

https://dspace.org/

The in vitro diffusion across exercised porcine skin of various formulations of compounds used topically in the treatment of skin afflictions

Elonga, Jessica

2023
University of the Witwatersrand, Johannesburg
https://hdl.handle.net/10539/43003
Elonga, Jessica. (2023). The in vitro diffusion across exercised porcine skin of various formulations of compounds used topically in the treatment of skin afflictions[Master's dissertation, University of the Witwatersrand, Johannesburg]. WireDSpace.https://hdl.handle.net/10539/43003

Downloaded from a DSpace repository. https://dspace.org/





The *in vitro* diffusion across exercised porcine skin of various formulations of compounds used topically in the treatment of skin afflictions.

Jessica Elonga

A dissertation submitted to the Faculty of Health Sciences, University of the Witwatersrand, Johannesburg, in fulfilment of the requirements of the degree of Master of Science in Medicine Johannesburg, 2023

Endurance produces proven character, and proven character produces hope ~ Romans 5:4

Abstract

Introduction and Aim: Skin afflictions have been treated with topically applied active compounds since the ancient Greek era. Topical compounds mostly avoid first-pass metabolism and move directly into the local region of the skin or mucous membranes to exert their therapeutic effects. In this study, the aim was to investigate the *in vitro* diffusion characteristics of active compounds commonly used in topical formulations, such as caffeine, theophylline, retinol, L-carnitine, and Co-enzyme Q10 across porcine skin, used as a model for human skin. These compounds were tested alone and in combination within different topical formulations (liquid, gel, and cream) to investigate skin permeation, skin accumulation and effect on skin integrity.

Methods: Method development and validation were performed to detect and quantitate all compounds tested by using a RP C18 HPLC system. Mobile phases included the following: caffeine and theophylline (Methanol:water [40:60], 20°C), retinol (Methanol:water [95:5], 20°C), L-carnitine (Sodium Phosphate buffer (pH 3.0):Methanol [99:1], 40°C) and Co-enzyme Q10 (Methanol:2-propanol [40:60], 25°C). All analyses were performed at 1 ml/min and injection volume of 20 µl. *In vitro* diffusion studies were performed using a PermeGear 7-in-line flow-through system. Either caffeine (2.5%), theophylline (2%), retinol (0.3%), L-carnitine (2%) or Coenzyme Q10 (0.5%) in various formulations alone, and in combinations were loaded into the donor compartments and PBS (pH 7.4) was pumped through the acceptor chambers at 1.5 ml/h (32°C, over 4 hours and 24 hours). The fluid collected (every 30 min or 2 hours) was analysed by RP HPLC. Skin accumulation for each compound was performed after completion of each experiment and skin integrity was established by measuring tissue resistance.

Results: HPLC methods were found to be sensitive and valid for linearity, precision, accuracy and robustness. Retention times were as follows: caffeine 2.57±0.02 min, theophylline 2.18±0.03 min, retinol 2.91±0.02 min, L-carnitine 3.0±0.009 min and Co-enzyme Q10 3.15 ±0.003 min. From the *in vitro* diffusion studies of active compounds alone, caffeine within all formulations had the highest diffusion rate compared to theophylline and L-carnitine (caffeine>theophylline>L-carnitine). Retinol and Co-enzyme Q10 did not diffuse across the skin within a 24-hour time-period. In combination with Co-enzyme Q10, the diffusion of caffeine increased from both gel and cream formulations ($p<0.05$), while retinol increased the diffusion of theophylline from a liquid formulation ($p<0.05$). Theophylline increased the diffusion of L-carnitine from both liquid and gel formulations ($p<0.05$). Liquid and gel formulations without compounds, decreased the skin's integrity after 24 hours and 2 hours, respectively. After 24 hours, the skin's integrity decreased after exposure to all compounds tested (liquid and gel formulations), while the cream formulation mostly kept the integrity of

the skin intact. Caffeine accumulated much more in the skin (>13%) compared to all the other compounds (<2.5%) for all three different formulations tested (caffeine>>L-carnitine>theophylline>retinol>Co-enzyme Q10). Combination studies mostly caused a decrease in accumulation of all compounds within the skin, except the following: retinol increased theophylline accumulation from a gel formulation and vice versa, Co-enzyme Q10 increased caffeine accumulation from all formulations and L-carnitine's accumulation mostly increased when combined with other compounds.

Conclusion: Caffeine was found to diffuse across and accumulate within the skin to a higher extent as compared to all the other compounds due to its ideal physicochemical characteristics. Very lipophilic compounds like retinol and Co-enzyme Q10 only accumulated to some degree in the skin. The findings indicated that the preferable combinations to increase efficacy, would be Co-enzyme Q10 in combination with caffeine, especially from a cream formulation, retinol in combination with theophylline (gel) and any of the compounds combined with L-carnitine (gel and cream). Cognisance must however be taken about possible systemic side effects.

Acknowledgements

I would like to thank my almighty Father, Jesus Christ, for giving me the strength and perseverance to push past my limits and complete this dissertation. The Lord knows it has been a long journey, but I have grown tremendously throughout this path, and I am forever thankful.

I would like to express my deepest gratitude and appreciation to my supervisor, Dr. Van Eyk. Thank you for the guidance, advice, trust, encouragement and helping me develop my knowledge and inspiring me continuously throughout the course of this project. Most importantly thank you for the support, understanding and patience through some of the tough times. The knowledge I gained, and experience has been invaluable, and this would have not been possible without your guidance.

I would like to express my sincerest gratitude and appreciation to the following people for the love, support and guidance given to me during this study:

- My lovely parents – Thank you both for always pushing me to do better and be better. Thank you for believing in me but most of all thank you for showing me unconditional love throughout this journey. This would not have been possible without your continuous support.

- My siblings- Glody, Johna and Naomi, thank you for continuously supporting me and making this journey fun by sharing laughter with me when all I wanted to do was cry.

- All my friends and colleagues who supported me through this study. Lizeka, Kim, Sahil, Puleng, Magali and Kekeletso. I appreciate your encouraging words shared with me.

Publications and conference presentations

Poster Presentation:

J.Elonga, Dr Van Eyk. The In Vitro diffusion characteristics across exercised porcine skin of various compounds used topically in the treatment of adiposis edematosa. The Annual Conference of South-African Society and Clinical Pharmacology Conference. University of the Free State, 01 -04 October 2017.

Poster Presentation:

Dr Van Eyk, J. Elonga.The In Vitro diffusion characteristics of various formulation containing Caffeine, Theophylline and Retinol across exercised porcine skin. Wits Faculty of Health Sciences (FHS) Research Day and Postgraduate Expo. University of Witwatersrand, September 2018.

Poster presentation:

Dr Van Eyk, **J. Elonga**.The In Vitro diffusion characteristics of L-Carnitine and Co-enzyme Q10 in liquid, gel and cream formulation across porcine skin. The Annual Conference of South-African Society and Clinical Pharmacology Conference. University of the Free State, 5th-7th October 2019.

Poster Presentation:

J.Elonga, **Dr Van Eyk** .The In Vitro diffusion of various active compounds from a cream formulation across skin. Wits Faculty of Health Sciences (FHS) Research Day and Postgraduate Expo. University of Witwatersrand, 15 October 2020

International conference:

Armorel van Eyk, Jessica Elonga. In vitro pharmacokinetics of topically applied compounds from various formulations across porcine skin.2021 4th Edition of Global Conference on Pharmaceutics and Novel Drug Delivery Systems September 6-8, 2021 | Virtual Event

Research day 2021:

Armorel van Eyk, Jessica Elonga. In vitro pharmacokinetics of topically applied compounds from various formulations across porcine skin.

Research day and oral presentation 2022:

Armorel van Eyk, Jessica Elonga. The effect of compounds in topical formulations on the barrier function of porcine skin.

SASBCP: poster presentation 2022:

Armorel van Eyk, Jessica Elonga.*In vitro* diffusion characteristics of topically applied compounds from three formulations across porcine skin.

In preparation: 2023 manuscript for peer reviewed Journal: Experimental Dermatology Journal

Armorel D van Eyk and Jessica Elonga. The *in vitro* diffusion characteristics of caffeine and retinol, alone and in combination from various formulations across porcine skin.

Table of Contents

Abstract *3*

Acknowledgements *5*

Publications and conference presentations *6*

Table of Contents *8*

1. Chapter 1: General introduction *19*

1.1 The Skin **19**

1.1.1 Overview of the Human Skin 19
1.1.2 Epidermis 20
1.1.3 Stratum Basale 21
1.1.4 Stratum Spinosum 21
1.1.5 Stratum Granulosum 21
1.1.6 Stratum Corneum 21
1.1.7 Tight Junctions 22
1.1.8 Dermis 23
1.1.9 Hypodermis 23

1.2 Skin afflictions **23**

1.2.1 Inflammatory Afflictions 24
1.2.2 Age and Hormone related afflictions 27

1.3 Topical treatment of skin afflictions **31**

1.3.1 Topical Treatment 31
1.3.2 Topical Formulations 32
1.3.3 Penetration Enhancers 33

1.4 Active compounds used in topical formulations **36**

1.4.1 Xanthine compounds 36
1.4.2 Retinol 42
1.4.3 L-Carnitine 45
1.4.4 Coenzyme Q10 (Ubiquinone-10) 48

1.5 Diffusion across skin **50**

1.5.1 Trans-appendageal pathway 51
1.5.2 Trans-epidermal pathway 51
1.5.3 Factors Affecting Transdermal Drug Delivery 53
1.5.4 Kinetics of Drug Absorption 54

1.6 Models for human skin **54**

1.6.1 Porcine skin 55
1.6.2 Rat skin 55
1.6.3 Rabbit skin 55
1.6.4 3D Cultured human skin models 56

1.7 Methods used for *in vitro* diffusion of chemicals across skin **56**

1.7.1 Franz Cells 57
1.7.2 Static cell (Side-bi- Side) 57
1.7.3 Continuous Flow cell or Flow-through-cell 58

1.8 Aims and objectives of the study **60**

Chapter 2: Experimental Methods and Materials *61*

2.1 High Performance Liquid Chromatography **61**

2.1.1 Introduction 61
2.1.2 Materials 62
2.1.3 Chromatographic apparatus 63
2.1.4 Preparation of mobile phases 64
2.1.5 Chromatographic Conditions 66

2.2 Preparation of Standards 66
2.2.1. Caffeine stock solution 66
2.2.2 Theophylline stock solution 67
2.2.3 Retinol stock solution 67
2.2.4 L-carnitine stock solution 67
2.2.5 Coenzyme Q10 stock solution 68

2.3. Preparation of phosphate buffered 68

2.4. HPLC Method Validation 68
2.4.1 Linearity 68
2.4.2 Limit of detection and limit of quantification 69
2.4.3 Precision 69
2.4.4 Accuracy 70
2.4.5 Ruggedness 71

2.4.6 Stability 72

2.5 In vitro Diffusion Studies 72
2.5.1 Introduction 72
2.5.2 Preparation of formulations 73
2.5.3 Combination Studies 74
2.5.4 Collection and storage of porcine skin tissue samples 75
2.5.5 Equipment used 76

2.6 Statistic Analysis 81

Chapter 3.1: Results – Validation 81

3.1 HPLC Method Validation 82
3.1.1 Linearity 82
3.1.2 Accuracy and Precision 93
3.1.3 Ruggedness 108
3.1.4 Temperature Variation 109
3.1.5 Mobile Phase Variation 119
3.1.6 Flow Rate Variation 133
3.1.7 Stability 147

3.1 Chapter 3.2: Results - In Vitro diffusion of active compounds 148
3.2.1 HPLC Specificity of compounds in formulations 148
3.2.2 *In vitro* diffusion of active compounds across the skin from liquid, gel, and cream, formulations 153
3.2.3 In Vitro Diffusion parameters of active compounds alone and in combination 159
3.2.4 TEER values 181
3.2.5 Skin Extraction 184

Chapter 4: Discussion 189

4.1. Method development and Validation of Active compounds 189
4.1.1 Caffeine 189
4.1.2 Theophylline 191
4.1.3 Retinol 192
4.1.4 L-carnitine 193
4.1.5 Coenzyme Q10 194

4.2. In vitro diffusion of active compounds across skin 195
4.2.1 Caffeine 196

4.2.2 Theophylline 197
4.2.3 L-Carnitine 199
4.2.4 Retinol and Coenzyme Q10 (CoQ10) 200

4.3 In Vitro Diffusion of compounds in combination 201
4.3.1 Caffeine alone and in combination in liquid, gel, and cream formulations 201
4.3.2 Theophylline alone and in combination in liquid, gel, and cream formulations 203
4.3.3 L-carnitine alone and in combination in liquid, gel, and cream formulations 205

4.4. Skin barrier Function (Skin integrity) 208
4.4.1 Liquid Formulation 209
4.4.2 Gel Formulation 210
4.4.3 Cream Formulation 211

4.5 Skin accumulation of active compounds alone 212
4.5.1 Caffeine 212
4.5.2 Theophylline 213
4.5.3 Retinol 214
4.5.4 L-carnitine 214
4.5.5 Co-enzyme Q10 215

4.6 Skin accumulation in combination 217
4.6.1 Skin accumulation of Caffeine in combination 217
4.6.2 Skin accumulation of Theophylline in combination 219
4.6.3 Skin accumulation of Retinol in combination 222
4.6.4 Skin accumulation of CoQ10 in combination 224
4.6.5 Skin accumulation of L-carnitine in combination 225

5. Chapter 5: Final Conclusion 228

5.1 Method validation of active compounds 228

5.2 *In vitro* diffusion of active compounds across skin 228

5.3 Skin accumulation of active compounds alone and in combination 229

5.4 Skin integrity 229

5.5. Future recommendations 230

6. Chapter 6: References 231

7. 7. Appendices 249

List of Figures

FIGURE 1.1: TRANSVERSE SECTION OF THE HUMAN SKIN (KHAVKIN AND ELLIS, 2011). 19
FIGURE 1.2: HISTOLOGICAL CROSS-SECTION OF THE EPIDERMIS LAYER (KHAVKIN AND ELLIS, 2011). 20
FIGURE 1.3: SCHEMATIC OVERVIEW OF THE SKIN INCLUDING PUTATIVE PENETRATION PATHWAYS. 22
FIGURE 1.4: POTENTIAL ILLUSTRATION SHOWING THE MECHANISM OF STAPHYLOCOCCUS AUREUS IN ATOPIC DERMATITIS. 25
FIGURE 1.5: SCHEMATIC ILLUSTRATION OF THE MECHANISM BEHIND THE ACTIVATION OF PSORIASIS. 26
FIGURE 1.6: ILLUSTRATION OF MODERATE ACNE ON A PATIENT (WILLIAMS ET AL., 2012).. 27
FIGURE 1.7: TRANSVERSE VIEW OF A NORMAL SEBACEOUS FOLLICLE REPRESENTED IN (A) AND INFLAMMATORY ACNE LESION WITH RUPTURE OF FOLLICULAR AND SECONDARY INFLAMMATION REPRESENTED IN (B) (WILLIAMS ET AL.,2012). 28
FIGURE 1.8: (A) VISUAL GRADING SCALE FOR ORANGE PEEL APPEARANCE. (B) SCHEMATIC ILLUSTRATION OF THE MAJOR MECHANISM INVOLVED IN ADEPOSIS ADEMATOSA..... 30
FIGURE 1.9: ILLUSTRATION OF PIGMENTED MACULES CAUSED BY MELASMA ON THE FOREHEAD (NICOLAIDOU AND KATSAMBAS., 2014). 31
FIGURE 1.10: AN ILLUSTRATION OF HLB SCALE (AS ET AL., 2018). 35
FIGURE 1.11: THE CHEMICAL STRUCTURE OF CAFFEINE (MONTEIRO ET AL., 2016). 38
FIGURE 1.12: THE CHEMICAL STRUCTURE OF THEOPHYLLINE (MONTEIRO ET AL., 2016)..... 41
FIGURE 1.13: CELLULAR MECHANISMS OF RETINOID ACTION IN PHOTODAMAGED SKIN. 42
FIGURE 1.14: STRUCTURAL FORMULAS OF RETINAL PALMINATE, RETINOL AND RETINOIC ACID (ZASADA AND BUDZISZ, 2019). 44
FIGURE 1.15: (A) ILLUSTRATION OF L-CARNITINE BIOSYNTHESIS PATHWAYS (STRIJBIS ET AL., 2010). 45
FIGURE 1.16: ILLUSTRATION OF THE MITOCHONDRIAL TRANSPORT OF FATTY ACID (LONGO ET AL., 2016) 46
FIGURE 1.17: STRUCTURAL FORMULA OF L-CARNITINE (HOPPEL, 2003). 48
FIGURE 1.18: STRUCTURAL FORMULA OF CO-ENZYME Q10 (PARKINSON ET AL., 2013). 49
FIGURE 1.19: MITOCHONDRIAL ELECTRON TRANSFER CHAIN AND THE REDOX REACTION OF CO-ENZYME Q10 (PARKINSON ET AL., 2013). 50
FIGURE 1.20:DRUG PERMEATION THROUGH THE TRANS-EPIDERMAL PATHWAY (TRANSCELLULAR AND INTERCELLULAR ROUTE) AND TRANS-APPENDAGEAL PATHWAY (SWEAT DUCTS, SEBACEOUS GLAND, AND HAIR FOLLICLE) (N'DA, 2014)..... 52
FIGURE 1.21: (A) ILLUSTRATION OF FRANZ CELL (B) SCHEMATIC ILLUSTRATION OF FRANZ CELL (BARTOSOVA AND BAJGAR, 2012). 57

FIGURE 1.22: SCHEMATIC ILLUSTRATION OF THE SIDE-BI-SIDE STATIC CELL APPARATUS (PERMEGEAR, 2018). 58
FIGURE 1.23: SCHEMATIC ILLUSTRATION OF THE CONTINUOUS FLOW OR FLOW-THROUGH CELL (PERMEGEAR, 2018). 59
FIGURE 2.1: SCHEMATIC DIAGRAM OF HPLC SYSTEM (CZAPLICKI 2013:102). 61
FIGURE 2.2: PERKIN ELMER HPLC SYSTEM. 63
FIGURE 2.3: ULTRASONIC SONICATOR (JANKE & KUNKEL- ULTRA-TURRAX). 73
FIGURE 2.4: ILLUSTRATION OF (A) ANTERIOR AND (B) SUPERIOR VIEW OF IN VITRO DIFFUSION APPARATUS AUTOMATED SYSTEM CONTAINING 7-IN-LINE FLOWS (ILC07) FROM PERMEGEAR INC (HELLERTOWN, PA,USA). 76
FIGURE 2.5: ILLUSTRATION OF PORCINE SKIN DIVIDED INTO 4-5 MM SECTIONS TO BE MOUNTED IN FLOW-THROUGH DIFFUSION CELLS (EXPOSED AREA 0.039 CM^2). 77
FIGURE 2.6: MILLIPORE MILLICEL® ERS-2 HAND-HELD RESISTIVITY METER. 80
FIGURE 3.1: LINEAR REGRESSION CURVE OF CAFFEINE (0 - 200 µG/ML) 83
FIGURE 3.2: LINEAR REGRESSION CURVE OF CAFFEINE (0 - 30 µG/ML). 84
FIGURE 3.3: CHROMATOGRAM OF CAFFEINE. 84
FIGURE 3.4: LINEAR REGRESSION CURVE OF THEOPHYLLINE (0 - 25 µG/ML). 85
FIGURE 3.5: CHROMATOGRAM OF THEOPHYLLINE. 86
FIGURE 3.6: LINEAR REGRESSION CURVE OF RETINOL (0 – 100 µG/ML). 86
FIGURE 3.7: LINEAR REGRESSION CURVE OF RETINOL (0 – 10 µG/ML). 88
FIGURE 3.8: CHROMATOGRAM OF RETINOL. 88
FIGURE 3.9: LINEAR REGRESSION CURVE OF CO-ENZYME Q10 (0 – 100 µG/ML). 89
FIGURE 3.10: LINEAR REGRESSION CURVE OF CO-ENZYME Q10 (0 – 10 µG/ML). 90
FIGURE 3.11: CHROMATOGRAM OF COENZYME Q10. 90
FIGURE 3.12: LINEAR REGRESSION CURVE OF L-CARNITINE (0 – 1000 µG/ML). 91
FIGURE 3.13: CHROMATOGRAM OF L-CARNITINE. 92

List of Tables

TABLE 1.1 PHYSICOCHEMICAL PROPERTIES OF CAFFEINE (WILKINSON ET AL., 2006; AGYEMANG-YEBOAH AND OPPONG, 2013; MONTEIRO ET AL.,2016). 39
TABLE 1.2 PHYSICOCHEMICAL PROPERTIES OF THEOPHYLLINE (THEOPHYLLINE, 2023). ... 41
TABLE 1.3 PHYSICOCHEMICAL PROPERTIES OF RETINOL (RETINOL, 2023). 44
TABLE 1.4 PHYSICOCHEMICAL PROPERTIES OF L-CARNITINE (L-CARNITINE, 2023). 47
TABLE 1.5 PHYSICOCHEMICAL PROPERTIES OF CO-ENZYME Q10 (COENZYME Q10, 2023) . 49
TABLE 2.1 CHROMATOGRAPHIC CONDITIONS OF CAFFEINE, THEOPHYLLINE, RETINOL, L-CARNITINE, AND COENZYME Q10. 66
TABLE 3.1: PRECISION OF CAFFEINE. 94
TABLE 3.3: PRECISION OF THEOPHYLLINE. 95
TABLE 3.4:PRECISION OF RETINOL. 96
TABLE 3.5:PRECISION OF CO-ENZYME Q10. 97
TABLE 3.6: PRECISION OF L-CARNITINE. 98
TABLE 3.7: INTERMEDIATE PRECISION OF CAFFEINE **(20 µG/ML).** 99
TABLE 3.8: INTERMEDIATE PRECISION OF THEOPHYLLINE **(10 µG/ML).** 100
TABLE 3.9: INTERMEDIATE PRECISION OF RETINOL **(40 µG/ML).** 101
TABLE 3.10: INTERMEDIATE PRECISION OF CO-ENZYME Q10 **(100 µG/ML).** 102
TABLE 3.11: INTERMEDIATE PRECISION OF L-CARNITINE **(500 µG/ML).** 103
TABLE 3.12: PEAK AREA AND PERCENTAGE RECOVERY OF CAFFEINE. 104
TABLE 3.13: PEAK AREA AND PERCENTAGE OF THEOPHYLLINE. 105
TABLE 3.14: PEAK AREA AND PERCENTAGE OF RETINOL. 106
TABLE 3.15: PEAK AREA AND PERCENTAGE OF CO-ENZYME Q10. 107
TABLE 3.16: PEAK AREA AND PERCENTAGE OF L-CARNITINE. 108
TABLE 3.17A: TEMPERATURE VARIATION OF CAFFEINE **(20 µG/ML)** 109
TABLE 3.18A: TEMPERATURE VARIATION OF THEOPHYLLINE **(5 µG/ML)** 112
TABLE 3.19A – TEMPERATURE VARIATION OF RETINOL **(1.0 µG/ML)** 114
TABLE 3.20C: TEMPERATURE VARIATION OF L-CARNITINE **(700 µG/ML)** 117
TABLE 3.21A: TEMPERATURE VARIATION OF COENZYME Q10 **(0.1 µG/ML)** 118
TABLE 3.22A: MOBILE PHASE VARIATION OF CAFFEINE **(10 µG/ML).** 120
TABLE 3.23A: MOBILE PHASE VARIATION OF THEOPHYLLINE **(4 µG/ML).** 123
TABLE 3.24A: MOBILE PHASE VARIATION OF RETINOL **(1.0 µG/ML).** 126
TABLE 3.25A: MOBILE PHASE VARIATION OF L-CARNITINE **(300 µG/ML).** 129
TABLE 3.26A: MOBILE PHASE VARIATION OF COENZYME Q10 **(0.1 µG/ML).** 131
TABLE 3.27: FLOW RATE VARIATION OF CAFFEINE **(150 µG/ML).** 134
TABLE 3.28A: FLOW RATE VARIATION OF THEOPHYLLINE **(5 µG/ML).** 135

TABLE 3.29A: FLOW RATE VARIATION OF RETINOL **(0.5 µG/ML).** 138
TABLE 3.30A: FLOW RATE VARIATION OF L-CARNITINE **(300 µG/ML).** 141
TABLE 3.31A: FLOW RATE VARIATION OF CO-ENZYMEQ10 **(0.1 µG/ML).** 144
TABLE 3.32: STABILITY OF STANDARD COMPOUNDS OVER A 2 – 3- DAY PERIOD AFTER STORAGE AT 4OC OR EXPOSED TO 32°C (IN VITRO DIFFUSION EXPERIMENT IN FORMULATIONS). RETINOL AND COENZYME Q10 WERE PROTECTED FROM LIGHT AT ALL TIMES DURING THIS TIME PERIOD. 147

Abbreviations

A – Area

ANOVA – Analysis of Variance

C – Concentration

°C – Degrees Celsius

cAMP – Cyclic adenosine monophosphate

CE – Chemical enhancer

CERs – Ceramides

cm^2 – Centimetres square (units of area)

CoA – Coenzyme A

COPD – Chronic Obstructive Pulmonary Disease

CoQ10 – Coenzyme Q_{10}

CRABP – Cellular retinoic acid-binding proteins

CRBP – Cellular retinol-binding proteins

Ct – The drug concentration in a particular compartment at time (t)

ddh2O – Double distilled water

DHT – Dihydrotesterone

DNA – Deoxyribonucleic acid

g – Grams

g/l - Gram per L

g/mol - Gram per mole

HLB – Hydrophilic-lipophillic Balance

HPLC - High performance Liquid chromatography

HPMC.FAM – Hydroxypropyl methyl cellulose

IL-10 – Interleukin 10

Jss – The steady- state flux or rate of drug absorption

Kg/m^3- Kilogram per cubic metre

KPa – Kilopascal

LOD – Limit of detection

LOQ – Limit of quantification

M – Molar

mg – Milligram

$mg/cm^2/h$ - Milligram per square centimetre per hour

min - Minutes

ml - Milliliter

ml/min - Milliliter per min

mL/H – Milliliters per hour

mg/mL – Microgram per Litre

mmHg - Millimetre(s) of mercury

mm - Millimeters

MPG – Monopropylene glycol

NF-kB – Nuclear Factor $_K$B

ng – Nanogram

Nm – nanometers

o/w - Oil in water

Papp – Permeability coefficients

PBS - Phosphate Buffer Saline

PDE – Phosphodiesterase

% - Percentage

pH - Acidity or Alkalinity of a solution

PIH – Post-inflammation Hyperpigmentation

ΔQ – The change in drug amount over a specific time interval

Qt – Total amount of drug at a time (t).

R - Retinoid molecule

r^2 – The coefficient of determination

RAR – Retinoid nuclear acid receptor

RARE – Retinoic acid elements

RP-C18 – Reverse phase-Column 18

RRE – Retinoid response elements

%RSD – Relative Standard Deviation

Rt – Retention time

RXR – Retinoid X receptor

SD – Standard Deviation

SE – Standard Error

tA – Duration of drug absorption multiplied by the absorption area

TEER – Trans-epithelial electrical resistance

TEWL – Transepidermal water loss

µl - Microlitre

µm - Micrometre

UVB - Ultraviolet B

UV – Ultraviolet

V – Volume

v/v - Volume per volume

Vt – Volume of distribution of the drug at time (t)

w/o - Water in oil

2D – Two dimensional

3D – Three dimensional

Chapter 1: General introduction

1.1 The Skin

1.1.1 Overview of the Human Skin

The skin is the largest organ of the human body and makes up sixteen percent of the human body weight. This complex organ acts mainly as a protective mechanism against foreign particles by being a permeability barrier to the environment (Kruger, 2010) as well as preventing water loss (Nolan and Marmur, 2012). The skin has various other functions including regulating temperature, synthesis of Vitamin D, playing a part in the immune system as well as receiving stimuli through the numerous nerves ending (Lebonvallet *et al*., 2010). The skin consists of three layers; epidermis, dermis and a fatty subcutaneous layer known as the hypodermis (Figure 1.1). Both epidermis and dermis have been found to be the prominent layers which are separated by the basement membrane, the extracellular matrix is a thin layer that forms part of the dermal layer (Evan *et al*., 2013). Furthermore, the epidermis consists of stratified squamous epithelium containing various cell types including Langerhans cells, melanocytes, and keratinocytes (Hwa *et al*., 2012).

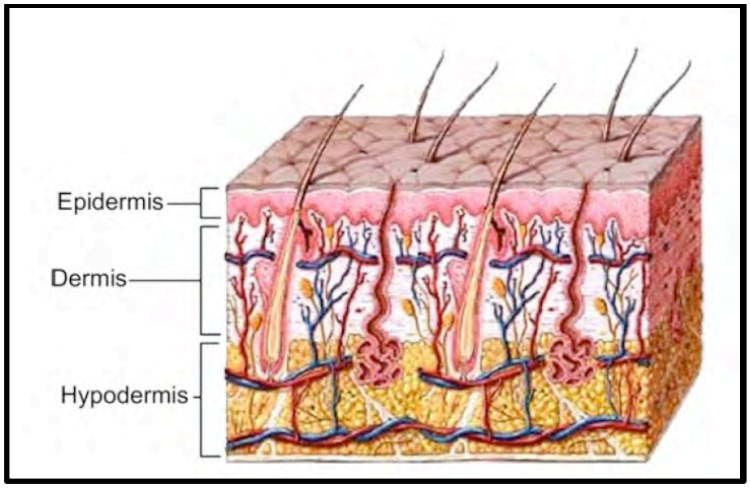

Figure 6.1: Transverse section of the human skin (Khavkin and Ellis, 2011).

1.1.2 Epidermis

The epidermis, being the outmost hydrophilic layer (70% water) (Bolzinger *et al*., 2012), varies in thickness from 0.06 mm on the eyelids to 0.8 mm on the palm of the hand and sole of the feet (Benson and Watkinson, 2012, p4). This layer is made up of stratified epithelial cells which consist of keratinocytes, these cell types are protein-rich cells containing keratin, that are responsible in providing structure and tensile strength and make up 95% of the epidermis layer; keratinocytes are hydrophilic and are separated from each other by a lipophilic layer (Hwa *et al*., 2011; Khavkin and Ellis, 2011).Within the epidermis, keratinocytes are arranged differently, forming the following layers: stratum basale (basal layer), stratum spinosum, stratum granulosum and stratum corneum (Figure 1.2) (Hwa *et al*., 2011).

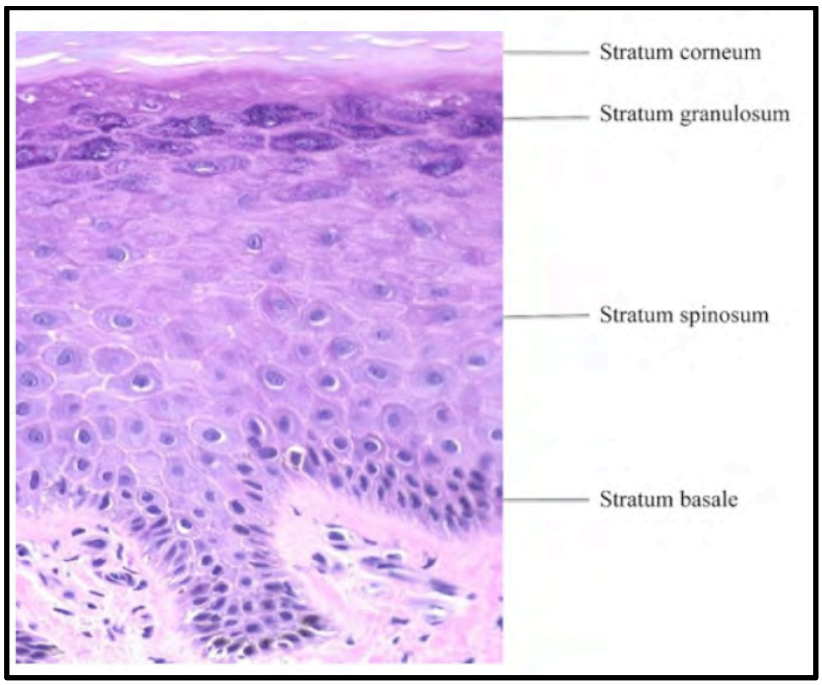

Figure 6.2: Histological cross-section of the Epidermis layer (Khavkin and Ellis, 2011).

1.1.3 Stratum Basale

The stratum basale, also called the stratum germinativum, is the basal (base) layer of the epidermis. It is the layer that is closest to the blood supply lying underneath the epidermis. Basal cells are responsible for proliferation. The cells can divide via the process of mitosis, which means that skin cells germinate here. Through the process of mitosis, keratinocytes arise. These cells are responsible for producing the most important protein called keratin. Keratin makes the skin tough and provides it with much-needed protection from microorganisms, physical harm, and chemical irritation (Piipponen *et al*., 2020).

1.1.4 Stratum Spinosum

Keratinocytes move from the stratum basale into the stratum spinosum, where secretion of keratin occurs thus forming lamellae bodies (secretary bodies). This gives the layer a spiny appearance. The stratum spinosum is partly responsible for the skin's strength and flexibility (Benson and Watkinson, 2012, p6).

1.1.5 Stratum Granulosum

The keratinocytes continue to migrate into the stratum granulosum, the cells undergo differentiation and therefore become flatter, brittle granular cells with no nuclei; these are known as keratohyalin (Benson and Watkinson, 2012, p6). The keratohyalin granules secrete a phosphoprotein known as profilagrin, which is responsible for the formation of corneocytes as well as intracellular metabolites which contribute to stratum corneum hydration and pH (Thyssen and Kezic, 2014).

1.1.6 Stratum Corneum

The Stratum Corneum is the outmost layer consisting of 10 - 25 layers of corneocytes, which have originated from keratinocytes that have undergone differentiation. The thin epithelial layer is impermeable to water as well as water-soluble substances (Bolzinger *et al*., 2012). The stratum corneum is the main penetration barrier when it comes to topical administration of drugs (Ochalek *et al*., 2012). The layer serves as the protective layer against harsh environmental conditions, additionally the layer plays a

vital role in water permeability. Studies have shown that the layer consist of natural moisturizing factors such as free amino acids, organic acids, urea and inorganic acids. These factors bind to water while the organization of lipids in the layer are responsible for the creation of the barrier (Menon *et al*., 2012). The major lipid classes found in the stratum corneum are as follows: cholesterol, free fatty acids and ceramides (CERs). Studies have shown that CERs play a vital role, a change in CERs composition will cause an impairment in the skin barrier (Van Smedden *et al*., 2011).

1.1.7 Tight Junctions

Epithelial tissue consists of cell-to-cell interactions by means of junctional complexes, this means cell structures can communicate by means of the arrangement of complex proteins which provides contact between neighbouring cells (Bäsler *et al*., 2016). Junctional complexes comprise of tight junctions, adherens junctions, desmosomes and gap junctions (Bäsler *et al*., 2016). Tight junctions are found below the stratum corneum at the level of the stratum granulosum (Figure 1.3), they act as a barrier and regulate the pathway of water, ions, and solutes through the paracellular pathway (De Benedetto *et al*., 2011). Furthermore, they have been found to play a crucial role in establishing as well as maintaining cell polarity in tissues (Bäsler *et a*l., 2016). Both the stratum corneum and the tight junctions act as the epithelium skin barrier structure, they interact together to ensure that the skin maintains a barrier (De Benedetto *et al*.,2011).

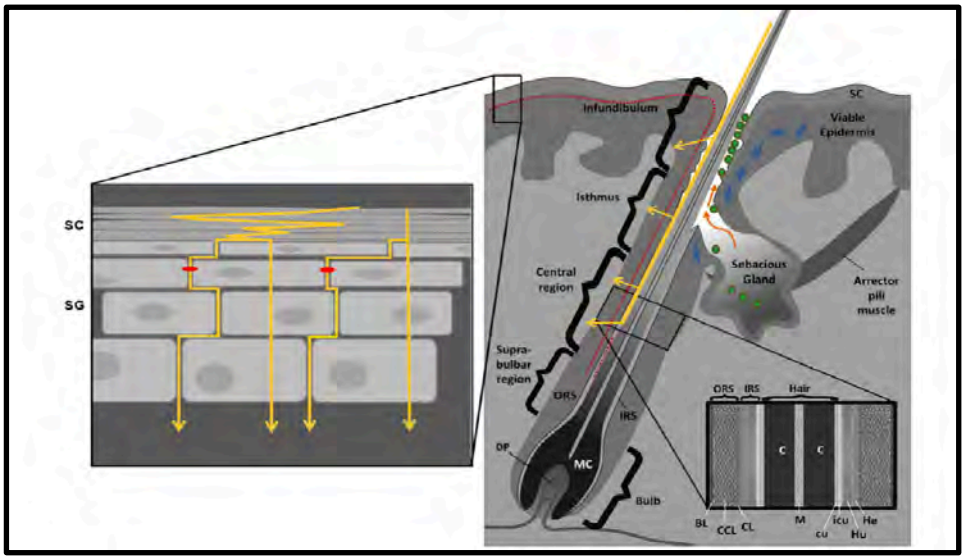

Figure 6.3: Schematic overview of the skin including putative penetration pathways.

Abbreviations: BL: basal cell layer of HF, C: Cortex, CCL: central cell layer of HF, CL: companion cell layer of HF, cu: cuticle of hair shaft, He: Henle's layer, Hu: Huxley's layer, icu: cuticle of IRS, IRS: inner root sheath, M: Medulla, MC: matrix cells, ORS: outer root sheath, SC: stratum corneum, SG: stratum granulosum. Yellow arrows: putative paracellular and transcellular penetration pathways. Red dots: tight junctions, blue stars: Langerhans cells, orange arrows: sebum, green circles: microbiota (Bäsler et al., 2016).

1.1.8 Dermis

The dermis is the layer found beneath the epidermis and it contains tough connective tissue, blood vessels, hair follicles, smooth muscle, lymphatic tissue as well as sweat glands. The dermis consists of fibroblast cells that are responsible for secreting collagen, elastin and proteoglycans which give support and elasticity to the skin. Furthermore, the dermal layers provide nutrients for the epidermis (Khavkin and Ellis, 2011).

1.1.9 Hypodermis

Hypodermis is the deepest layer, located below the dermis and above the underlying muscle (Khavkin and Ellis, 2011). The layer is composed of adipocytes arranged in lobules, fibroblasts, lymphocytes and mast cells and serves as an insulator and shock absorber (Kruger, 2010). The hypodermis is found to insulate and protect the body from mechanical injuries as well as a reserve energy supply (Khavkin and Ellis, 2011).

1.2 Skin afflictions

With the skin being the outermost human organ, which is in direct contact with the environment, it is increasingly exposed to stress that may cause skin afflictions. Skin afflictions refers to disorders that affect the skin, this can be characterized as minor or severe conditions.

The disturbance of the epithelial barrier of both the stratum corneum and tight junctions has been recognized as a feature of inflammatory diseases (Khavkin and Ellis, 2011). The impairment of the human stratum corneum barrier can lead to an increase in

transdermal water loss which in turns causes the skin to become susceptible to penetration of toxins thus resulting in various forms of skin afflictions (Del Rosso and Levin., 2011). Some skin afflictions can be categorized as situational cases due to stress or they may be from a genetic outcome. The following skin afflictions will be discussed in more detail: atopic dermatitis, psoriasis, acne vulgaris, adeposis adematosa and hyperpigmentation.

1.2.1 Inflammatory Afflictions

1.2.1.1 Atopic Dermatitis

Atopic Dermatitis, also known as eczema, is an inflammatory skin disease that is characterized by dryness and itch. Studies have shown that more than 85 % of the population is affected from childhood. The causality of the disease has not been determined, however there are two hypotheses that support the mechanism (Nutten, 2015):

- The inflammation is due to an immune defect, genetic studies have linked the causality of atopic dermatitis to various mutations, which support the hypothesis.
- The skin inflammation can be due to the primary defect of the stratum corneum, making the layer susceptible to penetration of microorganisms such as *Staphylococcus aureus,* a gram-positive bacterium (Figure 1.4). The *S. aureus* bacterium causes alteration of the lipid composition in the stratum corneum leading to skin inflammation.

Atopic dermatitis affects the facial and extensor surface of the limbs in infants whilst older children and adults have rashes on the flexural areas of the neck, elbows and knee areas (Ong., 2009; Nutten., 2015).

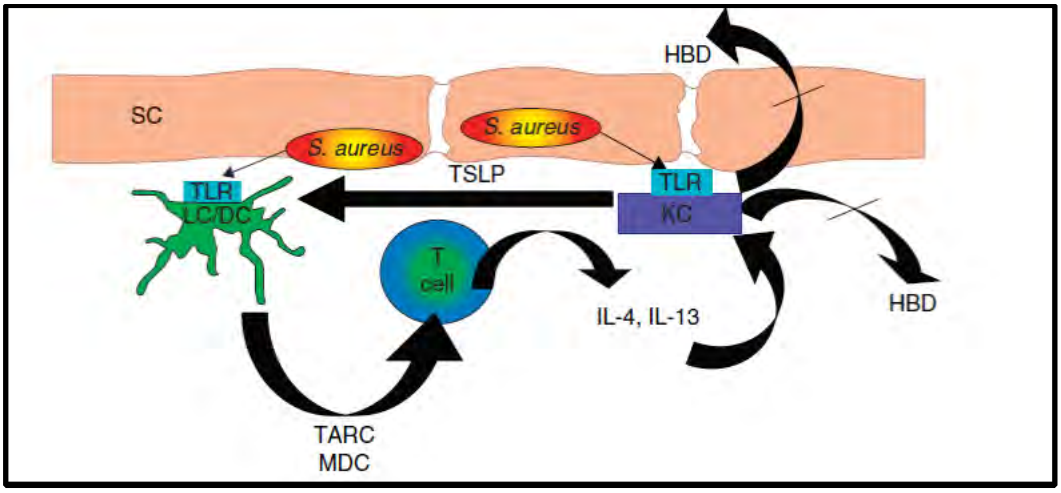

Figure 6.4: Potential Illustration showing the mechanism of Staphylococcus aureus in Atopic dermatitis.

On encountering *Staphylococcus aureus (S.aureus)*, Toll-like receptors (TLR) polymorphisms may lead to an increased Thymic stromal lymphopoietin (TSLP) and a decreased Human beta-defensin (HBD) production in Atopic dermatitis (AD). Increased Thymic stromal lymphopoietin (TSLP) leads to an increased T-Helper type 2 (TH2) response, whereas decreased Human beta-defensin, which is known to attract C-C chemokine receptor (CCR6+), leads to a decreased T-Helper type 1 (TH1) response. HBD production may be further suppressed by Interleukin-4 (IL-4)/Interleukin-13(IL-13). (Solid lines indicate pathway blocks.) (Ong, 2009).

Abbreviations: KC: Keratinocyte; LC/DC: Langerhans cells/dendritic cells; MDC: Macrophage-derived chemokine; SC: Stratum corneum (skin barrier); TARC: Thymus and activation-regulated chemokine (Ong, 2009).

1.2.1.2 Psoriasis

Psoriasis is known as an immune-mediated inflammatory disorder, a common chronic relapsing inflammatory skin disease. The immune system is dysregulated from the normal immune response (Rendon and Schäkel., 2019). This disorder is found to be more prominent in adults and affect 2 – 3 % of the world's population. Studies have found that there are several causalities which induces the disease (Enamandram and Kimball, 2013).

In psoriasis, T lymphocytes migrate from the immune system to the skin, there is no evidence which explain this hypothesis however, studies relate it to the genetic

susceptibility of the disease. The T lymphocytes are activated due to an immune response, the activation of T lymphocytes causes the development of red scaly skin lesions which results in inflammation of the skin. Furthermore, evidence has shown a correlation between tumour necrosis factor alpha (TNFα) and psoriasis. The cell signalling protein which is normally involved in systemic inflammation is found to promote and sustain psoriasis lesions however the aetiophatogenesis remains unclear (Figure 1.5) (Krueger and Bowcock, 2005; Campanati *et al*., 2010).

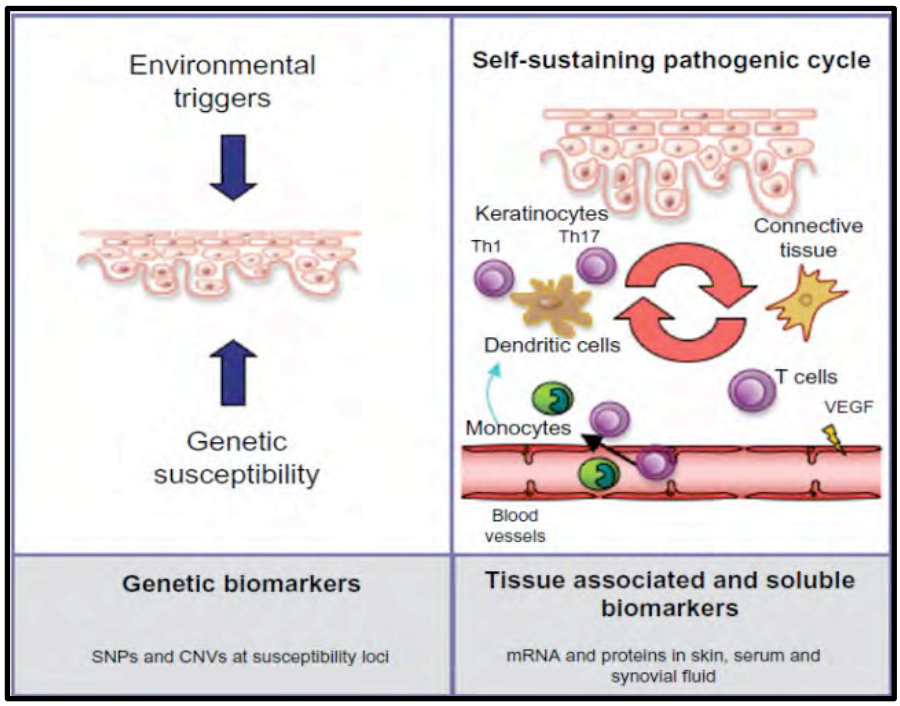

Figure 6.5: Schematic illustration of the mechanism behind the activation of Psoriasis.

Skin plaque formation is induced by environmental triggers in genetic predisposed subjects. Maintenance of the plaque is mediated by a self-sustaining pathogenic cycle constituted by T cells, dendritic cells, connective tissue (fibroblasts) and skin epithelium (keratinocytes). Moreover, the increased vascularity of the derma allows the migration from the circulation into the inflamed tissue of T cells and monocytes that will differentiate into mature dendritic cells. The systemic inflammatory condition characterizing psoriasis is evidenced by the high circulating levels of inflammation markers and, in a fraction of patients, causes the development of comorbidities, such as psoriatic arthritis and cardiovascular diseases.

Abbreviations: SNP, single-nucleotide polymorphism; CNV, copy number variation; VEGF, vascular endothelial growth factor. (Molteni and Reali, 2012).

1.2.1.3 Erythema solare (Sunburn)

Solar UV radiation has been known to be vital in the production of Vitamin D which plays a role in the synthesis of calcium and contributes to bone growth (Biniek *et al*., 2012). Studies have found that continuous exposure of UV radiation alters the function of the stratum corneum and thus leads to severe skin damage (Werth *et al*., 2011; Biniek *et al*., 2012). UVB radiation (280-320 nm) is absorbed by the epidermis and alter the morphology of the stratum corneum by increasing the thickness of the layer. This causes an alteration in the permeability of the layer thus allowing an increase in transdermal water loss resulting in a decrease in hydration of the layer. Due to this structural change, the skin is thus more susceptible to chapping and cracking due to the decrease in hydration, further aggravation can cause inflammation such as atopic dermatitis, itchthyosis vulgaris and chronic xerosis (Biniek *et al*., 2012).

1.2.2 Age and Hormone related afflictions

1.2.2.1 Acne vulgaris

Acne is a disorder which affects 80% of adolescents and young adults from the age of 11 and can persist into adulthood, with 12%-14% of cases affecting both the psychological and social wellbeing of an individual (Figure 1.6) (Almezani, 2018).



Figure 6.6: Illustration of moderate acne on a patient (Williams et al., 2012).

The cause of acne can be explained by the pilosebaceous unit being affected, this unit consisting of a hair follicle, hair shaft, arrector pili muscle and sebaceous gland (oil gland). The pathophysiological factors which induce acne includes:

- Seborrhea - this is due to the enlargement of the gland and the overproduction of sebum (free fatty acid).
- Hyperkeratinisation – Keratinocytes are hyper-proliferated around the hair follicle, this become dense with lipid droplets and thus forming acne lesions. There are two types of lesions formed:
    - Non-inflammatory - made up of whiteheads and blackheads
    - Inflammatory lesions - pores are infected with bacteria and have turned into papules and pustules; pimples containing pus (Figure 1.7).
- *Propionibacterium acnes* – The bacteria (*P. acnes*) migrate and colonizes the follicle duct and causing inflammation (Nakano *et al*., 2015; Dawson and Dellavalle., 2013).

The distribution of acne corresponds to the density of the pilosebaceous unit, this unit is commonly found on the face, neck, upper chest, shoulders and back. Acne is usually characterized by the scarring and inflammation of the skin (Williams *et al*., 2012).

A) 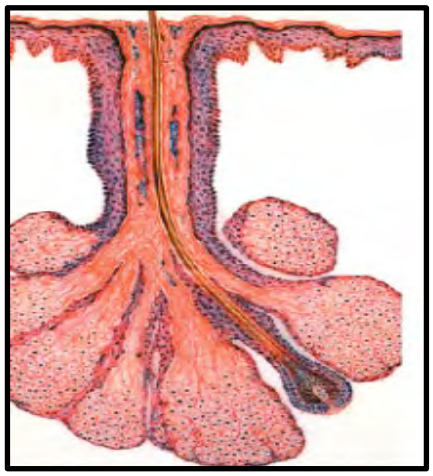 B) 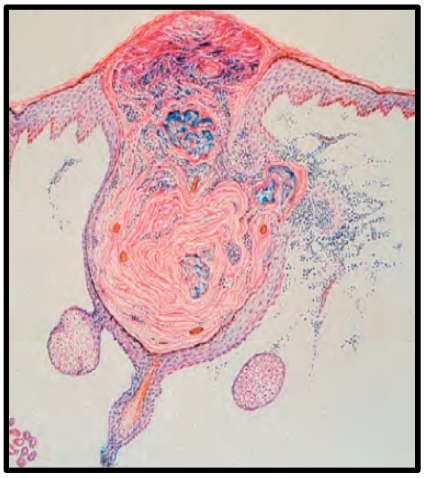

Figure 6.7: Transverse view of a normal sebaceous follicle represented in (A) and inflammatory acne lesion with rupture of follicular and secondary inflammation represented in (B) (Williams et al.,2012).

1.2.2.2 Adeposis adematosa (Cellulite)

Cellulite can be defined as a localized metabolic disorder of the subcutaneous tissue which results in the alteration of the appearance of the skin in women (Djajadisastra *et al*., 2014). It is an undesirable aesthetic problem which affects more than 85% of women; it usually begins at puberty and progresses throughout life (Tokarska *et al*., 2018; Hexsel and Mazzuco.,2013). This condition was often mistaken with Cellulitis, which is a progressive bacterial infection in the form of gangrenous bacteria spreading within the subcutaneous tissue (Bauer *et al*., 2020). With time, cellulite has been characterized as an alteration of the skin surface which gives rise to an orange peel effect (Figure 1.8 (A)) or mattress appearance (Tokarska et al., 2018). Its occurrence is mainly due to damaged blood vessels or accumulation of toxins from the lipolysis process in lymph vessels thus resulting in decreasing microcirculation. This causes accumulation of lymph fluid in the dermis as well as fat accumulation in the subcutaneous adipose tissue (Figure 1.8 (B)) (Djajadisastra *et al*., 2014; Herman and Herman, 2012). Cellulite occasionally occurs around the breast, abdomen, and upper arms, but it is mostly present on the pelvic region (gluteal-femoral region) (Rawlings, 2006; Velasco *et al*., 2008). Furthermore, cellulite can be classified into two distinct categories: incipient cellulite and advanced cellulite. Incipient cellulite is barely noticeable, it is usually recognized by an orange peel appearance demonstrated by the pinch test. In the case of full blown or advanced cellulite, there are irregular dimples which are highly noticeable on the skin surface; this stage of cellulite is also known as soft cellulite (Tokarska *et al*., 2018; Bauer *et al*., 2020).

A) 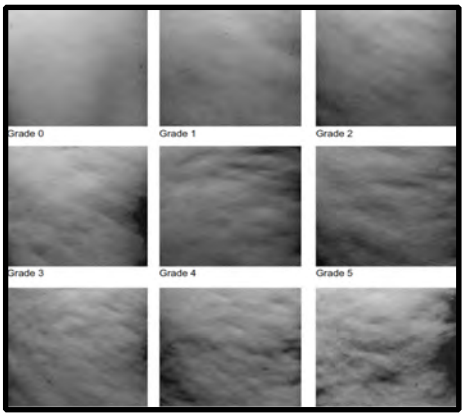

B) 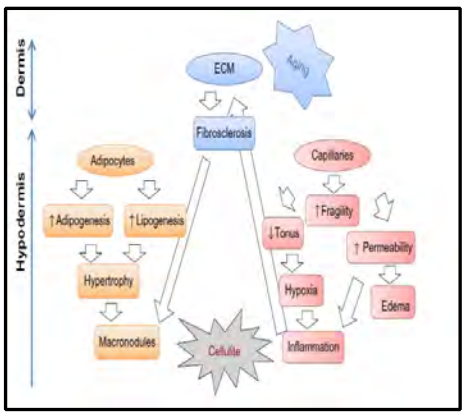

Figure 6.8: (A) Visual grading scale for orange peel appearance. (B) Schematic illustration of the major mechanism involved in Adeposis adematosa.

The exact etiology of cellulite is still a matter of debate, but most scientists agree on the involvement of reduced microcirculation, interstitial liquid infiltration (edema), localized hypertrophy of adipocytes, oxidative stress, and persistent low-grade inflammation, combined with extracellular matrix (ECM). Cellulite and skin aging may influence each other (Dupont *et al*., 2014).

1.2.2.3 Hyperpigmentation

Hyperpigmentation is a common skin problem that affects a large portion of the female population. Studies have shown that 90% of women can be affected whilst 50-70% of women experience skin discoloration during pregnancy (Almezani, 2018). Furthermore, hyperpigmentation is found to affect all population groups but seems to be more within population groups with darker skin types (skin types IV-VI) than lighter skin types; the darker the skin the more melanocytes in the epidermis (Davis and Callender, 2010; Qarqaz and Al-Yousef 2018; Almezani, 2018). Hyperpigmentation is related to the excess production of melanin; pigmentation responsible for skin hair and eye colour (Leyden *et al*., 2011). Studies have shown that UV light exposure stimulates melanocyte activity, thus causing excess production of melanin (Leyden *et al*., 2011; Almezani, 2018).

Melasma and post-inflammatory hyperpigmentation (PIH) are common pigmentation disorders that lead to darker marks on the surface of the skin (Davis and Callender ,2010; Nicolaidou and Katsambas, 2014)

- Melasma - This is clinically represented as irregular macules (area of discoloration). The cause of melasma is unknown; however, studies show that factors contributing to the disorder includes genetic predisposition, UV light exposure and estrogen exposure (Figure 1.9) (Nicolaidou and Katsambas., 2014).

- Post-inflammatory Hyperpigmentation (PIH)- PIH is related to a physiological response due to inflammation of the skin such as acne, atopic dermatitis, lichen planus and psoriasis (Davis and Callender, 2010; Rachmin *et al*., 2020). In this

case, melanocytes are stimulated by the inflammation (Davis and Callender, 2010; Rachmin *et al*., 2020).



Figure 6.9: Illustration of pigmented macules caused by melasma on the forehead (Nicolaidou and Katsambas., 2014).

1.3 Topical treatment of skin afflictions

1.3.1 Topical Treatment

Topical treatment has been found to be an effective way to treat local medical conditions and they are low in cost (Fleischer *et al*., 2017). Transdermal deliveries of therapeutic agents are an alternative and advantageous route of delivery compared to oral intake and hypodermic injections (Prausnitz and Langer, 2008). These advantages include:

1. Avoidance of hepatic first pass metabolism
2. Ability to discontinue administration by removal of the agent
3. The ability to control drug delivery for a longer time compared to the usual gastrointestinal transit of the oral dosage form
4. The ability to modify the properties of the biological barrier of absorption (Pathan and Setty, 2009).

1.3.2 Topical Formulations

Dermal and transdermal drug delivery can be dated back to the ancient Greeks, they used to apply a mixture of water, olive oil and lead oxide as an ointment on the skin (Morrow *et al*., 2007). Transdermal drugs have been used in the new era to treat skin diseases as well as aid with skin aesthetics. Most transdermal drugs are prepared in various formulations with different consistency such as liquids, solid powders, or semi-solids; where the semi- solid formulations consist of creams, gels and ointments (Morrow *et al*., 2007; Bartosova and Bajgar, 2012).

1.3.2.1 Topical solutions

Topical solutions are liquids which consist of one or more dissolved chemical substances. The solution often contains a mixture of solvents such as alcohol, polyols, and water (Ueda *et al*., 2009).

1.3.2.2 Gels

Gels also called jellies are semisolid substances which can be characterized as two different systems. Two-phase system gels are composed of small inorganic particles or large organic molecules mixed in with a liquid. Single phase system gels are composed of organic macromolecules which are uniformly distributed throughout the liquid, thus not creating an apparent boundary between the macromolecules and liquid (Ueda *et al*., 2009). Gels are composed using hydroxypropyl methylcellulose (HPMC) or carpobol, these agents are found to be effective in enhancing the drug permeation through the human skin (Al-Suwayeh *et al*., 2014).

1.3.2.3 Creams

Creams are emulsions of oleaginous (rich in oil) substances and water which spreads easily over the skin compared to ointments. Topical creams can be prepared in two manners: oil-in-water (o/w) or water-in-oil (w/o). O/W refers to oil being dispersed in water or aqueous solutions; these types of creams are water washable as well as cosmetic and aesthetically accepted. W/O refers to water or aqueous solution dispersed in oil or oleaginous phase; this mixture is not water washable and cannot absorb water (Ueda *et al*., 2009).

1.3.3 Penetration Enhancers

The stratum corneum is the main barrier for drug penetration and it is known to limit the transdermal penetration of molecules (Maghraby *et al*., 2008). Penetration enhancers are chemicals that are used to promote the delivery of active ingredient across the stratum corneum (Ubaid *et al*., 2016).

1.3.3.1 Chemical enhancement

1.3.3.1.1 Carbopol

Carbopol is a family of commercial polymers which are commonly used in cosmetic, pharmaceutical paint and food industry. There are more than 10 different grades of carbopol polymers, which are known to have a high molecular weight, hydrophilic characteristics and crosslinked polyacrylic acid polymer (Varges *et al*., 2019). The hydrophilic and cross-linked properties of Carbopol form a microgel which is useful for dermatological applications (Al-Suwayeh *et al*., 2014; Ubaid *et al*., 2016). The physical hydrogel has a three-dimensional polymer network which absorb water and presents a temporary reversible entanglement that are stronger when compared to chemical hydrogel (Varges *et al*., 2019). Studies have found that these polymers open tight junction in the stratum corneum, which improves the permeability of active agents through the paracellular pathway of the skin (Balakrishnan *et al*., 2015).

1.3.3.1.2 Ethanol

Ethanol commonly known as alcohol (CH_3CH_2OH or C_2H_6O) is a clear colourless liquid that is readily used as a topical disinfectant due to its antimicrobial effect. For this reason, the agent is widely used in various products with direct contact with human skin such as hand disinfectants, cosmetics or mouthwash. Ethanol has a molecular weight of 46.07 g/mol with a boiling point of 78.37 °C and melting point of -114.1 °C. Furthermore, the liquid molecule has a density of 789 kg/m^3, a vapor pressure of 5.95 KPa at 20 °C and an acid dissociation constant (pKa) of 15.9 (Ethanol, 2023). Ethanol is commonly used in transdermal formulations, it is also combined with water during *in vitro* permeation experiments as it diffuses through the skin rapidly with a steady

state flux of approximately 1mg/cm^2/h (Mathur *et al*., 2010). Ethanol increases permeation rate of drugs through the skin due to the following:

- the liquid can act as a solvent and increases the solubility of the drug
- ethanol can increase solubility of permeants that deplete during the steady state diffusion study
- application of ethanol on the skin can increase the permeation of the stratum corneum by loosening the tight junctions which in turns alters the permeability of the tissue
-the highly volatile property of ethanol modifies the thermodynamic activity of the drug within the formulation, which allows for the drug to become more concentrated and therefore create an over-saturated diffusion through the skin (Williams and Barry, 2012).

1.3.3.1.3 Propylene glycol

Propylene glycol is an emollient and emulsifier found in various ranges of consumer, professional and industrial uses such as carrier molecule in production. The liquid molecule can be described as a small carbon molecule ($C_3H_8O_2$) which form part of the monopropylene glycol (MPG) family (Jacob *et al*., 2018; Fowles *et al*., 2013). The molecule has a molecular weight of 76,09 g/mol with a boiling point of 186 °C and a melting point of -60 °C. Propylene glycol has a density of 1.0361 g/cm^3 and thus extremely soluble in water. Furthermore, the molecule has a vapor pressure of 106.6 at 20 °C and a pKa of 14.8 at 25 °C (Propylene-glycol, 2023).

In a study conducted by William Griffin (Pasquali *et al*., 2008), emulsifiers were classified according to a theory known as hydrophilic-lipophilic balance (HLB). This theory simply states that the emulsifier consists of a molecule that combines both hydrophilic and lipophilic groups. The balance of the size and the strength of these two opposite groups is known as HLB (Pasquali *et al*., 2008). The numerical value of HLB determines the nature of the emulsifier and the type of the emulsion. In other words, this will help to determine whether the emulsifier has more of a hydrophilic or lipophilic affinity. The lower the HLB value of an emulsifier, the more hydrophobic the emulsifier becomes. The HLB scale ranges from 0 to 20 (Sondari and Tursiloadi., 2018). According to the William Griffins classification (Pasquali *et al*., 2009), propylene

glycol has a HLB value in the range of 3.4 - 4.5; this indicates that propylene glycol is a lipophilic molecule that forms a w/o emulsion (Pasquali *et al*., 2008). The HLB scale is illustrated in Figure 1.10 (As *et al*., 2018).

Propylene glycols, as mentioned, has been used as a chemical enhancer for optimum topical transdermal formulation delivery. Chemical enhancers are agents that modifier the function of the stratum corneum. Propylene glycol works similarly by increasing permeation and loosening the α-keratin bonds, found in the epidermal layer, and therefore reducing the drug-tissue binding (Haque and Talukder, 2018).

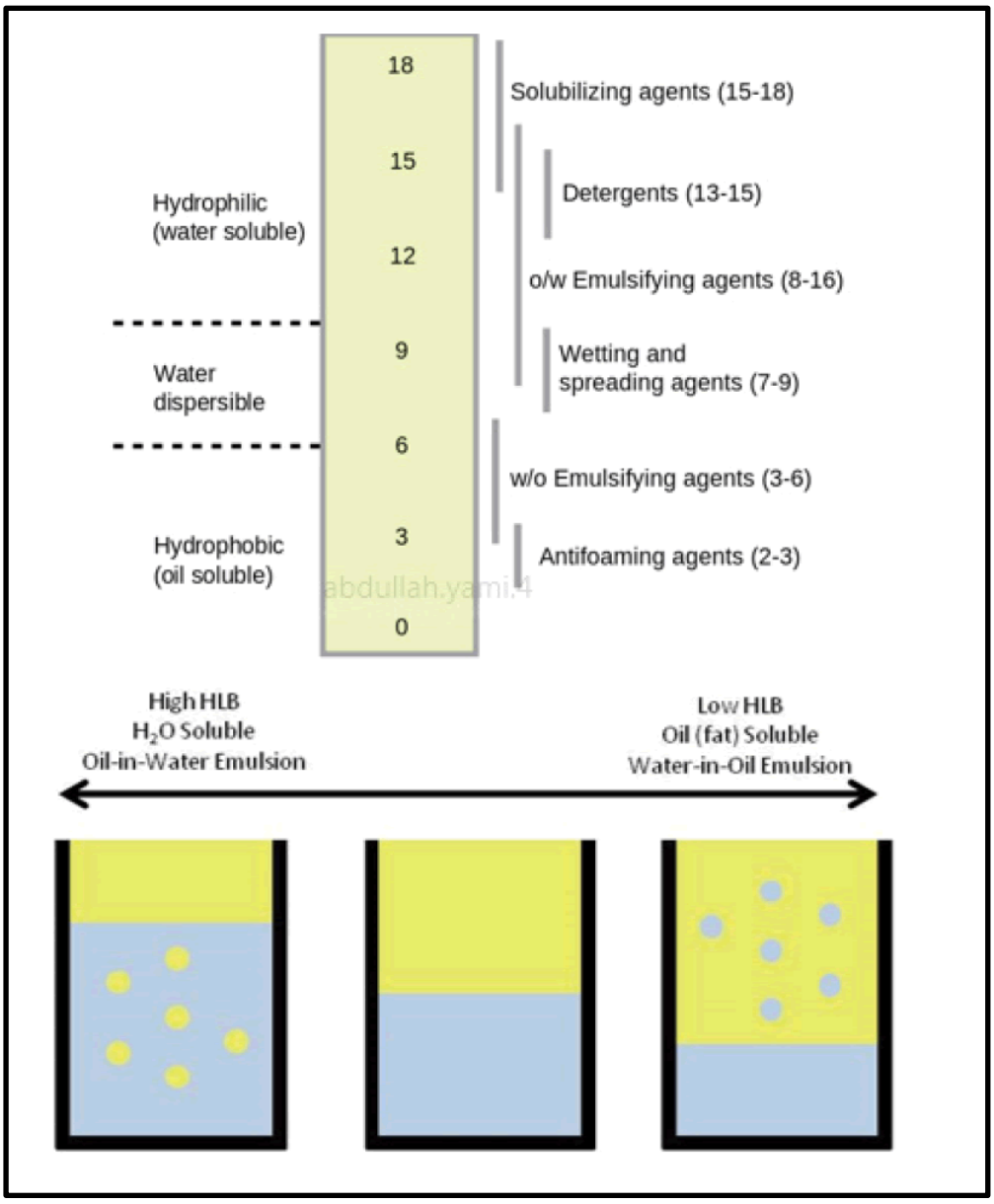

Figure 6.10: An illustration of HLB scale (As *et al*., 2018).

1.3.3.1.4 Olive oil

Olive oil is characterized as a natural oil, which can be used as an emulsifier, stabilizer or solubility enhancer. Natural oils are heterogeneous lipids which consist of triglycerides, diglycerides, free fatty acids, phosphatides, sterols, fatty alcohols and fat -soluble vitamins. Studies have found that free fatty acids are responsible for the structural change of the skin barrier, thus increasing the permeation of hydrophilic and hydrophobic compounds (Pham *et al*., 2016; Cizinauskas *et al*., 2017). Free fatty acids enter the hydrophobic tail of the stratum corneum lipid bilayer and disrupt the structure, by disrupting the inner structure it increases the fluidity and decreases the diffusional resistance resulting in an increase in permeation (Kim *et al*., 2020).

1.4 Active compounds used in topical formulations

1.4.1 Xanthine compounds

Xanthine compounds, chemically known as 3,7-dihydropurine-2,6-dione contains a purine base found in most human body tissues and fluids. The compound itself is a bi-product which results from the xanthine oxidase enzyme converting hypoxanthine to xanthine and finally to uric acid (Sarici *et al*., 2009). A methyl group attaching itself to a xanthine compound forms a methylated compound known as methylxanthine. Caffeine and theophylline are both methylxanthines. These two compounds are found to affect cells and tissues in the human body. The mechanism of action of both caffeine and theophylline includes (Monteiro *et al*., 2016):

- blocking of the adenosine receptors which results in the increased release of norepinephrine, dopamine, and serotonin,
- central nervous system stimulation,
- bronchodilation (mostly used in the treatment of asthma),
- stimulation of diuresis,
- regulation of glycogen metabolism.

Furthermore, caffeine and theophylline inhibit phosphodiesterase (PDE). The inhibition of PDE stimulates lipolysis, which is beneficial in the treatment of skin afflictions such as Adeposis adematosa (Herman and Herman, 2012). Moreover,

methylxanthines have also been known to be used in various topical creams with the aim of reducing skin related afflictions. A study conducted by Mitani *et al*., 2007 shows that plant extracts such as cocoa bean and cola nuts are rich in xanthine derivatives (Caffeine and theophylline). Furthermore, their research found that extracts of these plants have an effect against photo damage such as wrinkles, sunburn or tumors. The study suggest that the xanthine derivatives suppress the formation of wrinkles by preventing the neutrophil infiltration which is caused by UV exposure (Mitani *et al*., 2007).

1.4.1.1 Caffeine

Caffeine is a popular ingredient found in anti- cellulite creams as well as shampoos (Luo and Lane, 2015). Studies have shown that caffeine stimulate hair growth through follicular penetration (Otberg *et al*., 2008). The hair follicle serves as a long-term reservoir for topically applied agents, these agents can be stored in the reservoir for several days (Lademann *et al*., 2010). As caffeine is topically applied, the molecule penetrates the hair follicle through the trans-appendageal pathway. The molecule than moves from the pathway into the blood capillaries which surrounds the hair follicle (Lademann *et al*., 2008). Due to the follicular absorption of caffeine, shampoos are found to contain caffeine as an active ingredient in the formulation (Otberg *et al*., 2008).

Caffeine has been found to activate the lipolysis process by increasing the secretion of catecholamines, which in turn activates the β-adrenergic receptors that inhibit PDE and increases cyclic adenosine monophosphate (cAMP) in the cells. This activates the hormone sensitive lipase (HSL) in the lipolysis process. The caffeine molecule is also known to inhibit binding of insulin on the α-adrenergic receptor, therefore preventing the fat deposition which could lead to the appearance of adeposis adematosa. Caffeine stimulates the drainage of lymph systems found in adipocyte tissue by removing toxins, which arise during the lipolysis process (Herman and Herman, 2013).

5-α-Reductase is an enzyme that converts testosterone into an active form called dihydrotestosterone (DHT) which is responsible for baldness. Topical application of caffeine reduces the smooth muscle tension around the hair follicle allowing the agent to diffuse into the blood capillaries. As caffeine enters the blood circulation, it inhibits

the activity of the 5-α-reductase enzyme, which allows for a renewed growth phase of the hair. Furthermore, stimulation of hair growth can occur by inhibiting the PDE enzyme activity, which increases intracellular cAMP concentration that leads to cellular metabolism (Herman and Herman, 2013; Raker *et al*., 2016). The elevated levels of cAMP in the cell suppresses the inflammatory pathway by upregulating Nur77 expression (gene expression linked to inflammation) which weakens the monocyte inflammatory function. This is beneficial in patients who suffer from atopic dermatitis or psoriasis (Raker *et al*., 2016). Caffeine has been found to act as an antagonist on the A_{2A} receptor. A_{2A} receptors play a role in the heart by regulating myocardial oxygen consumption and coronary blood flow as well as control anti-inflammatory effects in the body (Dall'Igna *et al*., 2007).

1.4.1.1.1 Physiochemical properties of Caffeine

Caffeine (Figure 1.11) also known as 1,3,7- trimethylxanthine with a chemical formula of $C_8H_{10}N_4O_2$ (Table 1.1) is naturally found in coffee, cocoa, tea, and cola nuts. Caffeine can also be classified as an alkaloid as it is formed from the metabolism of nitrogen. This molecule is found to contain a lipophilic component and therefore is expected to easily permeate through the cell membrane (Monteiro *et al*.,2016). A synopsis of the physical and chemical properties of caffeine is provided in Table 1.1.

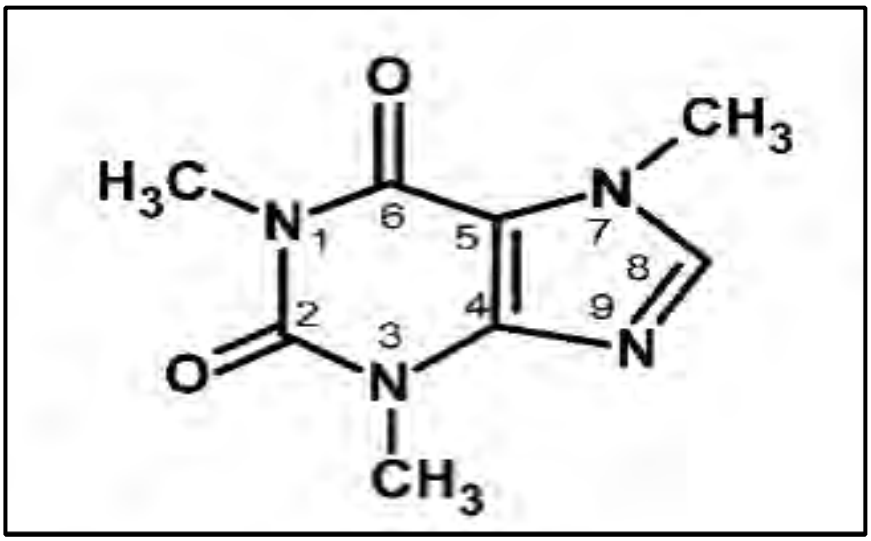

Figure 6.11: The chemical Structure of Caffeine (Monteiro *et al*., 2016).

Table 6.1 Physicochemical properties of caffeine (Wilkinson et al., 2006; Agyemang-Yeboah and Oppong, 2013; Monteiro et al.,2016).

Chemical names	1,3,7- trimethylxanthine, caffeine 58-08-2, Guaranine
Molecular weight	194.194 g/mol
Appearance	Odourless white powder with bitter taste
Solubility	Soluble in water (2.17%) and soluble in ethanol
pH	6.9
log P (Partition coefficient)	-0.07
Dissociation constant (pKa)	14 at 25°C
Melting point	238°C
Boiling point	178°C
Vapor Pressure	1010 kPa at 178°C
Density	1.2 g/cm^3
Volatility	0.5%

1.4.1.2 Theophylline

Theophylline is combined with ethylene diamine in anhydrous alcohol to form aminophylline which breaks down fat and cellulite through the activation of enzymes (Wang *et al*., 2007). Theophylline occurs naturally in tea and cocoa (Barnes, 2013). Theophylline was first extracted in 1985 from tea, it was further synthesized chemically to form a diuretic agent (Barnes, 2013). With time, its bronchodilator property was

discovered and therefore it became the first line of treatment in chronic obstructive pulmonary (COPD) disease (Barnes, 2013). Theophylline has been found to have several molecular mechanisms of action (Barnes, 2013):

- PDE inhibition: as mentioned in section 1.4.1, theophylline act as a PDE inhibitor, however compared to caffeine theophylline is found to be a weak non-selective inhibitor.
- Adenosine Receptor Antagonism: Theophylline blocks adenosine A_1 and A_2 receptors which is the mechanism of action for its bronchodilator effects.
- Increased IL-10: IL-10 is a cytokine with anti-inflammatory properties, the concentration of IL-10 decreases in the presence of asthma or COPD. An increase in theophylline relatively increases the concentration of IL-10, however, this can be counter-parted by the PDE inhibition process.
- Effects of transcription: Theophylline prevents the migration of the pro-inflammatory transcription factor called nuclear factor kappa B cells into the nucleus by inhibiting the degradation of the inhibitory protein I-$_K$Bα (nuclear factor of kappa light polypeptide gene enhancer in B-cells inhibitor, alpha). Inhibition of pro-inflammatory transcription factors reduces the inflammatory genes in asthma and COPD which contributes to theophylline bronchodilator function (Barnes, 2010).
- Decreases insulin resistance and hyperglycaemia: Theophylline has the potential to treat insulin resistance and hyperglycaemia by decreasing the secretion of IL-6 (Pro-inflammatory adipokines- Interleukin) which is characterized by an increase in adipose tissue (Mitani *et a*l., 2018).

1.4.1.2.1 Physiochemical properties of Theophylline

The theophylline molecule, also known as 1,3-Dimethylxanthine (Figure 1.12) with a chemical formula $C_7H_8N_40_2$ is a methyl xanthine which is derived from tea with diuretic, smooth muscle relaxant, bronchial dilation, and central nervous system activities (Theophylline, 2023). The theophylline molecule is described as a polar molecule and therefore requires the aid of a pro-drug when being administrated topically to enhance transdermal delivery. A pro-drug can be defined as a molecule which attaches to an organic/inorganic moiety and chemically modifies the molecule to increase the

chances of permeation through the skin transdermal delivery (N'Da, 2014). A synopsis of the physical and chemical properties of Theophylline is provided in Table 1.2.

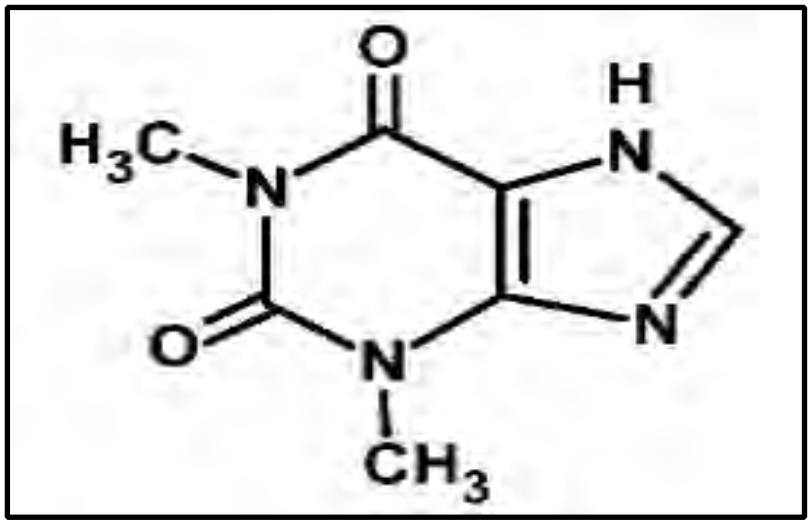

Figure 6.12: The chemical Structure of Theophylline (Monteiro et al., 2016).

Table 6.2 Physicochemical properties of theophylline (Theophylline, 2023).

Chemical names	1,3-dimethyl-7H-purine-2,6-dione
Molecular weight	180.167g/mol
Appearance	Odourless white crystalline powder with bitter taste
Solubility	Slightly soluble in water at a range of 5.5 to 8.3 g/l Slightly soluble in ethanol and chloroform
pH	3.0 - 4.7
log P (Partition coefficient)	-0.02
Dissociation constant (pKa)	8.81 at 25°C
Melting point	274°C
Boiling Point	313°C
Vapor Pressure	$5.12X10^{-9}$ mm Hg at 25 °C
Density	1.36 g/cm^3

1.4.2 Retinol

Vitamin A or Retinol A has been found to be very effective in the treatment of skin problems including aging (Jazzpollard, 2013), the compound is known to play a role in epithelial homeostasis (Oliveira *et al*., 2018).

The topical application of retinol can be beneficial to the skin in the treatment of psoriasis and severe acne, as it contains anti-inflammatory properties (Dawson and Dellavalle, 2013; Zasada and Budzisz, 2019). As retinol is topically administrated, the compound diffuses through the skin and binds to retinoid nuclear acid receptor (RAR). Once the compound has bound to the receptor, the receptor binds to a specific region on DNA known as retinoic acid elements (RARE). This activates transcriptional activity. Retinol is known to be lipophilic and can therefore diffuse through cellular and phospholipid membranes. Figure 1.13 shows a schematic overview of retinoid effects on photoaged skin (Sorg *et al*., 2006). The retinoid extract found in retinol A has been found to increase dermal content of collagen and dermo-epidermal protein, thus helping the skin look firmer and toned, which is beneficial in the treatment against wrinkles and skin aging (Zasada and Budzisz, 2019).

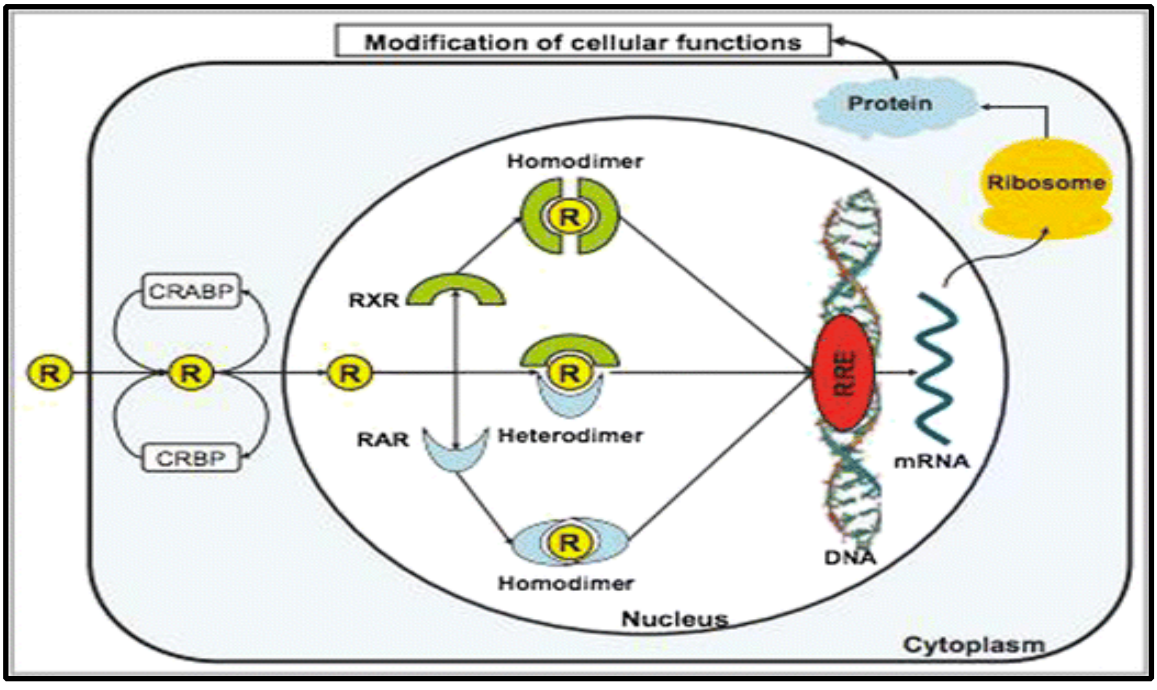

Figure 6.13: Cellular mechanisms of retinoid action in photodamaged skin.

The retinoid molecule (R) enters the cell by diffusion and is transported from the cytoplasm to the nucleus by cellular retinol-binding proteins (CRBP) or by cellular retinoic acid-binding proteins (CRABP). All-trans-retinoic acid, which is an active metabolite of vitamin A, can be metabolized immediately after binding to CRABP. CRBP and CRABP influence the bioavailability of retinoids. In the nucleus, R binds to either retinoic acid receptor (RAR) or to retinoid X receptor (RXR). Both RXR and RAR as homodimers (identical proteins) and/or heterodimers (different proteins) act as ligand-dependent transcription factors and bind to specific elements in the promoter genes, i.e., retinoid response elements (RRE). Transcription is modulated by transcriptional activation through specific DNA sites or by inhibiting transcription factors, e.g., activator protein-1 (Darlenski *et al*., 2010).

1.4.2.1 Physiochemical properties of Retinol

Retinol A or Vitamin A ($C_{20}H_{30}O$) (286.459 g/mol) also known as (2E,4E,6E,8E)-3,7-dimethyl-9-(2,6,6-trimethylcyclohexen-1-yl) nona-2,4,6,8-tetraenoic acid is an ester which naturally occurs in the skin with retinol and retinyl esters being the most abundant forms. These compounds are stored in the liver (Babamiri and Nassab, 2010; O'Byrne and Blaner., 2013). Retinol is formed in the small intestines by hydrolysis of retinyl esters by means of esterase enzymes. It is further oxidized by alcohol dehydrogenase and converted in many tissues to retinoic acid (300.43 g/mol), Figure 1.14 illustrates the chemical structure of retinol derivatives (Yourick *et al*., 2008; Babamiri and Nassab, 2010). In commercial cosmetic creams, retinol derivatives such as retinyl palminate, retinyl acetate and retinyl propionate are ingredients widely used as they are found to be more stable than retinol, which is found to degrade when exposed to light (Mukherjee *et al*., 2006). Retinol and its derivatives are known to be lipophilic molecules and can therefore diffuse through cellular and phospholipid membranes (Sorg *et al*., 2006), once inside the cell membrane they bind to the respective receptor respective receptor as mentioned in section 1.4.2. A synopsis of the physical and chemical properties of caffeine is provided in Table 1.3.

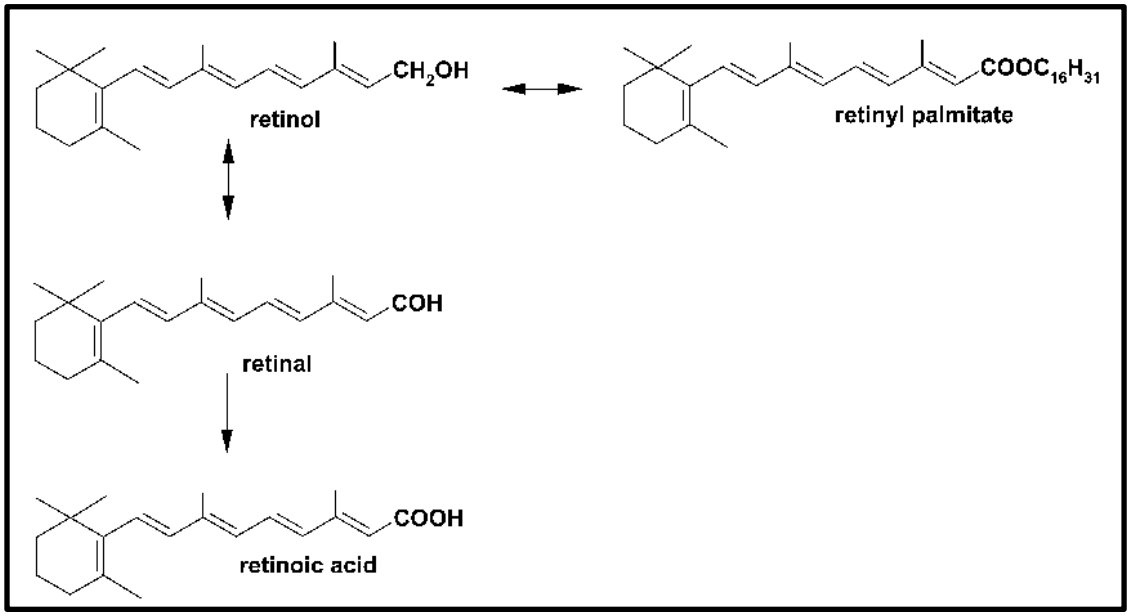

Figure 6.14: Structural formulas of Retinal palminate, retinol and Retinoic Acid (Zasada and Budzisz, 2019).

Table 6.3 Physicochemical properties of retinol (Retinol, 2023).

Chemical names	Vitamin A, all-trans-Retinol 68-26-8, Vitamin A1
Molecular weight	286.459 g/mol
Appearance	Yellow or light orange crystalline powder
Solubility	Insoluble in water (0.671 mg/l) and soluble in methanol
log P (Partition coefficient)	5.68
Dissociation constant (pKa)	16.4: Strongest acidic -2.2: Strongest basic
Boiling point	138°C at $1X10^{-6}$ mmHg
Melting point	63.5°C
Vapor Pressure	$7.5x10^{-8}$ mmHg at 25°C

1.4.3 L-Carnitine

L-carnitine is the biological stereoisomer of carnitine which is a compound predominantly found in food from animal sources (Flanagan *et al*., 2010), the compound can also be synthesized in eukaryotes (Strijbis *et al*., 2010). In eukaryotes, L-carnitine is synthesized from proteic trimethyllysine (amino acid) in the liver, brain and kidney. The biosynthetic pathway of L-carnitine involves four different enzymes which forms three substrates of the carnitine biosynthesis pathway (Strijbis *et al*., 2010). The pathway starts with the hydroxylation of trimethyllysine (TML) by TML dioxygenase (TMLD) into 3-hydroxy-N^6-trimethyllysine (HTML). The second enzyme performs a pyridoxal 5'-phosphate (PLP)-dependent aldolytic cleavage of HTML resulting in 4-N-trimethylaminobutyraldehyde (TMABA). The third enzymatic reaction includes the dehydrogenation of TMABA by TMABA dehydrogenase (TMABADH) which forms gamma-butryobetaine (γ-BB). In the fourth enzymatic step, γ-BB is hydroxylated by gamma-butryobetaine dioxygenase (BBD) to form L-carnitine. This biosynthetic pathway is illustrated in Figure 1.15 (Strijbis *et al*., 2010).

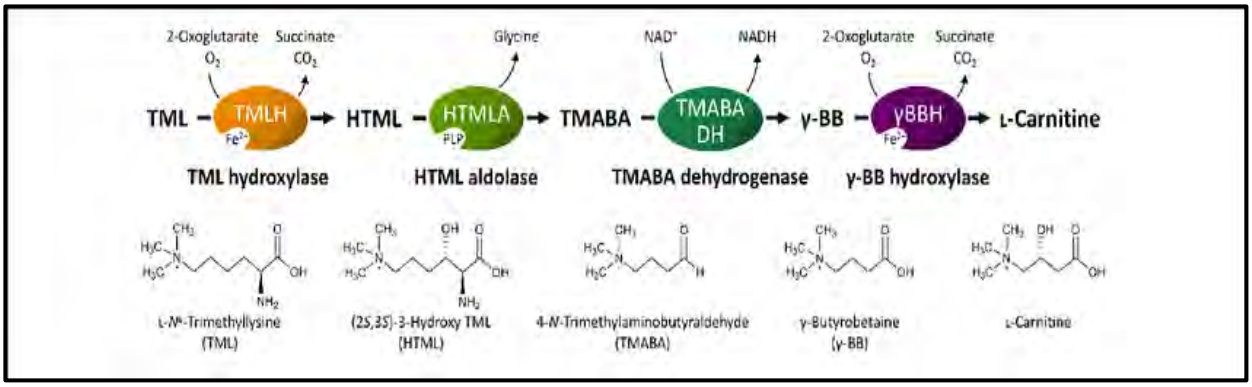

Figure 6.15: (A) Illustration of L-carnitine biosynthesis pathways (Strijbis et al., 2010).

L-carnitine is known to reduce sebum secretion, by transporting the sebum fatty acid chain inside the mitochondria and thus plays a role in energy metabolism (Foitzik *et al*., 2007). The L- carnitine isomer, also known as BT vitamin, is biologically active and acts as a co-factor in the process of fatty acid metabolism, it transports fatty acid chains to the inner mitochondria membrane. The activation of the long- chain to form acyl CoA occurs in the endoplasmic reticulum and the outer surface of the mitochondrial outer membrane (Figure 1.16). Acyl CoA moves from the outer membrane to the mitochondrial intermembrane space and is converted into

acylcarnitine by means of the malonyl-CoA-sensitive carnitine palmitoytransferase I (CPT-I). Carnitine-acylcarnitine translocase transports acylcarnitine from the intermembrane space into the mitochondrial inner membrane. Acylcarnitine binds to carnitine palmitoytransferase II (CPT-II) and breaks down the compound releasing carnitine and Acyl CoA in the mitochondrial inner membrane matrix. Acyl CoA then enters the β-oxidation pathway where the fatty acid is broken down to produce ATP (Figure 1.16) (Longo *et al*., 2016). This mechanism has been effective in the topical treatment of human sebocytes (Peirano *et al*., 2012). As mentioned previously, L-carnitine causes oxidization of free fatty acids, this again plays a positive role in the treatment of adeposis adematosa. Topical anti-cellulite creams use L-carnitine alongside methylxanthines with the objective of enhancing the process of lipolysis with the expectation of reducing the orange peel appearance (Rossi and Vergnanini, 2000; Jazzpollard, 2013). In a study conducted by Arslam *et al* (2003), the topical application of L-carnitine was found to be effective in the treatment of skin afflictions such as burn injuries and inflammation through the process of increasing the level of cellularity (Arslan *et al*., 2003).

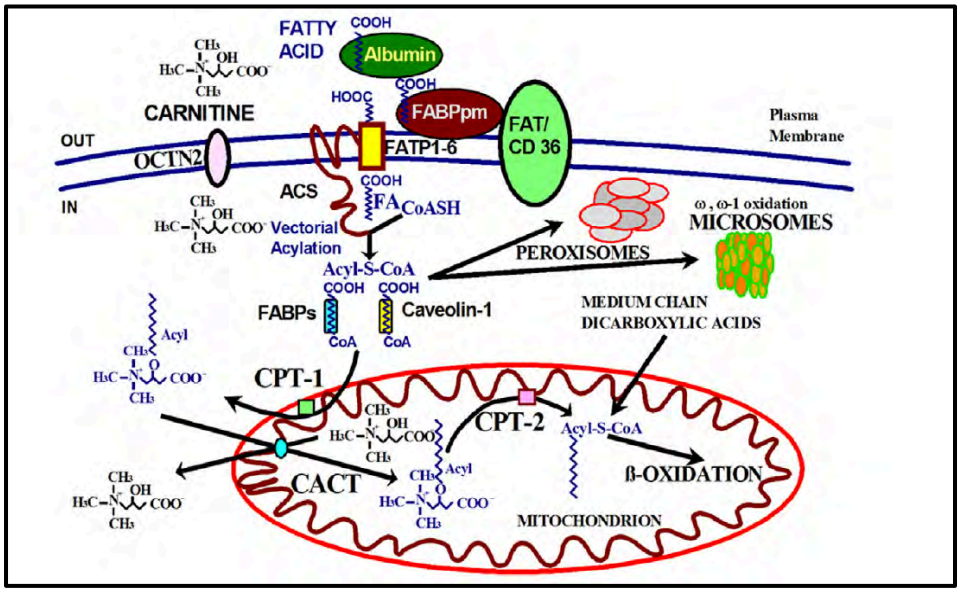

Figure 6.16: Illustration of the mitochondrial transport of fatty acid (Longo *et al*., 2016)

Fatty acids bound to albumin are transferred across the plasma membrane by the action of fatty acid transport proteins (FATP), fatty acid translocase (FAT/CD36), caveolins and plasma membrane fatty acid binding proteins (FABPpm). Inside the cell, fatty acids undergo vectorial acylation, a process catalysed by acyl-CoA synthases

(ACS), that traps them in the cytoplasm as acyl-CoA thioesters. The acyl-CoA thioesters are then conveyed through different metabolic pathways in mitochondria, peroxisomes and microsomes based on the cell energy status. ACS: acyl-CoA synthases; CACT: carnitine acyl carnitine translocase; CPT-1: carnitine palmitoyl transferase-1; CPT-2: carnitine palmitoyl transferase-2; FA: fatty acid; FABPpm: plasma membrane fatty acid binding proteins; FAT/CD36: fatty acid translocase; FATP: fatty acid transport proteins; OCTN2: organic cation transporter novel 2 (Longo et al., 2016).

1.4.3.1 Physiochemical properties of L-Carnitine

L- Carnitine also known as hydroxy-γ-N-trimethylaminobutyricacid, 3-hydroxy-4-N, N, N trimethylaminobutyrate (Figure 1.17) is a white crystalline hygroscopic powder. The molecule retains moisture and is hydrophilic. A synopsis of the physical and chemical properties of L-carnitine is provided in Table 1.4.

Table 6.4 Physicochemical properties of L-carnitine (L-carnitine, 2023).

Chemical names	hydroxy-γ-N-trimethylaminobutyricacid,3-hydroxy-4-N, N, N trimethylaminobutyrate
Molecular weight	161.201 g/mol
Appearance	Crystalline hygroscopic powder
Solubility	Soluble in water $1x10^6$ mg/l at 25°C Insoluble in acetone
pH	6.5-8.5
log P (Partition coefficient)	-5.48
Dissociation constant (pKa)	3.8 at 25°C
Melting point	197°C
Boiling point	287.5°C
Density	0.64 g/cm^3

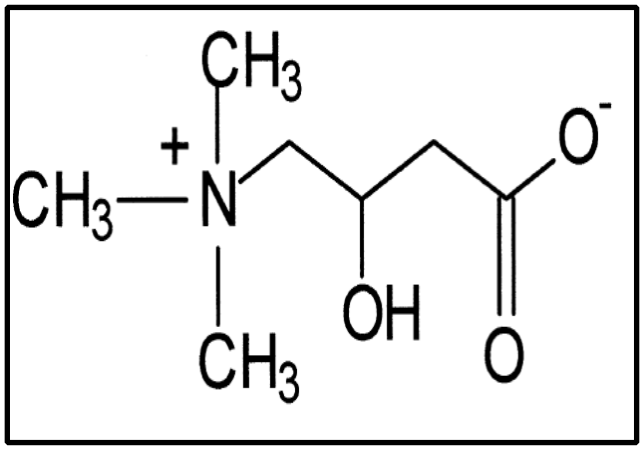

Figure 6.17: Structural formula of L-carnitine (Hoppel, 2003).

1.4.4 Coenzyme Q10 (Ubiquinone-10)

Coenzyme Q_{10} (CoQ_{10}) is a fat-soluble (lipophilic) anti-oxidant which is found naturally in the phospholipid bilayer membrane in every single cell in the body (Borekova *et al*., 2008). The compound enhances mitochondrial activity, maintains bioenergetic activities in human tissue, transport electrons to the mitochondrial membrane and enhances the immune system (Crane, 2001; Borekova *et al*., 2008; Lopez *et al*., 2010). With age and continuous exposure of the sun, there is a decrease in the level of CoQ_{10} in the epidermis. This promotes skin aging (Baumann, 2007; Huang *et al.*,2009). Topical application of CoQ_{10} replenishes the levels in the epidermis, which increases the synthesis of collagen and elastin, thus resulting in the reduction in the appearance of wrinkles (Huang, Lin and Fang, 2009; Knott *et al*., 2015). Topical application of CoQ_{10} with Vitamin E and Vitamin C protects the stability of the epidermis membrane from free radical oxidative damage and can regenerate the synthesis of other antioxidants such as tocopherol and ascorbate (Borekova *et al*., 2008).

1.4.4.1 Physiochemical properties of Coenzyme Q10

Coenzyme Q10 is chemically known as 2,3-dimethoxy-5-methyl-6-polisoprene parabenzoquinone and is a naturally occurring orange lipophilic molecule with a large molecular mass of 863.34 g/mol (Figure 1.18) (Borekova *et al*., 2008; Huang, Lin and Fang, 2009). CoQ_{10} is an isoprenoid, a hydrocarbon that is structurally based on

multiple isoprene units. Due to the fact that Co-enzyme has 10 isoprenoid units, it is therefore named Co-enzyme Q_{10}. The compound is found not to be stable at high temperatures of about 46°C where it starts to degrade. A synopsis of the physical and chemical properties of coenzyme Q10 is provided in Table 1.5 below.

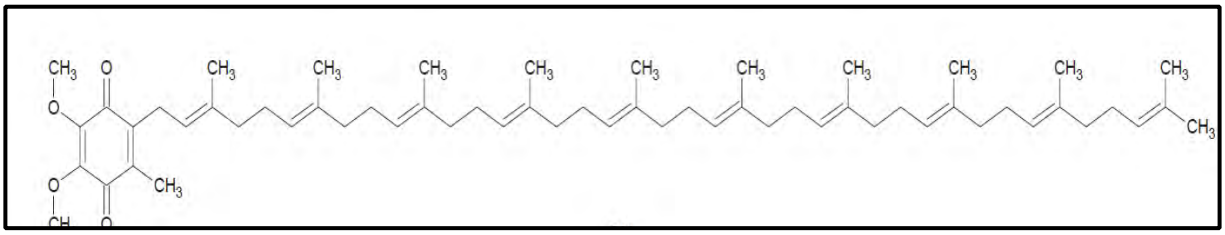

Figure 6.18: Structural formula of Co-enzyme Q10 (Parkinson et al., 2013).

Table 6.5 Physicochemical properties of Co-enzyme Q10 (Coenzyme Q10, 2023)

Chemical names	2[(2E,6E,10E,14E,18E,22E,26E,30E,34E)-3,7,11,15,19,23,27,31,35,39-Decamethyltetraconta-2,6,10,14,18,22,26,30,34,38-decaenyl]-5,6-dimethoxy-3-methylcyclohexa-2,5-diene-1,4-dione
Molecular weight	863,3 g/mol
Appearance	Solid
Solubility	Soluble in water 0.00019 g/l
log P (Partition coefficient)	10
Dissociation constant (pKa)	-4.7
Melting point	50-52°C
Boiling point	865.2±65°C
Density	0.96±0.1 g/cm^3

CoQ_{10} exists in three alternative redox states; the fully reduced ubiquinol form (CoQ10 H2), the radical semiquinone intermediate (CoQ10 H.), and the fully oxidized

ubiquinone form (CoQ10) (Raizner, 2019). A redox state refers to a reduction-oxidation reaction where reduction gains electrons or decreases the oxidation state by a molecule, atom or ion, while oxidation loses electrons or increases the oxidation state by a molecule, atom or ion (Parkinson *et al*., 2013). As illustrated in Figure 1.19, ubiquinone is in a fully oxidized form, which is reduced into semiquinone by the addition of two hydrogen atoms, semiquinone is a free radical form which is reduced into Ubiquinol (Figure 1.18) (Borekova *et al*., 2008). The redox reaction of CoQ_{10} plays a role in the production of ATP, the compound transfers electrons between complexes I (ubiquinone) and complex II (semiquinone). The oxidation of the fatty acids and amino acids moves the electron into complex III (ubiquinol) which results in the production of ATP as explained in Figure 1.19 (Parkinson *et al*., 2013).

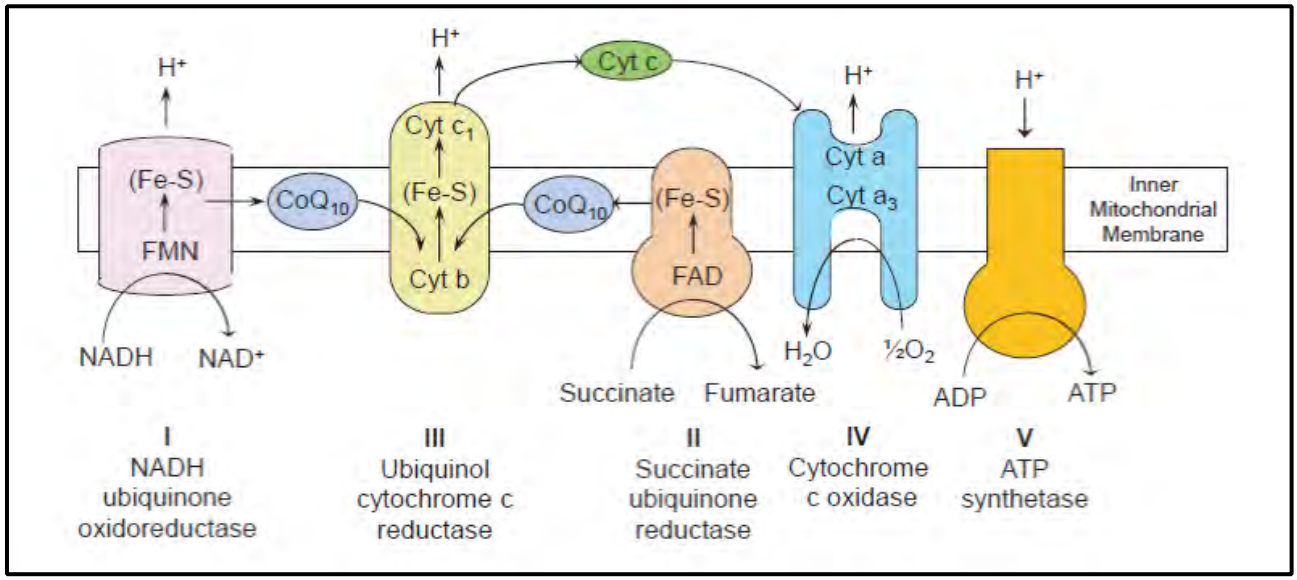

Figure 6.19: Mitochondrial Electron Transfer chain and the redox reaction of Co-enzyme Q10 (Parkinson et al., 2013).

1.5 Diffusion across skin

Penetration of drug molecules across the skin occurs initially through the stratum corneum. The movement of molecules across the skin occurs through the following two pathways: the trans-appendageal pathway and the trans-epidermal pathway (Mathur *et al*., 2010; N'Da, 2014).

1.5.1 Trans-appendageal pathway

The trans-appendageal pathway (Figure 1.20) consist of the sweat ducts, hair follicles and sebaceous glands which represents only 0.1% of the diffusion of molecules across the skin (Mathur *et al*., 2010; Ruela *et al*., 2016). This pathway which is also known as the shunt route, provides a pathway for molecules that have difficulty diffusing through the intact stratum corneum due to either a high molecular weight or being charged (polar molecules) (Mathur *et al*., 2010; N'Da, 2014). The follicular pathway refers to permeation of drug molecules through the hair follicle, this pathway has been found to be more advantageous to molecules that are hydrophilic and have a high molecular weight. Hair follicles, form invaginations within the skin surface reaching the dermis layer, thus increasing the surface area for penetration (Trauer *et al*., 2009).

1.5.2 Trans-epidermal pathway

As the drug is transported into the skin it is dissolved and released from the formulation. The drug molecule moves into the stratum corneum through the intercellular lipid matrix and moves into the dermis layer where it is absorbed through the capillary vessels (Ruela *et al*., 2016). The transepidermal pathway consists of two different routes, the intra cellular and the transcellular route (Figure 1.20).

1.5.2.1 Intracellular route

The intracellular route, which is also known as the transcellular pathway, provides a permeation route for molecules that move through the stratum corneum, the molecules thus diffuse through the cell (Figure 1.20) (Trauer *et al*., 2009). The molecule diffuses through the corneocytes, which are differentiated keratinocytes found in the stratum corneum. The keratinocytes of the stratum corneum is highly hydrophilic and therefore making it easy for hydrophilic drugs to diffuse through. However, the keratinocytes are enveloped in lipophilic layers that prevent hydrophilic drugs to diffuse through this pathway. This makes it hard for a drug molecule as it needs to diffuse through the lipophilic area followed by the hydrophilic area (Mathur *et al*., 2010). The first conception was that only hydrophilic drugs diffused through the intracellular route however it was found that the intracellular route is the predominant pathway for most drugs, this route accommodates both hydrophilic and lipophilic molecules. There is a

series of partitioning and diffusion stages between the hydrophilic corneocytes and lipid envelope surrounding the corneocytes (Haque and Talukder, 2018).

1.5.2.2 Intercellular route

The intercellular route, also known as the paracellular pathway, provides a pathway whereby substances diffuse across the epithelium layer by passing through the intercellular spaces between cells which consist of lipid lamellae (Trauer *et al*., 2009). This pathway allows for diffusion of lipophilic or non-polar molecules (Alkilani et al., 2015), and is the most predominant route of diffusion (Trauer *et al*., 2009).

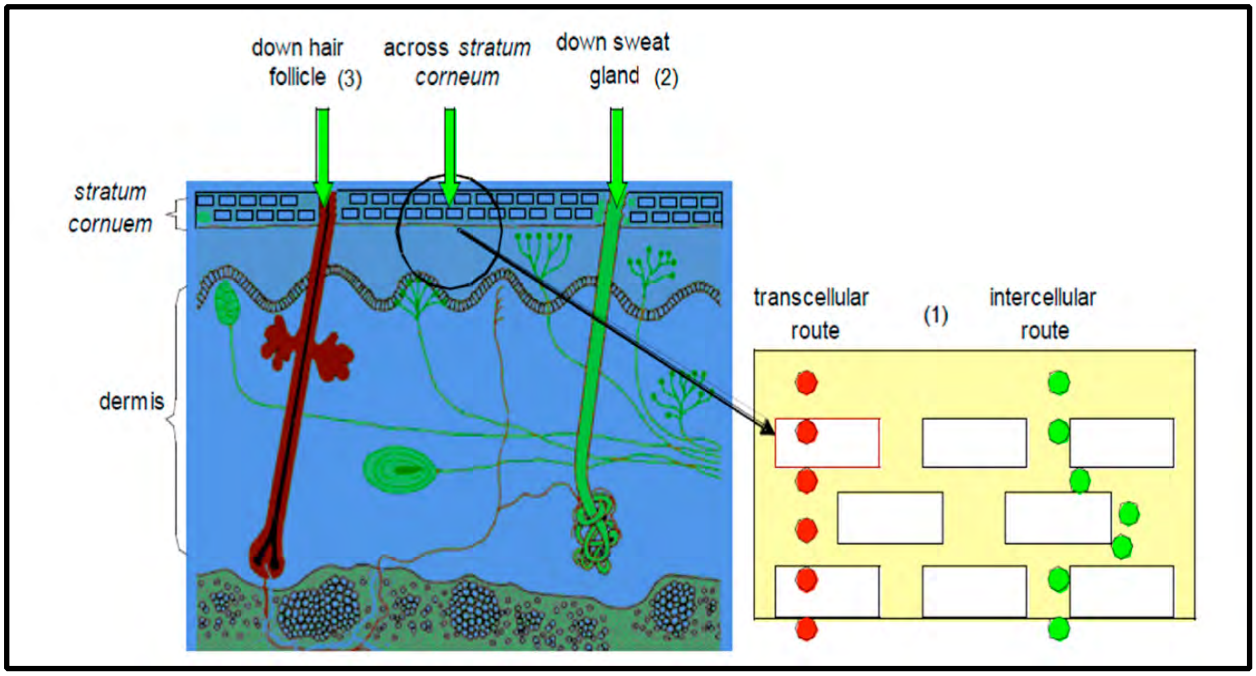

Figure 6.20:Drug permeation through the Trans-epidermal pathway (transcellular and intercellular route) and Trans-appendageal pathway (sweat ducts, sebaceous gland, and hair follicle) (N'Da, 2014).

1.5.3 Factors Affecting Transdermal Drug Delivery

1.5.3.1 Tissue Integrity

To optimize an efficient delivery of transdermal drug, it's important to study and understand the integrity of the tissue as this will influence the bioavailability of compounds that pass through specific skin compartments (Gorzelanny *et al*., 2020). They are various factors put in place to investigate the integrity of the tissue; these factors include the following (Jhawat *et al*., 2013; Gorzelanny *et al*., 2020):

- Trans-Epidermal water loss (TEWL) - This method measures barrier function/molecular flow, in other words it's the amount of water which passively evaporates through the skin into the external environment.

- Trans-Epithelial/trans-Endothelial electrical resistance (TEER) - This method measures the electrical resistance across tissue. This a very sensitive and reliable way to confirm the integrity and permeability of tissue (Srinivasan *et al*., 2015).

- Physiological and pathological condition of the skin – Physiological and pathological conditions may alter the permeation of the drug through the skin.

- Regional Site of skin- It's important to understand the skin's anatomical features such as hair follicle, thickness of stratum corneum or sweat glands as these will affect the percutaneous absorption.

1.5.3.2 Physiochemical properties of drug

Other than understanding the integrity of the skin to optimize drug delivery, it is equally important to study the drug molecule itself as they are factors that might impede in the delivery of the molecule. These factors include the following (Jhawat *et al*., 2013):

- Size of the drug molecule and molecular weight - The greater the size or molecular weight of the drug molecule the lower the absorption rate. Kadam and colleagues (2014) stated that the molecular weight of a drug should lie between 100-500 Dalton for transdermal delivery to occur.

- Partition coefficient and solubility – This determines the solubility or diffusion of drug in a lipid or aqueous system. Drugs which consist of both lipid and water solubility have a greater rate of absorption as the skin consist of a lipid bilayer.
- Drug concentration – Drugs will move according to the concentration gradient - from a high concentration to a low concentration. Therefore, the higher the concentration of the drug, the greater the absorption rate through the skin.
- pH conditions- This plays a role in determining the extend of the absorption rate, where unionized drugs have a better absorption rate than ions or ionic drugs.

1.5.4 Kinetics of Drug Absorption

As mentioned in section 1.5.3.2, a drug molecule adopts a passive diffusion which means that the drug will move from a high concentration (being on the skin surface) to a low concentration (that being inside the skin) (Jhawat *et al*., 2013). The rate of drug absorption by passive diffusion is controlled by Fick's law of diffusion seen in Equation 1 below (Zhou *et al*., 2015):

$$J = D \frac{dC}{dx} \quad (1)$$

J: This refers to the flux, the number of molecules flowing through a cross-sectional are per unit time.
D: This refers to the diffusion coefficient of penetrant (diffusant) in cm^2/sec, which is assumed to be constant.
dC: This refers to the concentration in g/cm^3.
dx: This refers to the distance in centimetre of movement perpendicular to the surface of the barrier.

1.6 Models for human skin

In vitro skin penetration studies are essential for the development of transdermal drugs. Due to the difficulty in obtaining human skin, many animal and tissue culture models are used effectively to predict the *in vivo* human penetration/permeation of topically applied chemicals (Schmook *et al*., 2001; Todo, 2017). Characteristics such

as thickness, lipid content, hair follicle density and enzyme activity are attributes reviewed when choosing a good animal model to represent human skin percutaneous absorption (Todo., 2017).

1.6.1 Porcine skin

Porcine skin is the most frequent model used for *in vitro* permeation studies due to the anatomical similarity to human skin (Schmook *et al*., 2001; Herron, 2010). The porcine skin epithelial layer is structurally similar to human epidermal thickness and the dermal-epidermal thickness ratios are also similar. Pigs and humans have similar hair follicle and blood vessel patterns in the skin. Porcine skin consists of dermal collagen and elastic content which is like humans. Furthermore, studies have shown that porcine skin have similar physical and molecular responses to various growth factors than human skin (Herron,2010).

1.6.2 Rat skin

Rodents skin has been found to be freely available and inexpensive, and usually used in permeation and regulatory toxicity studies. However, the rodent skin is found to have a higher permeation rate compared to the human skin. This can be explained by the following: in rodent skin the epidermis is found to be thinner, the appendage number is higher, intercellular lipid composition of the stratum corneum is different and the corneocyte surface is lower (Jung and Maibach, 2015).

1.6.3 Rabbit skin

Rabbit skin is generally more permeable than human skin. In a study conducted by Nicoli and colleagues (2008) a comparison was done between skin of a rabbit ear and skin of pig ear. The result showed that the rabbit ear skin had a thicker stratum corneum, increase amount of lipid found in stratum corneum, high hair density and is less hydrophilic than pig ear skin (Jung and Maibach, 2014). The stratum corneum is primarily known as the skin barrier, the thickness of the stratum corneum gives an indication on the number of cell layers which in turn determines the skin permeation flux. The lipid content of the stratum corneum gives an indication of the lipophilicity of the barrier which in turn affects the diffusion of topically applied drugs (Todo, 2017).

Studies have shown that hair follicles plays a role in drug permeation, as they increase the absorption of the substance through the appendageal pathway and into the blood capillary (Mohd *et al*.,2016).

1.6.4 3D Cultured human skin models

Various pathophysiological studies have been conducting using two-dimensional (2D) cell culture, also known as the standard laboratory practice. In this practice, cells are grown in a monolayer on a solid flat surface. The cells are kept alive using specific conditions such as: supplying of nutrients (amino acids, carbohydrates, vitamins, gases (O_2 and CO_2)), and regulation physio-chemical environment (pH, osmotic pressure, temperature). The 2D cell culture system has provided a key understanding in molecular signalling, cellular morphology, and drug discovery. However, there are limitations that could impact on the cellular responses from morphology, proliferation, migration, and differentiation to biochemical signalling. These limitations include mechanical forces, spatial orientation, physiological oxygen, nutrient and signalling gradient which are associated with a three dimensional (3D) *in vivo* environment (Randall *et al*., 2018)

The 3D model is a highly physiological three-dimensional cellular system which consist of a stratified epithelium derived from human skin biopsy (Szymański *et al*., 2020). The problem with producing a 3D human skin model is the limited tissue availability, donor variability, structural differences, and ethical consideration (Randall *et al*., 2018; Szymański *et al*., 2020). The cells grown in a 3D system replicate the physiological process and complexity found in the *in vivo* microenvironment. For this reason, the 3D system is used as an alternative for drug and cosmetic evaluation (Idrees *et al*., 2021).

1.7 Methods used for *in vitro* diffusion of chemicals across skin

Transdermal drug delivery has been an alternative way to diffuse a drug into the systemic circulation system as compared to conventional oral therapy or injections (Bartosova and Bajgar, 2012). Pharmaceutical and cosmetic industries have used this non-invasive *in vitro* diffusion method, which in turn has evolved research methodology (Ng *et al.*, 2010).

1.7.1 Franz Cells

Franz cells are used to measure the dermal absorption through *in vitro* diffusion (Salamanca *et al*., 2018). The Franz cell apparatus (Figure 1.21) consist of a versatile blown glass diffusion cell which places the membrane horizontally and is used in the development of transdermal products having a donor chamber open to the air and a stirred receptor chamber (Permegear Catalog, 2018).

(A)



(B)

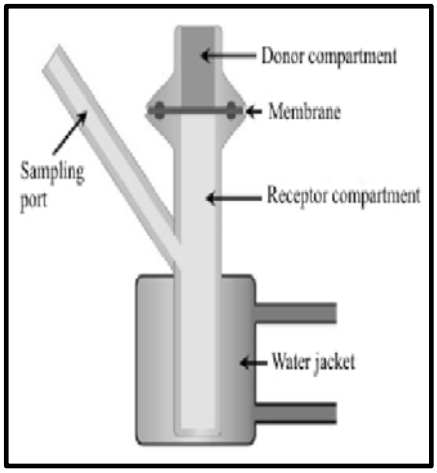

Figure 6.21: (a) Illustration of Franz Cell (b) Schematic illustration of Franz Cell (Bartosova and Bajgar, 2012).

1.7.2 Static cell (Side-bi- Side)

The side-bi-side cell consist of two cells placed adjacent to each other. One cell compartment receives the sample receptor fluid while the other cell compartment consists of the donor compound. The temperature is controlled by means of two protruding openings which allows the heat to circulate. Figure 1.22 shows a schematic illustration of the side-bi-side static cell apparatus. The aim of this apparatus is to evaluate the compound uptake into a membrane and determine the rate at which the compound diffuses through the membrane as well as the concentration found in the receptor cell compartment (PermeGear, 2018).

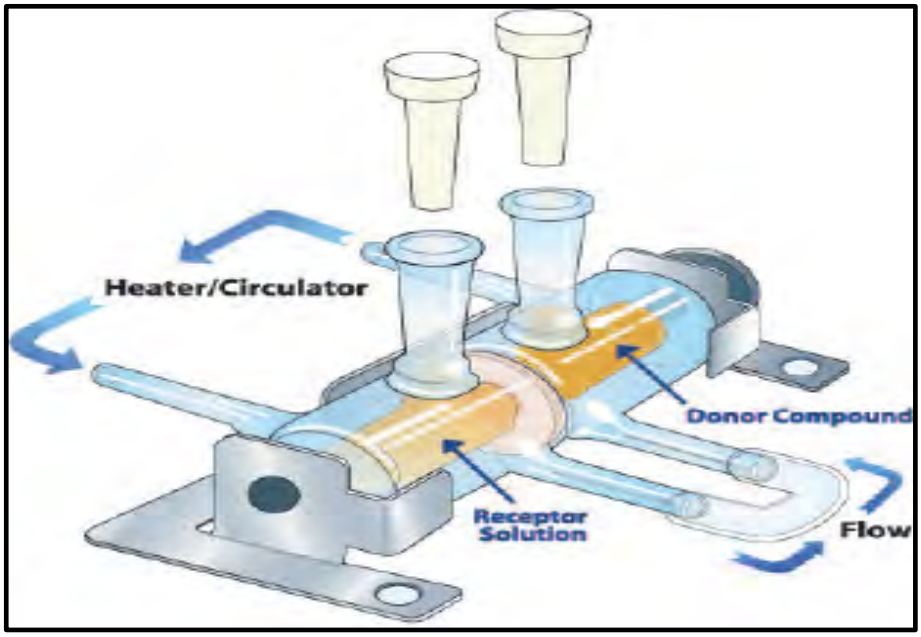

Figure 6.22: Schematic illustration of the Side-bi-side static cell apparatus (Permegear, 2018).

1.7.3 Continuous Flow cell or Flow-through-cell

The in-line continuous flow or flow-through cell (Figure 1.23) consists of two cell compartments. A fixed volume amount is injected in each receptor compartment. The apparatus consists of an automated machine that controls the temperature. In-line cells have a continuous flow which causes turbulence in the receptor chambers and stimulates stirring. The aim of this type of apparatus is to mimic the flow rate *in vivo*, and to evaluate compound uptake into the membrane, as well finite or infinite dose of permeation can be done. Furthermore, the rate at which the compound crosses the membrane (flux) is determined under continuous flow. The concentration in the receptor as well as the rate of clearance (flow rate) can be determined with the use of the apparatus (Fotaki., 2011; Permegear.,2018).

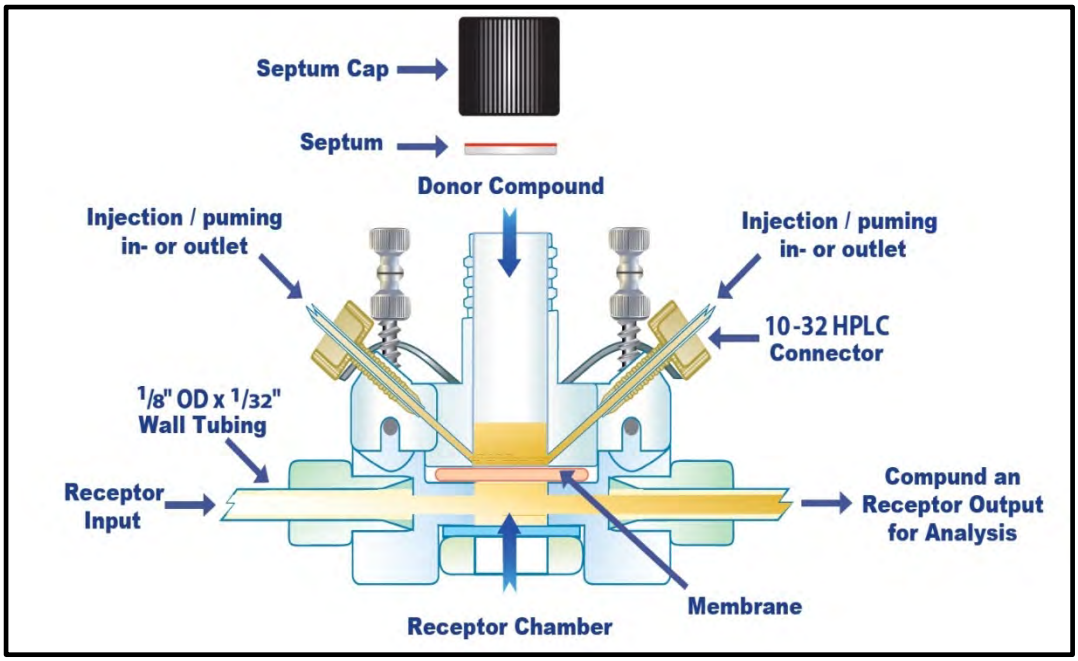

Figure 6.23: Schematic illustration of the Continuous flow or flow-through cell (Permegear, 2018).

1.8 Aims and objectives of the study

Aim

This study is intended to determine the effectiveness of penetration of various active compounds (Caffeine, Theophylline, Retinol, Co-enzyme Q_{10} and L-carnitine) in different formulations (Liquid, Gel and Cream) into and across porcine skin.

Objectives

To validate the HPLC method analysis for each active compound: Caffeine, Theophylline, Retinol, Co-enzyme Q_{10} and L-carnitine.

To compare the *in vitro* diffusion kinetic behavior of each active compound, alone and in combination, within three different formulations (liquid, gel and cream) across porcine skin, by using an ILC-07 (in-line flow cells) automated diffusion system over a 4-hour and/or 24-hour time period.

To compare the accumulation of each active compound, alone and in combination, within three different formulations (liquid, gel and cream) within porcine skin after the final established diffusion time period for each compound.

Chapter 2: Experimental Methods and Materials

2.1 High Performance Liquid Chromatography

2.1.1 Introduction

HPLC is seen as a multi-facet methodology which carries out an important and integral analytical function within the pharmaceutical industry (Kazakevich and Lubrutto, 2007: 77). HPLC has been known to be effective in detecting and estimating the quantity of a compound in a medium as well as separating the compound in a mixture. The HPLC system is made up of the mobile phase, pump, injector, column, and detector (Figure 2.1) (Dewe *et al*., 2004).

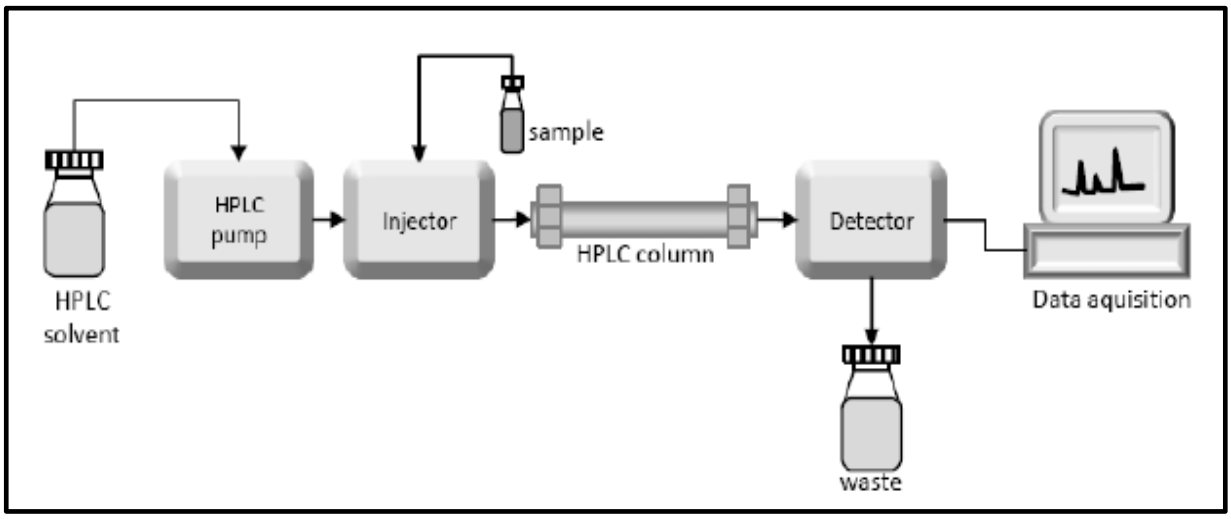

Figure 7.1: Schematic diagram of HPLC System (Czaplicki 2013:102).

Solvent reservoir: HPLC solvent storage for continuous operation of the system
Pump: The pump in the system is used to generate a specific flow rate for the mobile phase, generally this is recorded as millimeters per minute.
Injector: The analytes are introduced by the injector into a stream of the mobile phase as the sample enters the mobile phase it is carried out to the HPLC column.
Column: Also known as the centre of the HPLC system as it allows separation of and analysis of components in a mixture. The column acts as the position of contact between the mobile phase and stationary phase.

Detector: A detector registers specific physical properties of the column effluent. Commonly used, is the UV (wavelength) detector, this acts as a means of detecting compounds.
Data acquisition and control system: The HPLC-instrument is controlled by a computer-based system (Kazakevich and Lubrutto, 2007: 83).

The stationary phase is the part of the chromatographic system through which the mobile phase containing the injected samples flows through and is retained. In a HPLC machine, the separation and purification occur due to the relative affinities of the molecules for the stationary phase and the mobile phase (due to their polarity). In the case of a reverse phase liquid chromatography, molecules are bound to the hydrophobic matrix in an aqueous buffer (polar) and eluted from the matrix using a gradient of organic solvent (non-polar) (Ojha *et al*., 2013).

2.1.2 Materials

All pure standards were obtained from Sigma-Aldrich Co LLC (St Louis, Mo, USA) or Merck Co. LLC (NJ, USA). These pure standards included the following: Caffeine Anhydrous, Theophylline Anhydrous, Retinol, L-Carnitine Hydrochloride, Co-enzyme Q_{10}. Similarly, to the pure standards, analytical grade laboratory chemicals were purchased from Sigma-Aldrich Co LLC (St Louis, Mo, USA) or Merck Co. LLC (NJ, USA). These analytical grade laboratory chemicals included HPLC grade methanol and 2-propanol (HiPerSolv CROMANORM Methanol and 2-propanol.)

- propylene glycol
- Hydroxypropyl methyl cellulose (HPMC FAM)
- Beeswax- bleached
- Olive oil – Tested according to Ph.EUR

2.1.3 Chromatographic apparatus

2.1.3.1 Analytical instrument

Analyses were performed using the Perkin-Elmer Flexar HPLC system (Figure 2.2) containing a Flexar degasser, a binary pump, an autosampler, a column oven, a UV detector and Perkin-Elmer Chromera® software.

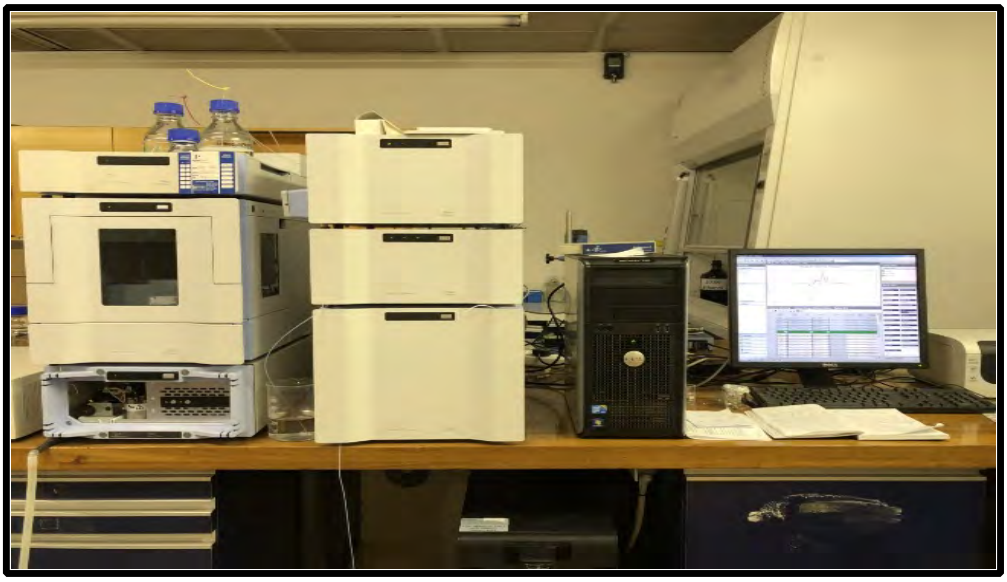

Figure 7.2: Perkin Elmer HPLC System.

Photograph illustrating an actual HPLC system in the laboratory. The photo displays the mobile phase reservoir as well as the different compartments which harbours the HPLC detector, pump, manual injector, and column oven. The picture also shows a computer which is responsible for data integration.

2.1.3.2 Column

A Phenomenex Kinetex column (Reverse Phase -Column 18 : 5µm, 150 mm x 4.6mm) containing a reverse phase – column 18 Security Guard Ultra cartridge (4.6 mm) were purchased from Separations (Pty) Ltd and used for the HPLC analyses.

2.1.4 Preparation of mobile phases

2.1.4.1 Water used for HPLC mobile phases

Milli-Q water was filtered through a 0.45 µm filter using a Millipore all-glass filtration unit (Merck) (Figure 2.2). The filtration removed water impurities prior to usage through the HLPC system.

Sodium azide is an inorganic compound used in filtered water to reduce the bacteria growth. A stock solution of 2% (w/v) was prepared and then diluted X100 to make a concentration of 0.02% (w/v) by adding 10 ml from the 2% (w/v) concentration to 990 ml of filtered water.

2.1.4.2 Preparation of Mobile phases

2.1.4.2.1 Caffeine

The mobile phase consisted of 400ml (A) of HPLC grade methanol and 600ml (B) of filtered water (A: B 40:60) (Naveen *et al*., 2018).

2.1.4.2.2 Theophylline

The mobile phase consisted of 400ml (A) of HPLC grade methanol and 600ml (B) of filtered water (A: B 40:60) (Charehsaz *et al*., 2014).

2.1.4.2.3 Retinol

The mobile phase consisted of 950 ml (A) of HPLC grade methanol and 50ml (B) of filtered water (A: B 95:5) (Kaur *et al*., 2004).

2.1.4.2.4 L-carnitine

The initial L- carnitine buffer consisted of 0.1 M ammonium acetate (Cao *et al*., 2007). Ammonium acetate ($C_2H_7NO_2$; 77.083 g/mol; 7.7083g) was added to 700ml of filtered water and dissolved using a magnetic stirrer. Ammonium acetate solution was adjusted with acetic acid to a pH of 3.5 using a pH meter. Once the correct pH was

reached, 300ml of acetonitrile was added until a final volume of 1000 ml was reached. The buffer was found to be unsuitable as it was found to block the column. In this case, phosphoric buffer was used instead (Khoshkam and Afshar, 2014). The phosphoric acid buffer (50 mM, pH 3.0) was prepared by dissolving $Na_2HPO_4 \cdot 12H_2O$ (17.907 g) into 1000 ml filtered water. Sodium Heptane sulfonate ($C_7H_{17}NaO_4S$; 0.56 g; 202.25 g/mol) was added to the buffer and then the pH was adjusted carefully using a pH meter. The pH of the solution was adjusted to 3.0 by diluting phosphoric acid in water until a pH 3 has been achieved. Sodium heptane sulfonate is an ion pairing reagent, it was added to the L-carnitine mobile phase to form ionic pairs with L-carnitine. This caused the L-carnitine to become more hydrophobic thus resulting in greater interaction with the Reverse Phase stationary phase and a longer retention time. Ion pairing agents are usually added to ionic samples, as they move out of the stationary phase without proper observation (Phechkrajang, 2010). Once the mixture was prepared, the final mobile phase consisted of 99% sodium phosphate buffer (pH 3): 1% HPLC grade methanol.

2.1.4.2.5 Coenzyme Q10

Coenzyme Q_{10} initial mobile phase consisted of a mixture of HPLC grade methanol: water (98:2 v/v) (Contin *et al*., 2011). The isocratic mobile phase proved unsuitable for the detection of coenzyme Q_{10}. The final mobile phase consisted of 400ml of HPLC grade methanol and 600ml of HPLC grade 2-propanol.

2.1.5 Chromatographic Conditions

The HPLC conditions for caffeine, theophylline, retinol, L-carnitine, and coenzyme Q_{10} were used as described Table 2.1 below:

Table 7.1 Chromatographic conditions of caffeine, theophylline, retinol, L-carnitine, and coenzyme Q10.

	Caffeine	Theophylline	Retinol	L-carnitine	Coenzyme Q_{10}
Flow rate	1.0 ml/min	1.0 ml/min	1.0 ml/min	1.0 ml/min	1.0 ml/min
Injection Volume	20µl	20µl	20µl	20µl	20µl
Detection (nm)	272	272	325	225	275
Run Time (min)	3.0	3.0	3.0	3.5	3.5
Temperature (°C)	20	20	20	40	25

2.2 Preparation of Standards

2.2.1. Caffeine stock solution

Caffeine stock solution was prepared by accurately weighing 5.0 mg caffeine in a 15 ml centrifuge tube and adding 5 ml caffeine mobile phase as mentioned in section 2.1.4.2. The solution was vortexed thoroughly to solubilize the caffeine after which the stock solution was filtered through a 0.45 µm syringe filter and stored at 4°C. A 2 ml working solution was prepared for the different points in the calibration curve. Those

solutions were obtained mixing the necessary reagent volume to attain different concentrations; 5, 10, 25, 30, 100, 150 and 200 µg/ml.

2.2.2 Theophylline stock solution

The stock solution was prepared by accurately weighing 5.0 mg Theophylline in a 15 ml centrifuge tube and adding 5 ml theophylline mobile phase as mentioned in section 2.1.4.2. The solution was vortexed thoroughly to solubilize the Theophylline where after the stock solution was filtered through a 0.45 µm syringe filter and stored at 4°C. A 2 ml working solution was prepared for the different points in the calibration curve. Those solutions were obtained mixing the necessary reagent volume to attain different concentrations; 1, 2,5,10,20,25, and 30 µg/ml.

2.2.3 Retinol stock solution

The stock solution was prepared by accurately weighing 3.0 mg retinol in a 15 ml centrifuge tube and adding 3 ml Retinol mobile phase as mentioned in section 2.1.4.2. The solution was vortexed thoroughly to solubilize the Retinol where after the stock solution was filtered through a 0.45 µm syringe filter. The stock solution was wrapped in foil, to avoid any degradation as it is sensitive to light and stored at 4°C. A 2 ml working solution was prepared for the different points in the calibration curve. Those solutions were obtained mixing the necessary reagent volume to attain different concentrations; 0.5, 2, 5, 10,40 and 100 µg/ml.

2.2.4 L-carnitine stock solution

The stock solution was prepared by accurately weighing 5.0 mg L-carnitine in a 15 ml centrifuge tube and adding 5 ml L-carnitine mobile phase as mentioned in section 2.1.4.2. The solution was vortexed thoroughly to solubilize the L-carnitine where after the stock solution was filtered through a 0.45 µm syringe filter and stored at 4°C. A 2 ml working solution was prepared for the different points in the calibration curve. Those solutions were obtained mixing the necessary reagent volume to attain different concentrations; 100, 200, 300, 400, 500 and 700 µg/ml.

2.2.5 Coenzyme Q10 stock solution

The stock solution was prepared by accurately weighing 10 mg Coenzyme Q_{10} in a 15 ml centrifuge tube and adding 10 ml Coenzyme Q_{10} mobile phase as mentioned in section 2.1.4.2. The solution was vortexed thoroughly to solubilize the Coenzyme Q_{10} where after the stock solution was filtered through a 0.45 µm syringe filter. The compound was handled at low light as it is light sensitive; it was then stored at 4°C in foil-covered container. A 2 ml working solution was prepared for the different points in the calibration curve. Those solutions were obtained mixing the necessary reagent volume to attain different concentrations; 0.1, 0.5, 1, 5, 10 and 50 µg/ml.

2.3. Preparation of phosphate buffered

The phosphate buffer saline (PBS), pH 7.4 was prepared by weighing out 16 g of sodium chloride (NaCl), 0.4 g of potassium chloride (KCl), 2.88 g of sodium phosphate (Na_2HPO_4), 0.48 g of potassium dihydrogen phosphate (KH_2PO_4) and added into 1600 ml of double distilled water (dd$H_2$0). Once the chemicals were dissolved, the pH was adjusted to 7.4 by means of Hydrochloric acid (HCL) and Sodium hydroxide solution. Once the pH was adjusted, ddH_2O was added to a total volume of 2000 ml.

2.4. HPLC Method Validation

2.4.1 Linearity

Linearity was expressed in terms of the determination coefficient (R^2) from plots of the integrated peak areas versus concentration of the standards, the data was best described by the linear equation: y= mx+c (Campas-Baypoli *et al*., 2009). Linearity was evaluated for each standard compound in the following ranges: Caffeine 5 µg/ml – 200 µg/ml, Theophylline: 1 µg/ml – 30 µg/ml, Retinol: 0.5 µg/ml – 100 µg/ml, L-carnitine: 100 µg/ml – 1000 µg/ml and Coenzyme Q_{10}: 0.1 µg/ml – 100 µg/ml. Standard curves were constructed for each standard compound using excel software, peak area was plotted against concentration (µg/ml). These samples were injected in triplicate into the HPLC system.

2.4.2 Limit of detection and limit of quantification

Limit of detection (LOD) and quantification (LOQ) are incorporated as analytical method development and validation parameters which aid with the process of drug synthesis. LOD refers to the lowest concentration of the analyte that is detected by an assay, but not necessarily quantified. LOQ refers to the lowest concentration of an analyte that can be quantified with a linear response (Benal; 2014).

Calculations of the LOD and LOQ were performed using Excel as follows (Apostol *et al*., 2009):

From the data analysis toolbar and using the linear regression formula the standard error (SE) of the intercept was calculated. The standard deviation (SD) of the intercept was calculated using the following equations (Apostol *et al*., 2009).

SD of intercept = SE intercept x Sqrt(N) (2)

Where N= number of concentrations tested.

LOD = 3.3 x (SD of intercept/slope of linear regression curve) (3)

LOQ = 10 x (SD of intercept/slope of linear regression curve). (4)

2.4.3 Precision

Precision is a measure of closeness of the analytical results obtained from a series of replicate measurements of the same measure under the conditions of the method (Peters *et al*., 2007).

2.4.3.1 Intra-day precision

Intra-day precision was determined by analysing samples on the same day at different times of the day; each sequence was repeated 3 times. The following concentrations were evaluated: Caffeine: 20 µg/ml, Theophylline: 10 µg/ml, Retinol: 40 µg/ml, Coenzyme Q_{10}: 100 µg/ml and L-carnitine: 500 µg/ml.

These samples were injected in the morning at 09h00 and in the afternoon at 14h00. The results were expressed as means, standard deviation and relative standard deviation (%RSD). This validation parameter was a way to measure variability, relative standard deviation should have been less or equal to 2% (Parsons *et al*., 2009; Reddy and Chevela., 2015)

2.4.3.2 Inter-day precision

Inter-day precision was determined by analysing samples on different days; each sequence was repeated 3 times. The following concentrations were evaluated:
Caffeine: 20 µg/ml, Theophylline: 10 µg/ml, Retinol: 40 µg/ml, Coenzyme Q_{10}: 100 µg/ml and L-carnitine: 500 µg/ml.

These samples were injected on two different days. The results were expressed as means, standard deviation and relative standard deviation (%RSD), RSD should have been less or equal to 2%. (Reddy and Chevela., 2015).

2.4.4 Accuracy

According to a study conducted by Menditto *et al*., (2007) accuracy can be defined as the closeness of agreement between a quantity value obtained by measurement and the true value of the measurement. This is a crucial measurement which determines the level of confidence of the result obtained, this allows to express the effectiveness quality, and safety of the compound. Three concentration levels of each compound were chosen to test, the samples were prepared as mentioned in section 2.2. HPLC analysis of each concentration was repeated six times to provide repeatability (Menditto *et al*., 2007).

1. Caffeine: 5 µg/ml, 30 µg/ml and 150 µg/ml
2. Theophylline: 2 µg/ml, 4 µg/ml and 10 µg/ml
3. Retinol: 2 µg/ml, 10 µg/ml, 100 µg/ml
4. Co-enzyme Q_{10}: 5 µg/ml, 10 µg/ml and 100 µg/ml
5. L-carnitine: 100 µg/ml, 400 µg/ml and 700 µg/ml

Results were expressed as percentage recovery (%), this was a validation parameter which showed that the expected value was measured accurately (Peters *et al*., 2007). Values for recovery were desired to be as close to 100% (90 – 110% for non-regulated products (Karnes *et al*., 1991).

2.4.5 Ruggedness

Ruggedness is defined as the degree of reproducibility of measurements required in specific laboratory conditions. The aim of this test is to evaluate the stability of the active ingredients by obtaining results using changing laboratory conditions minimally (Pereira *et al*., 2021). All 5 active compounds were tested under the following conditions and all results expressed as means and standard deviations.

2.4.5.1 Mobile phase variation

The % HPLC grade methanol was varied as follows:

- Caffeine: 39.5%, 40.0% and 40.5% (Table 3.21)
- Theophylline: 39.0%, 40.0% and 41.0% (Table 3.22)
- Retinol: 94.5%, 95%, 95.5% (Table 3.23)
- L-Carnitine: 99.5%, 99.0% (Table 3.24)
- Coenzyme Q_{10}: 39.5%, 40.0% and 40.5% (Table 3.25)

2.4.5.2 Flow rate

The flow rate was varied as follows: 0.95 ml/min, 1 ml/min and 1.1 ml/min.

2.4.5.3 Temperature variation

The column temperature was changed in the following manner for Caffeine, Theophylline and Retinol: 19.5°C, 20°C and 20.5°C. For Co-enzyme Q_{10} the column temperature was changed to 24.5°C, 25°C and 25.5°C. L-carnitine, the column temperature was changed to 39.5°, 40.0°C and 40.5°C.

2.4.6 Stability

The stability of the drug solution was determined by choosing 3 different concentrations of all 5 active compounds, which were further kept at room temperature for a week and then analyzed using each active ingredients HPLC conditions mentioned in section 2.1.5.

2.5 In vitro Diffusion Studies

2.5.1 Introduction

In the recent decades, there has been an increase in the number of dermal formulations utilised for the skin. Topical and transdermal formulations carry drugs or active ingredients which diffuse through the skin layers. The benefits of dermal formulation penetrating through the skin are as follows: dermal formulations are non-invasive treatment, gastrointestinal tract is protected, and the first pass metabolism of the liver is completely avoided (Zsikó *et al*., 2019). In a review conducted by Zsikó and colleagues, various methods which mimic in vivo conditions of skin penetration have been described. These methods include:

- The use of *in vitro* diffusion studies using diffusion cells. This tool consists of a chamber for active compound application. The active compound diffuses through the chamber into an acceptor chamber (Zsikó *et al*., 2019).
-
- Skin-PAMPA (Parallel Artificial Membrane Permeability Assay). This method consists of the usage of a 96-well plate-based method which determines the rapid passive membrane permeability of molecules (Sinkó *et al*.,2012; Zsikó *et al*., 2019)

- Tape stripping is a minimal invasive method that tests the penetration of topically applied formulations through the stratum corneum. An adhesive strip tape is used to remove the stratum corneum, which is quantitively analysed using HPLC (Zsikó *et al*., 2019).

- Two-photon microscopy

- Confocal laser scanning microscopy

- Confocal Raman microscopy

Diffusion cells can be broken down into two classes: static diffusion cells and flow-through cells. Studies have shown that the use of in-line flow-through diffusion cells is more suitable to simulate the *in vitro* drug diffusion process (Cordoba-Diaz *et al*., 2000).

2.5.2 Preparation of formulations

2.5.2.1 Liquid

The preparation of the liquid formulation was performed according to Moser *et al* (2001). Caffeine (0.25 g), Theophylline (0.2 g), Retinol (0.03 g), L-carnitine (0.2 g) and Co-enzyme Q_{10} (0.5 g) was respectively added to 3 g of 70% (v/v) ethanol and 6.75 g propylene glycol and MilliQ water added to a final volume of 10 ml. Both Ethanol and propylene glycol were added to the formulation to enhance penetration of the active compound across the skin barriers (Haque and Talukder, 2018). Each solution was then sonicated for 5 minutes at room temperature (Figure 2.3). Each liquid formulation was placed in a dark container and stored at 4°C until use.



Figure 7.3: Ultrasonic Sonicator (Janke & Kunkel-Ultra-Turrax).

Image showing an ultrasonic emulsification used in this research. The model used in this study was the Janke & Kunkel- Ultra- Turrax.

2.5.2.2 Gel

The preparation of Hydroxypropyl methyl cellulose (HPMC FAM) gel was performed according to Ghzaoui *et al* (2001). Caffeine (0.25 g), Theophylline (0.2 g), Retinol (0.03 g), L-carnitine (0.2 g) or Co-enzyme Q_{10} (0.5 g) was added to 0.3 g of HPMC FAM and 1.5 g propylene glycol and Milli Q water added to a final volume of 10ml. HPMC FAM was added to the formulation to form a gel. Each gel formulation was then sonicated for 5 minutes and placed in a dark container and stored at 4°C until use.

2.5.2.3 Cream

The preparation of the cream formulation was performed according to Sonia *et al* (2017). Bleached beeswax (0.8 g) was melted in a water bath at 70°C. Once the beeswax was completely melted, 6 ml of Olive oil was added and vigorously mixed with the beeswax. While still vigorously mixing the formulation, 4ml of MilliQ water containing either caffeine (0.25 g), theophylline (0.2 g) or L-carnitine (0.2g) was added to the formulation. The formulation was left to set for an hour before it was placed in a dark container and stored at 4°C until use. Retinol (0.03 g) or Co-enzyme Q_{10} (0.5 g) were added to the olive oil prior to mixing with the melted beeswax.

2.5.3 Combination Studies

Combination of active compounds within the different formulations were also used for the *in vitro* permeability studies. The aim of testing combination compounds was to study the effect of possible penetration enhancement or inhibition when compounds are combined. The combination studies included the following:

- Caffeine (0.25 g) + Retinol (0.03 g)
- Caffeine (0.25 g) + L- carnitine (0.2 g)
- Caffeine (0.25 g) + Co-enzyme q_{10} (0.05 g)
- Theophylline (0.2 g) + Retinol (0.03 g)

- Theophylline (0.2 g) + L-carnitine (0.2 g)
- Theophylline (0.2 g) + Co-enzyme q_{10} (0.05 g)
- L-carnitine (0.2 g) + Co-enzyme q_{10} (0.05 g)
- L-carnitine (0.2g) + Retinol (0.03g)
- L- carnitine (0.2g) + Caffeine (0.25g)

Each formulation (liquid, gel, and cream) was prepared as previously mentioned with the added combination, placed in a dark container, and stored at 4°C until use.

2.5.4 Collection and storage of porcine skin tissue samples

An Ethics waiver for the approval of the use of porcine skin was obtained from the University of the Witwatersrand Animal Research Ethics Committee as well as the Human Research Ethics Committee (*15.03.2016- O) (Addendum X).* The porcine skin samples were harvested from animals euthanized for other purposes at the Wits Research Animal Facility. Porcine skin is the most frequent model used for *in vitro* permeation studies due to is anatomical similarity to human skin (Schmook *et al*., 2001; Herron, 2010).

After collection, porcine skin was immediately placed in cold (PBS) (pH 7.4) solution and transported to the laboratory within an hour. Excess fat and connective tissue were removed, and the specimens were cut into 1x4 cm strips. The tissue stripes were then placed into cryovials, snap frozen in liquid nitrogen (-195°C) and stored at -70°C. No specimens were obtained or used with any signs of skin disease that might influence the permeability characteristics of the skin. The process of cryopreservation is a process in which organelles, cells and tissues are preserved by cooling to extremely low temperatures. Studies have shown that the process of cryopreservation might increase the permeability of the skin, however it is the method of choice to preserve skin samples when fresh skin cannot be utilized for these studies (Pouliot *et al*., 2017).

2.5.5 Equipment used

2.5.5.1 7-In-line flow cell diffusion apparatus

The *in vitro* diffusion apparatus consisted of an ILC07 (Figure 2.4) (A) and (B) automated system containing 7-in-line flow cells from PermeGear INC (Hellertown, PA, USA). An ISCO Retriever IV fraction collector, an Ismatec IPC peristaltic pump and a Thermoscientic Haake SC100 water bath were connected to the apparatus. Each flow cell contained an orifice area of 0.0397 cm^2 (Figure 2.5). Tissue viability was done by critically examining the tissue sample and looking for anything that could compromise the integrity of the skin barrier. The intactness of the skin barrier was measured by a TEER meter (Millicel ERS-2 electrical resistance system, EMD Millipore Corporationm) before and after each experiment (Musazzai *et al*., 2018). The diffusion behaviour between repeat tissue samples in an experiment was also compared for any changes in diffusion behaviour that would indicate a barrier compromise.

(A) 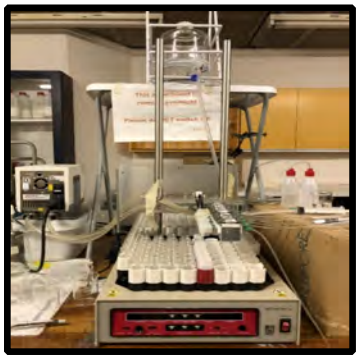 (B) 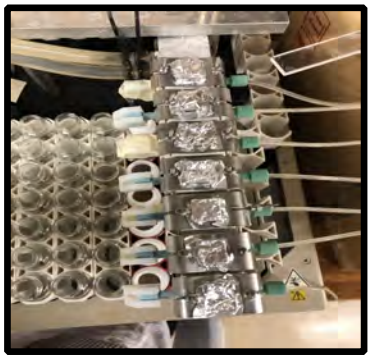

Figure 7.4: Illustration of (A) Anterior and (B) Superior view of in vitro diffusion apparatus automated system containing 7-in-line flows (ILC07) from PermeGear INC (Hellertown, PA,USA).



Figure 7.5: Illustration of porcine skin divided into 4-5 mm sections to be mounted in flow-through diffusion cells (exposed area 0.039 cm^2).

2.5.5.2 In vitro diffusion experiment

Prior to each permeability experiment, porcine skin samples were thawed for 10 minutes at room temperature in phosphate buffered saline (PBS, pH 7.4). Thereafter, excess fat and connective tissue were removed, and the skin divided into 4-5 mm sections and mounted in flow-through diffusion cells (Figure 2.4). Permeability experiments were performed for each compound tested. Equilibration of 10 minutes was allowed in the donor as well the acceptor compartments of the diffusion cells. Thereafter the PBS solution of the donor cell was replaced with the liquid, gel or cream formulation containing the active compounds. PBS at 37°C was pumped through the acceptor chambers at a rate of 1.5 ml/h and collected, by means of a fraction collector, at 30 min intervals for the first 4 hours and thereafter at 2-hour intervals for a final period of 24 hours initially. Thereafter, final collection periods were established as every 2 hours for a 24-hour period for each of caffeine, retinol, coenzyme Q_{10} and L-carnitine, while the collection period for theophylline remained as every 30 min for a 4-hour period. The study was performed under sink conditions (i.e. the concentration in the receptor cell never reached 10% of the donor cell concentration). The permeability experiment was repeated three times in different formulations (liquid, gel and cream) for each compound and combination of compounds) (caffeine, theophylline, retinol, l-carnitine and co-enzyme Q_{10}). As controls and to test for specificity of the compounds PBS, liquid, gel and cream formulations without any compounds were loaded into the donor compartments and experiments performed as above. At different time points the collected fluid in the receptor compartments was analysed by injecting 20 µl into the HPLC system and using the reverse-phase column 18 as mentioned in sections 2.1.4 and 2.1.5 above. From the chromatograms

obtained, the specific peaks of the compounds were identified from the retention times obtained from the corresponding standards. The areas of the peaks were then inserted into the linear regression equations of the standard curves obtained from the respective standards and solved for concentration.

2.5.5.2.1 Analysis of in vitro diffusion data

2.5.5.2.1.1 Calculation of Cumulative quantities

Cumulative quantities Qt (ng) refers to the quantity appearing in the receptor compartment of the diffusion per time period (min). The cumulative values were calculated by using Equation 5 below:

$$\mathrm{Qt} = \sum_{i=0}^{t} \mathrm{VtCt} \qquad (5)$$

Equation 5: Cumulative quantities (Where Qt is the cumulative quantities (ng), t (min) is the time period, Vt is the volume (ml) of the sample at t and Ct is the concentration of the sample (ng/ml) at t.

Data for the cumulative curves were expressed as the cumulative quantity per unit of skin surface are exposed (Equation 6, A=0.0397 cm^2).

Equation 6: Qt/A (6)

2.5.5.2.1.2 Steady State fluxes

Steady state fluxes (Jss) were calculated using GraphPad Prism Version 8.4.2. The values were calculated from the linear portion of the cumulative curves through linear regression analysis using Equation 7 below:

Equation 7: Steady state fluxes Jss = Δ(Q/(tA)). (7)

Data for the cumulative curves were expressed as the cumulative quantity per unit of skin surface are exposed (Equation 7, A=0.0397 cm^2).

2.5.5.2.1.3 Apparent permeability coefficient

Apparent permeability coefficients (Papp) were calculated by using Equation 8 below:

$$Papp = Jss/C_0 \qquad (8)$$

C_0 is the initial concentration of the compound in the donor compartment at t=0.
In this study, infinite dosing was used, which assumes that the compound concentration would not deplete over the experimental time period and there is very little change in initial concentration within the formulation throughout the experiment (Lau and Ng, 2017, p.2). The lag phase was calculated from the x-axis intercept after the linear regression of the linear portion of the cumulative diffusion curve.

2.5.5.3 Trans-epithelial electrical resistance (TEER) measurements testing skin integrity

Tissue viability was established prior to and after permeability experiments by measuring the tissue resistance using a Millipore Millicel ERS-2 hand-held resistivity meter (Figure 2.6). An experiment was also performed where tissue resistance was measured over a 24-hour time period (0, 2, 4 and 24 hours) after exposure to the 3 formulations without compounds (control) and with compounds so as to investigate the effect on skin barrier integrity. Experiments for both retinol and coenzyme Q_{10} took place under low light condition to reduce degradation of the compounds. Results at each time point were expressed as % of the initial resistance measurement (T = 0).

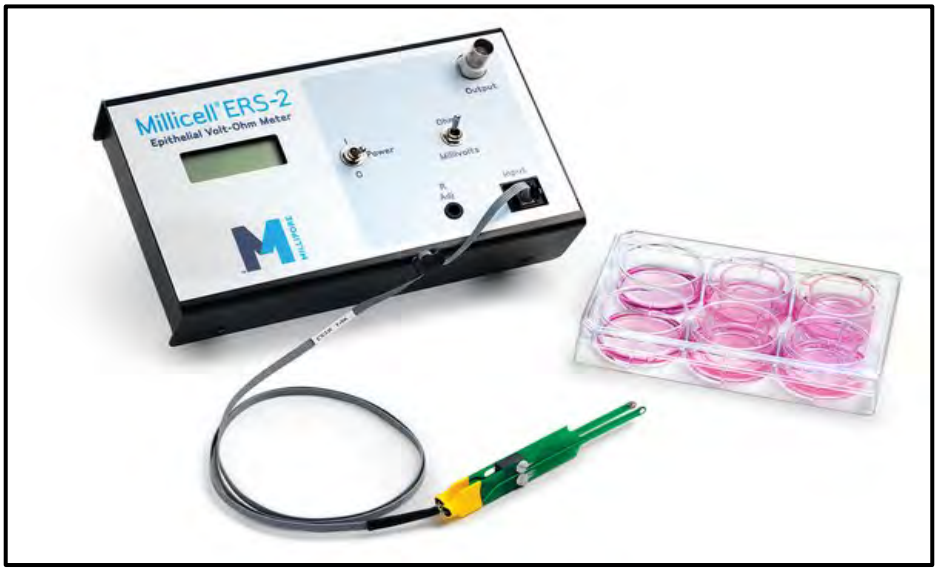

Figure 7.6: Millipore Millicel® ERS-2 hand-held resistivity meter.

2.5.5.4 Accumulation within the skin

Skin accumulation of active compounds (Qa) within the exposed skin (0.0397 cm^2) after the completion of the *in vitro* diffusion experiments was also accessed. After each experiment was completed, the tissue was placed within a 5 ml tube, 2 ml HPLC grade methanol was added and the tissue was homogenized for 10 min before being centrifuged at 1500 rpm for 5 min. The supernatant was removed and the compounds extracted was detected using the HPLC methods as previously mentioned in section 2.4. The quantity accumulated within the skin was calculated using Equation 9 below:

$$Qt\ (ng/cm^2) = CtV/A. \qquad (9)$$

Qt is the quantity accumulating in the skin after a certain time (t). Ct is the concentration of the extracted skin (in 2 ml methanol) after time (t). A is the skin area (cm^2) and V is the volume of methanol (2 ml). The percentage of the initial compound within the formulation that was applied to the skin, which accumulated within the skin, was calculated by using Equation 10 below:

$$Qt(\%) = (Qt/Q_0) \times 100 \qquad (10)$$

where Q_0 is the initial amount (µg or mg) of compound added to the donor compartment.

Once the diffusion experiment of the active compound alone was completed, the skin disk was removed and cleaned before the homogenised sample was analysed by HPLC. The skin disk was then homogenised in 2 ml methanol and centrifuged. After centrifugation, the sample was filtered through a 0.45 µm syringe filter and analysed using the HPLC machine.

2.6 Statistic Analysis

Data was analysed using Excel and GraphPad Prism Version 8.4.2. All experiments were repeated at least 3 times and parameters were expressed as Means ± standard deviation. Linear regression analysis was performed on all standard curve data and the linear regression formula (y= mx+c) used to calculate concentrations, cumulative amounts and to compute the steady state fluxes (Jss) and lag phases from the cumulative curves. ANOVA tests (2-way) were used to test for statistical significance ($p < 0.05$) between steady state flux values ($ng.cm^{-2}.min^{-1}$), skin accumulation (% of initial) and skin integrity (% of initial). For the two-way ANOVA test (Analysis of variance), the 2 independent variables were compounds (alone and in combination) and formulation (liquid, gel and cream).

Chapter 3.1: Results – Validation

The skin which is the largest organ of the human mainly acts as protective mechanism against foreign particles by means of acting as a permeability barrier to the environment. With time, the continuous exposure to the harsh environment, whether it be through over-exposure of sun rays, climate change or chemicals can give rise to skin afflictions (Balato *et a*l., 2014). Hyperpigmentation, erythema solare (sunburn), adiposis ademotosa (cellulite), to name a few are examples of skin afflictions.

In this study, a selection of active compounds (Caffeine, Theophylline, Retinol, Co-enzyme Q_{10} and L-carnitine) were validated using HPLC detection prior to the diffusion experiments. The active compounds were incorporated individually as well as in

combination in different topical formulations such as liquid, gel and cream. This was to evaluate the *in vitro* rate of diffusion of the active agents across skin, accumulation within the skin and whether the diffusion rate and accumulation would be influenced by various formulations or when combined with other agents. The aim was thus to establish which formulation and which combination shows the greatest efficacy. A 7-in - line flow cell diffusion system was used to evaluate the rate of diffusion across the skin and extent of accumulation of all 5 active compounds alone or in combination in liquid, gel, or cream formulations within porcine skin.

3.1 HPLC Method Validation

The intent of method validation is to provide scientific evidence that the analytical method is reliable and consistent and can therefore be used as a routine analysis. The key criteria for evaluation of an analytical method according to International Council of Technical Requirements for Pharmaceuticals for Human Use (ICH) guidelines are linearity, accuracy, precision, LOD, LOQ , ruggedness and sensitivity (Beloufa *et al*., 2017; Taleuzzaman, 2018).

3.1.1 Linearity

The linear regression model is the ability to predict values for a dependent variable whilst the independent value is known. The model determines the relationship of an independent variable on a dependent variable. The linearity of the model is expressed by means of a coefficient of correlation (r) or coefficient of determination (R^2) (Moosavi and Ghassabian, 2018). The coefficient of determination (R^2) is interpreted as the percent of variation shared between the two variables (Bruce Ratner, 2009; Hamilton *et al*., 2015). A coefficient of determination of 1.0 indicates that there is a perfect linear model while a value less 1.0 shows that not all variability in the data can be accounted by the model (Hamilton et al., 2015; Belouafa *et al*., 2017).

3.1.1.1 Caffeine

In Figure 3.1, the compound was linear between the following values: 5 – 200 μg/ml with regression equation of y= 19610x - 85893 and R^2 value of 0.9952. A slight

variation in the lower values (<50 ug/ml) can be observed. Due to the possibility that the lower values could potentially affect the regression line, analyses were performed on standards covering the lower regions of the concentration range (Figure 3.2): 5 – 30 µg/ml (Preparation of Calibration Curves, 2003). A regression equation of y= 46872x + 7462.4 with an R^2 value of 0.9988 was calculated from the latter caffeine curve. The LOD and LOQ were calculated from both Figure 3.1 and 3.2. In Figure 3.1 LOD and LOQ were found to be 22.06 µg/ml and 66.84 µg/ml respectively while in Figure 3.2 results were found to be 2.62 µg/ml and 7.95 µg/ml, respectively. The HPLC chromatogram of the caffeine standard is portrayed in Figure 3.3. The chromatogram shows the retention time of caffeine 2.57 ± 0.02 min.

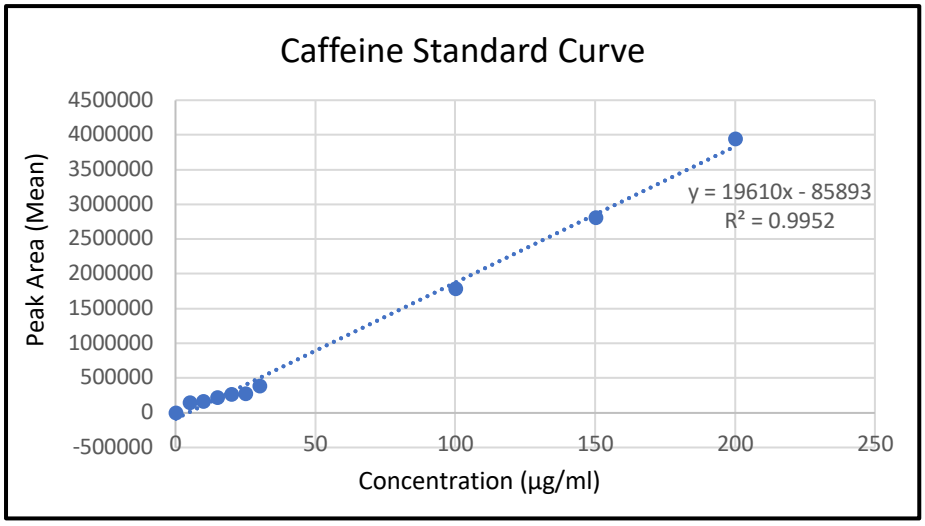

Figure 8.1: Linear regression curve of Caffeine (0 - 200 µg/ml)

The curve illustrates a regression equation of y= 19610x - 85893 and R^2 value of 0.9952. Values are the mean ± standard error of 3 replicates. When error bars are not visible, they fall within the size of the marker.

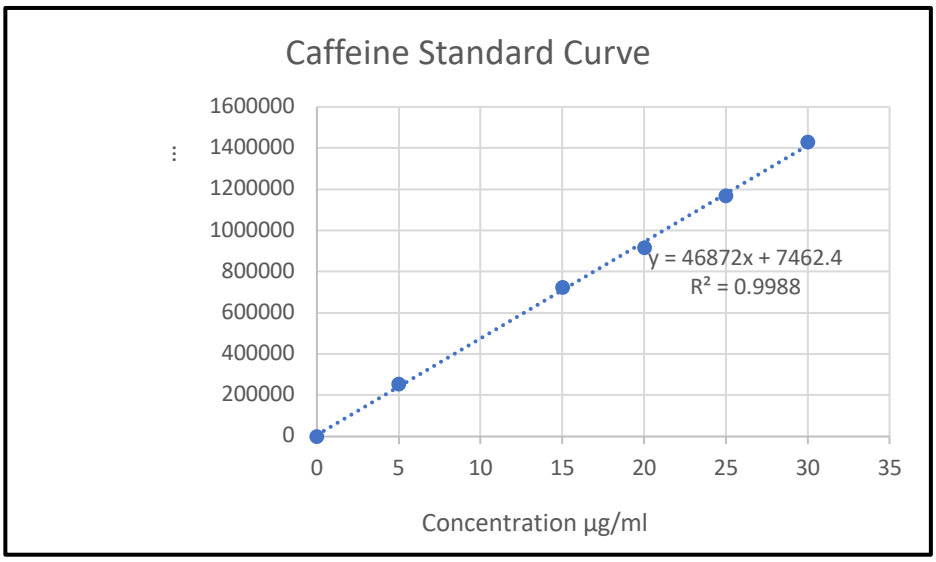

Figure 8.2: Linear regression curve of Caffeine (0 - 30 µg/ml).

The curve illustrates a regression equation of y= 46872x + 7462.4 and R^2 value of 0.9988. Values are the mean ± standard error of 3 replicates. When error bars are not visible, they fall within the size of the marker.

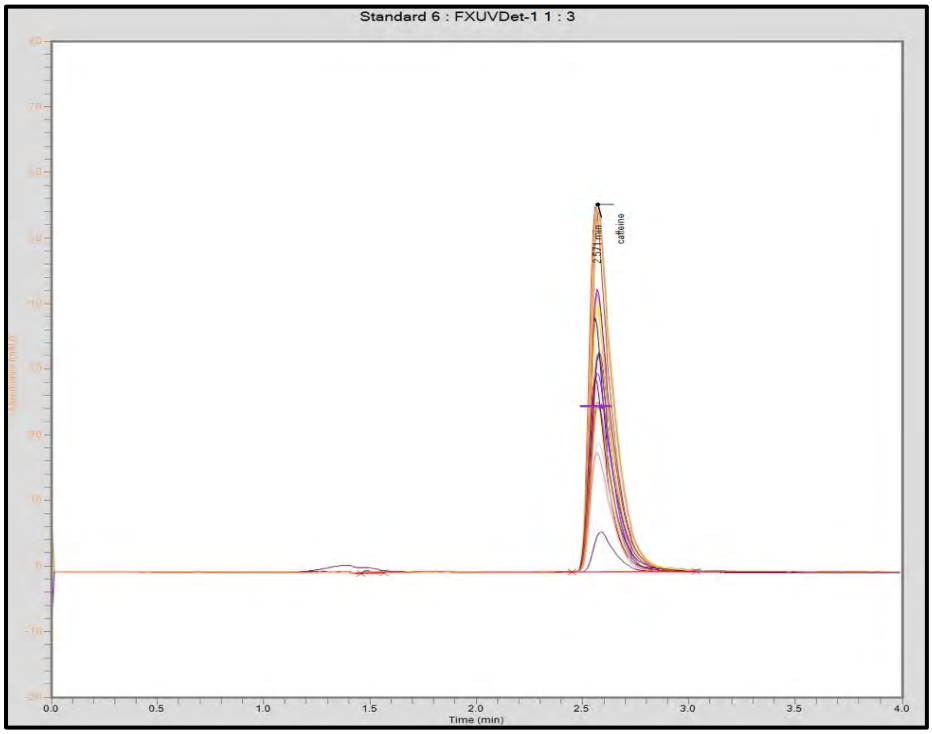

Figure 8.3: Chromatogram of Caffeine.

Caffeine peak was detected at a retention time of 2.57 ± 0.02 min at an absorbance of 56 milli-absorbance units (mAU). Chromatographic conditions were followed using table 2.1 in section 2.1.5.

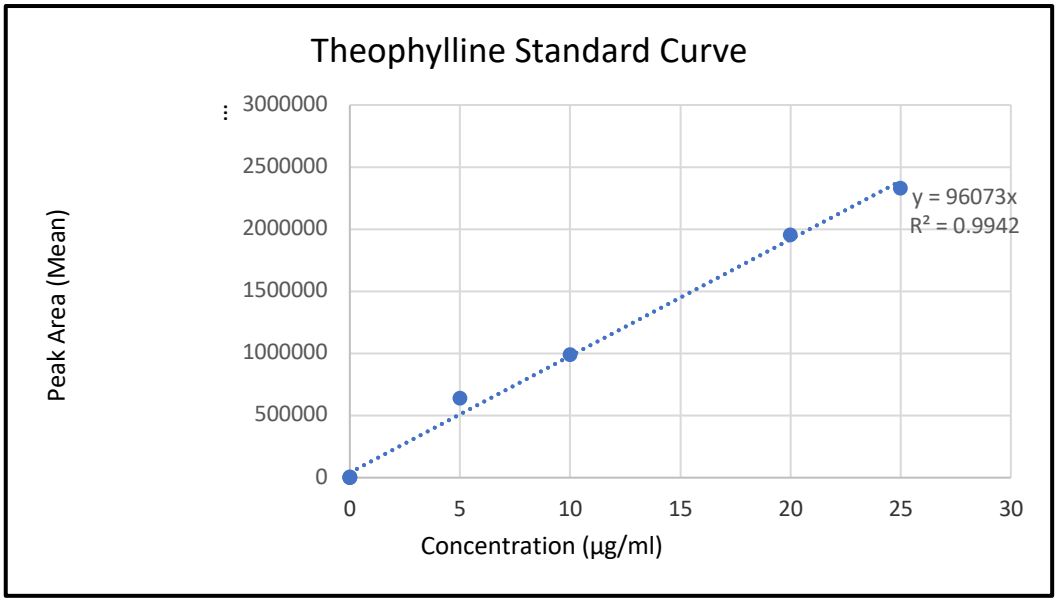

3.1.1.2 Theophylline

The linearity of Theophylline is demonstrated in Figure 3.4, within the concentration range 0 – 25 µg/ml. Theophylline showed a regression equation of y= 96073x with a R^2 of 0.9942. The LOD and LOQ were calculated from Figure 3.4 and were found to be 3.34 µg/ml and 10.13 µg/ml, respectively. The HPLC chromatogram of theophylline standard is portrayed in Figure 3.5. The chromatogram showed the retention time of theophylline 2.18 ± 0.03 min.

The curve illustrates a regression equation of y=96073x with a R^2 value of 0.9942. Values are the mean ± standard error of 3 replicates. When error bars are not visible, they fall within the size of the marker.

Figure 8.4: Linear regression curve of Theophylline (0 - 25 µg/ml).

Theophylline peak was detected at a retention time of 2.18 ± 0.03 min at an absorbance of 100 mAU. Additionally, a peak was detected at retention time of 1.482 at an absorbance of 6 mAU. Chromatographic conditions were followed using table 2.1 in section 2.1.5.

3.1.1.3 Retinol

The linearity of Retinol is demonstrated in Figure 3.6. Retinol showed a regression equation of y= 36849x + 72987 with a R^2 value of 0.9933, in the concentration range 0 – 100 µg/ml. The LOD and LOQ were calculated from Figure 3.6 and were found to be 14.83 µg/ml and 44.93 µg/ml, respectively. In the lower region of the standard curve, LOD and LOQ were calculated as 0.35 µg/ml and 1.06 µg/ml respectively. The

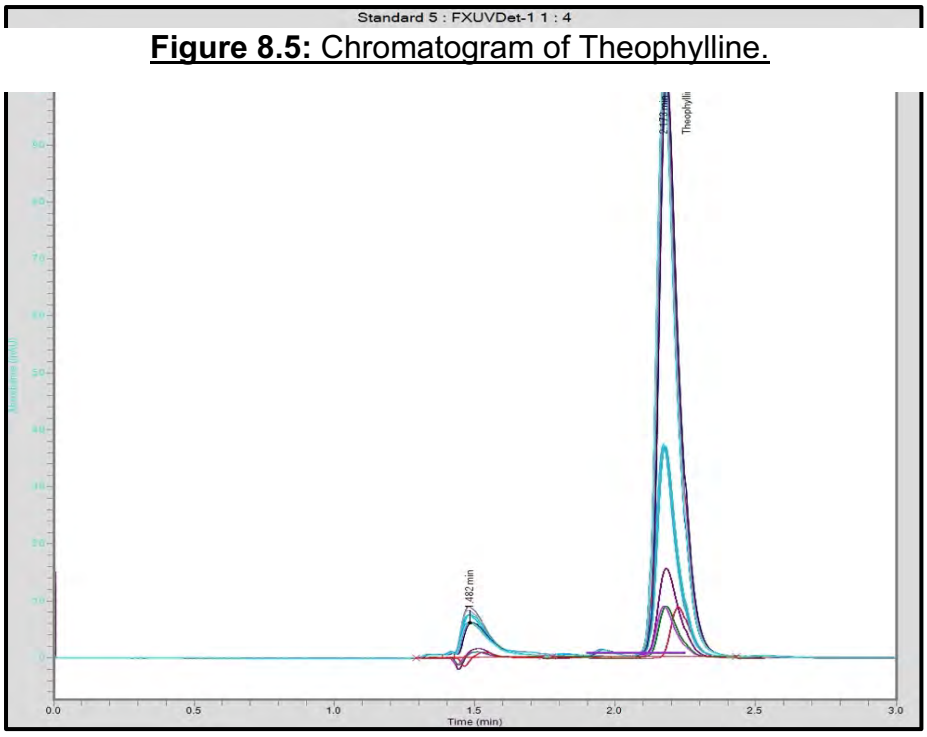

Figure 8.5: Chromatogram of Theophylline.

HPLC chromatogram of retinol standard is portrayed in Figure 3.8. The chromatogram showed the retention time of retinol 2.91 ± 0.02 min.

Figure 8.6: Linear regression curve of Retinol (0 – 100 µg/ml).

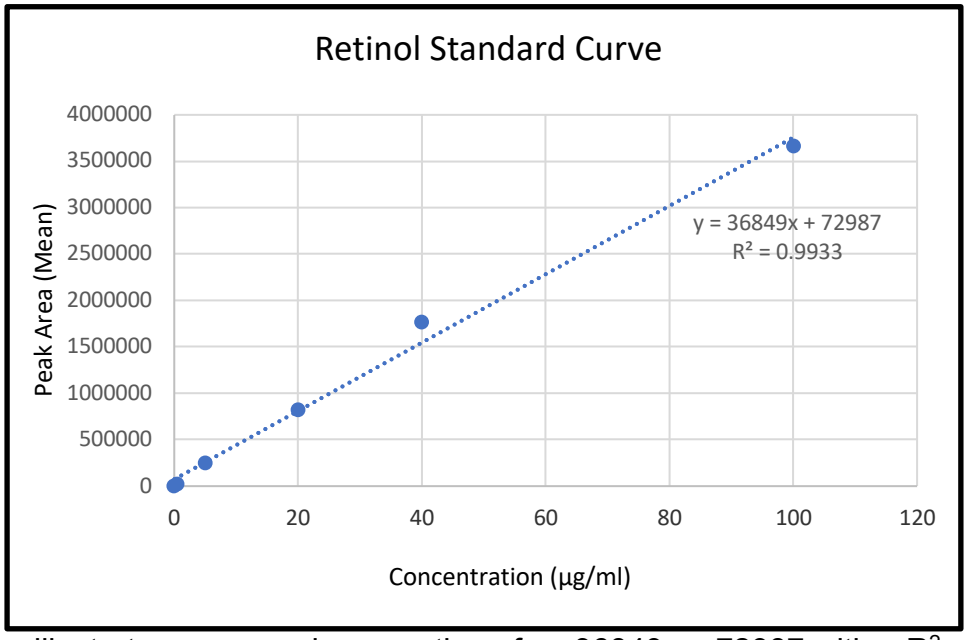

The curve illustrates a regression equation of y= 36849x + 72987 with a R^2 value of 0.9933. Values are the mean ± standard error of 3 replicates. When error bars are not visible, they fall within the size of the marker.

In figure 3.7, analyses were performed at the lower regions of the standard curve for retinol (0 – 10 µg/ml) due to slight variation in the lower concentration ranges. A regression equation of y= 52648x with a R^2 of 0.9995 was obtained.

Figure 8.7: Linear regression curve of Retinol (0 – 10 µg/ml).

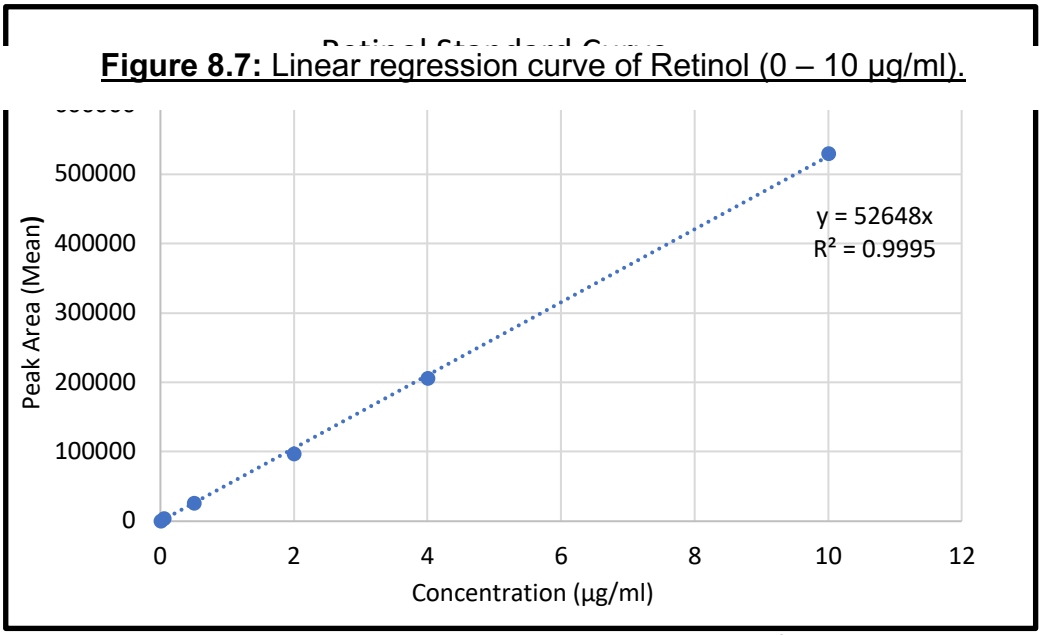

The curve illustrates a regression equation of y= 52648x with a R^2 value of 0.9995. Values are the mean ± standard error of 3 replicates. When error bars are not visible, they fall within the size of the marker.

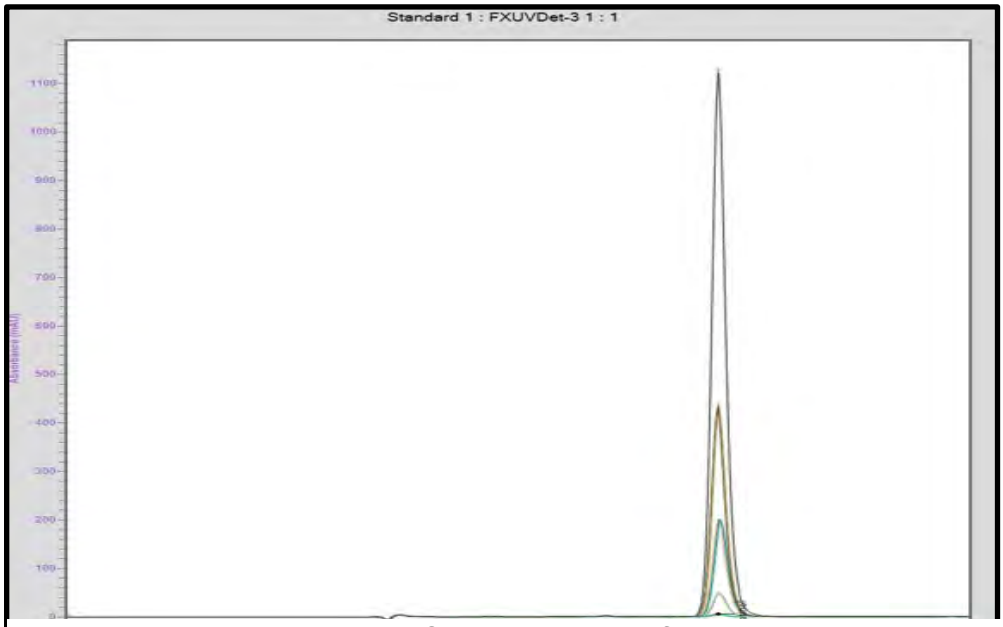

Figure 8.8: Chromatogram of Retinol.

Retinol peak was detected at a retention time of 2.91 ± 0.02 min at an absorbance of 1100 mAU. Chromatographic conditions were followed using table 2.1 in section 2.1.5.

3.1.1.4 Coenzyme Q10

The linearity of Coenzyme Q_{10} is demonstrated in Figure 3.9. Coenzyme Q_{10} showed a regression equation of y= 10175x + 23299 with a R^2 value of 0.9949. LOQ and LOD were calculated from Figure 3.9 and were found to be 12.73 µg/ml and 38.56 µg/ml, respectively. In the lower region of the standard curve LOD and LOQ were calculated as 0.69 µg/ml and 2.08 µg/ml respectively. The HPLC chromatogram of coenzyme Q_{10} standard is portrayed in Figure 3.11. The chromatogram showed the retention time of coenzyme Q_{10} 3.15 ± 0.003 min.

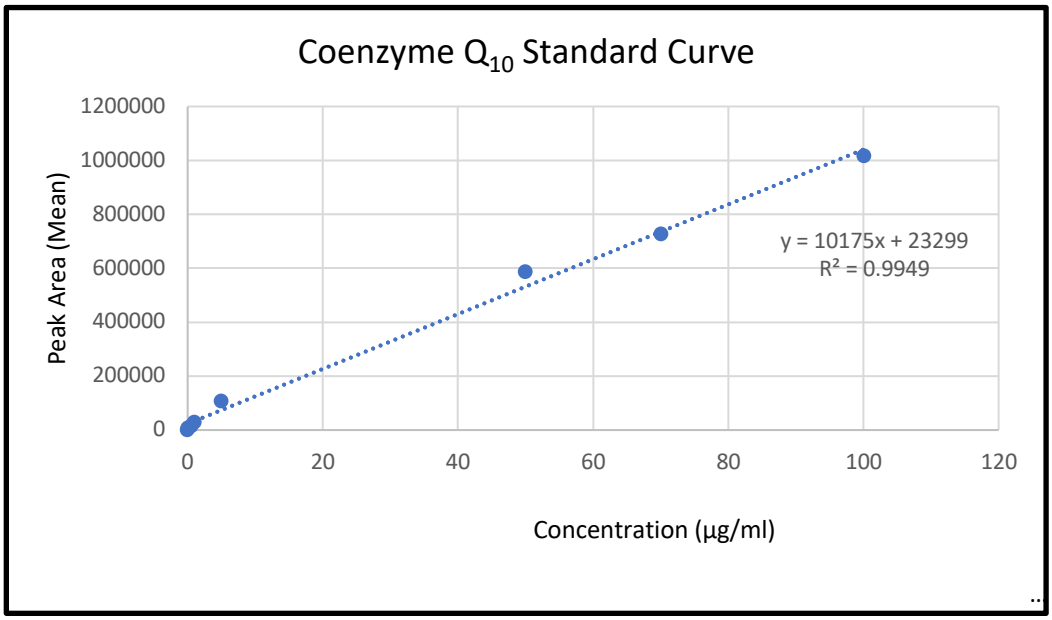

Figure 8.9: Linear regression curve of Co-enzyme Q10 (0 – 100 µg/ml).

The curve illustrates a regression equation of y=10175x + 23299 with a R^2 value of 0.9949. Values are the mean ± standard error of 3 replicates. When error bars are not visible, they fall within the size of the marker.

In figure 3.10, analyses were performed on standards covering the lower regions of the standard curve for coenzyme Q_{10} (0 – 10 µg/ml) due to slight variation in the lower concentration ranges. A regression equation of y=20188x + 5000.9 with a R^2 value of 0.9986 was obtained.

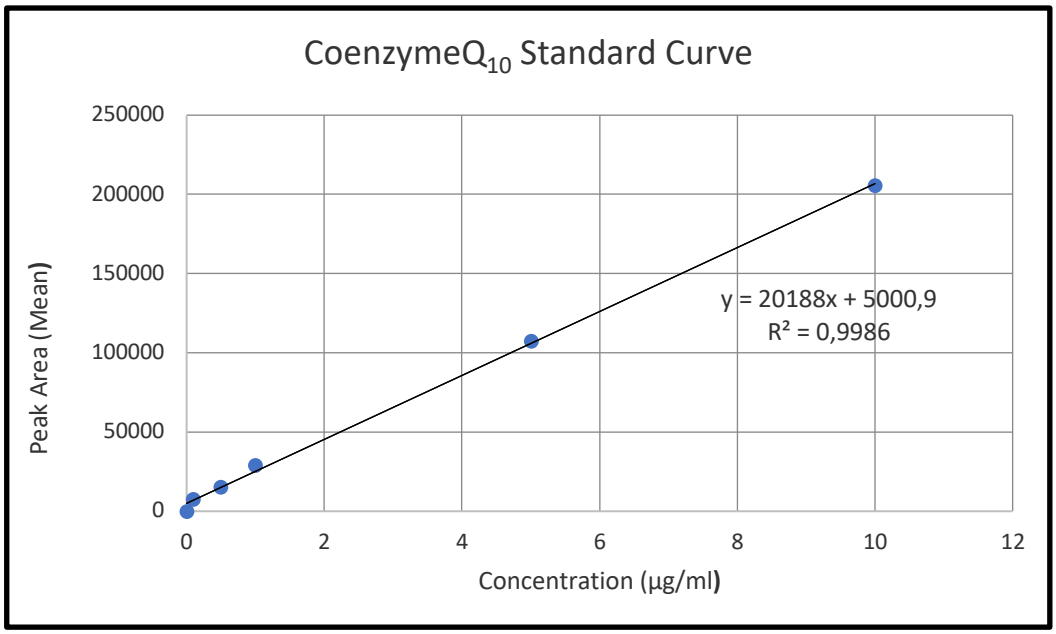

Figure 8.10: Linear regression curve of Co-enzyme Q10 (0 – 10 µg/ml).

The curve illustrates a regression equation of y=20188x + 5000.9 with a R^2 value of 0.9986. Values are the mean ± standard error of 3 replicates. When error bars are not visible, they fall within the size of the marker.

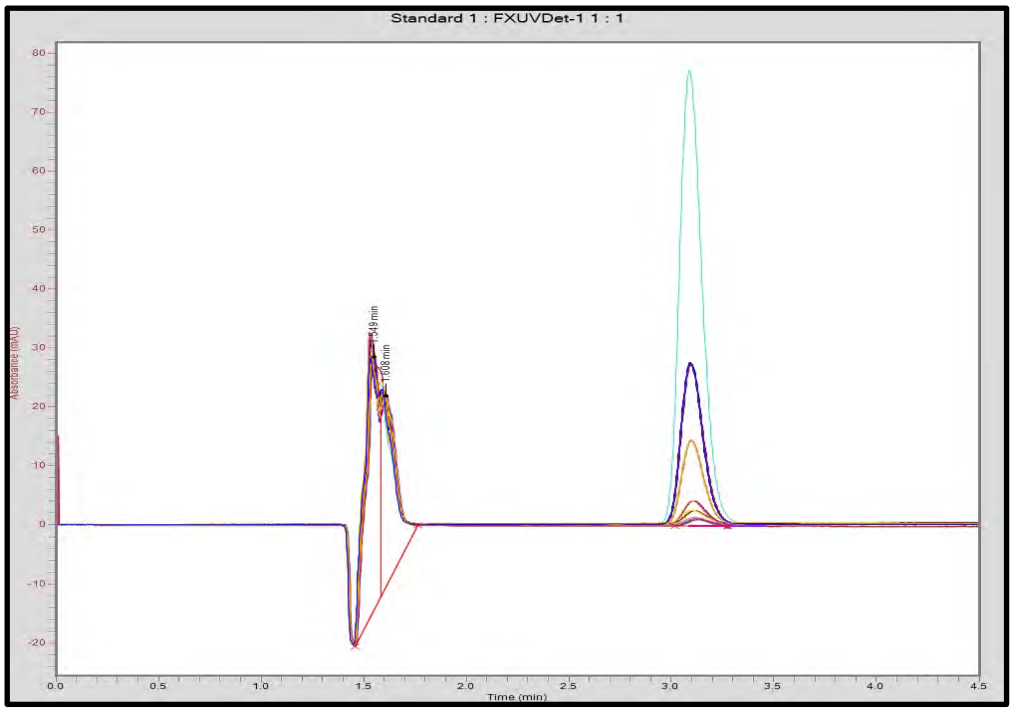

Figure 8.11: Chromatogram of Coenzyme Q10.

Coenzyme Q_{10} peak was detected at a retention time of 3.15 ± 0.003 min at an absorbance of 77 mAU. Additionally, two peaks were detected at 1.55 min at an absorbance of 28 mAU and at 1.61 min at an absorbance of 22 mAU. Chromatographic conditions were followed using table 2.1 in section 2.1.5.

3.1.1.5 L-Carnitine

The linearity of L-Carnitine is demonstrated in Figure 3.12. L-carnitine showed a regression equation of y= 86.385x + 1981.8 with a R^2 value of 0.9714. The concentration ranged from 100 – 1000 μg/ml. LOD was < 100 μg/ml and LOQ was 100 μg/ml. The HPLC chromatogram of L-carnitine standard is portrayed in Figure 3.13. The chromatogram showed the retention time of L-carnitine 3.0 ± 0.009 min.

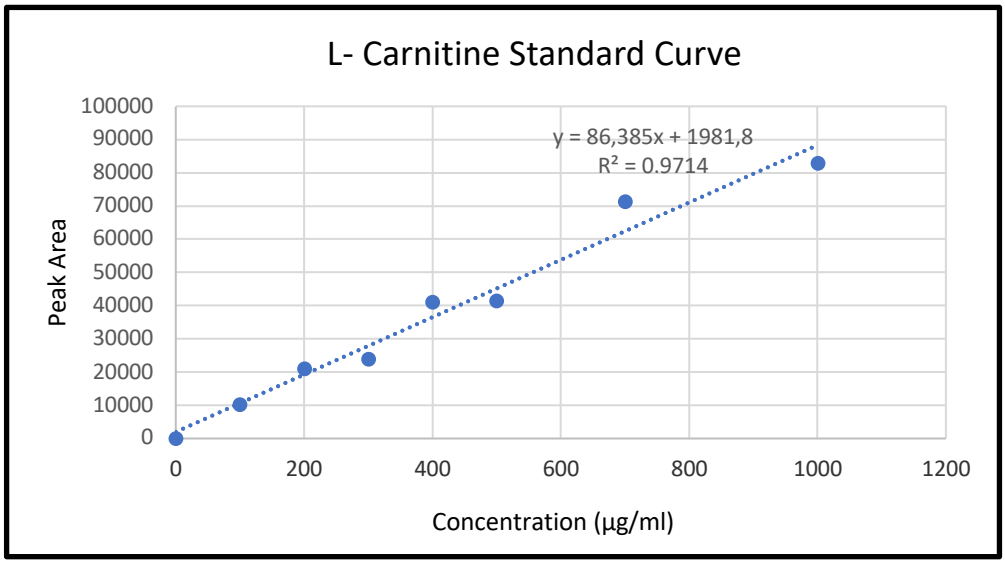

Figure 8.12: Linear regression curve of L-Carnitine (0 – 1000 μg/ml).

The curve illustrates a regression equation of y= 86.385x + 1981.8 with a R^2 value of 0.9714. Values are the mean ± standard error of 3 replicates. When error bars are not visible, they fall within the size of the marker.

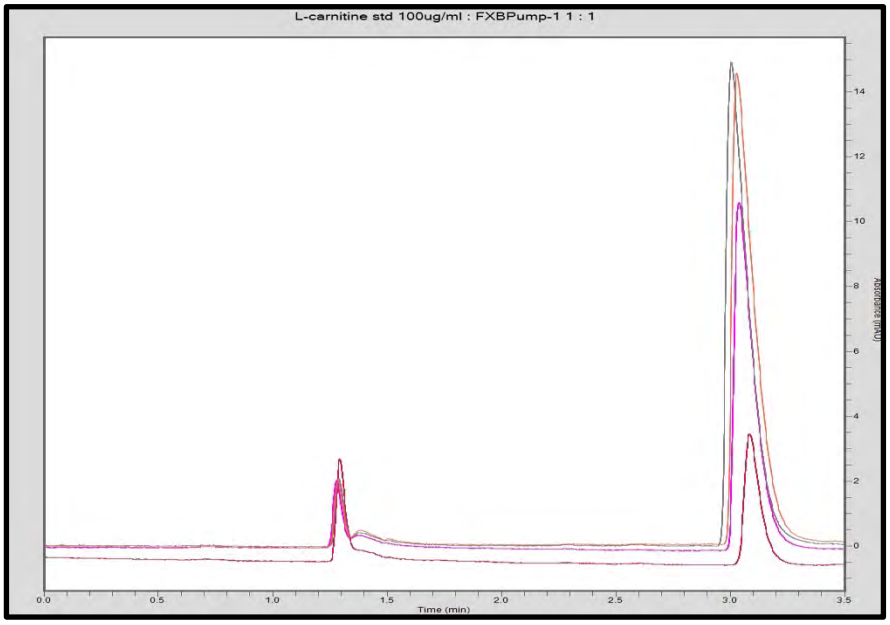

Figure 8.13: Chromatogram of L-carnitine.

L-carnitine peak was detected at a retention time of 3.0 ± 0.009 min at an absorbance of 18 mAU. Additionally, a peak was detected at a retention time of 1.3 min and absorbance of 2.2 mAU. Chromatographic conditions were followed using table 2.1 in section 2.1.5.

3.1.2 Accuracy and Precision

3.1.2.1 Precision

Precision refers to the closeness between a series of measurements obtained from multiple sampling of the same homogenous sample under the prescribed conditions. Precision is expressed as: repeatability, intermediate precision, and reproducibility (Kachave and Jadhav,2021). Tables 3.1 – 3.5 illustrates mean, standard deviation and %RSD data of Caffeine, Theophylline, Retinol, Co-enzyme Q_{10} and L-carnitine respectively.

RSD is defined as a coefficient of variation which is determined by the ratio of standard deviation and the mean. The measurement obtained by the ratio describes the dispersion of samples. In the pharmaceutical industry, RSD is used to determine multiple functions such as: the variability of the total dose of the active pharmaceutical ingredient (API), to determine the API in combination samples or to determine the variation in drug dissolution and bioavailability (Gao *et al*., 2013).

According to Shabir (2004), the accepted of %RSD varies according to the international regulatory agencies. The acceptance criteria for precision according to the Food and Drug Administration (FDA) should be 1% for drug substances and drug products, ± 2% for bulk drugs and finished products (Shabir, 2004). However, other regulatory Authorities, such as Health Canada (HC), states that RSD should be 1% for drug substances and 2% for drug products (Shabir, 2004). For minor components, it should be ± 5% but can reach a maximum value of 10%. The %RSD acceptance criteria of intermediate Precision should be ≤ 2% (Shabir, 2004; Gao *et al*., 2013). Intermediate precision refers to the intra-day and inter-day precision and a value of ≤ 2% indicates good precision of the method (Belouafa *et al*., 2017).

3.1.2.1.1 Caffeine

Table 3.1 shows precision of Caffeine at concentrations of 15, 30 and 150 µg/ml. Each concentration was repeated 3 times, and a mean and standard deviation were calculated. The (%) RSD was calculated for each concentration value. Results shows that the (%) RSD value exceeded the 2% acceptance criteria at the lower concentration levels, due to the variation in the data at these lower concentration ranges.

Table 8.1: Precision of Caffeine.

Concentration (µg/ml)	Number of Replicates	Peak Area	Mean ± SD	(%) RSD
15	Replicate 1	214 588	222 251 ± 9364	4.2
	Replicate 2	230 807		
	Replicate 3	221 357		
30	Replicate 1	387 453	392 143 ± 8667	2.2
	Replicate 2	386 830		
	Replicate 3	402 144		
150	Replicate 1	2 764 730	2 814 004 ± 51043	1.8
	Replicate 2	2 810 631		
	Replicate 3	2 866 659		

3.1.2.1.2 Theophylline

Results obtained in Table 3.2 shows precision of Theophylline at concentrations of 5, 10 and 20 µg/ml. Each concentration was repeated 3 times, and a mean and standard deviation were calculated. (%) RSD across all 3 concentrations were found to be ≤ 2%.

Table 8.2: Precision of Theophylline.

Concentration (µg/ml)	Number of Replicates	Peak Area	Mean ± SD	(%) RSD
5	Replicate 1	632 598	638 023 ± 9293	1.5
	Replicate 2	632 718		
	Replicate 3	648 753		
10	Replicate 1	991 966	992 654 ± 1491	0.2
	Replicate 2	991 631		
	Replicate 3	994 365		
20	Replicate 1	2 123 342	2 118 281 ± 4882	0.2
	Replicate 2	2 117 900		
	Replicate 3	2 113 600		

3.1.2.1.3 Retinol

Results obtained in Table 3.3 shows precision of Retinol at concentrations of 5, 40 and 100 µg/ml. Each concentration was repeated 3 times and a mean value and standard deviation were calculated. %RSD across all 3 concentrations were found to be ≤ 2%.

Table 8.3:Precision of Retinol.

Concentration (µg/ml)	Number of Replicates	Peak Area	Mean ± SD	(%) RSD
5	Replicate 1	212 122	213 972 ± 1612	0.8
	Replicate 2	214 717		
	Replicate 3	215 076		
40	Replicate 1	1 886 060	1 901 131 ± 20145	1.1
	Replicate 2	1 893 322		
	Replicate 3	1 924 012		
100	Replicate 1	5 010 981	5 000 983 ± 13652	0.3
	Replicate 2	5 006 540		
	Replicate 3	4 985 429		

3.1.2.1.4 Co-enzyme Q10

Results obtained in Table 3.4 shows precision of Co-enzyme Q_{10} at concentrations of: 5,10 and 70 µg/ml. Each concentration was repeated 3 times, and a mean value and standard deviation was calculated. %RSD across all 3 concentrations were found to be ≤ 2%.

Table 8.4:Precision of Co-enzyme Q10.

Concentration (µg/ml)	Number of Replicates	Peak Area	Mean ± SD	(%) RSD
5	Replicate 1	107 304	107 361 ± 55	0.05
	Replicate 2	107 414		
	Replicate 3	107 364		
10	Replicate 1	206 109	205 757 ± 542	0.3
	Replicate 2	205 133		
	Replicate 3	206 029		
70	Replicate 1	729 836	728 643 ± 1205	0.2
	Replicate 2	728 662		
	Replicate 3	727 427		

3.1.2.1.5 L-Carnitine

Results obtained in Table 3.5 shows precision of L-carnitine at concentrations of: 200, 500 and 1000 µg/ml. Each concentration was repeated 3 times, and a mean value and standard deviation was calculated. %RSD across all 3 concentrations were found to be ≤ 2%.

Table 8.5: Precision of L-Carnitine.

Concentration (µg/ml)	Number of Replicates	Peak Area	Mean ± SD	(%) RSD
200	Replicate 1	20 724	21 121 ± 354	1.7
	Replicate 2	21 404		
	Replicate 3	21 234		
500	Replicate 1	41 693	41 493 ± 227	0.6
	Replicate 2	41 540		
	Replicate 3	41 246		
1000	Replicate 1	82 977	82 972 ± 736	0.9
	Replicate 2	82 234		
	Replicate 3	83 706		

3.1.2.2 Intermediate precision

Intermediate precision was used to express within-laboratory variations (Belouafa et al., 2017) such as intra-day and inter-day precision. Results as seen in Tables 3.6 – 3.10 reports the intermediate precision data of Caffeine, Theophylline, Retinol, Co-enzyme Q10 and L-carnitine. The concentration was repeated 3 times on the same day and then repeated on day 2 to retrieve inter-precision data for each 5 active ingredients. An overall mean value was calculated over the two days The acceptance criteria for precision of data are expressed in (%)RSD with a value ≤ 2% as it indicates good precision of the method (Belouafa *et al*., 2017).

3.1.2.2.1 Caffeine

Results obtained in Table 3.6 shows intra- and inter-day precision of Caffeine at concentrations of 20 µg/ml. The (%) RSD was determined across inter and intra-day and a value ≤ 2% was found.

Table 8.6: Intermediate precision of Caffeine **(20 µg/ml).**

Number of Replicates	Peak Area Day 1	Peak Area Day 2
Replicate 1	214588	220904
Replicate 2	230807	225534
Replicate 3	221357	224032
Mean	222251 ± 8146	223490 ± 2362
%RSD	3.67	1.06
Overall Mean (Day 1 & Day 2)	222870	
SD	870	
%RSD	0.4	

3.1.2.2.2 Theophylline

Results obtained in Table 3.7 shows intra- and inter-day precision of Theophylline at concentrations of 10 µg/ml. The (%) RSD was determined across inter and intra-day, the value was found to be > 2%.

Table 8.7: Intermediate precision of Theophylline **(10 µg/ml).**

Number of Replicates	**Peak Area Day 1**	**Peak Area Day 2**
Replicate 1	653502	683541
Replicate 2	654227	692397
Replicate 3	653897	699547
Mean	653876 ± 363	691828 ± 8018
%RSD	0.056	1.16
Overall Mean (Day 1 & Day 2)	672852	
SD	26837	
%RSD	4.0	

3.1.2.2.3 Retinol

Results obtained in Table 3.8 shows intra- and inter-day precision of Retinol at concentrations of 40 µg/ml. The (%) RSD was determined across inter and intra-day, the value was found to be > 2%.

Table 8.8: Intermediate precision of Retinol **(40 µg/ml).**

Number of Replicates	**Peak Area Day 1**	**Peak Area Day 2**
Replicate 1	1886060	1960571
Replicate 2	1893322	1960344
Replicate 3	1924012	1987500
Mean	1901131 ± 20145	1969438 ± 15613
%RSD	1.06	0.79
Overall Mean (Day 1 & Day 2)	1 935 302	
SD	48324	
%RSD	2.5	

3.1.2.2.4 Co-enzyme Q10

Results obtained in Table 3.9 shows intra- and inter-day precision of Co-enzyme Q_{10} at concentrations of 100 µg/ml. The (%) RSD was determined across inter and intra-day, the value was found to be < 2%.

Table 8.9: Intermediate precision of Co-enzyme Q10 **(100 µg/ml).**

Number of Replicates	Peak Area Day 1	Peak Area Day 2
Replicate 1	1016 231	1337546 (*)
Replicate 2	1016782	1033461
Replicate 3	1016116	1035064
Mean	1016377 ± 356	1034263 ± 1133
%RSD	0.035	0.11
Overall Mean (Day 1 & Day 2)	1025356	
SD	12596	
%RSD	1.2	

* Value was omitted as it skewed the data.

3.1.2.2.5 L- Carnitine

Results obtained in Table 3.10 shows intra- and inter-day precision of l - carnitine at concentrations of 500 µg/ml. The concentration was repeated 3 times on the same day and then repeated on day 2 to retrieve inter-precision data. %RSD was determined across inter and intra-day. The value was found to be > 2%.

Table 8.10: Intermediate precision of L-Carnitine **(500 µg/ml).**

Number of Replicates	Peak Area Day 1	Peak Area Day 2
Replicate 1	41693	44628
Replicate 2	41540	45212
Replicate 3	41246	44489
Mean	41493 ± 227	44776 ± 384
%RSD	0.55	0.86
Overall Mean (Day 1 & Day 2)	43172	
SD	2374	
%RSD	6.4	

3.1.2.3 Accuracy

Accuracy refers to the closeness of agreement between the true value of the analyte concentration and the mean result obtained by spiked blank samples (Belouafa *et al.*, 2017). Table 3.11 – 3.15 represents the mean, SD and (%) RSD obtained for Caffeine, Theophylline, Retinol, L-carnitine, and Co-enzyme Q_{10} respectively. The acceptable range of % recovery was found between 80 and 120 % (Australian Pesticides & Veterinary Medicines Authority, 2004:5).

3.1.2.3.1 Caffeine

Table 3.11 reports the mean, SD and percentage recovery of Caffeine. The linear regression formula obtained from figure 3.2 was used to calculate accuracy. % Recovery of the spiked concentration of both 5 µg/ml and 30 µg/ml were within the acceptance criteria. The % recovery of the spiked concentration of 150 µg/ml was found to be over the acceptance criteria. Linear regression formula in Figure 3.1 was used to calculate the accuracy as it was out of range.

Table 8.11: Peak area and percentage recovery of Caffeine.

Numbers of Replicates	Concentration Spiked (µg/ml)		
	5	**30**	**150**
	Area under the Curve		
1	267219 (*)	1414609	4846016
2	266037 (*)	1426679	4824508
3	219667	1401058	4879801
4	216771	1436741	4931255
5	216826	1432558	4927854
6	219275	1434396	4919603
Mean	218135	1424340	4888173
SD	1552	13890	45429
RSD%	0.7	1.0	0.9
Recovery%	89.9	100.8	169.1

*Data points were excluded as they skewed data.

3.1.2.3.2 Theophylline

Table 3.12 reports the mean, SD, and percentage recovery of Theophylline. % Recovery of the spiked concentration of both 2 µg/ml and 4 µg/ml were within the acceptance criteria. % Recovery of the spiked concentration of 10 µg/ml was below the acceptance criteria.

Table 8.12: Peak area and percentage of Theophylline.

Number of Replicates	Concentration Spiked (µg/ml)		
	2	**4**	**10**
	Area under the Curve		
1	190307	355324	651648
2	190604	355587	650767
3	190306	356253	651069
4	190451	356923	651687
5	191035	357083	651520
6	190696	355897	650811
Mean	190567	356178	651250
SD	278	712	420
RSD %	0.1	0.2	0.07
Recovery %	80	84	65

3.1.2.3.3 Retinol

Table 3.13 reports the mean, SD and percentage recovery of Retinol. The linear regression formula used in Figure 3.7 was used to calculate the area under the curve for 2 and 10 µg/ml while formula in Figure 3.6 was used to calculate the area for 100 µg/ml. Due to the variation in the values in the lower concentration range, the % recovery values obtained when the blank was spiked with 2 µg/ml, was omitted. This low concentration resulted in the overestimation of the recovery.

Table 8.13: Peak area and percentage of Retinol.

Number of Replicates	Concentration Spiked (µg/ml)		
	2	**10**	**100**
	Area under the Curve		
1	346606	401187	2847528
2	317175	403927	2861261
3	312954	402250	2892785
4	315977	402145	2866226
Mean	323178	402377	2866950
SD	15719	1139	18952
%RSD	4.9	0.3	0.7
Recovery %	306.9 (*)	89.4	75.8

*Value was ignored due to the variation in the values in the lower concentration ranges which resulted in a wide variation in % recovery.

3.1.2.3.4 Co-enzyme Q10

In Table 3.14, reports the mean, SD and percentage recovery of Co-enzyme $Q_{10.}$ The percent recovery for Co-enzyme Q_{10} was reported to be within the acceptable range (80 – 120 %). The linear regression formula used in Figure 3.10 was used to calculate the area under the curve for 5 and 10 µg/ml while the formula in Figure 3.9 was used to calculate the area for 100 µg/ml.

Table 8.14: Peak area and percentage of Co-enzyme Q10.

Number of Replicates	Concentration Spiked (µg/ml)		
	5	**10**	**100**
	Area under the Curve		
1	107304.01	206108.8	1016231
2	107414.44	205132.9	1016782
3	107363.95	206028.5	1016116
Mean	107360.8	205756.7	1016377
SD	55.3	541.7	356
RSD%	0.05	0.3	0.03
Recovery%	101.4	99.4	97.6

3.1.2.3.5 L-Carnitine

Table 3.15 reports the mean, SD and percentage recovery of L-carnitine. % Recovery was found to be in the range between 63.9 and 80.3 %, acceptable range: 80 -120% (Australian Pesticides & Veterinary Medicines Authority, 2004:5).

Table 8.15: Peak area and percentage of L-Carnitine.

Number of Replicates	Concentration Spiked µg/ml		
	100	**400**	**700**
	Area under the curve		
1	7346	28528	50127
2	7556	28306	49969
3	7625	28236	53252
4	7173	30182	49148
5	7673	29936	49749
6	5713 (*)	30357	49567
Mean	7475	29257	50302
SD	210	1000	1485
RSD%	2.9	3.4	2.9
Recovery%	63.9	79.3	80.3

*Data point was excluded as it skewed data.

3.1.3 Ruggedness

Ruggedness is a measure by which laboratory conditions are varied slightly e.g., slight variations in temperature, mobile phase, and flow rate (Dejaegher and Heyden., 2007). A variation in temperature, mobile phase and flow rate results in a shift iin the retention time as compared to the normal condition set up (Chulikhit *et al*., 2023).

3.1.4 Temperature Variation

The temperature in the column was adjusted according to the chromatographic conditions of each active compound. Temperature was shifted 0.5 °C above and below the designated chromatographic condition of each active compound (César and Pianetti, 2009).

3.1.4.1 Caffeine

Table 3.16 a-c reported on the temperature variation of Caffeine at 3 different concentrations: 20,150,200 µg/ml, where the average retention time for caffeine was found to be 2.52 ± 0.02 min.

Table 3.16a reports on the temperature variation of Caffeine (20 µg/ml). At the temperature of 19.5°C, a high variation was reported amongst each replicate. Due to the high variation in the lower concentration of caffeine, these values were omitted. The mean retention time (min) with the temperature variation, was found to be 2.54 ± 0.03 min. The %RSD of retention time was found to be < 2% and the %RSD of area under the curve was > 2%.

Table 8.16a: Temperature Variation of Caffeine **(20 µg/ml)**

Temperatures (°C)	Number of Replicates	Retention Time (Min)	Area (a)
19.5	Replicate 1	2.63	4792*
	Replicate 2	2.53	267985*
	Replicate 3	2.54	-*
20	Replicate 1	2.53	794527
	Replicate 2	2.52	806572
	Replicate 3	2.51	827857
20.5	Replicate 1	2.54	934594
	Replicate 2	2.51	934991
	Replicate 3	2.52	933843
Mean		2.51	872064
SD		0.03	69198
%RSD		1.3	7.9

*Values were omitted as it skewed the data.

Table 3.16b reported the temperature variation of Caffeine (150 µg/ml). The mean retention time (min) was reported as 2.53 ± 0.01 min, the retention time remained constant despite the temperature variation. The %RSD of retention time was found to be < 2% and the %RSD of area was > 2%.

Table 8.16b: Temperature Variation of Caffeine **(150 µg/ml)**

Temperatures (°C)	Number of Replicates	Retention Time (Min)	Area (a)
19.5	Replicate 1	2.54	2097704
	Replicate 2	2.54	1931931
	Replicate 3	2.54	1855520
20	Replicate 1	2.53	2361369
	Replicate 2	2.52	2432551
	Replicate 3	2.52	2481345
20.5	Replicate 1	2.52	2725051
	Replicate 2	2.52	2719376
	Replicate 3	2.52	2661897
Mean		2.53	2362971
SD		0.01	331664
%RSD		0.4	14.04

Table 3.16c reported the temperature variation of Caffeine (200 µg/ml). The mean retention time (min) was reported as 2.53 ± 0.02 min, there was a slight variation in the retention time but remained overall constant. The % RSD was found to be < 2% and the % RSD of the area was > 2%.

Table 8.16c- Temperature Variation of Caffeine **(200 µg/ml)**

Temperatures (°C)	Number of Replicates	Retention Time (Min)	Area (a)
19.5	Replicate 1	2.53	3320432
	Replicate 2	2.54	3398690
	Replicate 3	2.54	3461625
20	Replicate 1	2.57	3874530
	Replicate 2	2.56	3868300
	Replicate 3	2.51	3953333
20.5	Replicate 1	2.51	3937739
	Replicate 2	2.52	3942848
	Replicate 3	2.51	3942369
Mean		2.53	3744430
SD		0.02	267188
%RSD		0.8	7.14

3.1.4.2 Theophylline

Temperature was varied 0.5°C above and below the designated chromatographic condition of each active ingredient. Table 3.17a-c showed temperature variation of Theophylline at 3 different concentrations; 5, 10 and 25 µg/ml. From the table below, the average retention time at which Theophylline was detected by the HPLC machine was 2.1 ± 0.03 min. The area under the curve was constant throughout the temperature variation.

Table 3.17a reports on the temperature variation of Theophylline (5 µg/ml). The mean retention time (min) was reported as 2.10 ± 0.02 min and remained constant despite the temperature variation. The % RSD of the retention time was found < 2% and the % RSD of the area was > 2%.

Table 8.17a: Temperature Variation of Theophylline **(5 µg/ml)**

Temperatures (°C)	Number of Replicates	Retention Time (Min)	Area (a)
19.5	Replicate 1	2.08	412870
	Replicate 2	2.09	397571
	Replicate 3	2.10	391230
20	Replicate 1	2.12	383393
	Replicate 2	2.13	383465
	Replicate 3	2.12	393183
20.5	Replicate 1	2.08	374148
	Replicate 2	2.09	372670
	Replicate 3	2.08	374934
Mean		2.10	387052
SD		0.02	13128
%RSD		0.94	3.4

Table 3.17b illustrated the temperature variation of Theophylline (10 µg/ml). The mean retention time (min) was reported as 2.10 ± 0.03 min and remained constant despite the temperature variation. The % RSD for retention time and the area was < 2%.

Table 8.17b: Temperature Variation of Theophylline **(10 µg/ml)**

Temperatures (°C)	Number of Replicates	Retention Time (Min)	Area (a)
19.5	Replicate 1	2.10	686153
	Replicate 2	2.09	659026
	Replicate 3	2.10	657177
20	Replicate 1	2.12	679429
	Replicate 2	2.13	679199
	Replicate 3	2.12	681072
20.5	Replicate 1	2.07	687502
	Replicate 2	2.07	692106
	Replicate 3	2.06	695026
Mean		2.10	679632
SD		0.03	13361
%RSD		1.43	1.97

Table 3.17c illustrated the temperature variation of Theophylline (25 µg/ml). The mean retention time (min) was reported as 2.09 ± 0.03 min, the retention time remained

constant despite the temperature variation. The % RSD for retention time and the area was < 2%.

Table 8.17c: Temperature Variation of Theophylline **(25 µg/ml)**

Temperatures (°C)	Number of Replicates	Retention Time (Min)	Area (a)
19.5	Replicate 1	2.08	2307709
	Replicate 2	2.08	2299867
	Replicate 3	2.06	2325761
20	Replicate 1	2.13	2333842
	Replicate 2	2.13	2325325
	Replicate 3	2.12	2327913
20.5	Replicate 1	2.06	2301433
	Replicate 2	2.06	2313292
	Replicate 3	2.06	2339002
Mean		2.09	2319349
SD		0.03	14227
%RSD		1.43	0.61

3.1.4.3 Retinol

Table 3.18a-c illustrates temperature variation of Retinol at 3 different concentrations; 0.5, 2 and 4 µg/ml with the average retention of Retinol of 2.91 ± 0.02 min.
Table 3.18a illustrated the temperature variation of 1.0 µg/ml. The mean retention time (min) was reported as 2.92 ± 0.03 min. The % RSD of the retention time was found < 2%, while the % RSD of the area was > 2%.

Table 8.18a – Temperature Variation of Retinol **(1.0 µg/ml)**

Temperatures (°C)	Number of Replicates	Retention Time (Min)	Area (a)
19.5	Replicate 1	2.95	68408
	Replicate 2	2.94	69212
	Replicate 3	2.94	70827
20	Replicate 1	2.92	71422
	Replicate 2	2.92	72295
	Replicate 3	2.91	72417
20.5	Replicate 1	2.91	77976
	Replicate 2	2.90	72662
	Replicate 3	2.90	72480
Mean		2.92	71967
SD		0.03	2716
%RSD		1.03	3.77

Table 3.18b illustrated the temperature variation of Retinol (6.0 µg/ml). The mean retention time (min) was reported as 2.91 ± 0.02 min, there was no change in the retention time despite the temperature variation. The % RSD of the retention time was found < 2% and the % RSD of the area was > 2%.

Table 8.18b: Temperature Variation of Retinol **(6.0 µg/ml)**

Temperatures (°C)	Number of Replicates	Retention Time (Min)	Area (a)
19.5	Replicate 1	2.93	285562
	Replicate 2	2.93	290456
	Replicate 3	2.93	292237
20	Replicate 1	2.91	288248
	Replicate 2	2.91	287397
	Replicate 3	2.91	292138
20.5	Replicate 1	2.89	273958
	Replicate 2	2.88	301057
	Replicate 3	2.89	291136
Mean		2.91	289132
SD		0.02	7189
%RSD		0.69	2.49

Table 3.18c illustrated the temperature variation of Retinol (10 µg/ml). The mean retention time (min) was reported as 2.91 ± 0.01 min, there was no change in the

retention time despite the temperature variation. The % RSD for retention time and the area was < 2%.

Table 8.18c: Temperature Variation of Retinol **(10 µg/ml)**

Temperatures (°C)	Number of Replicates	Retention Time (Min)	Area (a)
19.5	Replicate 1	2.92	588176
	Replicate 2	2.92	589899
	Replicate 3	2.92	594048
20	Replicate 1	2.91	585733
	Replicate 2	2.91	587988
	Replicate 3	2.92	597519
20.5	Replicate 1	2.88	588238
	Replicate 2	2.90	592320
	Replicate 3	2.89	590324
Mean		2.91	590472
SD		0.01	3625
%RSD		0.51	0.61

3.1.4.4 L-carnitine

Table 3.19a-c reports the temperature variation of L-carnitine at different concentrations; 300, 500 and 700 µg/ml with the average retention time of L-carnitine detected at 2.97 ± 0.009 min.

Table 3.19a illustrates the temperature variation of L-carnitine (300 µg/ml). The mean retention time (min) was reported as 2.98 ± 0.006 min, the retention time remained constant despite the variation in temperature. The % RSD for retention time and the area was < 2%.

Table 8 19a: Temperature Variation of L-carnitine **(300µg/ml)**

Temperatures (°C)	Number of Replicates	Retention Time (Min)	Area (a)
39.5	Replicate 1	2.98	31919
	Replicate 2	2.99	32316
	Replicate 3	2.99	32426
40	Replicate 1	3.00	32892
	Replicate 2	3.00	32635
	Replicate 3	3.00	32692
40.5	Replicate 1	2.99	33494
	Replicate 2	2.99	33435
	Replicate 3	2.97	33000
Mean		2.98	32757
SD		0.006	513
%RSD		0.20	1.57

Table 3.19b illustrates the temperature variation of L-carnitine (500 µg/ml). The mean retention time (min) was reported as 2.98 ± 0.014 min, the retention time remained constant despite the variation in temperature. The % RSD for retention time and the area was < 2%.

Table 8.19b: Temperature Variation of L-carnitine **(500 µg/ml)**

Temperatures (°C)	Number of Replicates	Retention Time (Min)	Area (a)
39.5	Replicate 1	2.99	43725
	Replicate 2	2.99	44357
	Replicate 3	2.99	43746
40	Replicate 1	3.00	41693
	Replicate 2	3.00	41540
	Replicate 3	3.00	71254*
40.5	Replicate 1	2.97	44561
	Replicate 2	2.96	44190
	Replicate 3	2.96	44392
Mean		2.98	43526
SD		0.014	1216
%RSD		0.5	2.79

*Values were omitted as it skewed the data.

Table 3.19c the temperature variation of L- carnitine (700 µg/ml). The mean retention time (min) was reported as 2.96 ± 0.013 min, the retention time remained constant

despite the variation in temperature. The % RSD for retention time and the area was < 2%.

Table 8.19c: Temperature Variation of L-carnitine **(700 µg/ml)**

Temperatures (°C)	Number of Replicates	Retention Time (Min)	Area (a)
39.5	Replicate 1	2.98	63625
	Replicate 2	2.97	64423
	Replicate 3	2.97	63158
40	Replicate 1	3.00	63341
	Replicate 2	3.00	62774
	Replicate 3	3.00	63898
40.5	Replicate 1	2.95	62819
	Replicate 2	2.95	63662
	Replicate 3	2.95	62529
Mean		2.96	63359
SD		0.013	68607
%RSD		0.43	0.96

3.1.4.5 Co-enzyme Q10

Coenzyme Q_{10} (CoQ_{10}) is a highly lipophilic molecule found naturally in the phospholipid bilayer membrane in every single cell in the body (Borekova *et al*., 2008). HPLC has been found to be an advantageous tool in determining the estimation of lipophilicity of a particular molecule, which is important when it comes to the pharmacodynamic and pharmacokinetic properties of a drug (Elmansi *et al*.,2019). In the instance of applying temperature variation to CoQ_{10} the area calculated was not consistent. There were extensive variations in the areas of the peaks and coenzyme Q_{10} tended to increase pressure of the column resulting in blocking of the guard column.

Table 3.20a-c illustrates the temperature variation of Coenzyme Q_{10} at different concentrations; 0.1, 10 and 100 µg/ml. The retention time of Coenzyme Q_{10} was detected through HPLC at 2.94 ± 0.009 min.

Table 3.20a illustrates the temperature variation of 0.1 µg/ml. The mean retention time (min) was reported as 2.91 ± 0.12. The Coenzyme Q_{10} retention time decreased with increased temperature. The % RSD for retention time and the area was > 2%.

Table 8.20a: Temperature Variation of Coenzyme Q10 **(0.1 µg/ml)**

Temperatures (°C)	Number of Replicates	Retention Time (Min)	Area (a)
24	Replicate 1	3.00	15299
	Replicate 2	3.00	14478
	Replicate 3	3.00	12689
25	Replicate 1	2.96	29470
	Replicate 2	2.97	184799*
	Replicate 3	2.97	28943
26	Replicate 1	2.75	17552
	Replicate 2	2.76	8238*
	Replicate 3	2.74	10899
Mean		2.91	18475
SD		0.12	7619
%RSD		4.05	41.24

*Values were omitted as it skewed the data.

Table 3.20b illustrates the temperature variation of Coenzyme Q_{10} (10 µg/ml). The mean retention time (min) was reported as 2.93 ± 0.16 min. The Coenzyme Q_{10} retention time decreased with increased temperature. The % RSD for retention time and the area was > 2%. At the low concentration range, the data varies thus leading to inaccurate data.

Table 8.20b: Temperature Variation of Coenzyme Q10 **(10 µg/ml)**

Temperatures (°C)	Number of Replicates	Retention Time (Min)	Area (a)
24	Replicate 1	3.10	40984*
	Replicate 2	3.09	102283
	Replicate 3	3.10	114563
25	Replicate 1	2.97	1056569*
	Replicate 2	2.96	179147
	Replicate 3	2.96	296191
26	Replicate 1	2.74	459966
	Replicate 2	2.74	-
	Replicate 3	2.74	417111
Mean		2.93	261543
SD		0.16	153967.2
%RSD		5.32	58.9

*Values were omitted as it skewed the data.

Table 3.20c the temperature variation of Coenzyme Q_{10} (100 µg/ml). The mean retention time (min) was reported as 2.97 ± 0.12 min. The Coenzyme Q_{10} retention time decreased with increased temperature. The % RSD for retention time and the area was > 2%. Coenzyme Q_{10} is an unstable compound, when injected in the HPLC columns it would easily block the column. This therefore resulted in some inaccurate data and integration of peaks by the software.

Table 8.20c: Temperature Variation of Coenzyme Q10 **(100 µg/ml).**

Temperatures (°C)	Number of Replicates	Retention Time (Min)	Area (a)
24	Replicate 1	3.09	1337546
	Replicate 2	3.08	793191*
	Replicate 3	3.08	1204816
25	Replicate 1	2.94	1289908
	Replicate 2	2.95	1173831
	Replicate 3	2.95	2062258
26	Replicate 1	2.75	233186*
	Replicate 2	ND	ND
	Replicate 3	ND	ND
Mean		2.97	1178060
SD		0.12	368415
%RSD		4.08	26

*Values were omitted as it skewed the data.

3.1.5 Mobile Phase Variation

Mobile phase plays a critical role in (HPLC). The solvent is responsible for moving the sample through the system to reach the stationary phase where identification of the separated components occur (Kupiec, 2004). The organic component of the mobile phase was adjusted according to the chromatographic conditions of each active ingredient. Furthermore, the organic component of the mobile phase concentration for each active compound was adjusted by 0.5% in a way that the total ratio adds up to 100%. In the case of theophylline, mobile phase was increased by 1%.

3.1.5.1 Caffeine

Table 3.21a-c showed mobile variation of caffeine at different concentrations (10,170 and 200 µg/ml) as well as the respective mean ± SD. For caffeine, the normal chromatic condition was 40% methanol and 60% water. The tables below showed that the retention time was not constant as the organic component of the mobile phase varied.

In Table 3.21a, the mobile phase ratio at 39.5:60.5 (methanol: water) had a retention time of 2.46 ± 0.06 min while at 40.5:59.5 (methanol: water), the retention time was 2.35± 0.025 min.

Table 8.21a: Mobile phase variation of Caffeine **(10 µg/ml).**

Mobile phase	Number of Replicates	Retention Time (min) ± SD	Area (a)
39.5 : 60.5	Replicate 1	2.47	487162
	Replicate 2	2.47	536148
	Replicate 3	2.43	496250
	Mean	**2.46**	**506520**
	SD	**0.06**	**26058**
	%RSD	**2.34**	**5.14**
40 : 60	Replicate 1	2.57	607909*
	Replicate 2	2.57	434661
	Replicate 3	2.57	400320
	Mean	**2.57**	**417491**
	SD	**0**	**24282.75**
	%RSD	**0**	**5.8**
40.5 : 59.5	Replicate 1	2.35	454036
	Replicate 2	2.32	456267
	Replicate 3	2.37	454020
	Mean	**2.35**	**464858**
	SD	**0.025**	**13128**
	%RSD	**1.07**	**8.89**

*Values were omitted as it skewed the data.

In Table 3.21b, the mobile phase ratio at 39.5:60.5 (methanol: water) had a retention time of 2.47 ± 0.017 min while at 40.5:59.5 (methanol: water), the retention time was 2.24 ± 1.32 min. The retention time decreased as the % organic component of the mobile phase increased.

Table 8.21b: Mobile phase variation of Caffeine **(170 µg/ml).**

Mobile phase	Number of Replicates	Retention Time (min) ± SD	Area (a)
39.5 : 60.5	Replicate 1	2.47	3638992
	Replicate 2	2.45	3629178
	Replicate 3	2.49	3527414
	Mean	**2.47**	**3598528**
	SD	**0.017**	**61781**
	%RSD	**0.68**	**1.72**
40 : 60	Replicate 1	2.31	3874530
	Replicate 2	2.34	3868300
	Replicate 3	2.37	4021440
	Mean	**2.34**	**392143**
	SD	**0.03**	**8667**
	%RSD	**1.23**	**2.21**
40.5 : 59.5	Replicate 1	2.21	3297923
	Replicate 2	2.25	3287145
	Replicate 3	2.27	3174220
	Mean	**2.24**	**3591016**
	SD	**0.030**	**296288**
	%RSD	**1.32**	**8.25**

In Table 3.21c, the mobile phase ratio at 39.5:60.5 (methanol: water) had a retention time of 2.51 ± 0.063 min while at 40.5:59.5 (methanol: water) mobile phase ratio the retention time 2.49 ± 0.03 min. The retention time remained relatively constant as the mobile phase ratio was varied.

Table 8.21c: Mobile phase variation of Caffeine **(200 µg/ml).**

Mobile phase	Number of Replicates	Retention Time (min) ± SD	Area (a)
39.5: 60.5	Replicate 1	2.58	4013523
	Replicate 2	2.47	4004797
	Replicate 3	2.47	4005802
	Mean	**2.51**	**4008041**
	SD	**0.063**	**4774.61**
	%RSD	**2.49**	**0.12**
40: 60	Replicate 1	2.46	4011585
	Replicate 2	2.43	4003412
	Replicate 3	2.43	3999021
	Mean	**2.43**	**4004673**
	SD	**0.015**	**6376**
	%RSD	**0.63**	**0.16**
40.5: 59.5	Replicate 1	2.45	4010379
	Replicate 2	2.51	4012918
	Replicate 3	2.50	4016647
	Mean	**2.49**	**4013315**
	SD	**0.03**	**3153**
	%RSD	**1.28**	**0.079**

3.1.5.2 Theophylline

Table 3.22a-c shows mobile phase ratio variation at different concentrations (4, 10 and 25 µg/ml) of theophylline. The HPLC mobile phase chromatic condition for Theophylline was 40% methanol and 60% water. The tables below illustrated the variation of the organic component of the mobile phase. The organic component of the mobile phase was adjusted by 1%. There was no particular reason why this amount was chosen, as mentioned in a study conducted by Pal and colleagues, the study proved that small and deliberate changes to flow rate (± 0.2 ml/min), column temperature (± 5 °), mobile and, phase and pH (± 0.2) have an effect on the retention time (Pal and Sundararajan, 2022).

In Table 3.22a, the mobile phase ratio at 39:61 (methanol: water) had a retention time of 2.23 ± 0.0019 min while at 41:59 (methanol: water) mobile phase ratio the retention time was 2.17 ± 0.0023 min. In normal chromatic condition, the retention time was shorter (2.17 ± 0.002 min) as compared to the mobile phase ratio at 39:61 (methanol:

water). The retention time decreased as the % organic component of the mobile phase increased.

Table 8.22a: Mobile phase variation of Theophylline **(4 µg/ml).**

Mobile Phase	Number of Replicates	Retention Time (min) ± SD	Area (a)
39: 61	Replicate 1	2.23	323851
	Replicate 2	2.23	323119
	Replicate 3	2.23	323841
	Mean	**2.23**	**323604**
	SD	**0.0019**	**420**
	%RSD	**0.087**	**0.13**
40: 60	Replicate 1	2.17	355324
	Replicate 2	2.18	355587
	Replicate 3	2.17	356253
	Mean	**2.17**	**355722**
	SD	**0.002**	**479**
	%RSD	**0.11**	**0.13**
41: 59	Replicate 1	2.17	319881
	Replicate 2	2.17	319473
	Replicate 3	2.17	318544
	Mean	**2.17**	**319300**
	SD	**0.0023**	**685**
	%RSD	**0.11**	**0.21**

In Table 3.22b, the mobile phase ratio at 39:61 (methanol: water) had a retention time of 2.08 ± 0.0088 min while at 41:59 (methanol: water) mobile phase ratio the retention time was 2.04 ± 0.012 min. In normal chromatic conditions, the retention time was 2.17 ± 0.0073 min. The retention time remained relatively constant as the mobile phase ratio was varied.

Table 8.22b: Mobile phase variation of Theophylline **(8 µg/ml).**

Mobile Phase	Number of Replicates	Retention Time (min) ± SD	Area (a)
39: 61	Replicate 1	2.07	699806
	Replicate 2	2.09	704733
	Replicate 3	2.08	693721
	Mean	**2.08**	**699420**
	SD	**0.0088**	**5516**
	%RSD	**0.42**	**0.79**
40: 60	Replicate 1	2.18	651648
	Replicate 2	2.17	650767
	Replicate 3	2.18	651069
	Mean	**2.17**	**651161**
	SD	**0.0073**	**447**
	%RSD	**0.33**	**0.069**
41: 59	Replicate 1	2.03	676685
	Replicate 2	2.05	693620
	Replicate 3	2.05	693803
	Mean	**2.04**	**688036**
	SD	**0.012**	**9831**
	%RSD	**0.59**	**1.43**

In Table 3.22c, the mobile phase ratio at 39:61 (methanol: water) had a retention time of 2.10 ± 0.017 min while at 41:59 (methanol: water) mobile phase ratio the retention time was 2.05 min ± 1.50. In normal chromatic conditions, the retention time was 2.12 min ± 0.0045. The retention time decreased at the higher % of organic phase component.

Table 8.22c: Mobile phase variation of Theophylline **(25 µg/ml).**

Mobile Phase	Number of Replicates	Retention Time (min) ± SD	Area (a)
39:61	Replicate 1	2.12	2297459
	Replicate 2	2.11	2284188
	Replicate 3	2.08	2296030
	Mean	**2.10**	**2292559**
	SD	**0.017**	**7285**
	% RSD	**0.81**	**0.32**
40:60	Replicate 1	2.12	2333841
	Replicate 2	2.13	2325325
	Replicate 3	2.12	2327913
	Mean	**2.12**	**2329026**
	SD	**0.0045**	**4366**
	% RSD	**0.21**	**0.19**
41: 59	Replicate 1	2.08	2323880
	Replicate 2	2.03	2327866
	Replicate 3	2.03	2327325
	Mean	**2.05**	**2326357**
	SD	**0.031**	**2162**
	% RSD	**1.50**	**0.093**

3.1.5.3 Retinol

Table 3.23a-c shows the mobile phase ratio variation at different concentrations (1 µg/ml, 5 µg/ml, and 10 µg/ml) of retinol. The HPLC mobile phase chromatic condition for retinol was 95% methanol and 5% water. The tables below illustrate the variation of the organic component of the mobile as the retention time altered the organic phase component was adjusted by 0.5%, which adds the total ratio to 100%. However, due to the lipophilic nature of Retinol the results obtained were inconsistent. This resulted in missing data at different replicates.

In Table 3.23a, the mobile phase ratio at 94.5:5.5 (methanol: water) had a retention time of 2.80 min while at 95.5: 4.5 (methanol: water) mobile phase ratio, the retention time was 2.82 ± 0.081 min. The retention time decreased at the higher % of organic phase component.

Table 8.23a: Mobile phase variation of Retinol **(1.0 µg/ml).**

Mobile Phase	Number of Replicates	Retention Time (min) ± SD	Area (a)
94.5: 5.5	Replicate 1	2.80	74747
	Replicate 2	ND	ND
	Replicate 3	ND	ND
	Mean	**2.80**	**74747**
	SD	**ND**	**ND**
	% RSD	**ND**	**ND**
95.0: 5.0	Replicate 1	2.92	74429
	Replicate 2	2.92	75339
	Replicate 3	2.92	75465
	Mean	**2.92**	**75078**
	SD	**0.004**	**565**
	% RSD	**0.0014**	**0.75**
95.5: 4.5	Replicate 1	2.92	78457
	Replicate 2	2.77	73657
	Replicate 3	2.78	73566
	Mean	**2.82**	**75094**
	SD	**0.081**	**1657**
	% RSD	**2.87**	**2.21**

*ND: Not determined. The mobile phase ratio of 94.5:5.5 was re-evaluated however no area value was determined.

In Table 3.23b, the mobile phase ratio at 94.5:5.5 (methanol: water) had a retention time of 3.0 ± 0.0036 min while at 95.5: 4.5 (methanol: water) organic phase ratio the retention time was 2.77 ± 0.0016 min. In normal chromatic conditions, the retention time was 2.92 ± 0.0076 min. The retention time decreased as the % organic component of the mobile phase increased.

Table 8.23b: Mobile phase variation of Retinol **(5 µg/ml).**

Mobile Phase	Number of Replicates	Retention Time (min) ± SD	Area (a)
94.5: 5.5	Replicate 1	3.00	271173
	Replicate 2	2.99	273795
	Replicate 3	3.00	276450
	Mean	**3.00**	**273806**
	SD	**0.0036**	**2638**
	% RSD	**0.12**	**0.96**
95: 5.0	Replicate 1	2.91	882037
	Replicate 2	2.92	879434
	Replicate 3	2.90	893943
	Mean	**2.92**	**885139**
	SD	**0.0076**	**7735**
	% RSD	**0.26**	**0.87**
95.5: 4.5	Replicate 1	2.77	280969
	Replicate 2	2.77	285605
	Replicate 3	ND	ND
	Mean	**2.77**	**291594**
	SD	**0.0016**	**22397**
	% RSD	**0.058**	**7.68**

*ND: Not Determined

In Table 3.23c, the mobile phase ratio at 94.5:5.5 (methanol: water) had a retention time of 2.99 min and the SD was not determined due to the concentration replicates not being detected. In the mobile phase of 95.5: 4.5 (methanol: water), the retention time was 2.77 ± 0.002 min. In normal chromatic conditions, the retention time was 2.90 ± 0.0012 min. The retention time decreased at the higher % of organic phase component.

Table 8.23c: Mobile phase variation of Retinol **(10 µg/ml).**

Mobile Phase	Number of Replicates	Retention Time (min) ± SD	Area (a)
94.5: 5.5	Replicate 1	2.99	599003
	Replicate 2	ND	ND
	Replicate 3	ND	ND
	Mean	2.99	**599003**
	SD	ND	ND
	% RSD	ND	ND
95: 5.0	Replicate 1	2.90	1886059
	Replicate 2	2.90	1893321
	Replicate 3	2.90	1924012
	Mean	**2.90**	**1901131**
	SD	**0.0012**	**20145**
	% RSD	**0.042**	**1.06**
95.5: 4.5	Replicate 1	2.77	587988
	Replicate 2	2.77	597519
	Replicate 3	ND	ND
	Mean	**2.77**	**588657**
	SD	**0.002**	**21953**
	% RSD	**0.076**	**3.73**

*ND: Not Determined. The mobile phase ratio of 94.5:5.5 was re-evaluated however no area value was determined.

3.1.5.4 L- carnitine

Table 3.24a-c shows the mobile phase ratio variation at different concentrations (300, 500 and 1000 µg/ml) of L-carnitine. The HPLC mobile phase chromatic condition for L-carnitine was 99% sodium phosphate buffer and 1% methanol. The tables below illustrated the variation of the organic component of the mobile phase. The organic phase component was adjusted by 0.5%, which adds the total ratio to 100%. Mobile phase was not run at 100% sodium phosphate buffer (pH 3) as this resulted in the column being completely blocked.

In Table 3.24a, the mobile phase ratio at 99.5:0.5 (buffer: methanol) had a retention time of 2.97 ± 0.0043 min. The retention time remained constant as the mobile phase ratio was varied.

Table 8.24a: Mobile phase variation of L-carnitine **(300 µg/ml).**

Mobile Phase	Number of Replicates	Retention Time (min) ± SD	Area (a)
99.5: 0.5	Replicate 1	2.97	33338
	Replicate 2	2.98	32340
	Replicate 3	2.98	32031
	Mean	**2.97**	**32570**
	SD	**0.0043**	**683**
	% RSD	**0.14**	**2.10**
99.0: 1.0	Replicate 1	2.98	32576
	Replicate 2	2.97	32409
	Replicate 3	2.97	32369
	Mean	**2.98**	**32511**
	SD	**0.0021**	**442**
	% RSD	**0.00073**	**1.36**

ND: Not Determined

In Table 3.24b, the mobile phase ratio at 99.5:0.5 (buffer: methanol) had a retention time of 2.96 ± 0.002 min. The retention time remained constant as the mobile phase ratio was varied.

Table 8.24b: Mobile phase variation of L-carnitine **(500 µg/ml)**.

Mobile Phase	Number of Replicates	Retention Time (min) ± SD	Area (a)
99.5: 0.5	Replicate 1	2.97	44348
	Replicate 2	2.96	44187
	Replicate 3	2.96	43936
	Mean	**2.96**	**44158**
	SD	**0.002**	**208**
	% RSD	**0.073**	**0.47**
99: 1	Replicate 1	2.97	44463
	Replicate 2	2.96	44288
	Replicate 3	2.96	43922
	Mean	**2.97**	**44225**
	SD	**0.002**	**276**
	% RSD	**0.069**	**0.62**

In Table 3.24c, the mobile phase ratio at 99.5:0.5 (buffer: methanol) had a retention time of 2.95 ± 0.0028 min. In normal chromatic condition, the retention time was 2.95 min ± 0.0017 min. The retention time remained constant as the mobile phase ratio was varied.

Table 8.24c: Mobile phase variation of L-carnitine **(1000 µg/ml).**

Mobile Phase	Number of Replicates	Retention Time (min) ± SD	Area (a)
99.5: 0.5	Replicate 1	2.95	71457
	Replicate 2	2.95	70190
	Replicate 3	2.95	69717
	Mean	**2.95**	**70455**
	SD	**0.0028**	**900**
	% RSD	**0.096**	**1.28**
99: 1	Replicate 1	2.95	70956
	Replicate 2	2.95	70523
	Replicate 3	2.95	70383
	Mean	**2.95**	**70621**
	SD	**0.0017**	**299**
	% RSD	**0.058**	**0.42**

3.1.5.5 Co-enzyme Q_{10}

As previously mentioned in section 3.1.3.1.5, Coenzyme Q_{10} (CoQ_{10}) is a highly lipophilic molecule found naturally in the phospholipid bilayer membrane in every single cell in the body (Borekova *et al*., 2008). In the instance of applying mobile phase variation to CoQ_{10} the area calculated was not consistent. There were extensive variations in the areas of the peaks and coenzyme Q_{10} tended to cause increase in pressure of the column resulting in blocking of the guard column.

Table 3.25a-c shows the mobile phase ratio variation at different concentrations (0.1 µg/ml, 10 µg/ml, and 100 µg/ml) of Coenzyme Q_{10}. The HPLC mobile phase chromatic condition for retinol was 40% methanol and 60% 2-propanol. The tables below illustrate the variation of the organic component of the mobile. The organic phase

component was adjusted by 0.5%, which adds the total ratio to 100%. However, due to the lipophilic nature of Coenzyme Q_{10} the results obtained were inconsistent for the areas. This resulted in missing data at different replicates and large variation in areas obtained.

In Table 3.25a, the mobile phase ratio at 39.5:60.5 (methanol: 2-propanol) had a retention time of 2.96 ± 0.05 min while at 40.5: 59.5 (methanol: 2-propanol) mobile phase ratio, the retention time was 3.03 min ± 0.01. The retention time remained constant as the % of organic component in the mobile phase changed.

Table 8.25a: Mobile phase variation of Coenzyme Q10 **(0.1 µg/ml).**

Mobile Phase	Number of Replicates	Retention Time (min) ± SD	Area (a)
39.5: 60.5	Replicate 1	2.89	1576*
	Replicate 2	2.99	16679
	Replicate 3	2.99	2618*
	Mean	**2.96**	ND
	SD	**0.05**	ND
	% RSD	1.64	ND
40: 60	Replicate 1	3.03	14803
	Replicate 2	3.05	23906
	Replicate 3	3.05	4987*
	Mean	**3.04**	**19354**
	SD	**0.01**	**6437**
	% RSD	**0.38**	**33.26**
40.5: 59.5	Replicate 1	3.03	2705*
	Replicate 2	3.03	22951
	Replicate 3	3.04	1759*
	Mean	3.03	ND
	SD	0.01	ND
	% RSD	0.19	ND

*ND: Not Determined. Values were omitted as it skewed the data.

In Table 3.25b, the mobile phase ratio at 39.5:60.5 (methanol: 2-propanol) had a retention time of 2.99 ± 0.01 min while at 40.5: 59.5 (methanol: 2-propanol) mobile phase ratio, the retention time was 3.05 min. The retention time remained constant as the % of organic component in the mobile phase changed.

Table 8.25b: Mobile phase variation of Coenzyme Q10 **(10 µg/ml**).

Mobile Phase	Number of Replicates	Retention Time (min) ± SD	Area (a)
39.5: 60.5	Replicate 1	2.98	250735
	Replicate 2	2.99	8633*
	Replicate 3	2.99	22828*
	Mean	**2.99**	ND
	SD	**0.01**	ND
	% RSD	**0.16**	ND
40: 60	Replicate 1	3.06	150351
	Replicate 2	3.05	24750*
	Replicate 3	3.05	17597*
	Mean	**3.05**	ND
	SD	**0.01**	ND
	% RSD	**0.19**	ND
40.5: 59.5	Replicate 1	3.05	4515*
	Replicate 2	ND	ND
	Replicate 3	ND	ND
	Mean	3.05	ND
	SD	ND	ND
	% RSD	ND	ND

*ND: Not Determined. Values were omitted as it skewed the data.

In Table 3.25c, the mobile phase ratio at 39.5:60.5 (methanol: 2-propanol) had a retention time of 2.99 min while at 40.5: 59.5 (methanol: 2-propanol) mobile phase ratio, the retention time was 3.05 min. The retention time remained constant as the % of organic component in the mobile phase changed. As mentioned prior, coenzyme Q_{10} is known to be an unstable compound that has a tendency of blocking the HPLC columns which results in unreliable data.

Table 8.25c: Mobile phase variation of Coenzyme Q10 **(100 µg/ml).**

Mobile Phase	Number of Replicates	Retention Time (min) ± SD	Area
39.5: 60.5	Replicate 1	2.99	297284
	Replicate 2	2.99	30023
	Replicate 3	2.99	50671
	Mean	2.99	ND
	SD	0	ND
	% RSD	-	ND
40: 60	Replicate 1	3.04	81716
	Replicate 2	3.03	106163
	Replicate 3	3.00	89189
	Mean	**3.02**	ND
	SD	**0.02**	ND
	% RSD	**0.69**	ND
40.5: 59.5	Replicate 1	3.05	22834
	Replicate 2	ND	ND
	Replicate 3	ND	ND
	Mean	3.05	ND
	SD	ND	ND
	% RSD	ND	ND

*ND: Not Determined

3.1.6 Flow Rate Variation

Flow rate impacts HPLC system pressure, chromatographic quality, and analysis time. A higher than usual flow rate may adversely affect the quality of the chromatography not giving the analyte sufficient time to interact with the stationary phase and to be detected. While a lower than usual flow rate may leave the analyst waiting for the peak to appear at the detector (Tarafder, Vajda and Guiochon, 2013). The Flow rate chromatographic condition of each active compounds was 1.0 ml/min, which was adjusted to 0.95 and 1.1 ml/min to obtain flow rate variation. The remaining HPLC condition such as temperature and mobile phase remained the same as described in section 2.1.5.

3.1.6.1 Caffeine

Table 3.26 shows the flow rate variation at 150 µg/ml. The retention times decreased as the flow rate increased. A slight decrease in the mean area of the peaks obtained was observed as the flow rate increased.

Table 8.26: Flow rate variation of Caffeine **(150 µg/ml).**

Flow rate (ml/min)	Number of Replicates	Retention Time (min)	Area (a)
0.95	Replicate 1	2.60	3937505
	Replicate 2	2.59	3939004
	Replicate 3	2.60	3928812
	Mean	**2.60**	**3935107**
	SD	**0.01**	**5503**
	%RSD	**0.22**	**0.14**
1.00	Replicate 1	2.46	3712102
	Replicate 2	2.46	3726401
	Replicate 3	2.45	3732940
	Mean	**2.46**	**3723814**
	SD	**0.01**	**10657**
	%RSD	**0.24**	**0.29**
1.10	Replicate 1	2.34	3565260
	Replicate 2	2.34	3558647
	Replicate 3	2.34	3574303
	Mean	**2.34**	**3566070**
	SD	**0**	**7860**
	%RSD	**-**	**0.22**

3.1.6.2 Theophylline

Table 3.27a-c showed flow rate variation at different concentrations (5, 10 and 25 µg/ml). The HPLC flow rate chromatic condition for Theophylline was 1ml/min. In this instance, the adjustments for flow rate variation were made by 1 ml/min instead of 0.5 ml/min. This is due to the lipophilic property of theophylline which may take longer for the compound to be detected by HPLC.

In table 3.27a, the retention time obtained at 1ml/min (2.98 ± 0.0038 min) was longer than the retention time obtained at 0.95 ml/min (2.09 ± 0.0091 min) and 1.1 ml/min (2.19 ± 0.016). The adjustment in flow rate shortens the retention time at which theophylline was detected in the HPLC machine.

Table 8.27a: Flow rate variation of Theophylline **(5 µg/ml).**

Flow rate (ml/min)	Number of Replicates	Retention Time (min)	Area (a)
0.90	Replicate 1	2.10	25808.14
	Replicate 2	2.10	25614.54
	Replicate 3	2.08	25932.84
	Mean	2.09	25785.17
	SD	0.0091	160.39
	%RSD	0.004	0.62
1.00	Replicate 1	2.07	409201.62
	Replicate 2	2.08	407801.82
	Replicate 3	2.07	405980.17
	Mean	2.98	407661.20
	SD	0.0038	1615.32
	%RSD	0.13	0.40
1.10	Replicate 1	2.20	34149.35
	Replicate 2	2.20	38128.47
	Replicate 3	2.17	-
	Mean	2.19	36138
	SD	0.016	2813.66
	%RSD	0.73	7.79

In table 3.27b, the retention time obtained at 1ml/min (2.07 ± 0.0084) and 0.90 ml/min (2.08 ± 0.002) was shorter than the retention time obtained at 1.1 ml/min (2.16 ± 0.017). The adjustment in flow rate at 1.1 ml/min increased the retention time at which theophylline was detected in the HPLC machine. Overall, the variation in flow rate impacted on the peak areas for all theophylline however, the optimal result was found at a flow rate of 1ml/min.

Table 8.27b: Flow rate variation of Theophylline **(10 µg/ml).**

Flow rate (ml/min)	Number of Replicates	Retention Time (min)	Area (a)
0.90	Replicate 1	2.08	41163
	Replicate 2	2.09	39874
	Replicate 3	2.08	37380
	Mean	2.08	39472.15
	SD	0.002	1923.10
	%RSD	0.096	4.87
1.00	Replicate 1	2.08	683541
	Replicate 2	2.07	692397
	Replicate 3	2.06	699547
	Mean	2.07	691828
	SD	0.0084	8017.79
	%RSD	0.41	1.16
1.10	Replicate 1	2.17	41220
	Replicate 2	2.17	41764
	Replicate 3	2.14	53585
	Mean	2.16	45523.33
	SD	0.017	6987.17
	%RSD	0.79	15.35

In table 3.27c, the retention time obtained at 1ml/min (2.06 ± 0.0084 min) was shorter than the retention time obtained at 0.90 ml/min (2.11 ± 0.011 min) and 1.1 ml/min (2.16 ± 0.017 min). The adjustment in flow rate increased the retention time at which theophylline was detected in the HPLC machine.

Table 8.27c: Flow rate variation of Theophylline **(25 µg/ml).**

Flow rate (ml/min)	Number of Replicates	Retention Time (min)	Area
0.90	Replicate 1	2.10	34249
	Replicate 2	2.12	31206
	Replicate 3	2.11	29740
	Mean	2.11	31732
	SD	0.011	2299.95
	%RSD	0.52	7.25
1.00	Replicate 1	2.06	2316696
	Replicate 2	2.06	2321443
	Replicate 3	2.07	2336938
	Mean	2.06	2325026
	SD	0.0038	10585.58
	%RSD	0.18	0.46
1.10	Replicate 1	2.14	72544
	Replicate 2	2.16	63819
	Replicate 3	2.18	62296
	Mean	2.16	66219.75
	SD	0.017	5529.67
	%RSD	0.79	8.35

3.1.6.3 Retinol

Table 3.28a-c showed flow rate variation at different concentrations (0.5, 2 and 4 µg/ml). The HPLC flow rate chromatic condition for Retinol was 1ml/min. In this instance, the adjustments for flow rate variation were made by 1 ml/min instead of 0.5 ml/min. This is due to the fact that Retinol is a lipophilic agent and therefore takes longer to be detected by HPLC.

In table 3.28a, the retention time obtained at 1ml/min (3.03 ± 0.004 min) was longer than the retention time obtained at 0.90 ml/min (2.89 ± 0.002 min) and 1.1 ml/min (2.63 ± 0.0081). The adjustment in flow rate decreased the retention time at which retinol was detected in the HPLC machine.

Table 8.28a: Flow rate variation of Retinol **(0.5 µg/ml).**

Flow rate (ml/min)	Number of Replicates	Retention Time (min)	Area (a)
0.90	Replicate 1	2.89	68832
	Replicate 2	2.89	69536
	Replicate 3	2.89	70167
	Mean	2.89	69511.84
	SD	0.002	667.85
	%RSD	0.069	0.96
1.00	Replicate 1	3.04	71422
	Replicate 2	3.03	72295
	Replicate 3	3.03	72417
	Mean	3.03	72044.67
	SD	0.004	542.68
	%RSD	0.0031	0.75
1.10	Replicate 1	2.63	69157.96
	Replicate 2	2.64	65162.04
	Replicate 3	2.64	64557
	Mean	2.63	66292.33
	SD	0.0081	2500.07
	%RSD	0.31	3.77

In table 3.28b, the retention time obtained at 1ml/min (3.03 ± 0.0031 min) was longer than the retention time obtained at 0.90 ml/min (2.88 ± 0.0058 min) and 1.1 ml/min (2.63 ± 0.005 min). The adjustment in flow rate decreased the retention time at which retinol was detected in the HPLC.

Table 8.28b: Flow rate variation of Retinol **(2 µg/ml).**

Flow rate (ml/min)	Number of Replicates	Retention Time (min)	Area (a)
0.90	Replicate 1	2.89	259730
	Replicate 2	2.88	262059
	Replicate 3	2.89	262866
	Mean	2.88	261551.57
	SD	0.0058	1628.61
	%RSD	0.20	0.62
1.00	Replicate 1	3.03	374653
	Replicate 2	3.03	375548
	Replicate 3	3.04	376150
	Mean	3.03	375450.4
	SD	0.0031	753
	%RSD	0.13	0.20
1.10	Replicate 1	2.63	237004
	Replicate 2	2.63	241567
	Replicate 3	2.62	239269
	Mean	2.63	239280
	SD	0.005	2281.41
	%RSD	0.19	0.95

In table 3.28c, the retention time obtained at 1ml/min (2.79 ± 0.21) was shorter than the retention time obtained at 0.90 ml/min (2.89 ± 0.0052) and longer than the retention time obtained at 1.1 ml/min (2.63 ± 0.005).

Table 8.28c: Flow rate variation of Retinol **(4 µg/ml).**

Flow rate (ml/min)	Number of Replicates	Retention Time (min)	Area (a)
0.90	Replicate 1	2.88	570076.67
	Replicate 2	2.89	576028.96
	Replicate 3	2.89	573342.80
	Mean	2.89	573149.48
	SD	0.0052	2980.85
	%RSD	0.18	0.52
1.00	Replicate 1	2.65	529681
	Replicate 2	2.65	528470
	Replicate 3	3.03	527316
	Mean	2.79	528489.1
	SD	0.21	1182.74
	%RSD	7.53	0.22
1.10	Replicate 1	2.62	522532.15
	Replicate 2	2.63	524948.63
	Replicate 3	2.63	527744.27
	Mean	2.63	525075.02
	SD	0.0050	2608.36
	%RSD	0.19	0.50

3.1.6.4 L-carnitine

Table 3.29a-c showed flow rate variation at different concentrations (300, 500 and 1000 µg/ml). The HPLC flow rate chromatic condition for L-carnitine was 1ml/min.

In table 3.29a, the retention time obtained at 1ml/min (2.98 ± 0.0033 min) was shorter than the retention time obtained at 0.95 ml/min (3.14 ± 0.0089 min) and 1.05 ml/min (3.00 ± 0.0059 min). The adjustment in flow rate increased the retention time at which L -carnitine was detected in the HPLC.

Table 8.29a: Flow rate variation of L-carnitine **(300 µg/ml).**

Flow rate (ml/min)	Number of Replicates	Retention Time (min)	Area (a)
0.95	Replicate 1	3.15	34997.95
	Replicate 2	3.13	35045.19
	Replicate 3	3.13	33764.62
	Mean	3.14	34602.58
	SD	0.0089	726.08
	%RSD	0.0028	0.021
1.00	Replicate 1	2.98	24009.31
	Replicate 2	2.98	23821.22
	Replicate 3	2.98	23862.85
	Mean	2.98	23897.79
	SD	0.0033	98.79
	%RSD	0.0011	0.0042
1.10	Replicate 1	3.00	33159.62
	Replicate 2	3.00	32726.17
	Replicate 3	3.00	32655.30
	Mean	3.00	32847.03
	SD	0.0059	273.02
	%RSD	0.002	0.0083

In table 3.29b, the retention time obtained at 1ml/min (2.96 ± 0.0028 min) was shorter than the retention time obtained at 0.95 ml/min (3.12 ± 0.0056 min) and 1.05 ml/min (3.00 ± 0.0022 min). The adjustment in flow rate increased the retention time at which l-carnitine was detected in the HPLC.

Table 8.29b: Flow rate variation of L-carnitine **(500 µg/ml).**

Flow rate (ml/min)	Number of Replicates	Retention Time (min)	Area (a)
0.95	Replicate 1	3.13	45383.65
	Replicate 2	3.12	45323.12
	Replicate 3	3.12	46921.40
	Mean	3.12	45876.06
	SD	0.0056	905.80
	%RSD	0.0018	0.020
1.00	Replicate 1	2.97	41693.12
	Replicate 2	2.96	41539.87
	Replicate 3	2.97	41246.08
	Mean	2.96	41493.03
	SD	0.0028	227.17
	%RSD	0.00096	0.0055
1.10	Replicate 1	3.00	44628.36
	Replicate 2	3.00	45211.81
	Replicate 3	3.00	44488.70
	Mean	3.00	44776.29
	SD	0.0022	383.58
	%RSD	0.00074	0.0086

In table 3.29c, the retention time obtained at 1ml/min (2.94 ± 0.0027) was shorter than the retention time obtained at 0.95 ml/min (3.11 ± 0.014) and 1.05 ml/min (2.98 ± 0.0033). The adjustment in flow rate increased the retention time at which l-carnitine was detected in the HPLC machine.

Table 8.29c: Flow rate variation of L-carnitine **(1000 µg/ml).**

Flow rate (ml/min)	Number of Replicates	Retention Time (min)	Area (a)
0.95	Replicate 1	3.10	66878.16
	Replicate 2	3.12	66075.35
	Replicate 3	3.11	66990.08
	Mean	3.11	66647.87
	SD	0.014	498.97
	%RSD	0.0045	0.0075
1.00	Replicate 1	2.93	82977
	Replicate 2	2.94	82234.11
	Replicate 3	2.94	83705.71
	Mean	2.94	82972.27
	SD	0.0027	735.82
	%RSD	0.00092	0.0089
1.10	Replicate 1	2.98	71742.10
	Replicate 2	2.98	71518.29
	Replicate 3	2.98	71355.89
	Mean	2.98	71538.76
	SD	0.0033	193.92
	%RSD	0.0011	0.0027

3.1.6.5 Co-enzyme Q10

Table 3.30a-c showed flow rate variation at different concentrations (0.1, 10 and 100 µg/ml). The HPLC flow rate chromatic condition for Co-enzyme Q10 was 1ml/min.
In table 3.30a, the retention time obtained at 1ml/min (2.99 ± 0.0024 min) was longer than the retention time obtained at 0.95 ml/min (2.96 ± 0.0043 min) and shorter than the retention time obtained at 1.05 ml/min (3.14 ± 0.099 min).

Table 8.30a: Flow rate variation of Co-enzymeQ10 **(0.1 µg/ml).**

Flow rate (ml/min)	Number of Replicates	Retention Time (min)	Area (a)
0.95	Replicate 1	2.96	29469.70
	Replicate 2	2.97	184798.76
	Replicate 3	2.97	28942.66
	Mean	2.96	81070.37
	SD	0.0043	89831.80
	%RSD	0.15	110.82
1.00	Replicate 1	2.99	15299.04
	Replicate 2	2.99	14477.79
	Replicate 3	2.99	12688.60
	Mean	2.99	14155.15
	SD	0.0024	1334.79
	%RSD	0.080	9.43
1.05	Replicate 1	3.25	11564.65
	Replicate 2	3.09	8175.42
	Replicate 3	3.07	13834.01
	Mean	3.14	11191.36
	SD	0.099	2847.70
	%RSD	3.15	25.45

In table 3.30b, the retention time obtained at 1ml/min (3.09 ± 0.0063 min) was slightly shorter than the retention time obtained at 0.95 ml/min (3.34 ± 0.009 min) and slightly longer than the retention time obtained at 1.05 ml/min (3.03 ± 0.0073 min). The adjustment in flow rate showed a slight variation in the retention time.

Table 8.30b: Flow rate variation of Co-enzyme Q10 **(10 µg/ml).**

Flow rate (ml/min)	Number of Replicates	Retention Time (min)	Area
0.95	Replicate 1	3.34	15338*
	Replicate 2	3.35	150351
	Replicate 3	3.33	1855348*
	Mean	3.34	ND
	SD	0.009	ND
	%RSD	0.27	ND
1.00	Replicate 1	3.09	40984.01*
	Replicate 2	3.09	102283
	Replicate 3	3.10	114563
	Mean	3.09	108423
	SD	0.0063	8683.27
	%RSD	0.20	8.01
1.05	Replicate 1	3.03	29578
	Replicate 2	3.03	31722
	Replicate 3	3.02	48501.1*
	Mean	3.03	30650
	SD	0.0073	1516.04
	%RSD	0.24	4.95

*ND: Not Determined. Values were omitted as it skewed the data. Coenzyme Q_{10} is an unstable compound which blocks the column in HPLC. This results in inaccurate data.

In table 3.30c, the retention time obtained at 1ml/min (3.08 ± 0.0051 min) was shorter than the retention time obtained at 0.95 ml/min (3.20 ± 0.21 min) and slightly longer than the retention time obtained at 1.05 ml/min (3.00 ± 0.0036 min). The adjustment in flow rate showed a slight variation in the retention time.

Table 8.30c: Flow rate variation of Co-enzyme Q10 **(100 µg/ml).**

Flow rate (ml/min)	Number of Replicates	Retention Time (min)	Area
0.95	Replicate 1	3.32	3078*
	Replicate 2	3.32	2531*
	Replicate 3	2.95	2062258
	Mean	3.20	689288.93
	SD	0.21	ND
	%RSD	6.57	ND
1.00	Replicate 1	3.09	1337546
	Replicate 2	3.09	793191*
	Replicate 3	3.10	1204816
	Mean	3.08	1271181
	SD	0.0051	93854.28
	%RSD	0.17	7.38
1.05	Replicate 1	3.01	130143
	Replicate 2	3.00	639368*
	Replicate 3	3.01	115527
	Mean	3.00	122835
	SD	0.0036	10335.07
	%RSD	0.12	8.4

*ND: Not Determined. Values were omitted as it skewed the data. Coenzyme Q_{10} is an unstable compound which blocks the column in HPLC. This results in inaccurate data.

3.1.7 Stability

Experiments were conducted over a 2 – 3-day period, and as such the stability of the compounds were observed after being stored at 4°C or exposed to 32°C (*in vitro* diffusion experiment in formulations) during this period. Retinol and Coenzyme Q_{10} were stored covered in foil or kept in the dark during the whole experimental procedure (Table 3.31). Fresh stock and working standards or samples were prepared for each set of experiments during the 2 – 3-day period. Changes in the formulations e.g. phase separation, changes in color and odor were also noted during the 2 – 3 day time period of the *in vitro* diffusion experiments.

The compounds remained stable over the 2 – 3-day time period in which experiments were performed (Table 3.31). For the formulations containing active compounds, no phase separation, alteration in odor or color were observed during storage at 4°C or during the 4 – 24-hour time period of the diffusion experiments (32°C). The same chromatogram conditions were applied as described in section 2.1.5.

Table 8.31: Stability of standard compounds over a 2 – 3- day period after storage at 4oC or exposed to 32°C (in vitro diffusion experiment in formulations). Retinol and Coenzyme Q10 were protected from light at all times during this time period.

Compound	% of initial	%RSD
Caffeine	100.6 ± 2.7	2.6
Theophylline	105.8 ± 1.2	1.1
L-Carnitine	107.9 ± 0.9	0.8
Retinol	103.6 ± 0.3	0.3
Coenzyme Q10	105.8 ± 1.2	1.1

3.1 Chapter 3.2: Results - In Vitro diffusion of active compounds

In vitro diffusion experiments have been used to replicate the complexity of the biological systems and it has become a way in which new formulations are developed (Bartosova and Bajgar, 2012; Ruela et al.,2016). Both Franz-type diffusion and in-line flow-through diffusion systems are employed to measure *in vitro* dermal absorption (Córdoba-Diaz *et al*., 2000). Studies have shown that the in-line flow-through diffusion systems are more suitable to simulate *in vivo* conditions, provides a good reproducibility of the temperature obtained at each diffusion point and more accurately reflects the movement of a compound from the donor compartment into the receptor medium. This is compared to the Franz-type diffusion, which needs to maintain a constant volume to flow into the receptor compartment. In summary, in-line flow-through diffusion is time efficient and an easier way to validate *in vitro* permeation studies compared to Franz-type diffusion apparatus (Córdoba-Diaz *et al*., 2000).
The *in vitro* permeation of active compounds Caffeine, Retinol, L-Carnitine and Co-enzyme Q_{10} from liquid, gel and cream formulations across porcine skin was monitored over a 24-hour time period compared to Theophylline which was monitored over a 4-hour time period.

3.2.1 HPLC Specificity of compounds in formulations

The analytical specificity is the ability to accurately identify and measure an analyte in the presence of other closely related compounds. Specificity shows how well an assay can detect only a specific substance and not the other closely related substances in the sample during an analysis (Chin et al., 2013).

3.2.1.1 Liquid, gel, and cream formulations without active compounds

In vitro diffusion experiments across porcine skin were performed (Section 2.5) where PBS, liquid, gel, or cream formulations without any compounds were loaded into the donor compartments of flow cells. Fluid that was collected in the receptor compartments were tested for interfering peaks with retention time similar to the active compounds.

The collected fluid in receptor compartments were also spiked with active compounds to indicate the Rt's of the individual active compounds.

3.2.1.1.1 Specificity of Caffeine

The HPLC chromatograms obtained from the receptor fluid collected when PBS, liquid, gel or cream formulations alone (without caffeine) were loaded into donor compartments, were all the same (Figure 3.14.a). Four peaks were observed, one small peak observed at the Rt (2.60min) for caffeine (compared to receptor fluid spiked with caffeine, Figure 3.14b).

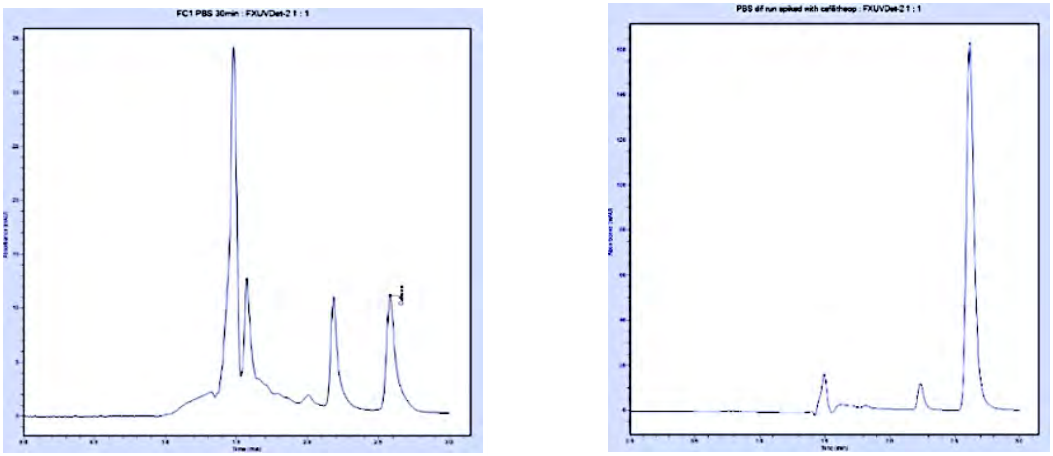

a. b.

Figure 9: HPLC Chromatogram of Caffeine

HPLC chromatograms of fluid collected in the receptor compartment of the *in vitro* flow cell after PBS, liquid, gel or cream without compounds (a) was loaded (1 ml) in the donor compartment and a diffusion experiment performed across porcine skin as described in section 2.5. Caffeine was detected at a retention time of 2.65 min at an absorbance of 10 AU; (b) receptor fluid spiked with caffeine and detected at a retention

time of 2.70 min with an absorbance of 100AU. Running conditions consisted of HPLC grade methanol: Milli Q water (40:60).

3.2.1.1.2 Specificity of Theophylline

The HPLC chromatograms obtained from the receptor fluid collected when PBS, liquid, gel, or cream formulations alone were loaded into donor compartments, were all the same (Figure 3.15.a). Four peaks were observed, one small peak observed at the Rt (2.11 min) for theophylline (compared to receptor fluid spiked with theophylline, Figure 3.15b).

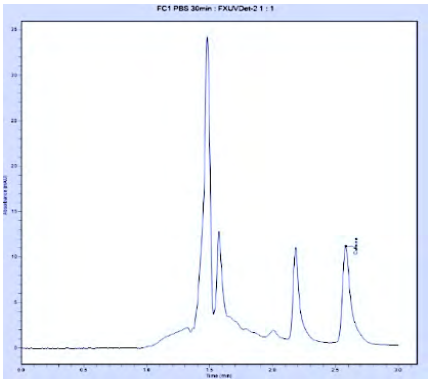

b.

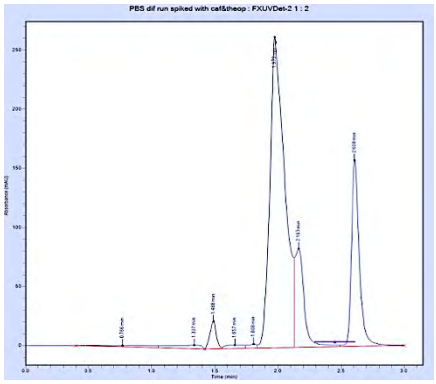

b.

Figure 9: HPLC Chromatogram of Theophylline

HPLC chromatograms of fluid collected in the receptor compartment of the *in vitro* flow cell after PBS, liquid, gel or cream without compounds (a) was loaded (1 ml) in the donor compartment and a diffusion experiment performed across porcine skin as described in section 2.5; (b) receptor fluid spiked with theophylline. Theophylline was detected at a retention time of 2.11 min at an absorbance of 110 AU. Running conditions consisted of HPLC grade methanol: Milli Q water (40:60).

3.2.1.1.3 Specificity of Retinol

The HPLC chromatograms obtained from the receptor fluid collected when PBS, liquid, gel or cream formulations alone were loaded into donor compartments, were all the same (Figure 3.16.a). Four peaks were observed, although there were no interfering peaks at the Rt (2.68 min) for retinol (compared to receptor fluid spiked with retinol, Figure 3.16b).

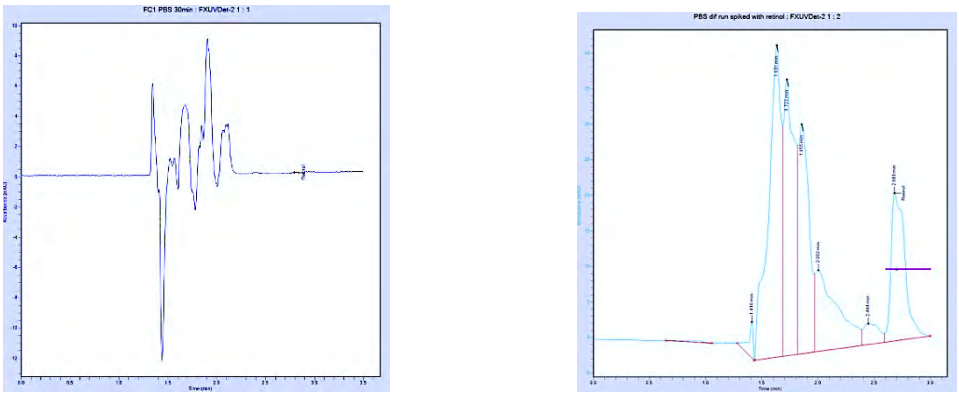

a. b.

Figure 9: HPLC Chromatograms of Retinol

HPLC chromatograms of fluid collected in the receptor compartment of the *in vitro* flow cell after PBS, liquid, gel or cream without compounds (a) was loaded (1 ml) in the donor compartment and a diffusion experiment performed across porcine skin as described in section 2.5; (b) receptor fluid spiked with retinol (Rt = 2.68 min). Retinol was detected at a retention time of 2.69 min at an absorbance of 23 AU. Running conditions consisted of HPLC grade methanol: Milli Q water (95:5).

3.2.1.1.4 Specificity of L-carnitine

The HPLC chromatograms obtained from the receptor fluid collected when PBS, liquid, gel or cream formulations alone were loaded into donor compartments, were all the same (Figure 3.17.a). Five peaks were observed, although there were no interfering peaks at the Rt (2.9- 3.2 min) for L-carnitine (compared to receptor fluid spiked with L-carnitine, Figure 3.17b). L-carnitine is a zwitterion and therefore is ionized easily. Due to the latter, a variation in retention time was observed for L-carnitine.

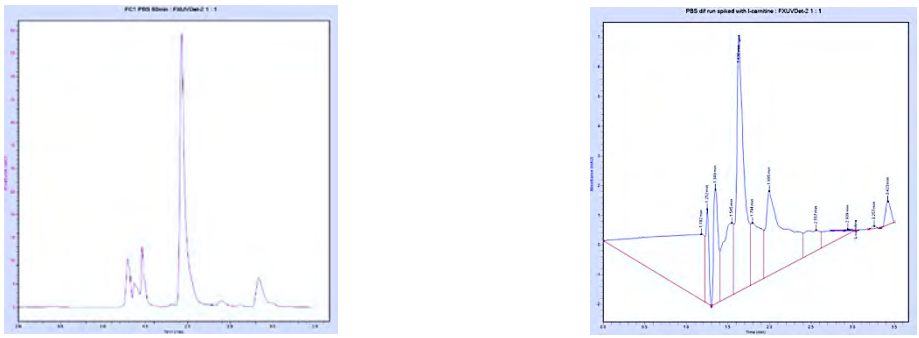

a. b.

Figure 9: HPLC Chromatograms of L-carnitine

HPLC chromatograms of fluid collected in the receptor compartment of the *in vitro* flow cell after PBS, liquid, gel or cream without compounds (a) was loaded (1 ml) in the donor compartment and a diffusion experiment performed across porcine skin as described in section 2.5; (b) receptor fluid spiked with L-carnitine (Rt = 2.9). Running conditions consisted of sodium phosphate buffer (pH 3.0): Methanol (99:1).

3.2.1.1.5 Specificity of Co-enzyme Q10

The HPLC chromatograms obtained from the receptor fluid collected when PBS, liquid, gel or cream formulations alone were loaded into donor compartments, were all the same (Figure 3.18.a). A large number of peaks were observed in the region of 1.5 – 2.0 min, although there were no interfering peaks at the Rt (3.0 min) for coenzyme Q10 (compared to receptor fluid spiked with coenzyme Q10, Figure 3.18b)

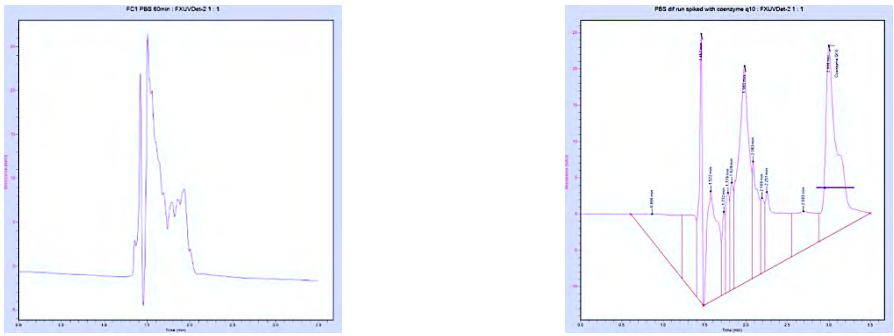

a. b.

Figure 9 :HPLC Chromatograms of Coenzyme Q10

HPLC chromatograms of fluid collected in the receptor compartment of the *in vitro* flow cell after PBS, liquid, gel, or cream without compounds (a) was loaded (1 ml) in the donor compartment and a diffusion experiment performed across porcine skin as

described in section 2.5; (b) receptor fluid spiked with coenzyme Q10 (Rt = 2.99 min). Coenzyme Q10 was detected at a retention time of 2.99 min at an absorbance of 24 AU. Running conditions consisted of HPLC grade methanol: HPLC grade 2-propanol (40:60).

3.2.2 *In vitro* diffusion of active compounds across the skin from liquid, gel, and cream, formulations

Diffusion curves of the cumulative amount of active compound ($ng.cm^{-2}$) diffusing across the skin versus time (min) were constructed for each compound in the different formulations to determine the steady state flux, apparent permeability coefficient and lag phase (min). The experimental methodology was fully explained in section 2.5.
The steady state flux (Jss) is a constant quantity of drug diffusing across a specific area of the skin in a time period. Lag phase (min) is the time for the compound to diffuse across the skin into the receptor fluid and to reach steady state. Apparent permeability ($cm.min^{-1}$) is the rate of compound penetration expressed as distance per time (Brodin *et al*., 2010). The table below (Table 3.32) shows a summary of retention time ± SD for each active compound in the various formulations. It can be seen that the retention times for all the compounds remained relatively constant and were not affected by the formulation in which the compounds were dissolved in. The diffusion process across the porcine skin itself did affect the retention times slightly as compared to the retention times found in mobile phase alone (section 3.1).

Table 9: Retention times (min) of the 5 compounds present in receptor fluid after in vitro diffusion experiments from the various formulations.

Compound	**Retention time (min)**		
	Liquid	Gel	Cream
Theophylline	2.11 ± 0.049	2.03 ± 0140	2.16 ± 0.026
Caffeine	2.60 ± 0.003	2.61 ± 0.002	2.62 ± 0.024
Retinol	2.68 ± 0.008	2.68 ± 0.004	2.68 ± 0.003
Coenzyme Q10	2.98 ± 0.001	2.98 ± 0.003	2.98 ± 0.001
L-Carnitine	2.87 ± 0.180	2.92 ± 0.038	2.97 ± 0.008

The table above does not include PBS but only 3 different formulations (liquid, gel, and cream).

3.2.2.1 Caffeine Diffusion

Figure 3.19 below illustrates the *in vitro* diffusion of caffeine (2.5% w/v: 0.25 g in 10 ml) in liquid, gel, and cream formulations across porcine skin over 24 hours. The active compound was monitored initially over a 24-hour period and then for a period of 4 hours (Figure 3.20). A 24-hour initial period was chosen to observe diffusion behavior prior to deciding on the final period to study. The final diffusion period for caffeine was established as 24 hours. Table 3.33 shows the steady state flux, lag phase and apparent permeability coefficient of caffeine across the 3 different formulations used (liquid, gel, and cream).

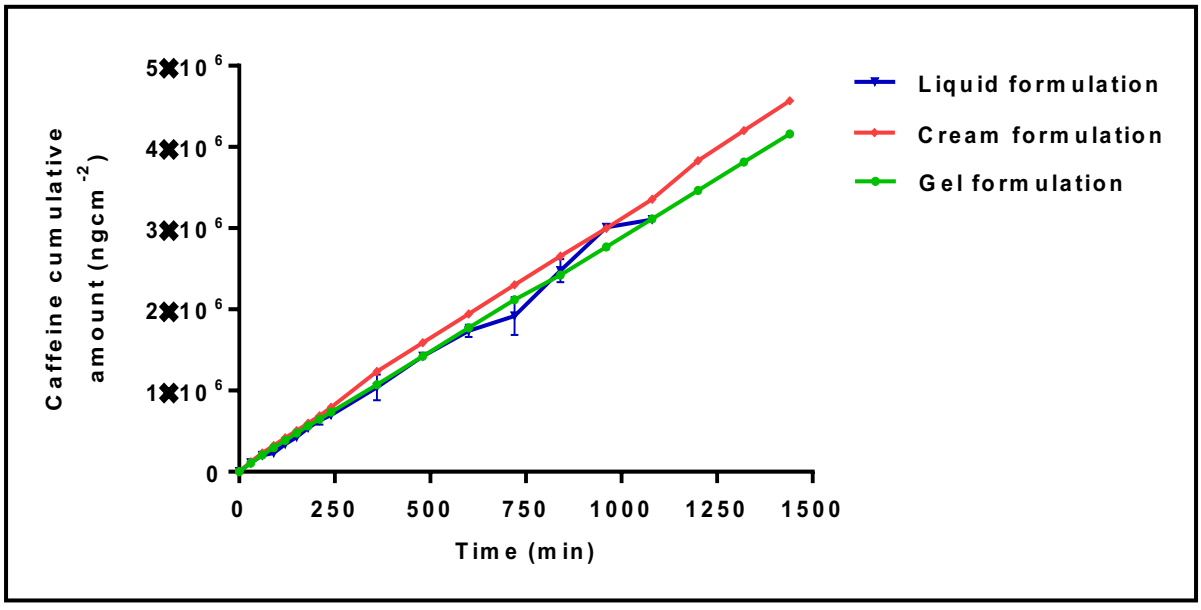

Figure 9: *In Vitro* Diffusion of Caffeine (2.5% w/v) from a liquid, gel, and cream formulation across porcine skin (0.0397 cm^2) over 24 hours

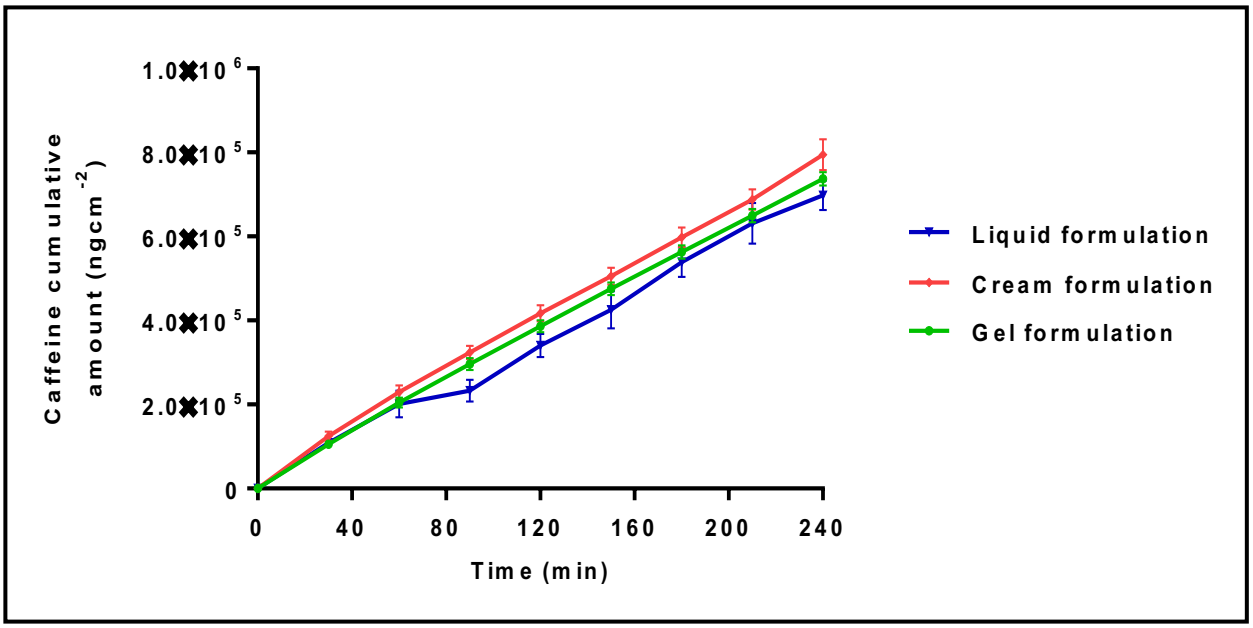

Figure 9: *In Vitro* Diffusion of Caffeine (2.5% w/v) from a liquid, gel, and cream formulation across porcine skin (0.0397 cm^2) over 4 hours.

The graph in Figure 3.20 above, shows the caffeine diffusion in liquid, gel, and cream formulations over the initial 4-hour time period. As can be seen from these graphs, caffeine diffused very rapidly across porcine skin and the rate remained constant over the 24-hour time period, irrespective of the formulation used. Caffeine present in a cream formulation diffused slightly quicker through porcine skin compared to caffeine from gel and liquid formulations. The differences in steady state flux rates were, however, not statistically significant ($p>0.8$). Approximately 0.64% (liquid and gel) – 0.73% (cream) of the original caffeine diffused across the skin into the receptor fluid over a 24-hour time period. The lag phase was found to be 0 min across all 3 formulations, indicating that diffusion occurred immediately through the skin. The apparent permeability coefficient (Papp: rate of diffusion into the skin ($cm.min^{-1}$) for caffeine from a cream formulation across porcine skin, was slightly higher than from gel or liquid formulations (Table 3.33).

Table 9*:* Steady state flux, Lag time and Apparent permeability coefficient (Papp) of Caffeine in a liquid, gel, and cream formulation.

Caffeine			
Formulations	**$Flux_{ss}$ (Jss) ($ng.cm^{-2}.min^{-1}$) Mean ± SD**	**Lag Time (min)**	**Papp Value ($cm.min^{-1}$)**
Liquid	2887 ± 308.83	0	1.15×10^{-4}
Gel	2867 ± 46.68	0	1.15×10^{-4}
Cream	3143 ± 64.56	0	1.25×10^{-4}

3.2.2.2 Theophylline Diffusion

Figure 3.21 below illustrates the *in vitro* diffusion of Theophylline (2% w/v: 0.2 g in 10 ml) from liquid, gel, and cream formulations across porcine skin. Theophylline was monitored over a period of 24 hours initially; however the active compound was not detected after 4 hours and was therefore monitored over a period of 4 hours only. Table 3.33 shows the steady state flux, lag phase and the apparent permeability coefficient of caffeine across the 3 different formulations (liquid, gel, and cream).

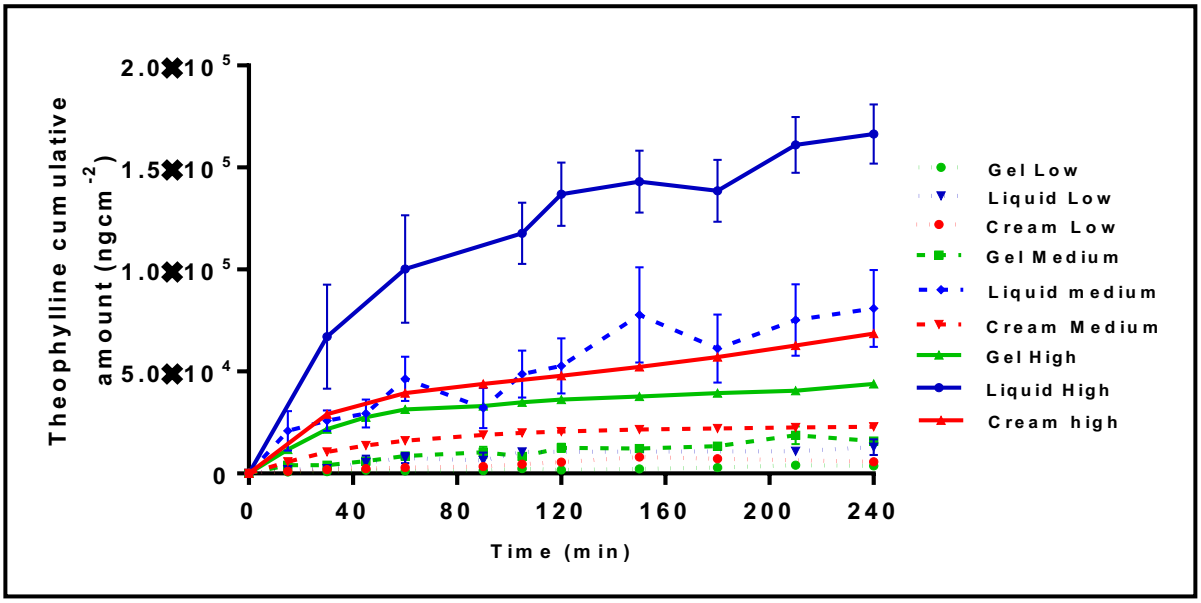

Figure 9: *In vitro* Diffusion of Theophylline (2% w/v) from a liquid, gel, and cream formulation across porcine skin (0.0397 cm^2) over 4 hours. The graph shows diffusion of theophylline at different ranges which is due to the high variability in diffusion.

Due to the high variability in the diffusion of theophylline across porcine skin, the *in vitro* diffusion graphs were divided into three different ranges (low, medium, and high diffusion) for each formulation. Theophylline from a liquid formulation diffused better than from a cream followed by a gel formulation (Table 3.34).

The diffusion rate for theophylline for all formulations seemed to decrease after 30 min exposure and in the low concentration ranges, flattened off significantly. The differences in steady state flux rates were, however, not statistically significant ($p>0.05$). Approximately 0.0025% - 0.0330% (liquid), 0.0008% - 0.0087% (gel) and 0.0012% - 0.0214% (cream) of the original theophylline diffused across the skin into the receptor fluid over a 4-hour time period. Theophylline from a liquid formulation diffused at a very high rate across the skin (0.0628% of initial amount diffused across the skin). The lag phase was found to be 0 min across all 3 formulations. The apparent permeability coefficients ($cm.min^{-1}$) for theophylline from the liquid and cream formulations across porcine skin were overall higher than from a gel formulation (Table 3.34).

As seen in figure 3.21, the graph depicting theophylline in cream (low) formulation and cream (medium) formulation overlaps with theophylline in gel low, liquid low and gel medium formulations.

Table 9: Steady state flux, Lag time and Apparent permeability coefficient (Papp) of Theophylline in a liquid, gel, and cream formulation over 4 hours.

Theophylline			
Formulations	**$Flux_{ss}$ ($ng.cm^{-2}.min^{-1}$) Mean ± SD**	**Lag Time (min)**	**Papp Value ($cm.min^{-1}$)**
Liquid (Low)	48.85 ± 31.60	0	2.44×10^{-6}
Liquid (Medium)	298.0 ± 378.63	0	1.49×10^{-5}
Liquid (High)	750.9 ± 161.88	0	3.75×10^{-5}
Gel (Low)	15.67 ± 7.64	0	7.83×10^{-7}
Gel (Medium)	16.26 ± 13.67	0	8.13×10^{-7}
Gel (High)	95.44 ± 42.57	0	4.78×10^{-6}
Cream	601.5 ± 247.77	0	3.01×10^{-5}

Table 3.34 shows the diffusion of theophylline in 3 different formulations. The table further depicts the different ranges at which theophylline was diffused, this is due to the high variability in theophylline through its diffusion process. The lag time was zero, this shows that diffusion occurred immediately has theophylline compound was added to the continuous flow (Figure 1.23).

3.2.2.3 L-Carnitine Diffusion

Figure 3.22 below illustrates the *in vitro* diffusion of L-Carnitine (2% w/v: 0.2g in 10 ml) from liquid, gel, and cream formulations across porcine skin over a 24-hour time period. A 24-hour initial period was chosen to observe diffusion behavior prior to deciding on the final period to study.

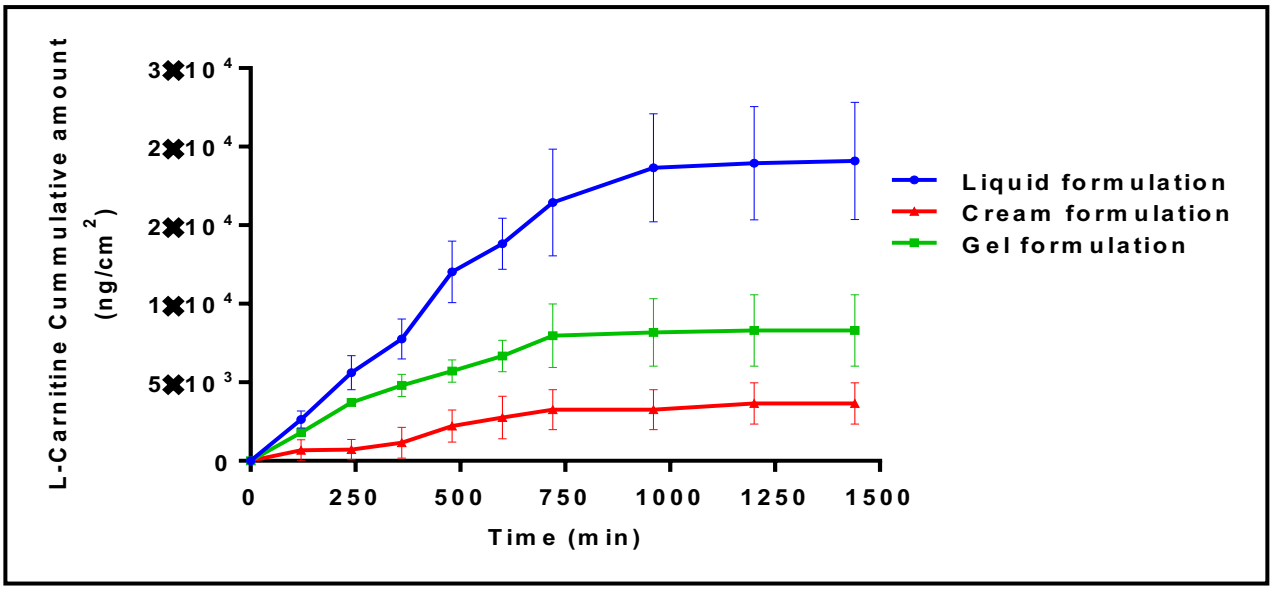

Figure 9*: In vitro* Diffusion of L-carnitine (2% w/v) from a liquid, gel, and cream formulation across porcine skin (0.0397 cm^2) over 24 hours.

As can be seen from the graph in Figure 3.22, L-carnitine diffused initially rapidly across porcine skin up till 750 min after which the rate declined up to 24 hours, irrespective of the formulation used. L-carnitine present in a liquid formulation diffused much quicker through porcine skin compared to caffeine in a gel formulation, where the rate was quicker than L-carnitine in a cream formulation (Liquid > gel > cream). The differences in steady state flux rates were, however, not statistically significant ($p>0.9$).

Approximately 0.0038% (liquid), 0.0017% (gel) and 0.0007% (cream) of the original L-carnitine diffused across the skin into the receptor fluid over a 24-hour time period. The lag phase was found to be 1.56 min for L-carnitine from a liquid formulation and 0 min for L-carnitine from the other two formulations. The apparent permeability coefficient (rate of diffusion into the skin ($cm.min^{-1}$) for L-carnitine from the three formulations into the porcine skin was in the following order: liquid > gel > cream (Table 3.35).

Table 9: Steady state, Lag time and Apparent permeability coefficient (Papp) of L-carnitine in a liquid, gel, and cream formulation.

L-carnitine			
Formulations	**$Flux_{ss}$ ($ng.cm^{-2}.min^{-1}$) Mean ± SD**	**Lag Time (min)**	**Papp Value ($cm.min^{-1}$)**
Liquid	23.25 ± 6.33	1.56	1.16×10^{-6}
Gel	10.62 ± 3.94	0	5.31×10^{-7}
Cream	5.60 ± 5.11	0	2.80×10^{-7}

3.2.2.4 Retinol and Coenzyme Q10

Due to the physiochemical of both retinol and Coenzyme Q10, both compounds were not detected in the receptor fluid within 24-hour time period and therefore were not quantified or illustrated in a graph.

3.2.3 In Vitro Diffusion parameters of active compounds alone and in combination

The pharmaceutical industry continuously tries to find ways to discover new drugs or improve the usage of drugs in new therapeutic areas; this is done through the process of drug repurposing. Drug combination is a type of drug repurposing, the process of drug combination involves the interaction of two or more drugs (Sun *et al*., 2016). The interaction of these drugs can either increase or decrease efficacy of the individual

drug or produce a new side effect that is unrelated to the initial side effect (Cascorbi, 2012).

In this study, the effect of one drug on the diffusion behavior of another was investigated by adding active compounds with each, as described in section 2.5.4.2. *In vitro* diffusion curves of cumulative amount of active compounds ($ng.cm^{-2}$) diffusing across the skin versus time (min) were constructed for Caffeine, Theophylline and L-carnitine alone and in combination with each other as well as with retinol and Coenzyme Q10. The diffusion parameters of caffeine, theophylline and L-carnitine alone and in combination across liquid, gel and cream formulation can be observed in Tables 3.33 – 3.35.1.

3.2.3.1 Caffeine alone and in Combination

The *in vitro* diffusion of caffeine from the three formulations (liquid, gel and cream), alone and in combination with co-enzyme Q10, retinol or L-carnitine are illustrated in the figures below (Figures 3.23 -3.25).

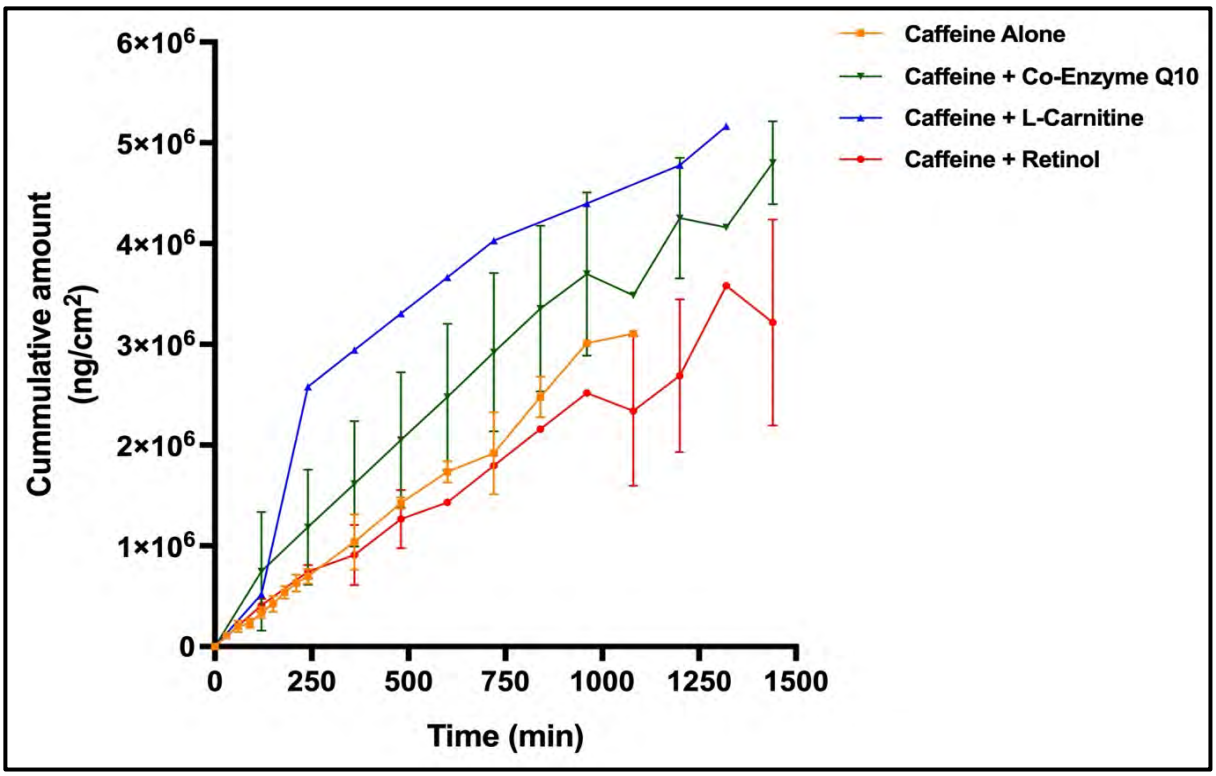

Figure 9: *In vitro* diffusion of caffeine alone and in combination from a liquid formulation across porcine skin (area = 0.0379 cm^2), (n=3) over 24 hours.

Table 9: Steady state flux, Lag time and Apparent permeability coefficient (Papp) of Caffeine in a liquid formulation.

Compound	In Combination with	$Flux_{ss}$ ($ng.cm^{-2}.min^{-1}$) Mean ± SD	Lag Time (min)	Papp Value ($cm.min^{-1}$)	Statistical significance of $Flux_{ss}$ (*p* value)
Liquid Formulation					
Caffeine	Caffeine Alone	2887 ± 308.83	0	1.15×10^{-4}	
	L-Carnitine	2299 ± 457.71	0	9.20×10^{-5}	0.6425
	CoQ10	3742 ± 1161.9	0	1.50×10^{-4}	0.5008
	Retinol	2486 ± 384.6	0	9.94×10^{-5}	0.7513

From the graphs above Figure 3.23 it can be seen that L-carnitine and coenzyme Q10 increased the cumulative amounts of caffeine from a liquid formulation across porcine skin slightly (L-carnitine > coenzyme Q10), while retinol seemed to slightly decrease the cumulative amount of caffeine slightly. The *in vitro* diffusion parameters are presented in Table 3.36 above indicate that the steady state flux rates, lag phases and Papp values were very similar with no statistically significant differences ($p>0.05$).

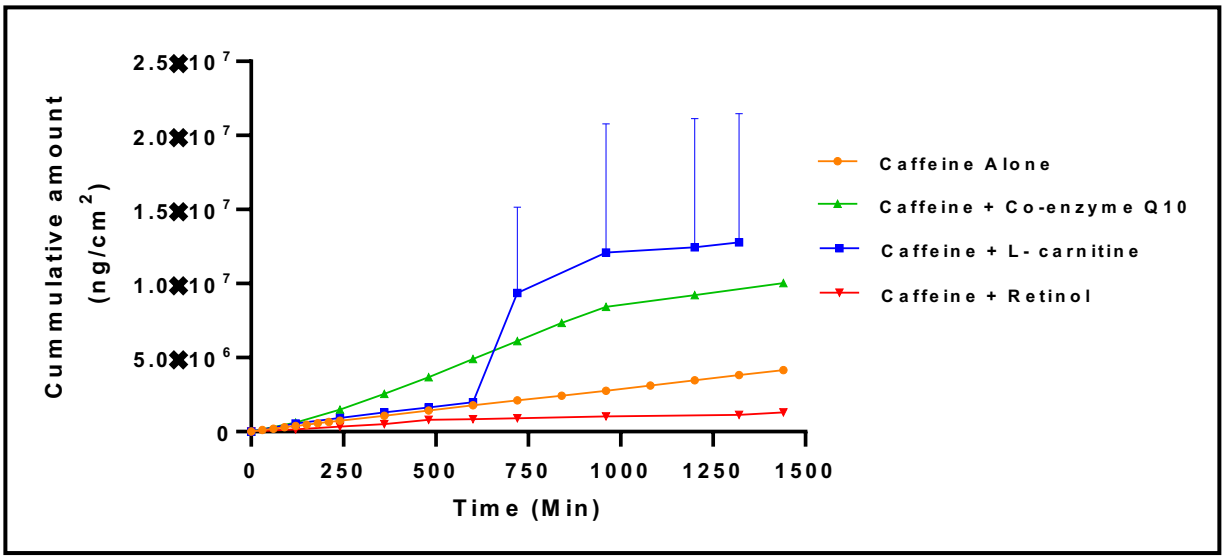

Figure 9: In vitro diffusion of caffeine alone and in combination from a gel formulation across porcine skin (area = 0.0379 cm^2), (n=3) over 24 hours.

Similarly, the graphs above (Figure 3.24) indicate that L-carnitine (750 min and above) and coenzyme Q10 increased the cumulative amounts of caffeine from a gel formulation across porcine skin (L-carnitine > coenzyme Q10), while retinol seemed to decrease the cumulative amount of caffeine. The cumulative amount of caffeine remained unchanged in combination with L-carnitine up to 600 min, after which a large increase in the cumulative amount was observed from 750 min. However, a large variation in the cumulative amount at each time point was observed for caffeine from 750 min onwards. The *in vitro* diffusion parameters are presented in Table 3.37 above. From Table 3.37 it can be seen that the steady state flux values and Papp values of caffeine were affected in the following order when combined: Coenzyme Q10 ($p<0.05$) > L-carnitine ($p>0.05$) >> Retinol ($p>0.05$). In combination with coenzyme Q10, the lag time of caffeine to reach steady state also increased from 0 – 10.55 min.

Table 9: Steady state flux, Lag time and Apparent permeability coefficient (Papp) of Caffeine in a gel formulation.

Compound	In Combination with	$Flux_{ss}$ ($ng.cm^{-2}.min^{-1}$) Mean ± SD	Lag Time (min)	Papp Value ($cm.min^{-1}$)	Statistical significance of $Flux_{ss}$ (*p* value)
Gel Formulation					
Caffeine	Caffeine Alone	2867 ± 46.68	0	1.15×10^{-4}	
	L-Carnitine	3247 ± 235.45	0	1.30×10^{-4}	0.7639
	CoQ10	5858 ± 3915	10.55	2.34×10^{-4}	0.0250*
	Retinol	476.5 ± 192.87	0	1.91×10^{-5}	0.0680

* Statistical significance $p < 0.05$

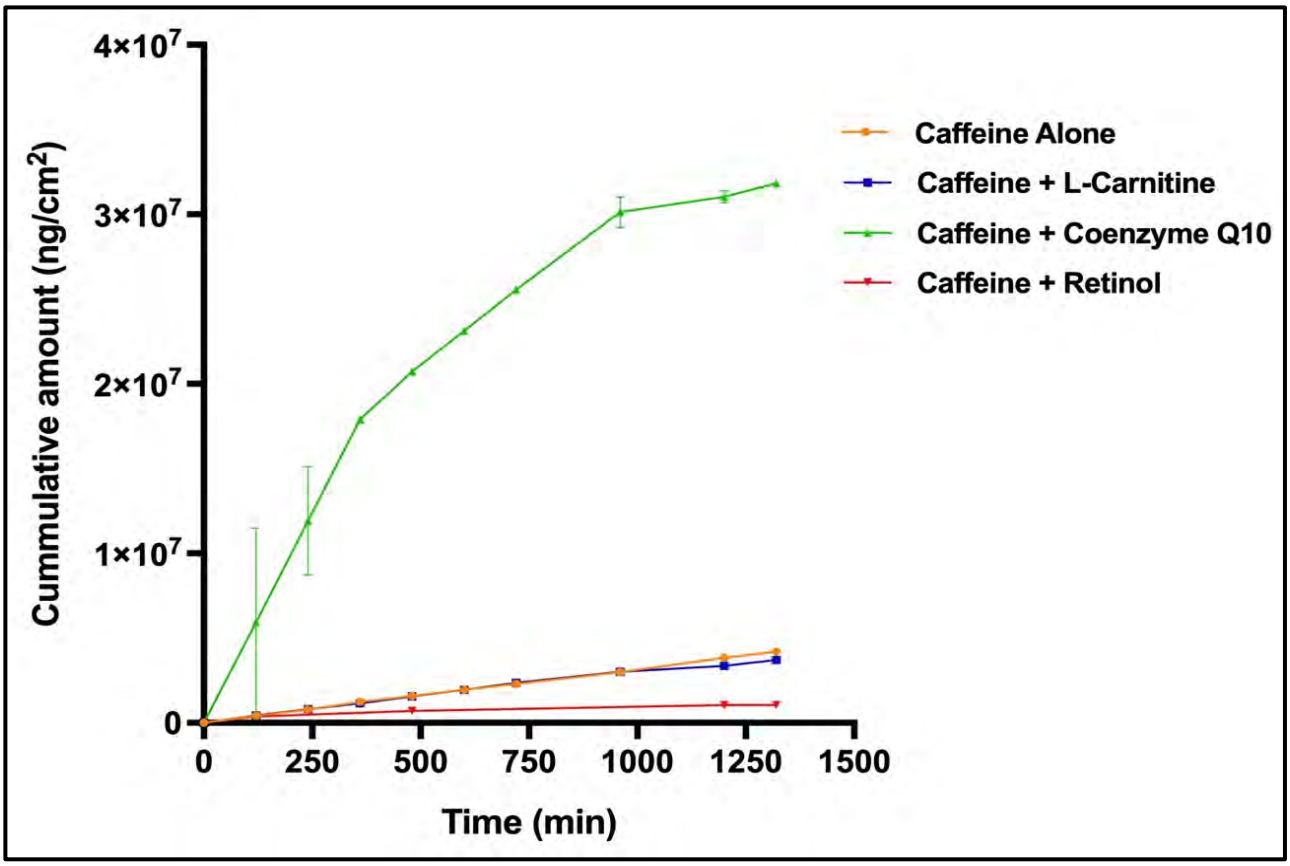

Figure 9: *In vitro* diffusion of caffeine alone and in combination from a cream formulation across porcine skin (area = 0.0379 cm^2), (n=3) over 24 hours.

The graphs above (Figure 3.25) indicate that caffeine in combination with coenzyme Q10 increased significantly ($p < 0.0001$) the cumulative amounts of caffeine from a cream formulation across porcine skin, while retinol decreased the cumulative amount of caffeine. L-carnitine seemed to have no effect on caffeine diffusion from a cream formulation. A large increase in the cumulative amount was observed for caffeine in combination with co-enzyme Q10 from 0 min. The *in vitro* diffusion parameters are presented in Table 3.38 below. From Table 3.38 it can be seen that the steady state flux values and Papp values of caffeine were affected in the following order when combined: Coenzyme Q10 ($p<0.05$) >>> Retinol ($p>0.05$) > L-carnitine ($p>0.05$). In combination with retinol, the lag time of caffeine to reach steady state increased to 6.43 min.

Table 9: Steady state flux, Lag time and Apparent permeability coefficient (Papp) of Caffeine in a cream formulation.

Compound	In Combination with	$Flux_{ss}$ ($ng.cm^{-2}.min^{-1}$) Mean ± SD	Lag Time (min)	Papp Value ($cm.min^{-1}$)	Statistical significance of $Flux_{ss}$ (*p* value)
Cream Formulation					
Caffeine	Caffeine Alone	3143 ± 64.56	0	1.25×10^{-4}	
	L-Carnitine	2808 ± 242.72	0	1.11×10^{-4}	0.7911
	CoQ10	20008 ± 3277.04	0	8.00×10^{-4}	<0.0001*
	Retinol	3089 ± 370.74	6.43	1.24×10^{-4}	0.9659

* Statistical significance $p < 0.01$

3.2.3.2 Theophylline alone and in Combination

The *in vitro* diffusion of theophylline from the three formulations, alone and in combination with co-enzyme Q10, retinol or L-carnitine are reported in the Figures (Figures 3.26 - 3.28). Due to the huge variation in diffusion rates of theophylline in combination with retinol from a liquid formulation, the lower graphs have been expanded for easier observation (Figure 3.26 a and b).

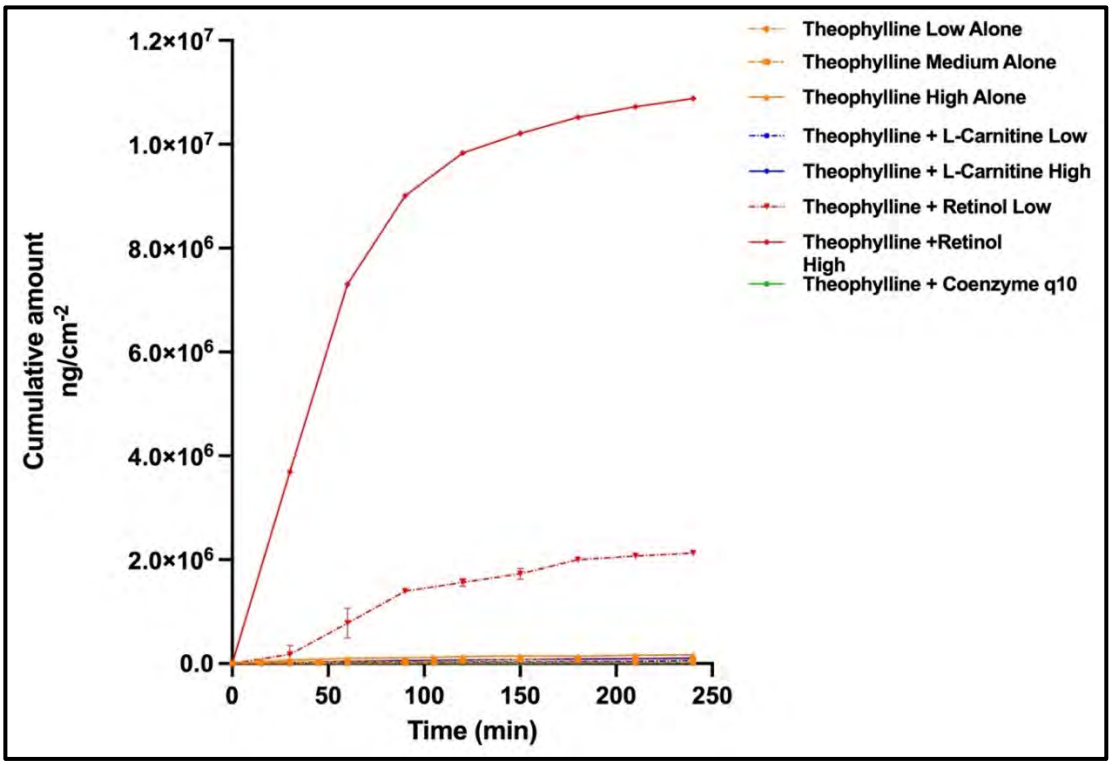

Figure 9 *In vitro* diffusion of theophylline alone and in combination from a liquid formulation across porcine skin (area = 0.0379 cm2), n=3 over 4 hours.

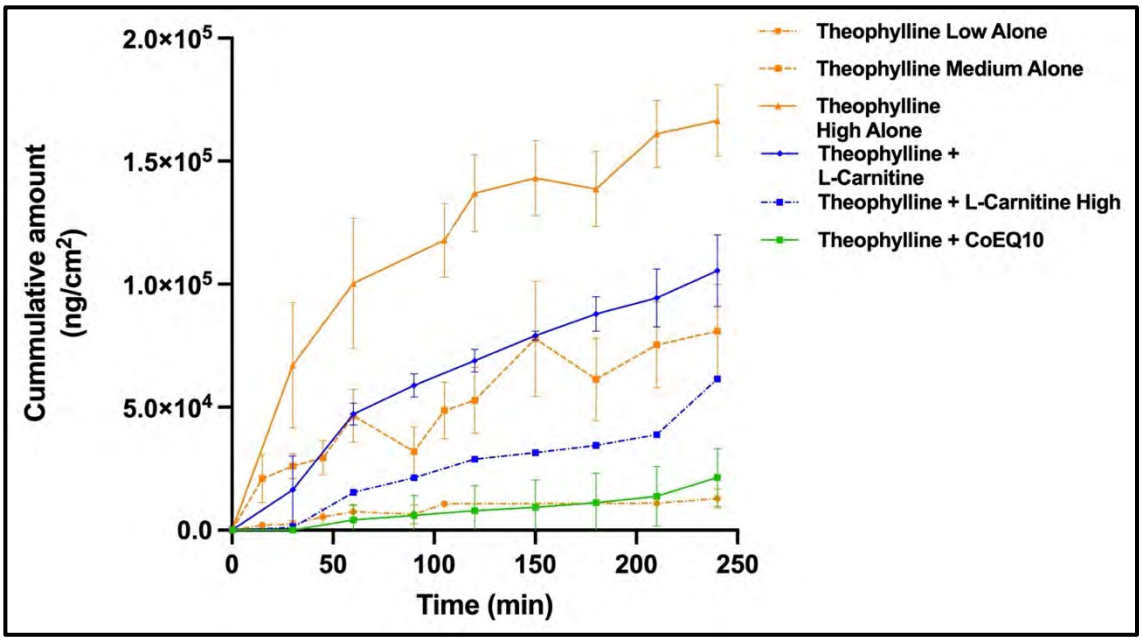

Figure 9: *In Vitro* diffusion of theophylline alone and in combination from a liquid formulation across porcine skin (area = 0.0379 cm2), n=3 over 4 hours.

Figure 3.26 a & b indicate that retinol increased the cumulative amounts of theophylline from a liquid formulation across porcine skin, while L-carnitine seemed to have minimal effect, if any. Coenzyme Q10 seemed to decrease the cumulative amount of theophylline. A large increase in the cumulative amounts was observed for theophylline in combination with retinol from 0 min in some instances.

The flux rate for theophylline varied (cumulative amount per unit time) greatly as mentioned before, however the steady state flux rate indicated no statistical significance (p>0.05). The *in vitro* diffusion parameters are presented in Table 3.39 above. From Table 3.36 it can be seen that the steady state flux values and Papp values of theophylline were affected in the following order when combined: Retinol (high) **(p<0.05)** > Retinol (low) (p>0.05) >> L-carnitine (high) (p>0.05) > L-carnitine (low) (p>0.05) > co-enzyme Q10 (p>0.05).

Table 9: Steady state flux, Lag time and Apparent permeability coefficient (Papp) of Theophylline in a liquid formulation.

Compound	In Combination with	$Flux_{ss}$ ($ng.cm^{-2}.min^{-1}$) Mean ± SD	Lag Time (min)	Papp Value ($cm.min^{-1}$)	Statistical significance of $Flux_{ss}$ (p value)
Liquid Formulation					
Theophylline	Theophylline Alone (Low)	48.85 ± 31.60	0	2.44×10^{-6}	
	Theophylline Alone (Medium)	298.0 ± 378.63	0	1.49×10^{-5}	>0.05
	Theophylline Alone (High)	750.9 ± 161.88	0	3.75×10^{-5}	>0.05
	L-Carnitine (Low)	151.5 ± 37.25	0	7.56×10^{-6}	0.9824
	L-Carnitine (High)	315.5 ± 105.33	0	1.58×10^{-5}	0.9542
	CoQ10	44.14 ± 66.72	0	2.21×10^{-6}	0.9992
	Retinol (Low)	5210 ± 1204.17	0	2.61×10^{-4}	0.2696
	Retinol (High)	11777 ± 4519.31	0	5.89×10^{-4}	0.0144*

* Statistical significance $p < 0.01$

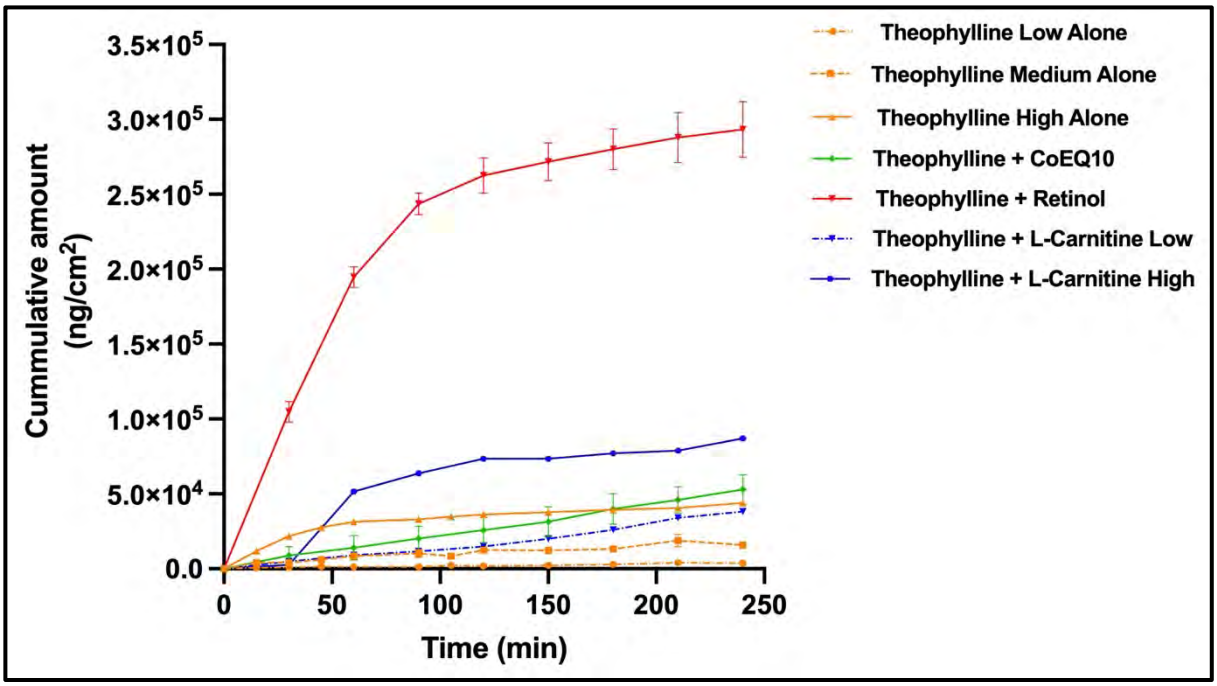

Figure 9: *In vitro* diffusion of theophylline alone and in combination from a gel formulation across porcine skin (area = 0.0379 cm2), n=3 over 4 hours.

The graphs above (Figure 3.40) indicate that retinol increased the cumulative amounts of theophylline from a gel formulation across porcine skin, while l- carnitine seemed to increase the cumulative amount in some instances. Coenzyme Q10 seemed to have minimal effect on the cumulative amount of theophylline. A large increase in the cumulative amount was observed for theophylline in combination with Retinol from 25 min onwards. The *in vitro* diffusion parameters are presented in Table 3.37 above. From Table 3.37 it can be seen that the steady state flux values and Papp values of theophylline were affected in the following order when combined: Retinol ($p>0.05$) > Co-enzyme Q10 ($p>0.05$) > L-carnitine (high) ($p>0.05$) > L-carnitine (low) ($p>0.05$). In combination with L-carnitine (high), the lag time of theophylline to reach steady state also increased from 0 – 7.22 min.

Table 9: Steady state flux, Lag time and Apparent permeability coefficient (Papp) of Theophylline in a gel formulation.

Compound	In Combination with	$Flux_{ss}$ ($ng.cm^{-2}.min^{-1}$) Mean ± SD	Lag Time (min)	Papp Value ($cm.min^{-1}$)	Statistical significance of $Flux_{ss}$ (*p* value)
Gel Formulation					
Theophylline	Theophylline Alone (Low)	15.67 ± 7.64	0	7.83×10^{-7}	
	Theophylline Alone (Medium)	16.26 ± 13.67	0	8.13×10^{-7}	>0.05
	Theophylline Alone (High)	95.44 ± 42.57	0	4.78×10^{-6}	>0.05
	L-Carnitine (Low)	108.5 ± 64.5	0	5.43×10^{-6}	0.9841
	L-Carnitine (High)	156.6 ± 25.43	7.22	7.83×10^{-6}	0.9237
	CoQ10	214.4 ± 90.99	0	1.07×10^{-5}	0.9658
	Retinol	317.2 ± 217.29	0	1.59×10^{-5}	0.9482

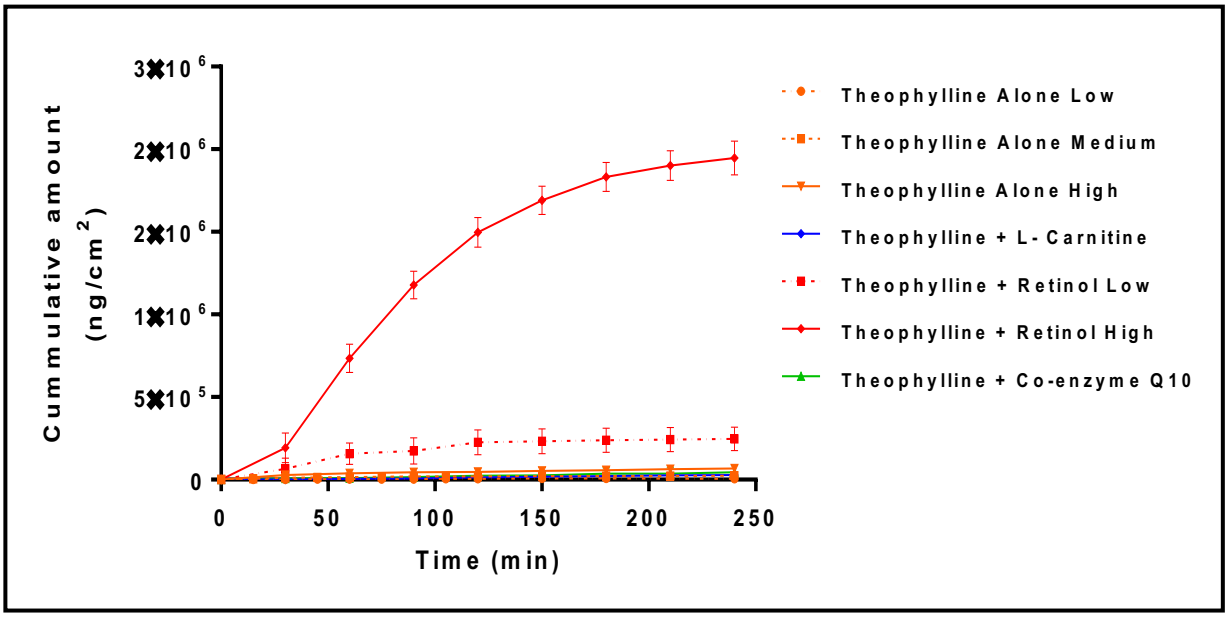

Figure 9: *In vitro* diffusion of theophylline alone and in combination from a cream formulation across porcine skin (area = 0.0379 cm2), n=3 over 4 hours.

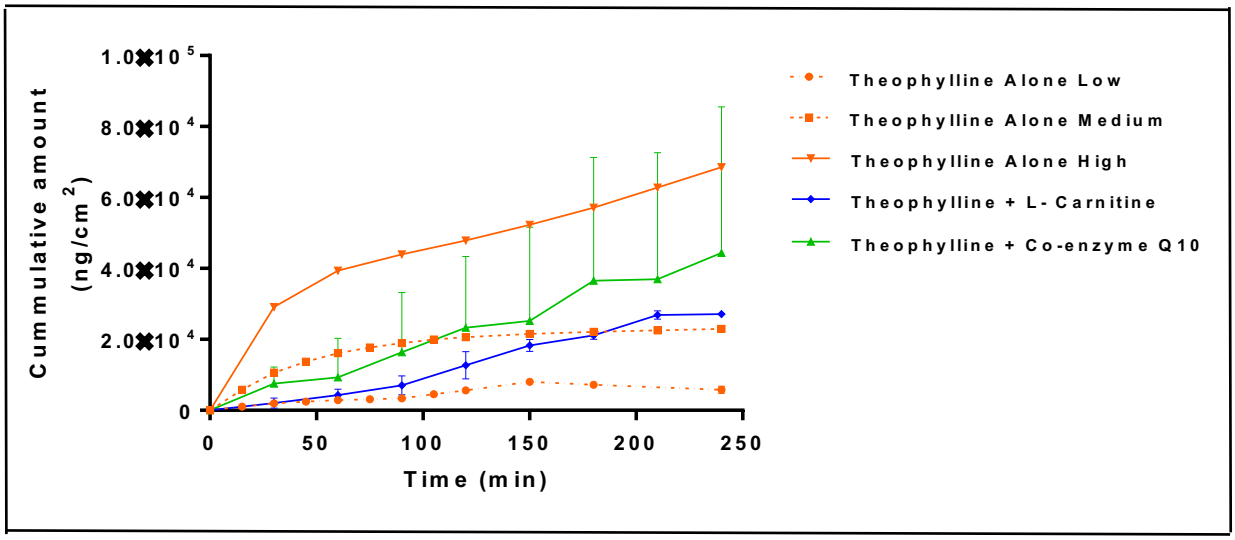

Figure 9 *In vitro* diffusion of theophylline alone and in combination from a cream formulation across porcine skin (area = 0.0379 cm2), n=3.

The graphs above (Figure 3.28a & b) indicated that Retinol increased the cumulative amounts of theophylline from a cream formulation across porcine skin, while co-enzyme Q10 and L-carnitine had minimal effect. A large increase in the cumulative amount was observed for theophylline in combination with Retinol at 25 min in some instances. The *in vitro* diffusion parameters are presented in Table 3.41 above. From Table 3.38 it can be seen that the steady state flux values and Papp values of theophylline were affected in the following order when combined: Retinol (p> 0.05) >> Co-enzyme Q10 (p>0.05) > L-carnitine (p>0.05). In combination with L-carnitine, the lag time of theophylline to reach steady state also increased from 0 – 15.26 min.

Table 9: Steady state flux, Lag time and Apparent permeability coefficient (Papp) of Theophylline in a cream formulation.

Compound	In Combination with	$Flux_{ss}$ ($ng.cm^{-2}.min^{-1}$) Mean ± SD	Lag Time (min)	Papp Value ($cm.min^{-1}$)	Statistical significance of $Flux_{ss}$ (*p* value)
Cream Formulation					
Theophylline	Theophylline Alone	601.5 ± 247.77	0	3.01×10^{-5}	
	L-Carnitine	126.8 ± 29.87	15.26	6.34×10^{-6}	0.9186
	CoQ10	182.7 ± 658.5	0	9.13×10^{-6}	0.9282
	Retinol	1945 ± 19311	0	9.73×10^{-5}	0.7724

3.2.3.3 L-Carnitine alone and in Combination

The *in vitro* diffusion of L-carnitine from the three formulations, alone and in combination with co-enzyme Q10, retinol or theophylline are illustrated in the figures below (Figures 3.29 - 3.31). Diffusion in combination with theophylline was kept to a 4-hour time period as it was found that theophylline became undetectable after 4 hours when used alone (Figure 3.21). Although L-carnitine could be detected when combined with caffeine in all formulations, it could not be quantitated. For the ease of interpretation, the figures for L-carnitine alone and in combination from all formulations are indicated separately.

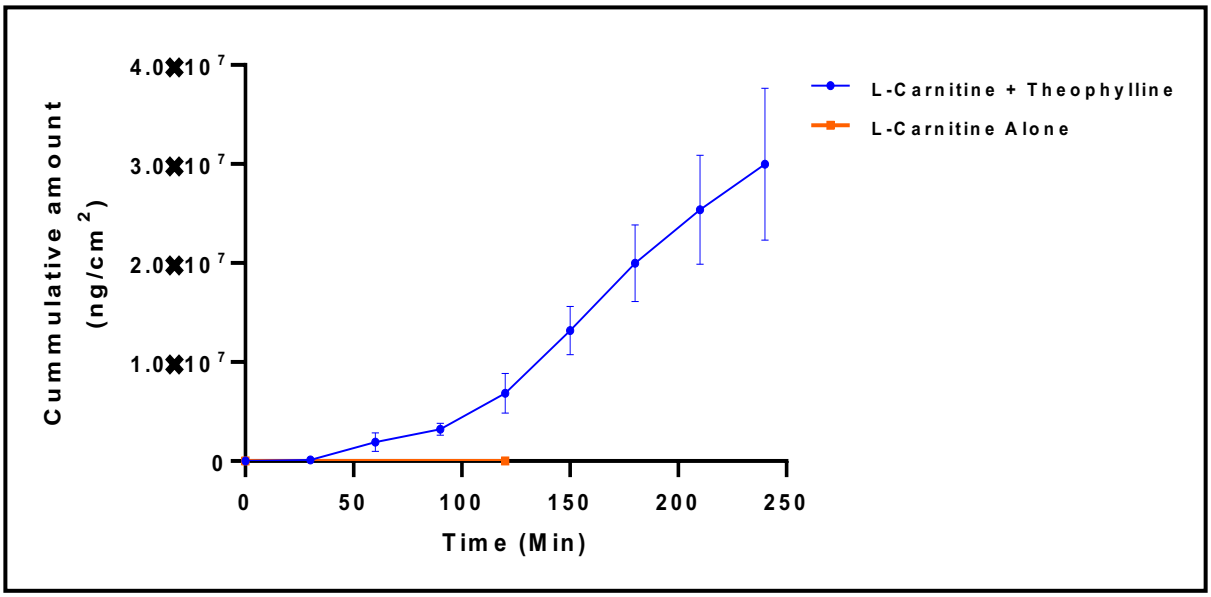

Figure 9: *In vitro* diffusion of L-carnitine alone and in combination with theophylline from a liquid formulation across porcine skin (area = 0.0379 cm2), n = 3.

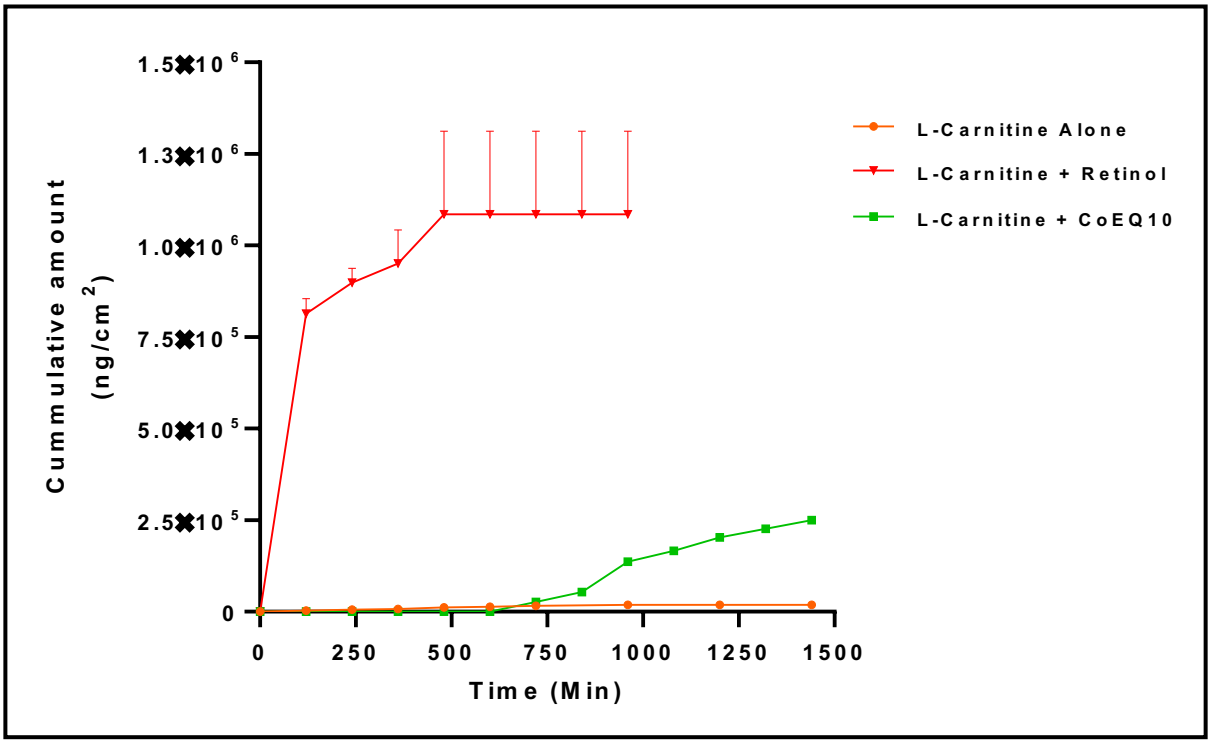

Figure 9: *In vitro* diffusion of L-carnitine alone and in combination with retinol and coenzyme Q10 from a liquid formulation across porcine skin (area = 0.0379 cm2), n = 3.

The graphs above (Figure 3.29 a & b) indicate that theophylline increased the cumulative amounts of L-carnitine from a liquid formulation across porcine skin. Retinol and coenzyme Q10 similarly enhanced the diffusion of L-carnitine (retinol >>> Coenzyme Q10), however to a much lesser extent than the enhancement observed by theophylline. The enhancement of L-carnitine diffusion by coenzyme Q10 was only observed from 600 min onwards. A large variation in the diffusion of L-carnitine in combination with retinol was observed at the time points 420 min onwards. The *in vitro* diffusion parameters are presented in Table 3.42 above. From Table 3.39 it can be seen that the steady state flux values and Papp values of L-carnitine were affected in the following order when combined: Theophylline **($p<0.05$)** >>> Retinol ($p>0.05$) > Coenzyme Q10 ($p>0.05$). In combination with theophylline, the lag time of L-carnitine to reach steady state increased from 1.56 – 77.02 min, while the lag time of L-carnitine in combination with co-enzyme Q10 increased from 1.56 - 377.8 min. No lag time was observed when L-carnitine was combined with retinol.

Table 9: Steady state flux, Lag time and Apparent permeability coefficient (Papp) of L-carnitine in a liquid formulation.

Compound	**In Combination with**	**$Flux_{ss}$ ($ng.cm^{-2}.min^{-1}$) Mean ± SD**	**Lag Time (min)**	**Papp Value ($cm.min^{-1}$)**	**Statistical significance of $Flux_{ss}$ (*p* value)**
Liquid Formulation					
L-Carnitine	L-Carnitine Alone	23.25 ± 6.33	1.56	1.16×10^{-6}	
	CoQ10	238.7 ± 26.88	377.8	1.19×10^{-5}	>0.05
	Theophylline	186885 ± 74378.78	77.02	9.34×10^{-3}	<0.0001*
	Retinol	852.2 ± 1672.4	0	4.26×10^{-5}	0.9714

* Statistical significance $p<0.01$

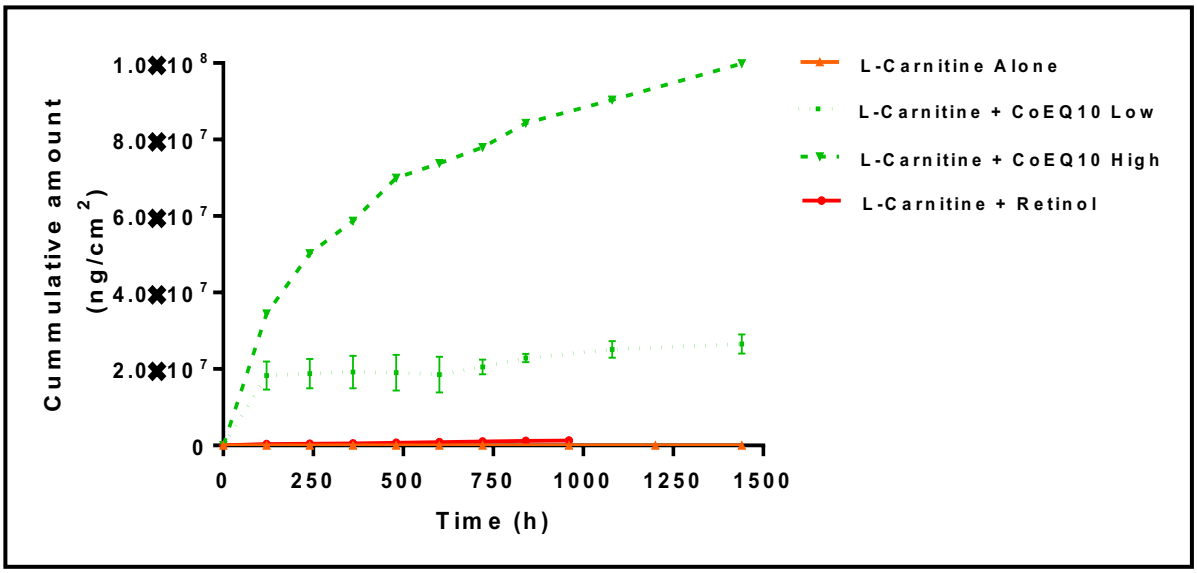

Figure 9: *In vitro* diffusion of L-carnitine alone and in combination with coenzyme Q10 and retinol from a gel formulation across porcine skin (area = 0.0379 cm2), n = 3.

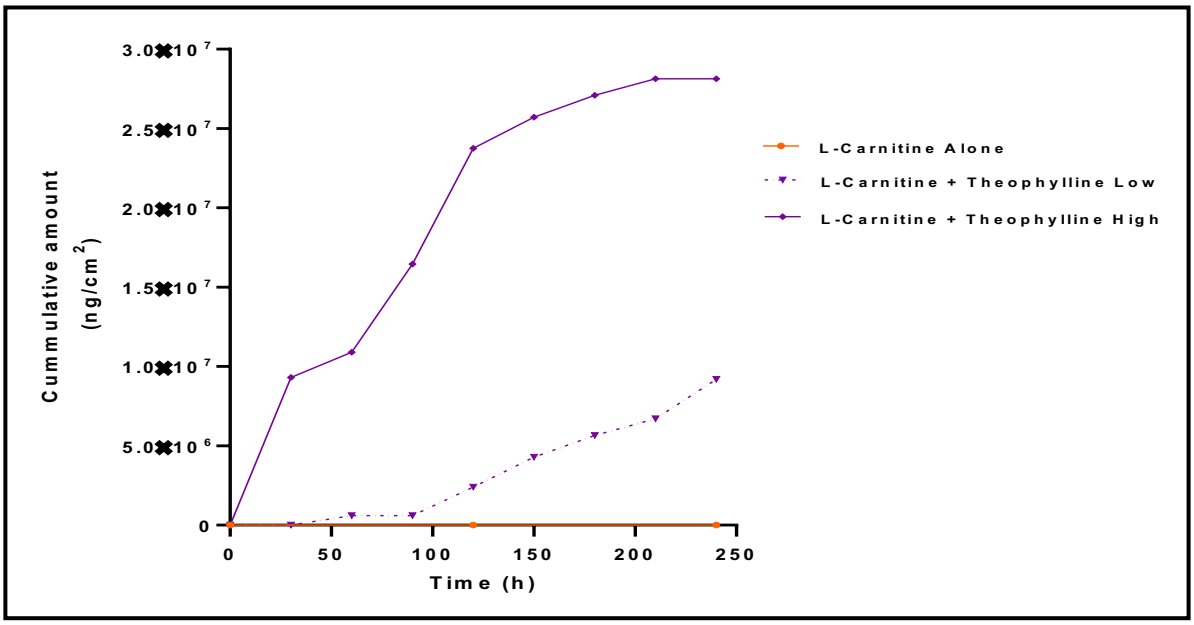

Figure 9: *In vitro* diffusion of L-carnitine alone and in combination with theophylline from a gel formulation across porcine skin (area = 0.0379 cm2), n = 3.

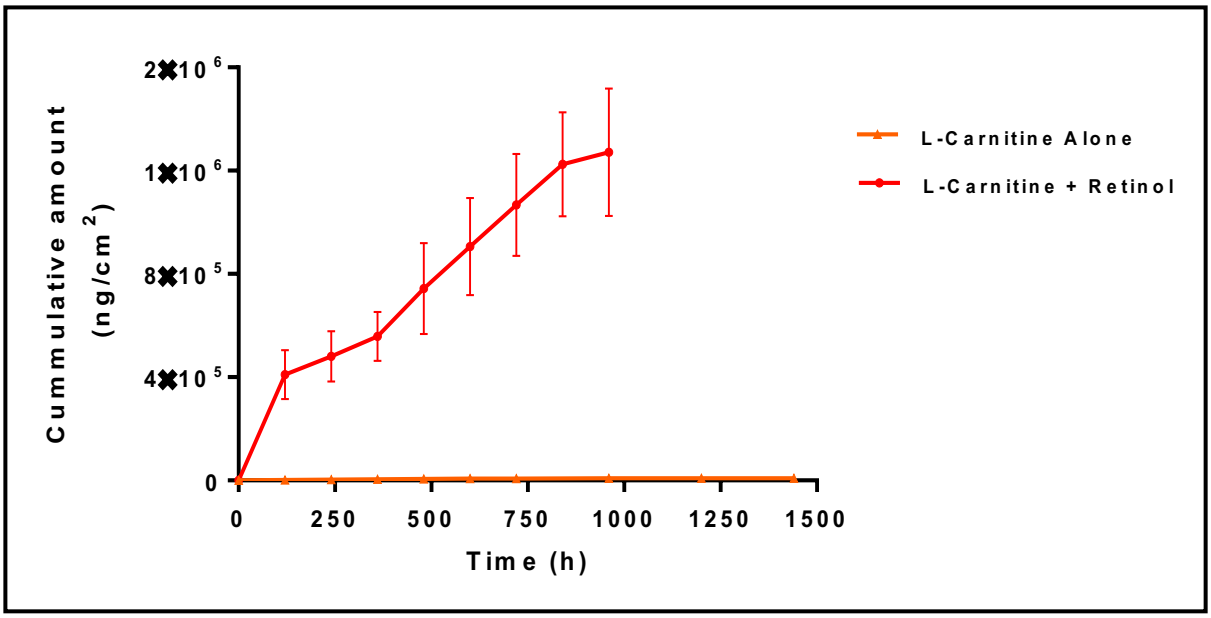

Figure 9: *In vitro* diffusion of L-carnitine alone and in combination with retinol from a gel formulation across porcine skin (area = 0.0379 cm2), n = 3.

The graphs above (Figure 3.30 a, b &c) indicate that theophylline, coenzyme Q10 and retinol increase the cumulative amounts of L-carnitine from a gel formulation across porcine skin (Coenzyme Q10 (high) >> Theophylline (high) > Coenzyme Q10 (low) > Theophylline (low) >> Retinol). In some instances, Coenzyme Q10 and theophylline caused very high diffusion rates for L-carnitine (Coenzyme Q10 (high) >> Theophylline (high) in the initial 4 hours. The *in vitro* diffusion parameters are presented in Table 3.40 above. From Table 3.43 it can be seen that the steady state flux values and Papp values of L-carnitine were affected in the following order when combined: Theophylline (high) **($p<0.05$)** > Theophylline (low) ≈ Co-enzyme Q10 (high) ($p>0.05$) > Co-enzyme Q10 (low) ($p>0.05$) > Retinol ($p>0.05$). In combination with theophylline, the lag time of L-carnitine to reach steady state also increased from 0 – 74.28 min.

Table 9: Steady state flux, Lag time and Apparent permeability coefficient (Papp) of L-carnitine in a gel formulation.

Compound	In Combination with	$Flux_{ss}$ ($ng.cm^{-2}.min^{-1}$) Mean ± SD	Lag Time (min)	Papp Value ($cm.min^{-1}$)	Statistical significance of $Flux_{ss}$ (*p* value)
Gel Formulation					
L-Carnitine	L-Carnitine Alone	10.62 ± 3.94	0	5.31×10^{-7}	
	CoQ10 (Low)	6950 ± 7172.05	0	3.46×10^{-4}	0.7641
	CoQ10 (High)	31497 ± 5616.21	0	1.57×10^{-3}	0.1786
	Theophylline (Low)	37274 ± 46776	0	1.86×10^{-3}	0.1132
	Theophylline (High)	53373 ± 12474	74.28	2.67×10^{-3}	0.0258*
	Retinol	1135 ± 484.79	0	5.68×10^{-5}	0.9612

*Statistical significance p< 0.05

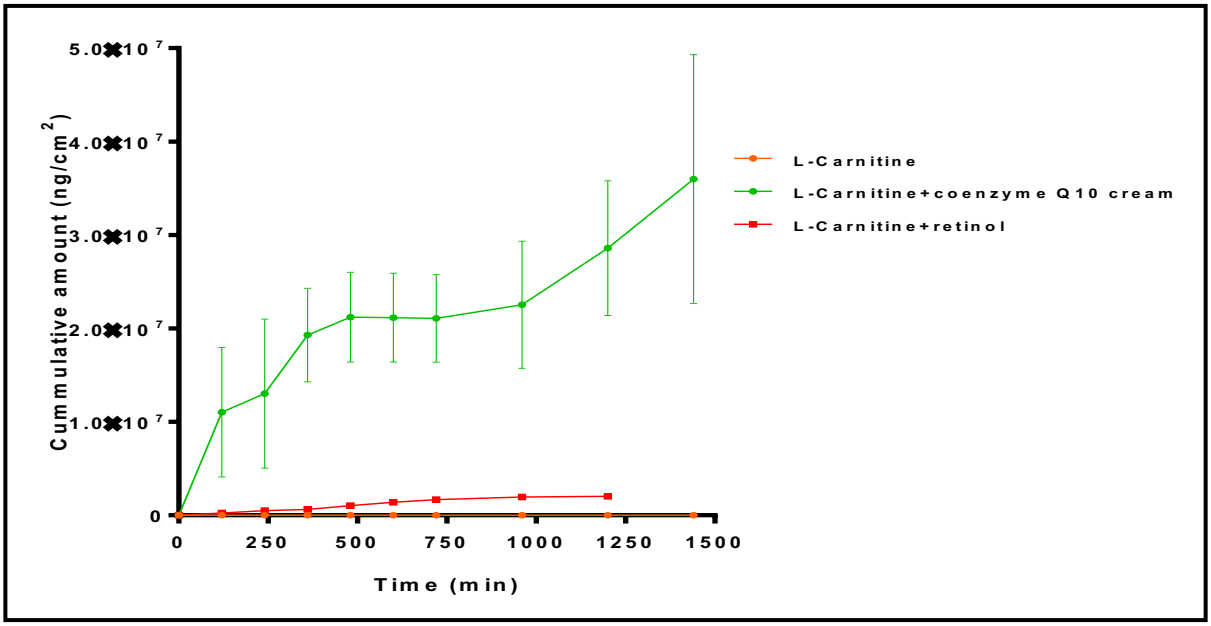

Figure 9: *In vitro* diffusion of L-carnitine alone and in combination with coenzyme Q10 and retinol from a cream formulation across porcine skin (area = 0.0379 cm2), n =3.

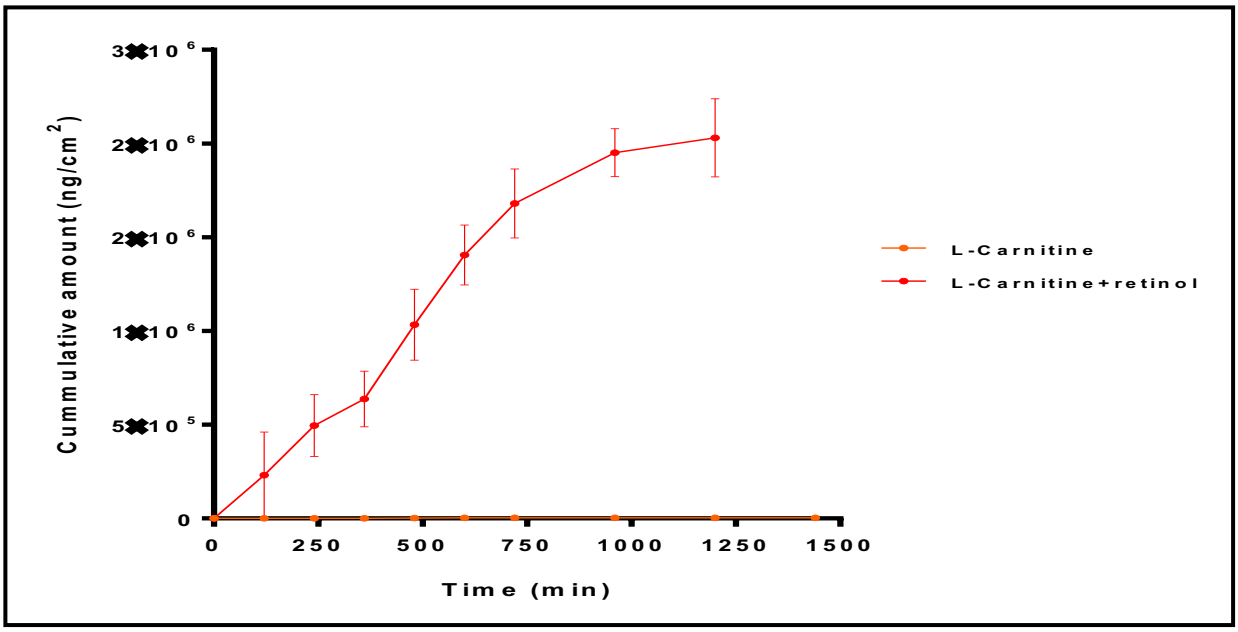

Figure 9: *In vitro* diffusion of L-carnitine alone and in combination with retinol from a cream formulation across porcine skin (area = 0.0379 cm2), n = 3.

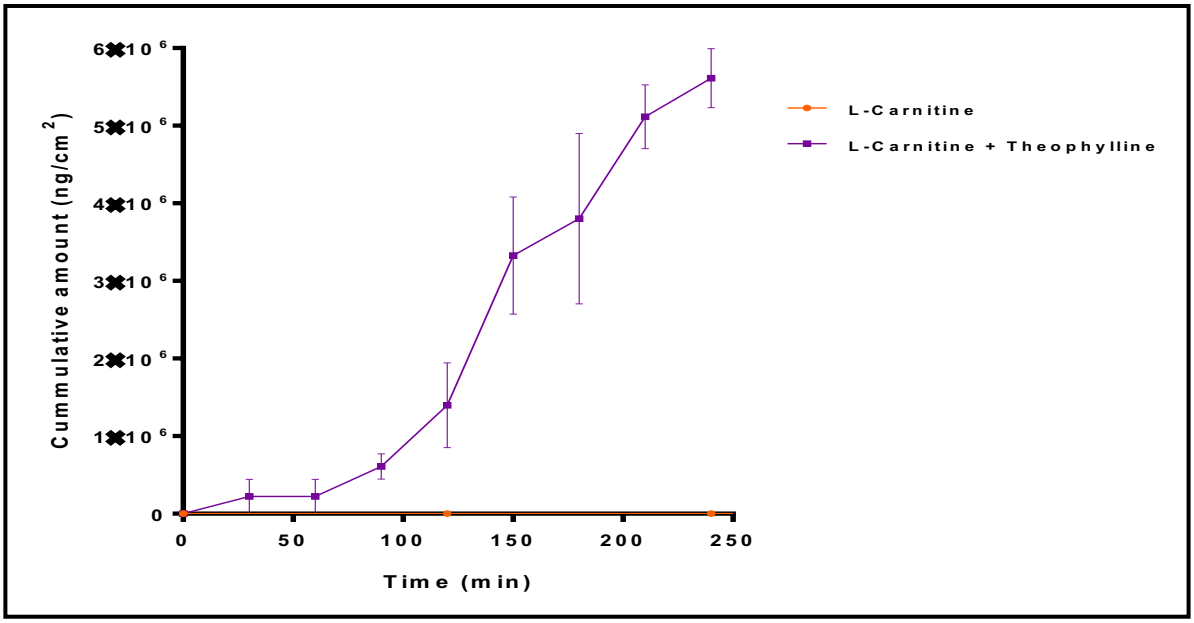

Figure 9:*In vitro* diffusion of L-carnitine alone and in combination with theophylline from a cream formulation across porcine skin (area = 0.0379 cm2), n = 3.

The graphs above (Figure 3.31 a, b &c) indicate that coenzyme Q10, retinol and theophylline increase the cumulative amounts of L-carnitine from a cream formulation across porcine skin (Coenzyme Q10 > Theophylline > Retinol). A large variation in the cumulative amount was seen for L-carnitine diffusion in combination with Coenzyme Q10. The *in vitro* diffusion parameters are presented in Table 3.41 above. From Table 3.44 it can be seen that the steady state flux values and Papp values of L-carnitine were affected in the following order when combined: Theophylline (p>0.05) ≈ Coenzyme Q10 (p>0.05) >> Retinol (p>0.05). In combination with theophylline, the lag time of L-carnitine to reach steady state also decreased from 118.5 – 62.62 min while, in combination with retinol, the lag time of L-carnitine to reach steady state also decreased from 118.5 – 18.82 min.

Table 9: Steady state flux, Lag time and Apparent permeability coefficient (Papp) of L-carnitine in a cream formulation.

Compound	**In Combination with**	**$Flux_{ss}$ ($ng.cm^{-2}.min^{-1}$) Mean ± SD**	**Lag Time (min)**	**Papp Value ($cm.min^{-1}$)**	**Statistical significance of $Flux_{ss}$ (p value)**
Cream Formulation					
L-Carnitine	L-Carnitine Alone	5.60 ± 5.11	118.5	2.8×10^{-7}	
	CoQ10	30647 ± 15864	0	1.53×10^{-3}	0.1903
	Theophylline	32837 ± 10667.53	62.62	1.64×10^{-3}	0.1612
	Retinol	2280 ± 450.9	18.82	1.14×10^{-4}	0.9216

All the *in vitro* diffusion parameters for caffeine, the summarized in Tables 3.45 – 3.47 below.

Table 9: Summary of steady state, Lag time and Apparent permeability coefficient (Papp) of Active compounds alone and in combination in a liquid formulation.

Compound	In Combination with	$Flux_{ss}$ ($ng.cm^{-2}.min^{-1}$) Mean ± SD	Lag Time (min)	Papp Value ($cm.min^{-1}$)	Statistical significance of $Flux_{ss}$ (*p* value)
Liquid Formulation					
Caffeine	Caffeine Alone	2887 ± 308.83	0	1.15×10^{-4}	
	L-Carnitine	2299 ± 457.71	0	9.20×10^{-5}	0.6425
	CoQ10	3742 ± 1161.9	0	1.50×10^{-4}	0.5008
	Retinol	2486 ± 384.6	0	9.94×10^{-5}	0.7513
Theophylline	Theophylline Alone (Low)	48.85 ± 31.60	0	2.44×10^{-6}	
	Theophylline Alone (Medium)	298.0 ± 378.63	0	1.49×10^{-5}	>0.05
	Theophylline Alone (High)	750.9 ± 161.88	0	3.75×10^{-5}	>0.05
	L-Carnitine (Low)	151.5 ± 37.25	0	7.56×10^{-6}	0.9824
	L-Carnitine (High)	315.5 ± 105.33	0	1.58×10^{-5}	0.9542
	CoQ10	44.14 ± 66.72	0	2.21×10^{-6}	0.9992
	Retinol (Low)	5210 ± 1204.17	0	2.61×10^{-4}	0.2696
	Retinol (High)	11777 ± 4519.31	0	5.89×10^{-4}	0.0144*
L-Carnitine	L-Carnitine Alone	23.25 ± 6.33	1.56	1.16×10^{-6}	
	CoQ10	238.7 ± 26.88	377.8	1.19×10^{-5}	>0.05
	Theophylline	186885 ± 74378.78	77.02	9.34×10^{-3}	<0.0001*
	Retinol	852.2 ± 1672.4	0	4.26×10^{-5}	0.9714

*Statistical significance of $Flux_{ss}$ comparison with compounds alone ($p<0.05$). A 1-way ANOVA test was used.

Table 9: Summary of steady flux, Lag time and Apparent permeability coefficient (Papp) of Active compounds alone and in combination in a gel formulation.

Compound	In Combination with	$Flux_{ss}$ ($ng.cm^{-2}.min^{-1}$) Mean ± SD	Lag Time (min)	Papp Value ($cm.min^{-1}$)	Statistical significance of $Flux_{ss}$ (*p* value)
Gel Formulation					
Caffeine	Caffeine Alone	2867 ± 46.68	0	1.15×10^{-4}	
	L-Carnitine	3247 ± 235.45	0	1.30×10^{-4}	0.7639
	CoQ10	5858 ± 3915	10.55	2.34×10^{-4}	0.0250*
	Retinol	476.5 ± 192.87	0	1.91×10^{-5}	0.0680
Theophylline	Theophylline Alone (Low)	15.67 ± 7.64	0	7.83×10^{-7}	
	Theophylline Alone (Medium)	16.26 ± 13.67	0	8.13×10^{-7}	>0.05
	Theophylline Alone (High)	95.44 ± 42.57	0	4.78×10^{-6}	>0.05
	L-Carnitine (Low)	108.5 ± 64.5	0	5.43×10^{-6}	0.9841
	L-Carnitine (High)	156.6 ± 25.43	7.221	7.83×10^{-6}	0.9237
	CoQ10	214.4 ± 90.99	0	1.07×10^{-5}	0.9658
	Retinol	317.2 ± 217.29	0	1.59×10^{-5}	0.9482
L-Carnitine	L-Carnitine Alone	10.62 ± 3.94	0	5.31×10^{-7}	
	CoQ10 (Low)	6950 ± 7172.05	0	3.46×10^{-4}	0.7641
	CoQ10 (High)	31497 ± 5616.21	0	1.57×10^{-3}	0.1786
	Theophylline (Low)	37274 ± 46776	0	1.86×10^{-3}	0.1132
	Theophylline (High)	53373 ± 12474	74.28	2.67×10^{-3}	0.0258*
	Retinol	1135 ± 484.79	0	5.68×10^{-5}	0.9612

*Statistical significance of $Flux_{ss}$ comparison with compounds alone ($p<0.05$). A 1-way ANOVA test was used.

Table 9: Summary of steady flux, Lag time and Apparent permeability coefficient (Papp) of Active compounds alone and in combination in a cream formulation.

Compound	In Combination with	$Flux_{ss}$ ($ng.cm^{-2}.min^{-1}$) Mean ± SD	Lag Time (min)	Papp Value ($cm.min^{-1}$)	Statistical significance of $Flux_{ss}$ (*p* value)
Cream Formulation					
Caffeine	Caffeine Alone	3143 ± 64.56	0	1.25×10^{-4}	
	L-Carnitine	2808 ± 242.72	0	1.11×10^{-4}	0.7911
	CoQ10	20008 ± 3277.04	0	8.00×10^{-4}	<0.0001*
	Retinol	3089 ± 370.74	6.43	1.24×10^{-4}	0.9659
Theophylline	Theophylline Alone	601.5 ± 247.77	0	3.01×10^{-5}	
	L-Carnitine	126.8 ± 29.87	15.26	6.34×10^{-6}	0.9186
	CoQ10	182.7 ± 658.5	0	9.13×10^{-6}	0.9282
	Retinol	1945 ± 19311	0	9.73×10^{-5}	0.7724
L-Carnitine	L-Carnitine Alone	5.60 ± 5.11	118.5	2.8×10^{-7}	
	CoQ10	30647 ± 15864	0	1.53×10^{-3}	0.1903
	Theophylline	32837 ± 10667.53	62.62	1.64×10^{-3}	0.1612
	Retinol	2280 ± 450.9	18.82	1.14×10^{-4}	0.9216

*Statistical significance of $Flux_{ss}$ comparison with compounds alone ($p<0.05$). A 1-way ANOVA test was used.

3.2.4 TEER values

Skin integrity (tissue resistance) was evaluated over a 24-hour time period to investigate whether caffeine, theophylline, L-carnitine and retinol in the different formulations had a negative effect on the skin barrier. TEER values for Co-enzyme Q10 were not obtained due to the instability of the compound. The TEER results can be observed in Figures 3.32a – c below.

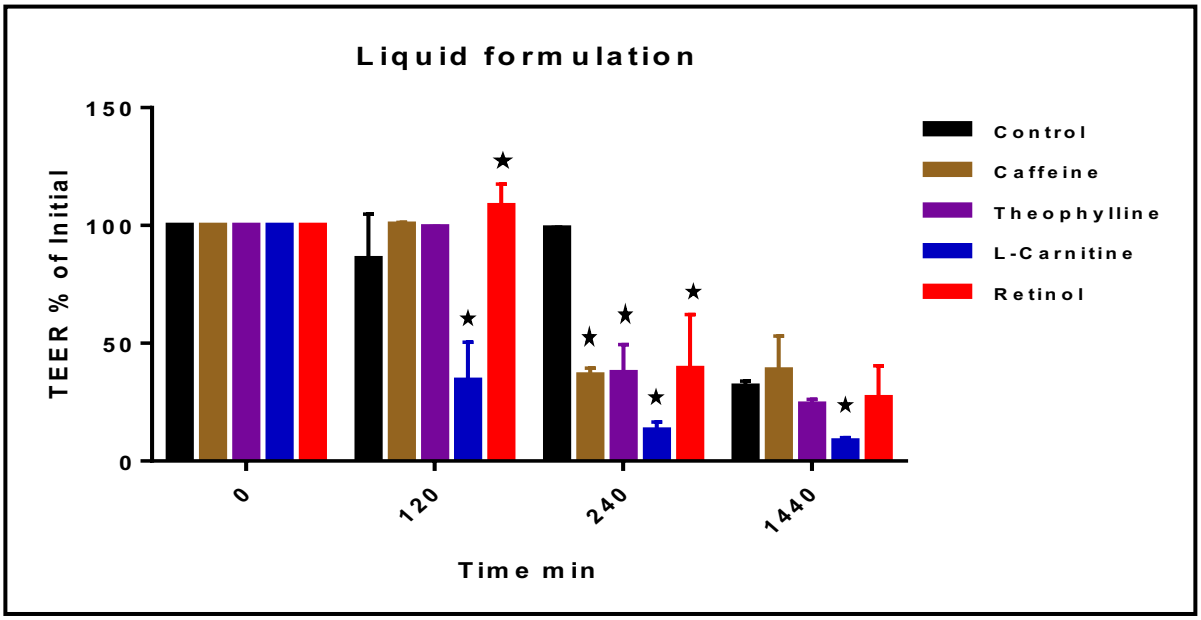

Figure 9: Skin integrity test (TEER) after exposure to active compounds in a liquid formulation compared to liquid formulation alone.***:** Statistically significantly different compared to control ($p<0.05$) (Caffeine: 2.5%, Theophylline: 2%, L-carnitine: 2%, Co-enzyme Q10: 0.5% and Retinol: 0.3%).

As can be seen from Figure 3.32a, skin barrier function remained mostly intact after 4 hours exposure to a liquid formulation without active compounds, however barrier function decreased with time and reached <50% after 24 hours exposure. Barrier function remained relatively intact with active compounds until 2 hours, except for L-carnitine which affected barrier function severely at this time point and beyond. All active compounds caused a decrease in skin barrier function after 24 hours exposure time, with theophylline and L-carnitine having the greatest effect on skin. Furthermore, l-carnitine was found to have a significant decrease in skin integrity as compared to all the other active ingredients.

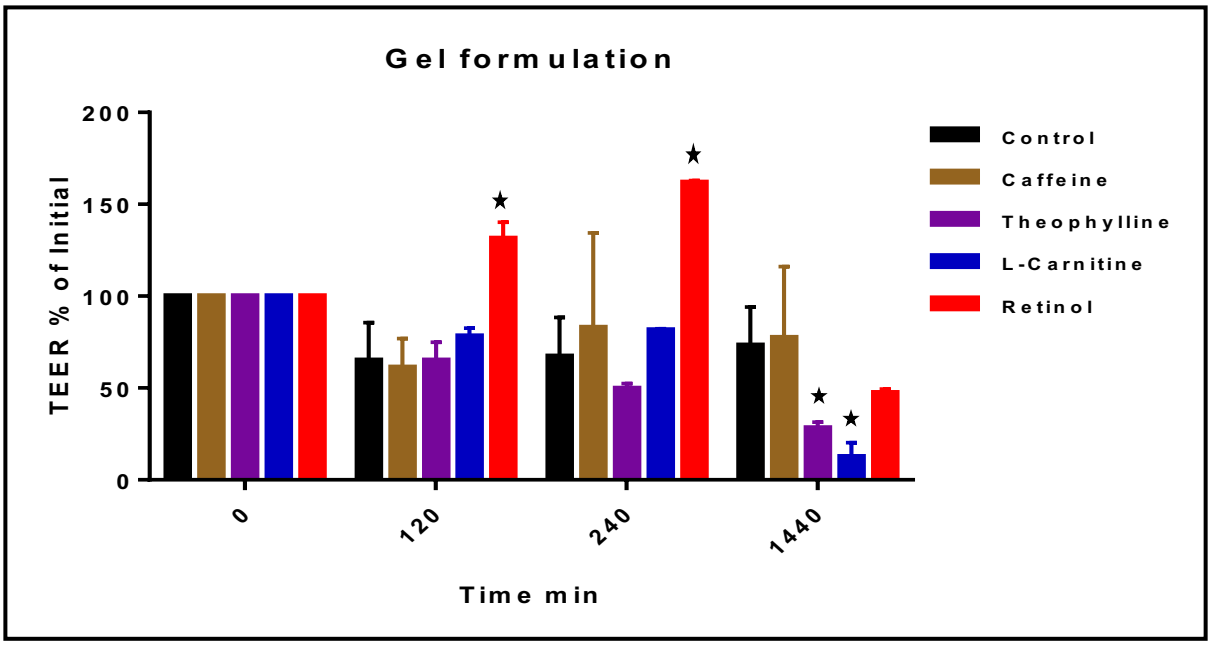

Figure 9:Skin integrity test (TEER) after exposure to active compounds in a gel formulation compared to gel formulation alone. ***:** Statistically significantly different compared to control ($p<0.05$) (Caffeine: 2.5%, Theophylline: 2%, L-carnitine: 2%, Co-enzyme Q10: 0.5% and Retinol: 0.3%).

From Figure 3.32b above, it can be seen that skin barrier function decreased after 2 hours exposure to approximately 70%. In contrast, retinol caused an increase in skin barrier function up between 2 to 4 hours of exposure retinol. However, skin integrity decreased by 50% after 24 hours exposure to retinol. Barrier function remained between 50 and 70% for the other active compounds till 4 hours, except for retinol. All active compounds caused a decrease in skin barrier function after 24 hours exposure time, with theophylline and L-carnitine having a significant effect on skin integrity.

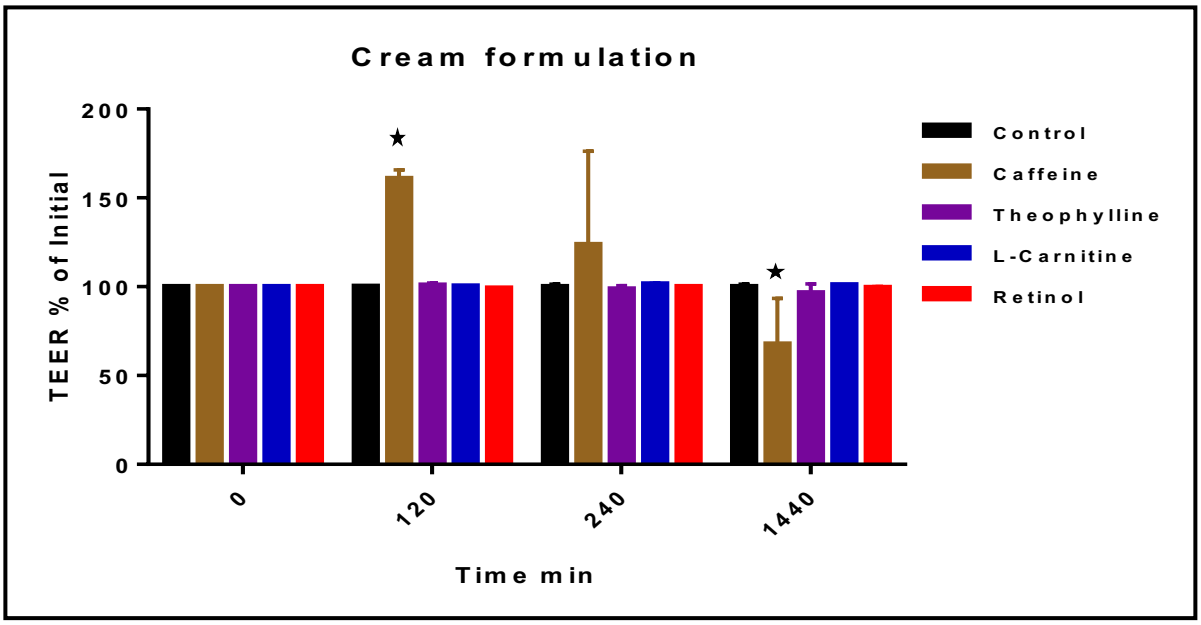

Figure 9: Skin integrity test (TEER) after exposure to active compounds in a cream formulation compared to cream formulation alone. *: Statistically significantly different compared to control ($p<0.05$).Caffeine: 2.5%, Theophylline: 2%, L-carnitine: 2%, Co-enzyme Q10: 0.5% and Retinol: 0.3%).

From Figure 3.32c above, it can be seen that skin barrier function remained relatively intact up till 24 hours exposure to active ingredients in a cream formulation. Caffeine caused a significant increase in skin barrier function after 2 – 4 hours of exposure, but decreased significantly after 24 hours exposure.

3.2.5 Skin Extraction

3.2.5.1 Skin extraction of active ingredients alone

After completing the diffusion experiment of the active compound alone, the skin disk was removed and cleaned. The homogenized sample was then analysed by HPLC. The skin disk was homogenized in 2 ml of methanol and subsequently centrifuged. Following centrifugation, the sample underwent filtration through a 0.45 µm syringe filter and was then analysed using the HPLC machine.

Table 3.49 presents the summary of the average percent accumulation (of the initial amount) of Caffeine, Theophylline, Retinol, L-carnitine, and Co-enzyme Q10 in three different formulations. For each active compound, the percentage of the initial active compound alone in three different formulations was extracted from the skin disk.

In the case of caffeine, the gel formulation exhibited a significantly higher percentage of caffeine accumulation compared to the liquid ($p < 0.05$) and cream ($p < 0.05$) formulations.

For theophylline, the liquid formulation showed a higher percentage of theophylline accumulation compared to the cream and gel formulations; however, this difference was not statistically significant ($p > 0.05$).

Analysing retinol skin accumulation over a 4-hour period revealed that the liquid formulation had a higher percentage of retinol accumulation compared to the cream and gel formulations ($p > 0.05$). Similarly, over a 24-hour period, the liquid formulation exhibited a higher percentage of retinol accumulation compared to the cream and gel formulations ($p > 0.05$).

Regarding L-carnitine skin accumulation, the liquid formulation demonstrated a higher percentage of L-carnitine accumulation compared to the cream and gel formulations ($p > 0.05$).

In the case of coenzyme Q10 skin accumulation, the liquid formulation showed a significantly higher percentage of coenzyme Q10 accumulation compared to the cream and gel formulations ($p > 0.05$).

Table 9: Summary of average percent accumulation (of initial amount) of Caffeine, Theophylline, Retinol, L-carnitine, and Co-enzyme Q10 in three different formulations.

Compound	Formulations	Average (%) Accumulation	Standard deviation
Caffeine (2.5%)	Liquid	13.70	0.61
	Cream	13.86	0.75
	Gel	16.14	1.15
Theophylline (2%)	Liquid	0.93	0.06
	Cream	0.69	0.04
	Gel	0.57	0.01
Retinol (4hrs) (0.3%)	Liquid	0.51	0.04
	Cream	0.25	0.14
	Gel	0.26	0.08
Retinol (24hrs) (0.3%)	Liquid	0.68	0.44
	Cream	0.21	0.01
	Gel	0.18	0.08
L-carnitine (2%)	Liquid	2.33	1.22
	Cream	1.32	0.81
	Gel	1.56	0
CoQ_{10}	Liquid	0.04	0.01
	Cream	0.006	0.004
	Gel	0.03	0.02

*Statistical significance **($p<0.05$)**:

Caffeine: Liquid vs Cream (p=0.8049); **Liquid vs Gel:** (p=0.0016*); **Gel vs Cream** (p=0.0027*). **Caffeine (Liquid, Gel & Cream) vs Theophylline, L-Carnitine, Retinol & Coenzyme Q10 in all formulations** (p<0.0001*). Theophylline: Liquid vs Gel (p=0.5799); Liquid vs Cream (p=0.7113); Gel vs Cream (p=0.8529). L-Carnitine: Liquid vs Gel (p=0.2450); Liquid vs Cream (p=0.1333); Gel vs Cream (p=0.7113).

L-Carnitine (Liquid) vs Retinol, Theophylline & Coenzyme Q10 in all formulations (p<0.05*). Retinol: Liquid vs Gel (p=0.6999); Liquid vs Cream

(*p*=0.6886); Gel vs Cream (*p*=0.9877). Coenzyme Q10: Liquid vs Gel (*p*=0.4354); Liquid vs Cream (*p*=0.4145); Gel vs Cream (*p*=0.9704). Statistical test: 2-way ANOVA.

3.2.5.2 Skin extraction of active compounds in combination

Once the diffusion experiment of active compound in combination was completed, the skin disk was removed and wiped down dry with a tissue paper to remove any formulation. The skin disk was then homogenised in 2 ml methanol and centrifuged. After being centrifuged, the sample was filtered through a 0.45 µm syringe filter and analysed using the HPLC machine. The percentage of initial active compound in combination in three different formulations, which was extracted from the skin tissue is shown in Table 3.49.

3.2.5.2.1 Combination Caffeine extraction

Caffeine was combined with Retinol, Co-enzyme Q10, and L-carnitine in three different formulations (liquid, gel, and cream). When combined with L-carnitine, the liquid formulation exhibited a higher percentage of caffeine accumulation compared to the cream ($p > 0.05$) and gel ($p > 0.05$). Similarly, in combination with retinol, the liquid formulation showed a higher percentage of caffeine accumulation compared to the cream ($p > 0.05$) and gel ($p > 0.05$). Furthermore, when combined with co-enzyme Q10, the liquid formulation demonstrated a higher percentage of caffeine accumulation compared to the cream ($p > 0.05$) and gel ($p > 0.05$).

3.2.5.2.2 Combination Theophylline extraction

Theophylline was combined with Co-enzyme Q10, L-carnitine, and Retinol in three distinct formulations (liquid, gel, and cream). When Theophylline was combined with Co-enzyme Q10, the liquid formulation exhibited a higher percentage of Theophylline accumulation compared to the cream ($p > 0.05$) and gel ($p > 0.05$). Similarly, when Theophylline was combined with L-carnitine, the liquid formulation demonstrated a higher percentage of Theophylline accumulation compared to the cream ($p > 0.05$) and gel ($p > 0.05$). Notably, Theophylline in combination with retinol revealed that the gel formulation had a significantly higher percentage of Theophylline accumulation compared to both the liquid ($p < 0.0001$) and cream ($p < 0.0001$) formulations.

3.2.5.2.3 Combination Retinol extraction

Retinol was combined with L-carnitine, Theophylline, and Caffeine in three different formulations (liquid, gel, and cream). When Retinol was combined with L-carnitine, the liquid formulation demonstrated a higher percentage of retinol accumulation compared to the cream ($p > 0.05$) and gel ($p > 0.05$). In the case of Retinol in combination with Theophylline, the gel formulation exhibited a significantly higher percentage of retinol accumulation compared to both the liquid ($p = 0.008$) and cream ($p = 0.0391$) formulations. Similarly, when Retinol was combined with Caffeine, the liquid formulation showed a higher percentage of retinol accumulation compared to the gel ($p > 0.05$) and cream ($p > 0.05$) formulations.

3.2.5.2.4 Combination Co-enzyme Q10 extraction

Coenzyme Q10 was combined with caffeine, L-carnitine, and Theophylline in three different formulations (liquid, gel, and cream). Results obtained from diffusion experiments, where Coenzyme Q10 was combined with L-carnitine and Theophylline, indicated detectable peaks; however, the quantification of Coenzyme Q10 was not feasible.

In the combination of Coenzyme Q10 and caffeine, the liquid formulation exhibited a significantly higher percentage of Coenzyme Q10 accumulation compared to both the gel ($p < 0.0001$) and cream ($p < 0.0001$).

3.2.5.2.5 Combination L-carnitine extraction

L-carnitine was combined with retinol, coenzyme Q10, caffeine, and theophylline in three different formulations (liquid, gel, and cream). When L-carnitine was combined with caffeine, the cream formulation exhibited a higher percentage of L-carnitine accumulation compared to the gel ($p > 0.05$), while the liquid formulation showed a significantly lower accumulation ($p = 0.0014$). In combination with coenzyme Q10, both the cream and gel formulations demonstrated a higher percentage of L-carnitine accumulation compared to the liquid, which was significantly lower ($p < 0.005$). Combining L-carnitine with retinol revealed that both gel and liquid formulations had a

higher percentage of L-carnitine accumulation compared to the cream (p = 0.0278). Lastly, in combination with theophylline, both gel and cream formulations showed a higher percentage of L-carnitine accumulation compared to the liquid, with the liquid formulation being significantly lower (p < 0.005).

Table 9: Summary of average percent accumulation (% of initial) of active compound in combination.

Combination Accumulation within skin			
	% of initial compound		
	Formulation		
Compound (% w/v)	**Liquid**	**Gel**	**Cream**
Caffeine (2.5%) + Retinol (0.3%)	Caff: 0.100 ± 0.057^{+} Ret: 0.032 ± 0.035$^{\&}$	Caff: 0.066 ± 0.035^{+} Ret: 0.0028 ± 0.003	Caff: 0.037 ± 0.0016^{+} Ret: 0.0008 ± 0.00026
Caffeine (2.5%) + CoQ10 (0.5%)	Caff: 0.510 ± 0.150^{+} CoQ10: 4.117 ± 0.715^{+}	Caff: 0.240 ± 0.015^{+} CoQ10: 0.15 ± 0.013	Caff: 0.120 ± 0.013^{+} CoQ10: 0.120 ± 0.008
Caffeine (2.5%) + L-carnitine (2%)	Caff: 0.480 ± 0.0^{+} L-car: 2.69 ± 0	Caff: 0.27 ± 0.14^{+} L-car: 5.53 ± 0$^{\#}$	Caff: 0.37 ± 0.0^{+} L-car: 6.50 ± 0^{+}
Theophylline (2%) + CoQ10 (0.5%)	Theo: 0.035 ± 0.027^{+} *CoQ10: - detected	Theo: 0.020 ± 0.01 *CoQ10: - detected	Theo: 0.003 ± 3.5x10^{-5+} *CoQ10: - detected
Theophylline (2%) + L-Carnitine (2%)	Theo: 0.034 ± 0.0006^{+} L-car: 2.87 ± 0	Theo: 0.014 ± 0.0003 L-car: 6.14 ± 0$^{\#}$	Theo: 0.003 ± 3.99x10^{-5+} L-car: 5.92 ± 0$^{\#}$
Theophylline (2%) + Retinol (0.3%)	Theo: 0.260 ± 0.007^{+} Ret: 0.059 ± 0.00049$^{\&}$	Theo: 1.330 ± 0.003 Ret: 0.470 ± 0.0023$^{\wedge}$	Theo: 0.630 ± 0.008$^{\$}$ Ret: 0.170 ± 0.00062
Retinol (0.3%) + L-carnitine (2%)	Ret: 0.008 ± 0.005$^{\&}$ L-car: 3.56 ± 1.53	Ret: 0.0005 ± 0.00012 L-car: 3.14 ± 2.42	Ret: 0.0011 ± 0.0011 L-car: 1.18 ± 0.74
L-carnitine (2%) + CoQ10 (0.5%)	L-car: 3.57 ± 1.33 *CoQ10: detected	L-car: 6.98 ± 1.04^{+} *CoQ10: detected	L-car: 7.23 ± 0.76^{+} *CQ10: detected

***** Coenzyme Q10 was detected in these samples, but could not be quantified
$^{+}$ Statistically significantly different compared to compound alone (p<0.0001)
$^{\$}$ Statistically significantly different compared to compound alone (p<0.030)
$^{\#}$ Statistically significantly different compared to compound alone (p<0.002)
$^{\&}$ Statistically significantly different compared to compound alone (p<0.001)
^ Statistically significantly different compared to compound alone (p<0.05)

Chapter 4: Discussion

Topical drug delivery has been found to be an effective route of drug administration due to the fact that the drug circumvents first-pass metabolism and has a direct local effect on the skin or mucous membranes. It also reaches the targeted areas faster and has reduced amount of side effects compared to the oral route (Ruela et al., 2016). The administration of topical drugs is found to achieve controlled or prolonged drug delivery (Ruela *et al*., 2016). The concept of topical application reveals that some drugs will remain on the surface of the skin (topical) or penetrate across the skin layers (transdermal) (Supe and Takudage, 2019). Various formulations have been used to deliver active compounds (caffeine, theophylline, L-carnitine, retinol and Coenzyme Q10, amongst others) to the skin for different skin afflictions e.g. wrinkles, UV damage, inflammation, cellulite, psoriasis etc (Wang *et al*., 2021; Desoqi *et al*., 2021)

The focus of this study was to investigate the efficacy of *in vitro* diffusion of active compounds such as Caffeine, Theophylline, Retinol, L-carnitine and Co-enzyme Q10, alone and in combination, from three different formulations (liquid, gel and cream) across exercised porcine skin. To reach this objective, HPLC methods used to detect these compounds were explored and validated. Furthermore, the amount of accumulation of these compounds, alone and in combination was investigated as well as the effect of the formulations and the compounds on the barrier properties of the exercised skin.

4.1. Method development and Validation of Active compounds

4.1.1 Caffeine

Caffeine is a xanthine derivative with a molecular weight of 194.19 g/mol (van Zyl *et al.,* 2008). This small molecule consists of an additional methyl group on position 7 of the chemical structure. Increasing the water solubility of caffeine which results in a slower distribution of compound through PBS (van Zyl *et al*., 2008). This theory can be seen in a study conducted by van Zyl and colleagues (2002), which compared the molecular diffusion of drugs across porcine bronchial tissue, and it was found that

theophylline has a greater flux value (620 ng.cm^{-2}.min^{-1}) as compared to caffeine and theobromine (380 ng.cm^{-2}.min^{-1}) (van Zyl *et al*., 2008).

The quantification of caffeine content was performed using the published and validated HPLC method by Chowdhury *et al*. (2012). This method was not altered as caffeine was detected at a retention time of 2.57± 0.02 min. Linearity of the caffeine calibration curve was good with a R^2 value of 0.9952 in the range of 0 – 200 µg/ml (y= 19610x - 85893). Variation of values was found in the lower region of the calibration curve. As such, a further analysis was performed using the lower concentrations and a strong linear relationship was indicated as seen in Figure 3.2 (0 - 30 µg/ml, R^2= 0.9988). The variation could be due to the mobile phase used in our study, as a mixture of methanol and water (40:60; v/v) was used. In a study conducted by Alkhamaisah and colleagues (2019), a low gradient mobile phase containing water, methanol, and acetonitrile in a ratio of 84:1:15 was used to measure the amount of caffeine in different beverages. Result obtained showed that the HPLC method used to detect caffeine content in beverages gave a R^2 value of 0.9995 in the range of 0.122-125 µg/ml (y=25686x + 21332). Acetonitrile is a strong eluotropic compound and is frequently used in reversed phase HPLC and capillary electrophoresis (Rudakov *et al*., 2018).

Precision RSD (%) was found to be 4.2%, 2.2% and 1.8% at concentration values of 15,30, and 150 µg/ml respectively in the lower concentration ranges (table 3.1). At a higher concentration (150 µg/ml) RSD was found to be ≤ 2%. This could be explained using the Horwitz function, as the concentration of the analyte decreases, the relative standard deviation reproducibility (RSDR) increases (Horwitz and Albert, 2006). Intra- and inter-day precision %RSD values were ≤2%, this confirms adequate sample stability and method reliability (Horwitz and Albert, 2006).

Accuracy of the method was analyzed by studying the % recovery using three different concentrations for each sample in replicates (n=6). The results obtained showed an % recovery within the ranges of 80-120%, which shows that the method was able to accurately quantify and estimate caffeine. The ruggedness of the method was measured by determining the effect of temperature variation, mobile phase variation and flow rate variation. The result obtained from the %RSD (≤2 %) (table 3.1) showed that the method was successfully applied to measure caffeine.

The stability of caffeine was determined by storing the caffeine working solution at a temperature of 4°C over a period of 2-3 days (table 3.31). The result demonstrated a %RSD of 2% which shows that stability was not kept completely intact. This could be

due to the period caffeine was stored for and the temperature it was stored at. In a study conducted by Al-Bratty and colleagues (2020), the short- and long-term stability of caffeine was investigated. The result showed that caffeine (10µg/ml) stored in room temperature for 48h, in a refrigerator at -7°C for 7 days and at -20°C for 30 days had a good stability (RSD ≤2%) (Al-Bratty *et al*., 2020). In another study conducted by Oliphant and colleagues (2022), the aim was to develop and validate a liquid chromatography assay *in vitro* and *in vivo* quantification of caffeine and this to determine the stability of caffeine citrate solution. The result obtained showed that caffeine found in saliva placed under freeze and thaw cycles (-20°C to ambient temperature for a total of 3 months) was stable in all three different concentration (1,15 and 30 µg/ml), RSD value was ≤ 2% (Oliphant *et al*., 2022). In both aforementioned studies, stability testing of caffeine was conducted at temperatures below 0°C for a duration exceeding three days.

4.1.2 Theophylline

Theophylline is a methylxanthine with a molecular weight of 180.16 g/mol and is a metabolite of caffeine (Moghimipour *et al*., 2012). This compound has been used to manage respiratory diseases. As a result of its capacity to elevate cyclic AMP levels by non-selectively inhibiting phosphodiesterase, caffeine induces the relaxation of bronchial smooth muscles, thereby exerting bronchodilatory effects (Moghimipour *et al*., 2012). The compound is more soluble in hot water, has a negative log P value and shows slight solubility in organic liquids (Gulaboski *et al*., 2007). Theophylline was quantified using the same method and conditions as used for the detection of caffeine (Chowdhury *et al*., 2012). Theophylline was detected at a retention time of 2.18 ± 0.03 min (figure 3.5), slightly earlier than caffeine, as expected due to its increased hydrophilicity. Linearity of the theophylline calibration curve was good with a R^2 value of 0.9942 in the range of 0 - 25 µg/ml (y=96073x) (figure 3.4). In a study conducted by Al-Salman *et al.* (2021), theophylline was detected 3.45 ± 0.011 min, with the calibration curvelinear in the concentration range 5- 25 µg/ml and indicating excellent correlation (R^2= 0.9998). The increase in retention time could be due to the difference in mobile phase used - Methanol:Acetonitrile (50:50), (v/v) and acetic acid at pH 4.5 (Al-salman *et al*., 2021).

Precision, intra-and inter-day precisions demonstrated %RSD values ≤ 2. This indicates that the method is reproducible and reliable. Accuracy (RDS %) was within the 80-120% range except for the concentration value of 10 µg/ml, which had a value of 65% (table 3.12). The method development for ruggdeness and stability showed a %RSD value ≤ 2, which indicated that the method was successfully applied to measure theophylline (table 3.31).

4.1.3 Retinol

Retinol, also known as vitamin A is a common ingredient used to improve the appearance of skin (Yourick *et al.,* 2008). It is a slightly larger molecule (286.459g/mol), which is described to be very lipophillic with a Log P value of 5.8 (National Center for Biotechnology Information, 2022). Retinol was detected and quantified utilizing a HPLC RP C18 column using the method described by Patriche *et al*. (2014). Due to the lipophilic nature of the compound, 99% methanol was used in the mobile phase for the elution of the molecule and to prevent it from adhering to the reverse column (Patriche *et al*., 2014). This method was validated for the detection of retinol at a retention time of 2.91 ± 0.02 min (figure 3.8). In a study conducted by Khan *et al.* (2010), retinol was detected at a shorter retention time of 2.10 min, this could be due to column and mobile phase used which is as follows: Perkin Elmer C18 (150mm x 4.6mm x 5µm; Norwalk, USA) precolumn guard cartridge, at 292nm wavelength, using methanol–water (99:1, v/v), in isocratic mode. In a study conducted by Prabakaran *et al.* (2014), the retention times for standard and sample of Vitamin A Acetate was 1.182 min and 1.165 min, respectively. The retention time can be attributed to the mobile phase used in the HPLC method; RP 18 (250 Å~ 4.6mm; 5µm) column using the mobile phase consists of Acetonitrile: Isopropyl alcohol: n-Hexane (400:400:200). The linearity of the retinol calibration curve was good with a R^2 value of 0.9933 in the range of 0 - 100 µg/ml (y= 36849x + 72987) (figure 3.6).
The precision (table 3.3), accuracy (table 3.13), ruggedness and stability (figure 3.31) parameters were evaluated for retinol, the laboratory result showed that the method was accurate and fully validated (%RSD ≤ 2).

4.1.4 L-carnitine

L-carnitine, is a water soluble molecule with a molecular weight of 161.2 g/mol (In *et al* ., 2019). The molecule plays a role in transporting long chain fatty acid across the mitochondrial membrane (Perano *et al*., 2012). L-carnitine is known as a zwitterion which is defined as a polymer that contains both a positive and negative charge along the chain. The charge stoichiometry can either be neutral or weighed towards the cation or anion charge, switching charges can be dependent on the environment the polymer finds itself in (Blackman *et al*., 2019). L-carnitine was initially detected by using HPLC conditions described by Cao *et al*. (2007) however, the method was found to be inadequate in detecting L-carnitine (section 2.1.4.2.4). The molecule was not retained in the C18 column as it was expelled into the void volume. A different method was used to detect L-carnitine, one described by Khoshkam and Afshar (2014), with slight variation. The mobile phase consisted of 0.05 M phosphate buffer (pH 3.0: methanol (99:1) containing 0.56 mg/ml of sodium 1-heptanesulfonate and the column temperature was set at 40°C instead of 50°C. Linearity of the L-carnitine calibration curve was adequate with a R^2 value of 0.9714 in the range of 0 – 1000 µg/ml (y= 86.385x + 1981.8) (figure 3.12).

In a study conducted by Manoharan (2021), L-carnitine showed a good linearity at concentration ranges between 70-1120 µg/ml with an R^2 value of 1. In the current study, L-carnitine had a retention time of 3.0 ± 0.009 min, while in the study conducted by Manoharan (2021), the retention time was more than double at 7.7 min. This could be due to the HPLC conditions used in this particular study, where the mobile phase consisted of 0.05M phosphate buffer (pH-3.2): Methanol (95: 5 v/v) (Manoharan, 2021).

The developed HPLC method showed that the precision, accuracy, ruggedness and stability was valid (%RSD ≤2). The intermediate precision of L-carnitine between two days showed an RSD value of 6.4%. The Recovery percentage of accuracy result for 100, 400 and 700 µg/ml was 63.9%, 79.3% and 80.3% respectively. The results obtained for intermediate precision (table 3.10) and accuracy (table 3.15) did not fall within the %RSD range (≤2%). There is no substantial reason for the results obtained, this could possibly be due to the degradation of the L-carnitine molecule due to temperature variation or pH of mobile phase.

4.1.5 Coenzyme Q10

Coenzyme Q10 (CoQ10), or ubiquinone (863.3 g/mol; log p value 10) is a fat-soluble (lipophilic) anti-oxidant which is found naturally in the phospholipid bilayer membrane in every single cell in the body (Borekova *et al*., 2008; National Center for Biotechnology Information (2022). PubChem Compound Summary for CID 5281915, Coenzyme Q10. Retrieved June 29, 2022). The compound enhances mitochondrial activity, maintains bioenergetic activities in human tissue, transport electrons to the mitochondrial membrane and enhances the immune system (Crane, 2001; Borekova *et al*., 2008 and Lopez *et al*., 2010). CoQ10 was quantified using RP HPLC utilizing the method described by Yuan *et al*., (2010). Chromatic separation was done on a Diamonsil C_{18} column with the UV detector set at 275nm. Mobile phase was prepared using methanol-2-propanol (40:60, v/v), which was identical to the one used in the current study. At first, mobile phase used for coenzyme Q10 was methanol:water (98:2 v/v), however this yielded to no detection peak on the HPLC.

Linearity of the coenzyme Q10 calibration curve was good with a R^2 value of 0.9986 in the range of 0 – 100 μg/ml (10175x + 23299) (figure 3.9). Due to variation in the lower region of the curve, analyses were performed on standards covering the lower regions of the standard curve for coenzyme Q10 (0-10 μg/ml), with an equation of (y=20188x + 5000.9) and a retention time of 3.15 ± 0.003 min (figure 3.10). In a study conducted by Sarkar *et al*. (2021), linearity of CoQ10 was obtained in the concentration range of 240-360 μg/ml with an R^2 value of 0.997 and a retention time of 4.46 min. The differences in retention time could be due to the HPLC condition used in this study such as Waters X Bridge C_{18} column was used as stationary phase and as mobile phase, a mixture of acetonitrile, tetrahydrofuran, and water (65:32:3 v/v) was used. The result obtained from HPLC method development showed that the precision (table 3.4), accuracy (table 3.14), ruggedness, and stability (table 3.31) was valid (RSD≤ 2%).

4.2. In vitro diffusion of active compounds across skin

Topical and transdermal drug delivery have shown increased benefits in clinical practice for drug delivery to targeted sites. The major benefits from this system are: it avoids first pass metabolism, controls, and prolongs the release of compounds and there is a reduction in the amount of side effects as compared to the oral route of administration (Ruela *et al*., 2016).

Studies have shown that certain drug molecules contain characteristics which are ideal for transdermal drug delivery across the stratum corneum. The epidermis' outermost layer serves as a barrier, recognized for its lipophilic nature. Consequently, molecules with high lipophilicity exhibit enhanced permeability across this membrane (N'Da, 2014; Neupane *et al*., 2020). Molecules should preferably have a low molecular weight (200-500 Da) to easily penetrate across the stratum corneum. In the case of a large molecular weight, penetration enhancers could be added to facilitate the movement of the molecule across the skin. In this regard, the development of an appropriate formulation to enhance drug delivery plays a role (Neupane *et al*., 2020). The solubility and the partition coefficient of the molecule determines the pathway the drug would follow to permeate across the skin. Hydrophilic molecules would use transcellular routes (through the cells) while lipophilic molecules would use intercellular routes (between cells or paracellular route). Ideally, a molecule should consist of both lipophilic and hydrophilic properties to simplify the transdermal drug delivery (N'Da, 2014). There is a third route of permeation, that is known as the shunt pathway or appendageal route. This pathway offers a path for molecules to move through hair follicles (the transfollicular route) or sweat glands and across the stratum corneum (Ng and Lau, 2015). Drugs that use this pathway consist of a high molecular weight (N'Da, 2014). However, according to a study conducted by Verma *et al*. (2016), the transfollicular route is more suitable for systemic delivery as it contributes insignificantly to local therapy. This could be due to the complex unit which has various barriers that can enhance or hinder the permeation of a molecule (Verma *et al*., 2016).

In this study, an *in vitro* diffusion method utilizing flow-through in-line cells (PermeGear) was used to investigate the movement of active compounds such as

Caffeine, Theophylline, Retinol, L-carnitine, and Co-enzyme Q10, across the layers of the skin.

4.2.1 Caffeine

Caffeine is a small molecule with a molecular weight of 194,19 g/mol, a log P value of approximately -0.07 and consists of both hydrophilic and lipophilic properties (Pubchem). These characteristics benefit the transdermal delivery of caffeine across the stratum corneum. A log P value > -1 is considered a good value for compounds that undergoes transdermal delivery (N'Da, 2014). In a study conducted by Yu and colleagues (2021), a description of favorable factors that influence percutaneous absorption were reviewed. Results showed that a Log P value between 1-3 is considered to have both hydrophilic and lipophilic properties and therefore considered a favorable molecule to diffuse through skin (Yu et al., 2021).

The results obtained from the current study showed that caffeine penetrated the skin immediately (no lag time), it gave linear kinetics (cumulative amount versus time) and did not reach a plateau after 24 hours. Caffeine contains hydrophilic properties, which allows it to be absorbed and distributed throughout a body of water and sufficient lipophilic properties which allow for the compound to pass through membranes (Caffeine for sustainment of Mental Task performance, 2001).

The different formulations used (liquid, gel, or cream) did not affect the penetration behaviour of caffeine across the skin and no statistically significant differences in steady state flux and Papp values were found between the 3 different formulations (table 3.33) ($p>0.05$). Similar to the results in this study, Mustapha *et al*. (2011) found that 1g caffeine in a gel formulation showed the highest absorption characteristics across skin compared to caffeine in a liquid or cream formulation.

The cumulative diffusion graph for caffeine (Figure 3.19) indicated that caffeine most probably used all 3 transdermal permeation routes (transcellular, intercellular and transappendageal route) to diffuse across the skin. Since caffeine was found to easily diffuse through the stratum corneum and dermis layer of the skin, there is a chance that the compound will reach the circulatory system, with resultant side effects e.g. tachycardia. In a study conducted by Trauer *et al*. (2009), where the data from *in vitro* follicular penetration of caffeine was compared to the data from *in vivo* experiments, it was found that in both experiments, caffeine diffused through the follicular pathway by

50%. Compared to the *in vitro* data however, the *in vivo* data indicated that caffeine was detected in the blood stream (Trauer *et al*., 2009). This could potentially lead to increased tension, anxiety, tremor, and palpitations in individuals that are sensitive to caffeine (Rodak *et al*., 2021).

4.2.2 Theophylline

Theophylline is a metabolite of caffeine with a small molecular weight of 180,14 g/mol and displays both hydrophilic and lipophilic properties. Due to the structural difference of having one less methyl group, theophylline is more hydrophilic (log P = -0.02) than caffeine (log P=-0.07) (Andrei, 2011). The molecule will therefore most probably use the transcellular route as its main pathway to diffuse across the skin (figure 3.21). It was found that theophylline from the liquid formulation had the highest diffusion rate (figure 3.21). This is most probably due to the presence of the penetration enhancers, ethanol, and propylene glycol within the liquid formulation (Haq and Michniak-kohn, 2018). Theophylline showed great variation in diffusion behaviour across the skin, irrespective of the formulation used and might be due to the fact that theophylline diffused across skin using both the paracellular (intercellular) and the intracellular (transcellular) pathways. Even though the paracellular pathway is not the preferred pathway for more hydrophilic molecules, the penetration enhancers found in the different formulations modify the corneocytes' protein structure in the stratum corneum and thus increases the permeability (Carrer *et al*., 2020).

Ethanol is often used in various pharmaceutical and cosmetic formulations, however there is no exact explanation behind the mechanism of ethanol as a penetration enhancer. In a study conducted by Gupta *et al*. (2020), it was found that ethanol enhanced bilayer permeability by extraction of skin lipids and enhancing the mobility of lipid chains (Gupta *et al*., 2020). This reasoning might support the finding in the current study that theophylline from a liquid formulation gave the highest diffusion rate (table 3.34).

In the cream formulation olive oil was added, which is a natural potent free fatty acid permeation enhancer (Masrijal *et al*., 2020). The natural occurring enhancer disrupts skin barrier and increases permeability across the skin. Theophylline from the cream formulation was found to diffuse across the skin, however at a lower rate as compared to from the liquid formulation (table 3.34). In a study conducted by Wang *et al*. (2007),

the permeation of aminophylline in three plant oils, including olive oil, were investigated. Results indicated that all plant oils did enhance the permeation of aminophylline. However, their permeation enhancing effects were less than that found for ethanol (Wang *et al*., 2007). These findings support the results in the current study as illustrated in Figure 3.21.

Propylene glycol, a chemical enhancer also found in the gel formulation, increases the solubility in the intercellular lipids of the stratum corneum (Carrer *et al*., 2019). In the result obtained for this study, the theophylline from the gel formulation had a lower diffusion rate as compared to that found from the liquid and the cream formulations. This could be due to propylene glycol used as co-solvent with ethanol in the liquid formulation where it works effectively in combination with ethanol, thus enhancing theophylline's permeation (Karande and Mitragotri, 2009). Furthermore, reasons why molecules from formulations containing propylene glycol resulted in a lower diffusion rate as compared to formulations containing ethanol, could be due to the mechanism of action of these two penetration enhancers. Ethanol disrupts the stratum corneum barrier by removing intercellular material and causing lipid fluidization and extraction, while propylene glycol increases permeability by solvating the alpha-keratin structure (Haq and Michniak-Kohn, 2018). A similar study was conducted by Duracher *et al*. (2009) investigating the *in vitro* transdermal diffusion of caffeine across pig skin in the presence of ethanol (5%), propylene glycol (5%) and a mixture of both ethanol and propylene glycol (25%:25%). The Duracher study indicated that ethanol on its own had the least effect on the diffusion of caffeine across porcine skin, followed by propylene glycol and, the most effective transdermal enhancer, was the mixture of ethanol and propylene glycol. These findings are in accordance with what was obtained in the current study, indicating that the two enhancers together do have a significant effect on the rate of diffusion of compounds across skin.

Another study was conducted by Pokorna *et al*. (2019) investigating the effectiveness of four different penetration enhancers on the diffusion behaviour of theophylline, prepared in a medium containing both propylene glycol and water. Results showed that all the chemical enhancers significantly improved the permeation of theophylline in range of 1-3 hours. The study also indicated that theophylline alone struggled to diffuse across tissue with a flux value of 6.60 ± 0.80 μg/cm^2/h which was the lowest value as compared to when used in combination with chemical permeation enhancers. Result obtained in the study showed Theophylline permeation with the chemical

permeation enhancers increased rapidly (29.84 ± 7.02 μg/cm^2/h) (Pokorna *et al*.,2019). A study conducted by Moghimipour *et al*. (2012) investigated the *in vitro* diffusion characteristics of theophylline across shaded snakeskin and the penetration enhancing effects of bile salts, sodium tauroglycocholate and sodium deoxycholate as well as skin modifiers such as oleic acid. Result indicated that enhancer-free samples showed almost no diffusion of theophylline across the skin (Moghimipour e*t al.*, 2012).

4.2.3 L-Carnitine

L- carnitine is a peptide derivative (161,20 g/mol) with a pKa of 3.8, a log P value of -5.58 and at a neutral pH of 7.4, it is a zwitterion with an overall neutral charge (National Center for Biotechnology Information (2022). PubChem Compound Summary for CID 10917, Levocarnitine. Retrieved June 29, 2022).

According to the results obtained, L-carnitine diffused across skin at a lower rate than Caffeine and Theophylline (Figures 3.19, 3.20 and 3,21). In a liquid formulation, L-carnitine reached a cumulative amount of approximately 2x10^4 ng/cm^2 after 24 hours (figure 3.22) while Caffeine and Theophylline reached cumulative values of approximately 8x10^5 ng/cm^2 (24 hours) (figure 3.20) and 1.5x10^5 ng/cm^2 (4 hours) (figure 3.21), respectively. The data obtained from this study shows how the hydrophilic L-carnitine molecule has limited transdermal penetration across the skin. According to In *et al.* (2019), when applied topically binds to the calcium positive charge (Ca^{2+}) found between the corneocytes in the stratum corneum. This resulted in a greater quantity of L-carnitine that remains in the surface area of the skin (In *et al*., 2019). Lim *et al,* (2018), performed a study that investigated different types of peptides and their skin permeation and effect on wrinkle reduction. They found that Acetyl hexapeptide-3 (also known as Acetyl hexapeptide-8, brand name Argireline (Arg0)), which is in a zwitterionic state, struggle to diffuse across the skin. Only 0.22% of the total amount that permeated across the skin was retained within the stratum corneum, while 0.01% of the peptide manage to permeate to the epidermis (Lim *et al*., 2018). This was due to the molecule large molecular weight (889 g/mol), hydrophilicity (log P = -6.3) and charged state.

From the results obtained in the current study (figure 3.22), L-carnitine in a liquid formulation, diffused at a greater rate as compared to the gel and cream formulations. The higher diffusion from the liquid formulation is due to ethanol and propylene glycol,

both penetration enhancers found in the liquid formulation. The gel formulation contained propylene glycol only, which is not as effective as ethanol, as it works better as a co-solvent (Haq and Michniak-kohn, 2018). The cream formulation had the lowest diffusion rate as compared to the liquid and gel formulations. The cream formulation consisted of olive oil, which is a free fatty acid natural penetration enhancer. The olive oil found in the cream formulation increased the diffusion of L-carnitine but was not able to deliver the compound to the target site as it forms a layer on the skin surface and inhibits L-carnitine to move through the hydrophilic part of the phospholipid bilayer. Similarly, a study conducted by Fox *et al*. (2011) that investigated the influence of a Pheroid (lipophilic enhancer) on the topical delivery and transdermal diffusion of L-carnitine through skin, indicated that the Pheroid increased the permeation of L-carnitine but did not improve the topical delivery to the target site (epidermis-dermis) as compared to PBS (Fox *et al*., 2011).

4.2.4 Retinol and Coenzyme Q10 (CoQ10)

Retinol and CoQ10 are larger molecules with molecular weights of 286 g/mol and 863.34 g/mol, respectively. Both these molecules are highly lipophilic with log P values of 5.68 and 10, respectively (National Center for Biotechnology Information. PubChem Database). The larger molecular weights and lipophilic natures of both molecules are factors that hinder the *in vitro* diffusion across skin resulting in accumulation within the skin surface (Yang and Hinner, 2015). In many studies, both Retinol and CoQ10 diffusion have been evaluated by using formulations containing penetration enhancers to increase transdermal delivery (Neupane *et al*., 2020). Due to the lipophilic nature and larger sizes of these molecules, both Retinol and CoQ10 are thought to penetrate the skin using the paracellular pathway (N'Da, 2014). This study did not detect any Retinol or CoQ10 in the receptor fluid even after 24 hours of exposure to the compounds.

4.3 In Vitro Diffusion of compounds in combination

Transdermal drug delivery is the process of administrating therapeutic agents across skin. This method is considered the most innovative way for a therapeutic agent to reach its target site as it presents numerous advantages. Most research studies have focused on single compound permeation or compounds with a permeation enhancer. These approaches do not take into consideration the effect one compound may have on the diffusion behavior of another when they are used in combination. As such, the diffusion behavior of compounds in combination from three formulations (liquid, gel, and cream) was investigated in the current study (Bird and Ravindra, 2020).

4.3.1 Caffeine alone and in combination in liquid, gel, and cream formulations

4.3.1.1 Liquid Formulation

Caffeine when combined with CoQ10, L-carnitine and Retinol (figure 3.23 and table 3.33) resulted in a linear diffusion rate similar to when caffeine alone diffused across porcine skin from a liquid formulation. There was a slight increase in caffeine diffusion when combined with L- carnitine and CoQ10, as compared to caffeine on its own however, the increases were not statistically significant ($p>0.05$). In contrast to the combinations of caffeine with either L-carnitine or CoQ10, when combined with Retinol, caffeine exhibited a slightly lower diffusion rate. However, this difference was not found to be statistically significant ($p > 0.05$). As mentioned before, previous studies have shown that L-carnitine influences the adhesion between corneocytes in the stratum corneum and this might result in the slight increase in caffeine diffusion when these two compounds are used in combination (In *et al.,* 2019). Both retinol and Coenzyme Q10 are very lipophilic molecules and tend to accumulate within the upper skin layers. As found in this study their effects on the diffusion behavior of caffeine from a liquid formulation is very similar to caffeine on its own (figure 3.23).

4.3.1.2 Gel Formulation

From the gel formulation, it was noticed that there is a greater diffusion rate of caffeine when combined with CoQ10 as compared to when on its own (figure 3.24). In combination with CoQ10, caffeine reached a cumulative amount after 24 hours of approximately $1x10^7$ ng/cm^2, while alone it reached a cumulative amount of approximately $4.6x10^6$ ng/cm^2 (table 3.37). This increase in diffusion was found to be statistically significant with a p value of 0.0250. A lag time was however noted (table 3.7). Thus, by combining CoQ10 and caffeine in a gel formulation containing propylene glycol as penetration enhancer, caffeine penetration would be more effective than it would be on its own. The mechanism of this increase in diffusion of caffeine when combined with coenzyme Q10 is unknown and it can only be speculated that it has to do with the enzymatic conversion of coenzyme Q10 in the skin and the hydrating/antioxidative effect of coenzyme Q10 in the skin that facilitated the movement of caffeine through the skin.

Caffeine, when combined with retinol showed a lower diffusion rate, compared to caffeine on its own. This effect was not statistically significant ($p>0.05$), but it shows that retinol impeded the diffusion of caffeine when the two compounds are used in combination. Although the mechanism of this is also unknown, it can be speculated that retinol accumulated in the skin (reservoir effect) and blocked the different pathways caffeine used to penetrate the skin, with the resultant slower diffusion rate of caffeine (Yourick et al., 2008). Caffeine in combination with L-carnitine, showed similar diffusion characteristics to caffeine on its own from 0-600 min (figure 3.24). After 600 min a great variation was observed which could be due to the fact that some of the caffeine molecules diffused rapidly through the transappendageal pathway (shunt). Looking at the large variation in the data, it could be assumed that the diffusion rate of caffeine when combined with L-carnitine would be superimposed on the caffeine-only curve and thus L-carnitine has no effect on the diffusion of caffeine from this gel formulation.

4.3.1.3 Cream Formulation

From a cream formulation, a similar pattern of caffeine diffusion as that observed from the gel formulation was noted. In combination with Coenzyme Q10, caffeine had a

statistically significantly greater cumulative amount after 24 hours of approximately 3.1x107 ng/cm^2 compared to caffeine on its own with a value of approximately 5x10^6 ng/cm^2 ($p<0.0001$, Table 3.35)). Similar to the gel formulation above, in combination with retinol, caffeine from a cream formulation had a lower cumulative amount after 24 hours ($p>0.05$). The reasons for the caffeine diffusion in the presence of coenzyme Q10 and retinol would be similar to that mentioned above. When combined with L-carnitine, caffeine had a similar diffusion pattern as found for caffeine alone (figure 3.25). This indicates that adding L-carnitine to caffeine did not affect the way in which caffeine diffuse across the skin from a cream formulation.

In summary across all three different formulations (liquid, gel, and cream), CoQ10 was found to have more of a significant enhancing effect on the diffusion behavior of caffeine (gel and cream: $p<0.05$; liquid: $p>0.05$) (table 3.45, table 3.46, table 3.47). Retinol across all three formulations impeded the diffusion of caffeine as compared to the other compounds (CoQ10 and L-carnitine). L- carnitine indicated little, if any effect on the diffusion behaviour of caffeine when used in combination from all three formulations. Compared with this study where retinol was found to impede the diffusion of caffeine, a study performed by Djajadisastra and Hadyanti (2014), found that tretinoin, also known as all-trans retinoic acid, had an enhancing effect on the diffusion of caffeine across rat skin. So far, there has been as yet very little, if any literature found on combination studies used for comparative purposes.

4.3.2 Theophylline alone and in combination in liquid, gel, and cream formulations

4.3.2.1 Liquid Formulation

As mentioned in the section 4.2 above, Theophylline struggled to diffuse across porcine skin due to the more hydrophilic nature of the molecule with a large variation observed in the diffusion data (cumulative amount after 4 hours: approximately 1.0 x 10^4 – 1.8 x 10^5 ng/cm^2) (figure 3.26a and 3.26b). A similar wide distribution pattern of diffusion data was observed when theophylline was used in combination from the

liquid formulation (figure 3.26a). The molecule also was not detected in the receptor fluid after 4 hours exposure. Combined with retinol, theophylline's diffusion rate from a liquid formulation increased statistically, from the range mentioned above to approximately 2.0 x 10^6 ($p>0.05$) and 1.1 x 10^7 ng/cm^2 ($p= 0.0144$) after 4 hours. This latter very high cumulative value is thought to be due to the rapid transappendageal pathway via the hair follicles. Although retinol is a slightly larger, lipophilic molecule and is known to accumulate within the skin and form a reservoir, it is thought to alter the barrier properties, in an unknown manner to facilitate the penetration of theophylline. The enzymatic conversion of retinol to retinyl esters and retinoic acid by active enzymes in the tissue after snap freezing in liquid nitrogen, could also play a role (O'Byrne and Blaner, 2013). This could possibly be by affecting the tight junctions in the stratum corneum, opening them up and increasing the diffusion of theophylline. L- carnitine had very little, if any effect on the diffusion of theophylline ($p>0.05$) when used in combination, while coenzyme Q10 resulted in a very low diffusion rate of theophylline ($p>0.05$). This is most probably due to coenzyme Q10 accumulating within the skin and blocking the penetration of theophylline.

4.3.2.2 Gel Formulation

Similarly, from the gel formulation, when theophylline was combined with Retinol, the theophylline cumulative amount after 4 hours was found to be increased from approximately 5 x 10^4 to 3 x 10^5 ng/cm^2, however the steady state flux rate increase (table 3.37) was not statistically significant. The diffusion of theophylline, when combined with retinol, was much higher from the liquid formulation (Retinol (high)- $p<0.05$) as compared to the gel formulation. This could partly be due to the penetration enhancers ethanol and propylene glycol in the liquid formulation. When combined with L- carnitine, a slight increase in the diffusion of theophylline was observed ($p>0.05$) while combined with CoQ10, theophylline's diffusion remained unaffected (figure 3.27).

4.3.2.3 Cream Formulation

As with both the liquid and gel formulations above, theophylline's diffusion was increased when combined with Retinol from a cream formulation, with cumulative

amounts of approximately 6.2 x 10^4 to 2 x 10^5 ng/cm^2 after 4 hours (figure 3.28a). The increase in steady state flux rates were however not statistically significant. When combined with L-carnitine, theophylline's diffusion was not altered and similarly when combined with coenzyme Q10, no alteration in the diffusion of theophylline was observed (table 3.41). As mentioned above, the increase in theophylline's diffusion when combined with retinol most probably was due to an effect of retinol on the tight junctions in the stratum corneum, opening the areas between keratinocytes and enhancing the diffusion of theophylline. This was evident in Figure 3.32c, where retinol maintains skin integrity within a cream formulation.

In summary, Theophylline diffused much better across skin in combination with Retinol, from all three formulations tested. This was found to be statistically significant in the liquid formulation (p=0.0144) as compared to the gel and cream formulations (table 3.41). The presence of the penetration enhancers ethanol and propylene glycol found in the liquid formulation would also have contributed to this enhanced diffusion. Across all three formulations, CoQ10 and L-carnitine had little, if any effect on the diffusion rate of theophylline. In a study by Djajadisastra and Hadyanti (2014), tretinoin, also known as all-trans retinoic acid, had a similar enhancing effect on the diffusion of aminophylline across rat skin.

4.3.3 L-carnitine alone and in combination in liquid, gel, and cream formulations

4.3.3.1 Liquid Formulation

When combined with theophylline, L-carnitine's diffusion across porcine skin from a liquid formulation increased significantly (p=0.0001) after a lag time of approximately 77 min (table 3.42) from cumulative amounts after 4 hours of <1 x 10^4 to 3 x10^7 ng/cm^2 (steady state flux rate: $p < 0.0001$). Although theophylline was found to increase the diffusion of L-carnitine, the opposite was not observed, as L-carnitine did not affect the diffusion of theophylline (section 4.3.2.1). The nature of this interaction and enhancing effect of theophylline on the diffusion of L-carnitine is surprising and worth further investigation.

Similarly, both retinol and coenzyme Q10, when combined with L-carnitine individually for a 24-hour time period, increased the diffusion of L-carnitine, however a long lag time of 378 min was noticed when combined with coenzyme Q10. These two lipophilic compounds have altered the tight junctions in the stratum corneum or affected the hydration of the corneocytes due to enzymatic conversion within the skin and thus increased the diffusion of the hydrophilic L-carnitine molecule. Curiously, no L-carnitine was detected in the receptor fluid when combined with caffeine, even after 24-hour exposure. This could be due to the degradation of L-carnitine over the 24hr collection period. The interaction is unexpected and needs further investigation.

4.3.3.2 Gel Formulation

From the gel formulation, L-carnitine's diffusion indicated a minimal cumulative amount over 24h, however in combination with CoQ10 resulted in an increase to two levels i.e., 2×10^7 and 1.0×10^8 ng/cm^2.However, the alteration in steady state flux rates (table 3.23) were not statistically significant i.e. the rate of diffusion/cm^2 did not increase significantly ($p>0.05$). The latter high cumulative amount may be attributed to the rapid transappendageal pathway via the fair follicles. Similarly, when combined with retinol, the cumulative amount of L-carnitine also increased to a value of 1×10^6 ng/cm^2 after 24 hours (figure 3.30c), which have been the reasons mentioned before in section 4.3.1.1. The change in steady state flux rate was however not statistically significant ($p > 0.05$). In combination with theophylline over a 4-hour time period, L-carnitine also showed an increase in diffusion, with cumulative amounts of 1×10^7 (lag time of 74 min) and 2.8×10^7 ng/cm^2, steady state flux rate: $p = 0.0258$ after 4 hours. The reason for this increase in diffusion needs further investigation. As with diffusion from the liquid formulation, no L-carnitine was detected in the receptor fluid after 24-hour exposure when combined with caffeine.

4.3.3.3 Cream Formulation

As found from the liquid and gel formulations above, the diffusion of L-carnitine from a cream formulation in combination with theophylline, retinol and CoQ10, increased, with CoQ10 (table 3.31a) having the largest effect, reaching a cumulative amount of

$3.7x10^7$ ng/cm^2 after 24 hours. In combination with theophylline, the cumulative amount of L-carnitine reached $5.7x10^6$ ng/cm^2 after 4 hours (table 3.31c) and combined with Retinol reached $2.2x10^6$ ng/cm^2 after 24 hours (table 3.31b). The possible reasons for the increased diffusion were mentioned in section 4.2, however the penetration enhancers within the formulations may also play a major role in the enhancement of the diffusion of L-carnitine across the skin when used in combination. It was noticed that from a cream formulation L-carnitine alone had a lag time of 119 min before diffusion occurred (table 3.44), this was most probably due to interaction with polar groups within the stratum corneum delaying diffusion as well as the hydrophilic molecule struggling to penetrate the skin from the cream that might form a layer on the skin surface (Schafer *et al*., 2023). The presence of theophylline and retinol resulted in decreased lag times. This decrease is attributed to reduced interaction between L-carnitine and calcium ions within the stratum corneum. This reduced interaction is hypothesized to occur because of the accumulation of other compounds (theophylline and retinol) in the stratum corneum as well. This suggests that the presence of theophylline and retinol somehow alters the dynamics of L-carnitine and calcium ion interactions in the skin, potentially affecting processes such as permeability or cellular signaling. No lag time was noticed when L-carnitine was combined with coenzyme Q10 (table 3.44), it could be speculated that this was probably due to the antioxidant and hydrating effect of this compound in the skin (Knott *et al*., 2015). No diffusion of L-carnitine occurred from the cream formulation in the presence of caffeine, due to a yet unknown mechanism.

In conclusion, it can be stated that theophylline, CoQ10 and Retinol all influenced the diffusion of L-carnitine across porcine skin (table 3.47). The effect of Theophylline on L-carnitine steady state flux rates was mostly found to be statistically significant (faster rate/cm^2), as compared to CoQ10 and Retinol. The mechanism behind this increase should be further investigated. In a previous study conducted by Alhomina (2001) with the aim to determine the effect of daily administration of theophylline on the activity of carnitine palmitoyltransferase in skeletal muscle, results showed a significant increase in the activity of palmitoyltransferase. The function of the palmitoyltransferase enzyme is that it binds the L-carnitine molecule to long-chain fatty acids for the l -carnitine cross into the inner membrane of mitochondria (Wang *et al*., 2021). One could speculate that Theophylline may lead to notable alterations in the distribution of carnitine not only

in plasma but also in various other tissues (Alhomina, 2001). Furthermore, in the current study it was found that CoQ10 and Retinol increased the diffusion of L-carnitine, although the steady state flux rates were not found to be significant ($p<0.05$) (table 3.47). The mechanisms could be due to the reasons stated in section 4.1.4. As previously mentioned, L-carnitine is a Zwitterion and encounters difficulty when diffusing through skin (In *et al*., 2019). Combining both CoQ10 and retinol with L-carnitine individually, would seem to enhance the diffusion of L-carnitine from all formulations. Both CoQ10 and Retinol are lipophilic molecules using predominantly the paracellular pathway to penetrate the skin (N'Da, 2014). Facilitation of the diffusion of L-carnitine through skin by these lipophilic compounds via the paracellular pathway might be a possibility, alternatively these molecules might drive the L-carnitine molecules to move to a greater extent via the transcellular pathway (N'Da, 2014).

4.4. Skin barrier Function (Skin integrity)

The skin is composed of several different types of barriers: physical, chemical, and immune barriers. The physical barrier located in the outmost layer of the skin is commonly known as the stratum corneum. It has been identified as the core tissue of the skin barrier (Proksch *et al*., 2006). The stratum corneum structure consist of corneocytes, which are held together by tight junctions, also known as desmosomes, and proteins which helps maintain the skin barrier (Hogan *et al*., 2012). The corneocytes are surrounded by a protein-lipid cornified cell envelope and the intercellular space between the corneocytes is filled with lipid lamellae which consist of ceramides, cholesterol, and free fatty acids. This structure is made in a way that prevents water loss from the body and protects the skin from external foreign pathogens (Haque and Talukder, 2018).

Due to the rigid complexity of the stratum corneum, transdermal delivery of certain compounds do not easily result in permeation through the skin. For this reason, penetration enhancers have been made available. The aim of using penetration enhancers is to modify the stratum corneum barrier function in a way so that molecules can penetrate through the skin (Haque and Talukder, 2018). In this study three penetration enhancers were used i.e., ethanol and propylene glycol used in the liquid formulation and propylene glycol used in the gel formulation. In the cream formulation,

olive oil was added which is categorized as a fatty acid penetration enhancer known to temporally cause a reversible disruption to the stratum corneum by increasing fluidity and diffusion through the skin (Haque and Talukder, 2018).

Furthermore, TEER method was used to measure the resistance across the skin (Gelker *et al*., 2018; Musazzi *et al*., 2018). The pupose of this was to investigate whether the different formulations containing the pernetration enhancers had an effect on the skin barrier after the diffusion period. The effect of the summary of active compounds added to the formulations on the barrier function of the skin was also investigated.

4.4.1 Liquid Formulation

The liquid formulation in our study contained ethanol and propylene glycol as penetration enhancers. According to Haque and Talukder (2018), ethanol extracts lipid and protein from the stratum corneum. Propylene glycol mainly increases drug permeation by improving the partition properties of drugs in the stratum corneum, it solvates the alpha-keratin and reduces drug tissue binding (Haque and Talukder, 2018). The TEER results in the present study showed that the skin integrity of porcine skin exposed to the control, which only consisted of the liquid formulation with no added compounds, remain relatively constant for up to 240 min (4hours) (figure 3.32a). At 24 hours (1440 min) the skin integrity decreased to just below 50% (figure 3.32a). This decrease in skin integrity was attributed to the two penetration enhancers in the liquid formulation.

In and colleagues (2019), reported that L-carnitine was found to influence the adhesion between corneocytes in the stratum corneum by causing chelation with calcium ions. The result obtained from the present study (figure 3.32a) showed that L-carnitine in the liquid formulation was found to significantly decrease the skin integrity (barrier function) in a time dependent manner. This could be due to the abovementioned action of L-carnitine. At 24 hours the skin integrity caused by exposure to L-carnitine within the liquid formulation was much lower as compared to the control (<25%) (figure 3.32a).

Retinol in the liquid formulation increased the barrier function after 2 hours exposure (120 min) and this was found to be statistically significant ($p<0.05$) (figure 3.32a).

Retinol is well known to keep the skin barrier intact, that is the reason the molecule is used in many anti-aging creams (Gruber *et al*., 2020). The fat-soluble molecule moves across the stratum corneum and binds to receptors found in the keratinocyte. When interacting with these receptors, retinol promotes the growth of keratinocytes, strengthens the function of the epidermis, and prevents the loss of transdermal water loss (Zasada and Budzisz, 2019). Furthermore, retinol is also known to reduce the degradation of collagen and inhibits the process of metalloproteinases which is responsible for breaking down the extracellular matrix (Mukherjee *et al*., 2006; Zasada and Budzisz, 2019). At 4 hours (240 min) the barrier function significantly decreased to 50% and decreased again at 24 hours, however this was not statistically significant compared to the liquid formulation alone ($p>0.05$) (figure 3.32a). Both caffeine and theophylline in the liquid formulation kept the skin integrity intact for the first 2 hours. This could have been to the protective function caffeine and theophylline have on the skin; caffeine is known to promote biosynthesis of collagen in the skin which increases the elasticity (Seleem *et a*l., 2022). Theophylline serves as an important antioxidant by decreasing apoptosis levels of epidermal keratinocytes and increasing melatonin levels to name a few (Sanabria-de la Torre *et al.,* 2020). At 4 hours there was a statistically significant ($p<0.05$) decrease of skin integrity to about 30% (figure 3.32a). All the components affected the skin barrier in a time dependent manner. CoQ10 was not tested as the component was found not to be stable with time.

4.4.2 Gel Formulation

Propylene glycol was also the penetration enhancer present in the gel formulation. At 2 and 4 hours after exposure it can be observed that Retinol, added to the gel formulation, significantly increased the skin integrity by over 100 % compared with formulation alone (Figure 3.32b). This could be explained by the fact that retinol is a lipophilic molecule which accumulates in the skin surface. The molecule is known to smooth out the stratum corneum and thicken the epidermis. It also reconstructs the underlying dermal and epidermal matrix proteins such as elastin and collagen (Gruber *et al*., 2020). Retinol thus enhances skin integrity and hydration; therefore, retinol can thus be considered to keep the skin barrier intact. At 24 hours however, retinol decreased the barrier function to 50% compared to formulation alone (figure 3.32b).

Both Theophylline and L-carnitine significantly decreased ($p<0.05$) the barrier function of the skin to below 10% after 24 hours exposure when added to the formulation (figure 3.32b), due to previously mentioned possible effects on the barrier property of the skin. All components affected the skin barrier in a time dependent manner (figure 3.32b). The skin barrier was still relatively intact after 24 hours for the control formulation alone, containing only propylene glycol and caffeine within the formulation, compared to the values found for the liquid formulation (figure 3.32a). This can partly be attributed to the gel formulation containing only propylene glycol and not propylene glycol and ethanol found in the liquid formulation, which is known to decrease the skin integrity to a greater extent (Carrer *et al*., 2019).

4.4.3 Cream Formulation

The cream formulation had olive oil added, this is known as a natural penetration enhancer. Since olive oil contains Free Fatty acids (oleic acid), having a C18 chain and 1 double bond, it disrupts the barrier function by causing the ordered structure of the lipids to be disrupted (Haque and Talukder, 2018). The results obtained in the current study showed that the barrier function of the skin remained intact after exposure to the cream formulation alone, as well as when all compounds were added individually to the cream formulation over the 24-hour period (figure 3.32c). The only significant change that occurred was when caffeine was present in the cream formulation. At 2 hours, caffeine increased the skin integrity and only decreased the barrier function at 24 hours. The barrier function remained above 50% after 24 hours, thus the barrier function was not affected significantly (figure 3.32c).
In a study conducted by Dewi and colleagues (2021), topical caffeine in concentrations of 0.25% and 0.5% in anti-wrinkle therapy was evaluated on skin elasticity. The results indicated that topical caffeine application can improve skin barrier function and increase the elasticity of the skin (Dewi *et al*., 2021).

4.5 Skin accumulation of active compounds alone

The amount of each active compound alone and in combination present within the three different formulations, that accumulated in the skin was evaluated at the end of each of the *in vitro* permeation experiments. The purpose was to evaluate the extent at which individual compounds accumulated within the skin that would result in a local effect, and how the presence of other compounds, when used in combination, would affect this accumulation.

4.5.1 Caffeine

Caffeine accumulated in the skin over a 24-hour time period in high amounts (Figure 3.33), which correlated well with the *in vitro* diffusion data across the skin obtained for caffeine within all 3-formulations. More than 10% of the initial quantity of caffeine that was applied onto the skin, accumulated within the skin, with the gel formulation yielding the highest quantity (16.14%; $p<0.05$, Table 3.45). The reason for the lower skin accumulation in the liquid formulation could be due to the penetration enhancers propylene glycol and ethanol in the liquid formulation that increased the diffusion of caffeine across the skin, resulting in a slightly lower accumulation in the skin as compared to the gel formulation that contained propylene glycol only. Propylene glycol was found in a study to increase *in vitro* diffusion of agents that are more soluble in alcohol than water, which could also explain the greater accumulation of caffeine in skin from a gel formulation, since caffeine is more soluble in water than ethanol (Veryser *et al*., 2013). The accumulation of caffeine from a cream formulation was found to be very similar to the liquid formulation. In a study done by Trauer *et al*. (2009), a similar concentration of caffeine (2.5% (w/w) was used to investigate follicular penetration of caffeine *in vitro* using the follicular closing technique. The formulation used in this study was composed of 2.5g of caffeine, 30 g of ethanol (70%) and 67.5g of propylene glycol. In this study, results showed an increase level of caffeine penetration in the epidermis layer with a value of 4.7% ± 0.57 (table 3.48).

4.5.2 Theophylline

The skin accumulation of theophylline from the 3 formulations (liquid, cream, and gel) over a 4–hour period was very low (< 1.0% of the initial amount of theophylline applied to the skin, Figure 3.34). Theophylline in a liquid formulation accumulated significantly ($p < 0.05$) (0.93%) as compared to theophylline in a cream (0.69%) and gel (0.57%) formulation respectively. The results for skin accumulation correlate very well with the *in vitro* diffusion results found in the study (figure 3.21). The increased theophylline accumulation from a liquid formulation as compared to from cream and gel formulations have been due to the penetration enhancers (ethanol and propylene glycol) found in the formulation. Ethanol is known to be greatly effective in increasing the permeation of compounds by various mechanisms such as: disruption of the Stratum corneum, weakening of the protein structure between the corneocytes and changing the environment in the bilayer (Williams and Barry, 2012). The olive oil in the cream formulation most probably also disrupted the lipid layers. All these factors lead to increased permeation of compounds in the skin and could have resulted in a corresponding increased accumulation of more hydrophilic compounds e.g., theophylline within the skin (Wang et al., 2007, Veryser *et al*., 2013). Another factor that might also have contributed was theophylline interacting with polar groups within the stratum corneum lipid bilayer. Furthermore, the skin accumulation data obtained across all 3 formulations were relatively low compared to caffeine. The time period in which skin accumulation was done was only after 4 hours which would also contribute to the low accumulation. The diffusion study was only done for 4 hours due to theophylline not diffusing further after 4 hours. This correlated well with what was discussed in section 4.2. Theophylline, being a more hydrophilic molecule than caffeine, encountered difficulty in diffusing across the skin, making use mostly of the transcellular pathway. This resulted in variations in the diffusion data obtained due to the molecule struggling to diffuse through the three different pathways. Compared to the present study, a higher amount of aminophylline was found to be present within skin by Ademola *et al*. (1992). The concentration of theophylline detected in the skin after topical application in vitro ranged from 2.8 ± 0.5% to 7.7 ± 7.7% according to Ademola et al. (1992), whereas in our current study, the concentrations were notably lower, measuring 0.93 ± 0.06% for the liquid formulation, 0.69 ± 0.04% for the cream formulation, and 0.57 ± 0.01% for the gel formulation.

4.5.3 Retinol

Retinol, from a liquid formulation had the greatest accumulation within the skin (0.51 % of the initial amount loaded onto the skin as compared to retinol within the cream (0.25%) and gel (0.26 %) formulations, this was not statically significant ($p>0.05$) (table 3.48). The penetration enhancers within the liquid formulation (ethanol and propylene glycol) most probably increased the penetration of retinol into the skin, causing a reservoir effect of retinol within the skin (Yourick *et al*., 2008). Due to the lipophilic nature of retinol, the affinity for the hydrophilic liquid formulation is less than for the lipophilic stratum corneum, causing the retinol to move into the skin. As compared to the liquid formulation, the gel formulation resulted in a lower accumulation of retinol in the skin (table 3.48), as it contained propylene glycol only. From the data this would indicate that ethanol most probably caused a disruption in the lipids surrounding the corneocytes, resulting in greater accumulation of retinol from the liquid formulation. Due to the lipophilic nature of the cream formulation, this most probably caused less retinol moving into the skin because of the greater affinity between the formulation and retinol (a very lipophilic molecule), resulting in retinol most probably remaining in the formulation on the skin. As mentioned before, retinol did not diffuse across the skin within the 24-hour time period and was not detected in the receptor fluid. Compared to the current study, Yourick *et al*. (2008) found that a retinol amount of 5.7 ± 0.8 % accumulated in human skin from a gel formulation, while an amount of 8.9 ± 2.0 % of retinol accumulated the skin from an oil-and-water emulsion after a 24-hour period. Furthermore, the study also showed an amount of 0.3 ± 0.1% retinol from a gel formulation and 1.3 ± 0.1% from an oil-and-water emulsion diffused across the skin after 24 hours, contrasting with the current study's findings of 0.68 ± 0.44% for the liquid formulation, 0.21 ± 0.01% for the cream formulation, and 0.18 ± 0.08% for the gel formulation.

4.5.4 L-carnitine

As mentioned before, L-carnitine is a zwitterion and contains a neutral overall charge at pH 7.4. When interacting with a phospholipid bilayer, the zwitterion interacts with a carbonyl oxygen found on the phospholipid bilayer which in turn changes the sodium (Na^+) and potassium (K^+) position on the phospholipid bilayer resulting in a

physiological change, this theory in an ongoing debate (Deplazes *et al*., 2020). Furthermore, L-carnitine in the skin is found to break up the calcium ion bond found between the desmosomes in the stratum corneum, this facilitates the penetration of L-carnitine through skin (In *et al*., 2019). In the cosmetic industry,L- carnitine is found to be used in exfoliating products due to the aforementioned reason, it is found to easily removed dead skin (In *et al*., 2019). As mentioned in the previous sections for caffeine, theophylline and retinol, each formulation had a penetration enhancer which would play a part in the diffusion of the compound (figure 3.37). Similarly to what was found for the other compounds, the accumulation of L-carnitine (2.5% w/v) from a liquid formulation (≈2.33%) was higher as compared to L-carnitine from gel (≈1.56%) and cream (≈1.33%) formulations. The value obtained for skin accumulation from a liquid formulation as compared to gel and cream formulations was not found to be statistically significant ($p>0.05$). The presence of ethanol and propylene glycol in the liquid formulation has been found to be more effective in increasing penetration compared to propylene glycol alone and olive oil. The skin accumulation data correlated, as seen before, with the *in vitro* diffusion data. In a study conducted by Fox *et al.* (2011), L-carnitine at an initial concentration of 2% in a PBS formulation, was found to accumulate in the skin at an average amount of 0.054 $\mu g/cm^2$ in the stratum corneum and 1.1343 $\mu g/cm^2$ in the epidermis-dermis. The study compared the accumulation of L-carnitine in PBS formulation to L-carnitine in combination with Pheroid. The results showed that L-carnitine in combination with Pheroid accumulated in the skin at an average amount of 0.022 $\mu g/cm^2$ in the stratum corneum and 0.777 $\mu g/cm^2$ in epidermis-dermis layer. The Pheroid combination enhanced L-carnitine permeation however not as great as the PBS formulation (Fox *et al*., 2011).

4.5.5 Co-enzyme Q10

CoQ10 showed similar results to Retinol, being highly lipophilic and struggling to diffuse across the skin. As observed before, the CoQ10 with an initial concentration of 0.5% (w/v) in liquid formulation resulted in a slightly greater accumulation (≈0.54%) as compared to CoQ10 within gel (≈0.03%) and cream formulations (0.006%) (figure 3.38), this was found not to be statistically significant ($p>0.05$). This can again be explained by the ethanol and propylene glycol penetration enhancing effects found in the liquid formulation. The CoQ10 from the lipophilic cream formulation, resulted in the

lowest skin accumulation. As mentioned for retinol above, due to the lipophilic nature of the cream formulation, this most probably caused less CoQ10 moving into the skin because of the greater affinity between the formulation and CoQ10 (a very lipophilic and large molecule), resulting in CoQ10 remaining in the formulation on the skin. An opposite effect was thus observed from the more hydrophilic gel and liquid formulations. As found for retinol, coenzyme Q10 did not diffuse across the skin within the 24-hour time period. Another possibility of the low skin accumulation could be that CoQ10 was reduced within the skin because of the interaction with light. CoQ10 is a very unstable compound, and it easily degrades when it encounters light (Tessema *et al*., 2020). Similar to this study, Tessema and colleagues (2020) found that CoQ10 from a hydrophilic cream accumulated in the skin to a greater extent as compared to CoQ10 from a lecithin-based microemulsion.

Overall data indicated that caffeine, theophylline, and L-carnitine in the different formulations diffused across the skin and accumulated within the skin. The lipophilic compounds, retinol, and coenzyme Q10 accumulated within the skin, however they did not diffuse across the skin. The accumulation was, however, dependent on the properties of the molecules. Caffeine had the highest skin accumulation (and the highest diffusion rate across skin), followed by L-carnitine, Theophylline, Retinol and CoQ10. This indicates that caffeine has the ideal lipophilic and hydrophilic characteristics for transdermal drug delivery. Furthermore, a liquid formulation containing ethanol and propylene glycol seems to indicate be a better formulation for transdermal delivery.

4.6 Skin accumulation in combination

Combination studies were done to evaluate not only the effect one compound may have on the diffusion rate of another compound, but also whether one compound influences the skin accumulation of another.

4.6.1 Skin accumulation of Caffeine in combination

4.6.1.1 Caffeine in combination with L-carnitine

Results obtained showed a very low (% of initial) caffeine accumulation in the skin when combined with L-carnitine from all formulations when compared to the % caffeine accumulation on its own (combined % accumulation <0.5% compared to alone ≈ 16%). Whereas caffeine from a gel formulation was the highest on its own (≈ 16%), when combined with L-carnitine, it indicated the lowest skin accumulation (<0.2%, Figure 3.39). This indicated that L-carnitine, being a zwitterion, impeded greatly caffeine's skin accumulation, however it had minimal effect on caffeine's diffusion across skin (Figures 3.23 – 3.25). The interaction of L-carnitine with charged molecules in the skin layer might prevent caffeine molecules also interacting with the same groups in the skin layers due to competition for the same sites, resulting in less caffeine accumulation. The presence of L-carnitine did not seem to impede the movement of caffeine through the skin nor did L-carnitine block the pathways caffeine molecules use to move through the skin. Compared to caffeine alone, the liquid formulation containing caffeine and L-carnitine was found to have the highest amount of caffeine accumulation in the skin compared to gel and cream formulations, the values were respectively as follows; 0.48%, 0.27% and 0.37% (table 3.49). The high amount of caffeine accumulation in liquid as compared to cream and gel was not statistically significant ($p>0.05$). The penetration enhancers found in the liquid formulation could be the reason for an increase in transdermal permeation and accumulation i.e., ethanol and propylene glycol, compared to propylene glycol only that are present in the gel formulation, for reasons mentioned previously. The penetration enhancing effect of the free fatty acids in olive oil present in the cream formulation, also increased caffeine accumulation in the skin slightly in the presence of L-carnitine. This could

also be attributed to caffeine being able to move into the skin layers more easily due to the disruption in the lipid layers caused by the FFAs.

4.6.1.2. Caffeine in combination with Retinol

Caffeine had a very low skin accumulation (% of initial) when in combination with retinol from all formulations, as compared to caffeine on its own (combined % accumulation ≤≈0.1% compared to alone ≈ 16%). Whereas caffeine from a cream formulation was ≈ 13% on its own, when combined with retinol, it indicated the lowest skin accumulation (<0.04%, Figure 3.40). Retinol however had minimal effect on caffeine's diffusion across skin from the liquid formulation (most probably due to the presence of ethanol and propylene glycol as penetration enhancers) but did decrease the diffusion of caffeine across skin from both the gel and cream formulations (Figures 3.23 – 3.25). Retinol thus seemed to greatly impede caffeine's skin accumulation from all formulations (liquid (≈0.100%), gel (0.066%), cream (≈0.037%)). As mentioned before, retinol is a very lipophilic molecule and moves through the skin using the lipophilic paracellular pathway as well as the transcellular and transappendageal pathways to a lesser degree. The paracellular pathway consists of more lipids which is favourable for retinol. In moving via these pathways, retinol forms a layer in the skin which lowers the diffusion of caffeine across the skin. Due the two molecules that might use the same pathways to diffuse into the skin, there might be competition between the two molecules with the larger, more lipophilic retinol blocking the movement of the caffeine molecule. This would result in less caffeine within the skin and more caffeine remaining on the skin surface.

4.6.1.3. Caffeine in combination with CoQ10

Caffeine had a very low skin accumulation (% of initial) when in combination with CoQ10 from all formulations, as compared to caffeine on its own (combined % accumulation ≤0.5% compared to alone ≈ 16%). Whereas caffeine from a cream formulation was ≈ 13% on its own, when combined with CoQ10, it indicated the lowest skin accumulation (≈0.1%, figure 3.41). CoQ10 increased caffeine's diffusion across skin from all formulations (cream>>gel>>liquid) most probably partly due to the presence of ethanol, propylene glycol and olive oil as penetration enhancers, Figures

3.23 – 3.25). It seemed to greatly impede caffeine's skin accumulation from all formulations (liquid (≈0.51%), gel (≈0.24%), cream (≈0.12%). As mentioned for retinol above, CoQ10 is also a very lipophilic and large molecule making use of the same pathways as retinol. However, curiously, as compared to retinol, CoQ10 significantly enhanced caffeine's diffusion greatly. In combination with CoQ10, caffeine also accumulated more in the skin compared to when combined with retinol. This could partly be due to enzymatic activity that occurs in the skin which alters CoQ10 into its reduced form, Ubiquinol (Knott *et al*., 2015, Tessema, 2020), therefore resulting in low levels of CoQ10 (ubiquinone) in the skin. Since the skin was snap frozen in liquid nitrogen, some enzymatic activity might still be preserved during the experimental process after defrosting (Söderquist M, 2013, Eliminating Biological Change after Excision. Genetic Engineering and Biotechnology News January 15, Vol 33, No 2, pg 16, https://doi.org/10.1089/gen.33.2.08). Ubiquinol might interact with groups in the stratum corneum, similarly to L-carnitine, disrupting the skin lipid layer which might result in less caffeine skin accumulation, but greater diffusion across the skin. The higher affinity between the lipophilic cream formulation and coenzyme Q10 and caffeine, might also impede movement of both compounds into the skin resulting in more caffeine on the skin surface due to coenzyme Q10 forming a layer on the skin and impeding its movement. This could result in the slightly lower skin accumulation as compared to the liquid and gel formulations.

4.6.2 Skin accumulation of Theophylline in combination

4.6.2.1. Theophylline in combination with CoQ10

Theophylline is more hydrophilic than caffeine and slightly smaller. The compound had an extremely low skin accumulation (% of initial) after 4 hours when in combination with CoQ10 from all formulations, as compared to on its own (combined % accumulation <0.07% compared to alone <1%). Whereas skin accumulation of theophylline from a cream formulation was ≈ 0.7% on its own, when combined with CoQ10, it indicated the lowest skin accumulation (≈0.003%, Figure 3.42). CoQ10 had minimal, if any effect on theophylline's diffusion across skin from all formulations, Figures 3.26a – 3.28b). CoQ10 seemed to greatly impede theophylline's skin accumulation. As mentioned before, CoQ10 is a very lipophilic and large molecule

(Çelik *et al*., 2017). As found with caffeine above, the possible enzymatic alteration of CoQ10 to ubiquinol, might have affected theophylline skin accumulation in a negative way. These large lipophilic molecules may also form a layer in the skin which in turn prevented Theophylline to accumulate inside the skin, however in this instance CoQ10 did not enhance the diffusion of theophylline across the skin, as was found with caffeine mentioned above (section 4.6.1.3). It could be speculated that theophylline uses mostly the transcellular pathway (as it is relatively hydrophilic) which might not be used by CoQ10 and in this way the diffusion is not affected. Theophylline in combination with CoQ10 from a liquid formulation (≈0.035%) had the highest amount of skin accumulation as compared to gel (≈0.02%) and cream (≈0.003%) formulations, which again, might be due to the effective penetration enhancer, ethanol as well as propylene glycol in this formulation. Other reasons for the poor skin accumulation in the presence of coenzyme Q10 are mentioned in the section on caffeine in section 4.6.1.3.

4.6.2.2 Theophylline in combination with L-carnitine

Very similar results were obtained for the skin accumulation of theophylline in combination with L-carnitine as observed in section 4.6.2.1 as well as the results found for caffeine in section 2.6.1.1. When combined with L-carnitine, theophylline's accumulation in the skin was extremely low, especially from a cream formulation (Figure 3.43). L-Carnitine, being a zwitterion impeded greatly theophylline's skin accumulation, however it had minimal effect on theophylline's diffusion across skin (Figures 3.26a – 3.28b). The interaction of L-carnitine with charged molecules in the skin layer might prevent theophylline molecules interacting with the same groups in the skin layers due to competition for the same sites, resulting in less theophylline skin accumulation. The presence of L-carnitine did not seem to impede the movement of theophylline through the skin, nor did L-carnitine block the pathways theophylline molecules used to move through the skin. As found earlier for theophylline alone, the liquid formulation (≈0.034%) was found to have the highest amount of theophylline accumulation in the skin after 4 hours compared to cream (≈0.003%) and gel (≈0.014%) formulations. This could partly have been due to the penetration enhancers found in the liquid formulation i.e., ethanol and propylene glycol. The poor skin

accumulation from a cream formulation in the presence of L-carnitine could be due to L-carnitine being a zwitterion, moving into the skin to a greater extent than the hydrophilic theophylline due to the low affinity between the lipophilic cream formulation and the compounds. There might be great competition between the two compounds for the transcellular diffusion pathway, resulting in theophylline being impeded by the L-carnitine binding to the Ca^{2+} ions found in the upper layers of the stratum corneum as mentioned before.

4.6.2.3 Theophylline in combination with Retinol

Theophylline had a slightly lower skin accumulation (% of initial) when in combination with retinol from the liquid and cream formulations, as compared to theophylline on its own (combined % accumulation ≈0.6% for cream and ≈0.25% for liquid compared to alone ≈ 1%). Curiously, the % theophylline's skin accumulation, in the presence of retinol, from the gel formulation increased to ≈1.33% (Figure 3.44). Retinol was found to increase theophylline's diffusion across skin from all formulations as well (Figures 3.26a – 3.28b). Retinol is a very lipophilic molecule making use of all three penetration pathways, but mostly the paracellular pathway. However, curiously, in comparison to when theophylline was combined with coenzyme Q10 (section 4.6.2.1), retinol enhanced theophylline's diffusion greatly, whereas coenzyme Q10 had little effect on theophylline's diffusion. In combination with retinol, theophylline also accumulated more in the skin compared to when combined with coenzyme Q10. Due to the differences in the lipophilicity of the two molecules as well as them making use of different pathways to diffuse into the skin, retinol seemed to accelerate the more hydrophilic theophylline molecule's diffusion, most probably via the transcellular pathway. Thus, although retinol accumulated in the skin and impeded some accumulation of theophylline, it may have forced more theophylline molecules to diffuse into the deeper layers of the skin and across the skin. The reasons for the increase in theophylline skin accumulation (from the gel formulation) and diffusion when combined with retinol from all formulations, is evidence for further investigation, but might be due to enzymatic alteration of retinol within the skin to retinoic acid which has a skin hydrating effect. This also disrupts the barrier allowing more of the hydrophilic theophylline to penetrate the skin. Enzymatic activity in the excised skin which was snap-frozen after collection, might still have been responsible for the

formation of retinoic acid during the experimental procedure (Söderquist M, 2013, Eliminating Biological Change after Excision. Genetic Engineering and Biotechnology News January 15, Vol 33, No 2, pg 16, https://doi.org/10.1089/gen.33.2.08).

4.6.3 Skin accumulation of Retinol in combination

4.6.3.1 Retinol in combination with L-carnitine

Retinol skin accumulation (%) in combination with L-carnitine was much lower (≤0.008%, liquid> gel>cream ; figure 3.45) than retinol accumulation on its own (≤0.7%, Figure 3.36). As mentioned in all the sections above, L-carnitine, being a small hydrophilic amino acid derivative thus impeded greatly retinol's skin accumulation. The interaction of L-carnitine with charged molecules in the phospholipid bilayer of the skin might alter the lipid bilayer as mentioned previously, this might have impeded the movement of retinol into the skin in some way. The original retinol compound might have been also detected to a lesser extent due to enzymatic conversion to retinoic acid within the skin. The retinol skin accumulation from the liquid formulation (≈0.008%) also was higher as compared to the gel (≈0.0005%) and cream (≈0.0011%) formulations. This might be due to ethanol and propylene glycol found in the liquid formulation that is known to be effective permeation enhancers, as mentioned before (Williams and Barry, 2012; Jacob *et al*., 2018)

4.6.3.2 Retinol in combination with Theophylline

Retinol's skin accumulation (% of initial) when in combination with theophylline from the liquid and cream formulations, was lower as compared to retinol on its own (combined % accumulation ≈0.12% for cream and ≈0.06% for liquid compared to alone in cream ≈ 0.25% and liquid ≈0.7%). Curiously, the % retinol's skin accumulation in the presence of theophylline from the gel formulation increased significantly from ≈0.25 to ≈0.47% ($p<0.05$).This tendency was also noticed where theophylline's skin accumulation also increased from the gel formulation when the two compounds were combined (section 4.6.2.3; table 3.49) The results indicated that retinol and theophylline in a gel formulation enhanced each other's skin accumulation via a yet

an unknown mechanism that needs further investigation. As mentioned in section 3.6.2.3, retinol also enhanced the diffusion of theophylline across the skin from all formulations, possibly due to the hydrating effect on the skin caused by the conversion of retinol to retinoic acid as mentioned above (section 4.6.2.3). However, no retinol was detected in the receptor fluid, thus theophylline did not enhance the diffusion of retinol across the skin.

4.6.3.3 Retinol in combination with Caffeine

Retinol had a very low skin accumulation (% of initial) when in combination with caffeine from all formulations, as compared to retinol on its own (combined % accumulation ≤0.032% compared to alone ≤0.7%). Whereas retinol from a cream formulation was ≈0.25% on its own, when combined with caffeine, it indicated the lowest skin accumulation (≈0.0008%, Figure 3.47). Caffeine thus seemed to greatly impede retinol's skin accumulation and vice versa. As mentioned before in section 4.6.1.2, retinol forms a layer in the skin which lowers the diffusion of caffeine across the skin, but due to the fact that the two molecules might use the same pathways to diffuse into the skin, there might be competition between the two molecules with the larger, more lipophilic retinol blocking the movement of the caffeine molecule and vice versa. Retinol, as found earlier, had minimal effect on caffeine's diffusion across skin from the liquid formulation, but did decrease the diffusion of caffeine across skin from both the gel and cream formulations (Figures 3.23 – 3.25). No retinol was detected in the receptor fluid when combined with caffeine, thus caffeine did not enhance the diffusion of retinol across the skin. The retinol accumulation was higher from the liquid formulation as compared to the gel and cream formulations which might be due to the presence of the two penetration enhancers, as mentioned before. Another reason contributing to the low detection of retinol might be the conversion of retinol to retinoic acid resulting in low levels on the original compound detected in the skin.

4.6.4 Skin accumulation of CoQ10 in combination

4.6.4.1 CoQ10 in combination with Caffeine

CoQ10 accumulation increased (% of initial) when in combination with caffeine from all formulations, as compared to CoQ10 on its own (combined % accumulation from liquid ≈4.1% ($p<0.05$), gel ≈0.15% and cream ≈0.12% compared to alone ≤0.04%, Figure 3.48). The greatest accumulation was from a liquid formulation in the presence of caffeine, which might partly be due to the penetration enhancers as well as the lower affinity between the lipophilic coenzyme Q10 and the hydrophilic formulation causing more coenzyme Q10 to move into the skin. As mentioned in section 4.6.1.3, CoQ10 also increased caffeine's diffusion across skin from all formulations (cream>>gel>>liquid, Figures 3.23 – 3.25), but this was not the case in reverse. Caffeine did not increase the diffusion of CoQ10 across the skin as no coenzyme Q10 was detected in the receptor fluid. A possible contributing mechanism for the higher levels of coenzyme Q10 in the presence of caffeine could be that caffeine in some way prevents the conversion of coenzyme Q10 to ubiquinol in the skin, with the resultant higher levels of coenzyme Q10 detected in the skin.

4.6.4.2 CoQ10 in combination with Theophylline and L-Carnitine

Detectable, but no quantifiable levels of coenzyme Q10 were detected within the skin from all formulations when combined with theophylline or L-carnitine. The mechanisms behind this can only be speculated. Both theophylline and L-carnitine are small hydrophilic molecules and could most probably enhance the enzymatic metabolism of CoQ10 to ubiquinol, resulting in very low levels of ubiquinone (CoQ10) in the skin. CoQ10 however, caused decreased accumulation of theophylline as opposed to increased accumulation of L-Carnitine inside the skin. (Figures 3.42 and 3.49). An interesting finding and has most probably to do with the increased levels of ubiquinol and decreased levels CoQ10 in the skin. This needs further investigation.

4.6.5 Skin accumulation of L-carnitine in combination

4.6.5.1 L-Carnitine in combination with Caffeine

Results obtained showed higher levels (% of initial) of L-carnitine in the skin when combined with caffeine from all formulations when compared to the % L-carnitine accumulation on its own (combined % accumulation cream: ≈6.5%, gel: ≈5.5%, liquid: ≈2.7% compared to alone ≤2.3%, Figure 3.49). Interestingly, no L-carnitine was detected in the receptor fluid when combined with caffeine from all formulations (Section 3.2.3.3). This implied that caffeine caused L-carnitine to accumulate in the skin, but not to diffuse across the skin. From section 4.6.1.1 above, L-carnitine, being a zwitterion, impeded greatly caffeine's skin accumulation, however it had minimal effect on caffeine's diffusion across skin (Figures 3.23 – 3.25). As mentioned before, caffeine and L-carnitine might interact with the same groups in the skin layers due to competition for the same sites, resulting in less caffeine accumulation, but more L-carnitine accumulation due to the presence of charged reactive groups within L-carnitine. Caffeine moves easily across the skin, being more lipophilic and uses multiple pathways, however L-carnitine being very hydrophilic, and using mostly the transcellular pathway, might struggle moving across skin in the presence of caffeine due to competition for the transcellular pathway to cross the skin. Interestingly, the liquid formulation in the presence of caffeine, yielded the lowest L-carnitine accumulation and the gel and cream formulations the highest. Thus, the penetration enhancers found in the liquid formulation i.e. ethanol and propylene glycol, did increase the diffusion of L-carnitine across the skin, however prevented it from accumulating in the skin to a greater extent as compared to the other two formulations. It might be due to the fact that L-carnitine is hydrophilic and its affinity for the hydrophilic liquid formulation is high, thus more of the compound will remain on the skin surface, the opposite would be true for the cream formulation.

4.6.5.2 L-carnitine in combination with CoQ10

A similar trend was observed as described in section 4.6.5.1 above. Higher levels (% of initial) of L-carnitine in the skin were observed when combined with coenzyme Q10 from all formulations when compared to the % L-carnitine accumulation on its own (combined % accumulation cream: ≈7.2%, gel: ≈7.0%, liquid: ≈3.6% compared to alone ≤2.3%, Figure 3.50). Coenzyme Q10 also increased L-carnitine's diffusion across skin phenomenally (Figures 3.29b, 3.30a and 3.31a, section 3.2.3.3). As mentioned in section 4.6.4.2, L-carnitine in turn decreased coenzyme Q10's accumulation in the skin. (Figures 3.23 – 3.25). These effects could be due to the levels of ubiquinol compared to ubiquinone (coenzyme Q10) in the skin as mentioned in section 4.6.4.2. As mentioned in section 4.6.5.1, the liquid formulation also yielded the lowest L-carnitine skin levels and could be due to the reasons mentioned in that section.

4.6.5.3 L-carnitine in combination with Retinol

Results obtained showed higher levels (% of initial) of L-carnitine in the skin when combined with retinol from the liquid and gel formulations when compared to the % L-carnitine accumulation on its own (combined % accumulation gel: ≈3.1%, liquid: ≈3.6% compared to alone ≤2.3%, Figure 3.51). Alternatively, L-carnitine greatly impeded the retinol's skin accumulation for possible reasons (section 4.6.3.1) and also did not enhance retinol diffusion across the skin, as no retinol was detected in the receptor fluid. Retinol was also found to enhance L-carnitine's diffusion greatly across the skin (Figures 3.29b, 3.30c, 3.31b). Due to the differences in the lipophilicity of the two molecules (L-carnitine being hydrophilic and retinol being lipophilic) as well as them making use of different pathways to diffuse into the skin, retinol seemed to accelerate the more hydrophilic L-carnitine's diffusion via the transcellular pathway. Thus, retinol may have forced more L-carnitine molecules to diffuse into the deeper layers of the skin and across the skin. The reasons of the increase in L-carnitine skin accumulation (from the liquid and gel formulations) and diffusion when combined with retinol from all formulations, give a cause for further investigation, but could in part be due to the presence of the penetration enhancers in the two formulations and the hydrating effect on the skin caused by the conversion of retinol to retinoic acid (section 4.6.2.3).

4.6.5.4 L-carnitine in combination with Theophylline

A similar trend as described in sections 4.6.5.1 and 4.6.5.2 was observed when L-carnitine was combined with theophylline. Higher levels (% of initial) of L-carnitine in the skin were observed when combined with theophylline from all formulations when compared to the % L-carnitine accumulation on its own (combined % accumulation cream: ≈5.9%, gel: ≈6.1%, liquid: ≈2.9% compared to alone ≤2.3%, Figure 3.52). Theophylline also greatly increased L-carnitine's diffusion across skin (Figures 3.29a, 3.30b and 3.31c). As mentioned in section 4.6.2.2, L-carnitine again impeded greatly theophylline's skin accumulation, but had minimal effect on its diffusion across skin (Figures 3.26a – 3.28b) for possible reasons mentioned in that section. As mentioned in sections 4.6.5.1 and 4.6.5.2 above, the liquid formulation also yielded the lowest L-carnitine skin levels and could be due to the reasons mentioned in those sections. Theophylline might cause some disruption in the barrier layer of the skin that might cause increased amounts of L-carnitine to diffuse into and across the skin, and this mechanism needs further investigation.

From the results reported above, it would seem that L-carnitine's diffusion across the skin and accumulation in the skin are positively affected by all compounds combined with it and when combined in all formulations. However, this compound negatively affects most other compounds' skin accumulations but have minimal effect on their diffusion across the skin. All compounds affect caffeine's skin accumulation in a negative way, however when combined with coenzyme Q10, its diffusion is greatly enhanced across the skin which might increase the risk of systemic side-effects. This combination however, also results in more coenzyme Q10 accumulation in the skin, especially from a liquid formulation, with resultant beneficial effects. Combined with retinol, theophylline's diffusion across the skin increases, which might also increase the risk of systemic side-effects, however retinol accumulation in the skin increases from a gel formulation with resultant beneficial effects.

5. Chapter 5: Final Conclusion

The purpose of this study was to investigate the effectiveness of penetration of various active compounds in different formulations (Liquid, Gel and Cream) in and across porcine skin. Five different active compounds (Caffeine, Theophylline, Retinol, L-carnitine and CoenzymeQ10) were detected and the methods validated by HPLC analysis compared the *in vitro* kinetic behaviour of each active compound alone and in combination. Furthermore, the accumulation of each active compound alone and in combination was evaluated within the three different formulations (liquid, gel, and cream). Skin integrity was observed by evaluating the effect of active compound in different formulation on the barrier intactness.

5.1 Method validation of active compounds

The proposed HPLC method is suitable for the detection of caffeine, theophylline, retinol, coenzyme Q10 and L -carnitine. Furthermore, the method showed to be linear, precise, accurate and robust across all five active compounds.

5.2 *In vitro* diffusion of active compounds across skin

Each active compound was prepared in three different formulations (liquid, gel, and cream) and the diffusion behaviour was investigated across the porcine skin.

Caffeine alone in a cream formulation penetrated at a slightly greater rate as compared to caffeine in gel and in liquid. This can be due to composition of the formulations; cream contains olive oil which act as a natural occurring enhancer. When looking at caffeine in combination, its shows that caffeine in combination with coenzyme Q10 showed a significant increase in skin permeation in a gel and cream formulation as compared to liquid. Both gel and liquid formulation contained chemical enhancer, propylene glycol and ethanol respectively, which contributes an increase in skin permeation.

Theophylline was found to be a complex compound to diffuse through skin, this is due to its greater hydrophilic nature. The study showed that Theophylline alone had a greater diffusion rate from a liquid formulation as compared to gel and cream formulations. This again can be attributed to the chemical enhancer found in liquid,

ethanol. When looking at Theophylline in combination with retinol, it was found that theophylline had a greater permeability across all three formulations (liquid, gel, and cream). L- carnitine alone, which is known as a zwitterion, diffused at a greater rate in a liquid formulation. L-carnitine in combination with theophylline had a significant greater diffusion in liquid and gel formulation. Both retinol and co-enzyme Q10 have lipophilic properties which makes it difficult for compounds to diffuse through the skin.

5.3 Skin accumulation of active compounds alone and in combination

Due to the nature of certain active compounds, skin accumulation was found to be more prominent for some compounds as compared to others. When looking at skin accumulation on its own, Caffeine was found to significantly accumulate in the skin over a period of 24hours from a gel formulation compared to liquid and cream formulation. Theophylline and L-carnitine had an increase in skin accumulation in the liquid formulation, however this was not found to be statistically significant. Retinol and Coenzyme Q10 are both lipophilic compounds that struggled to diffuse through the skin. Result obtained showed that both compounds accumulated in the skin and that a higher accumulation percentage was found from a liquid formulation for Retinol and coenzyme Q10. Skin accumulation in combination showed that adding a secondary compound to the formulation can increase the accumulation percentage of the primary compound as seen in theophylline, retinol co-enzyme Q10 and L-carnitine. Theophylline in combination with retinol showed a significant accumulation of theophylline across all 3 formulations. Retinol in combination with theophylline showed a significant amount of retinol accumulation from a gel formulation. Coenzyme Q10 in combination with caffeine showed a significant accumulation of co-enzyme from a liquid formulation. L-carnitine was found to significantly accumulate in skin from a liquid formulation when in combination with Caffeine, Theophylline, Retinol and Coenzyme Q10.

5.4 Skin integrity

As a general overview, skin barrier function was found to disintegrate after exposure to active compounds over a period of 24-hours in liquid and gel formulation, the cream formulation showed that the skin barrier remained relative intact over the same period.

When exposed to a liquid formulation containing L-carnitine, skin barrier function significantly after 2 hours while retinol increased the barrier function after 2 hours then decreased barrier function after 4 hours.
Both Caffeine and Theophylline only affected the barrier function after a 4hour exposure.

From the gel formulation, retinol caused significant increase in the skin barrier function after 2 hours to 4 hours. The compound only decreased skin integrity at 24 hours. Theophylline and L carnitine decreased barrier function significantly after 24 hours while, caffeine remained relatively constant. From a cream formulation, the skin barrier function remained consistently intact over 24 hours. Caffeine increased the barrier function at 2 hours and significantly decreased skin barrier function at 24 hours.

5.5. Future recommendations

In future, researchers and policy makers should consider testing different formulation such as emulsion, emulgel, or ointments to observe the diffusion characteristics of these compounds; Caffeine, Theophylline, L-carnitine, Retinol and CoQ10. Furthermore, other chemical enhancers can be evaluated to see how they affect the permeation rate of active compounds across skin. Various chemicals have been known to disrupt the stratum corneum, these chemicals include poly-alcohols, amines, pyrrolidones, amides, sulphoxides, fatty acids, alkanes, esters, surfactants, terpenes, and phospholipids. The assessment of skin integrity can be done using transdermal water loss (TEWL), this is a common way in chich skin barrier is evaluated.

6. Chapter 6: References

A-f, C. A. L. (2007). *Theophylline Theophylline*. 2–4.
Abebe Belay. (2011). Some biochemical compounds in coffee beans and methods developed for their analysis. *International Journal of the Physical Sciences*, *6*(28). https://doi.org/10.5897/ijps11.486

Al-Bratty, M., Alhazmi, H. A., Rehman, Z. ur, Javed, S. A., Ahsan, W., Najmi, A., Khuwaja, G.,
Makeen, H. A., & Khalid, A. (2020). Determination of Caffeine Content in Commercial Energy
Beverages Available in Saudi Arabian Market by Gas Chromatography-Mass Spectrometric Analysis. *Journal of Spectroscopy*, *2020*(2008). https://doi.org/10.1155/2020/3716343

Alkhamaisah, S. I., Younes, K. M., Gaipov, A., & Aljofan, M. (2019). Development and validation of a
simple and sensitive HPLC method for the determination of liquid form of therapeutic substances. *Electronic Journal of General Medicine*, *16*(6).

Al-Salman, H. N. K., Jasim, E. Q., Hussein, H. H., & Shari, F. H. (2021). Theophylline determination in pharmaceuticals using a novel high-performance liquid chromatographic process. *NeuroQuantology*, *19*(7), 196–208. https://doi.org/10.14704/nq.2021.19.7.NQ21103

Al Qarqaz, F., & Al-Yousef, A. (2018). Skin microneedling for acne scars associated with pigmentation in patients with dark skin. *Journal of Cosmetic Dermatology*, *17*(3), 390–395. https://doi.org/10.1111/jocd.12520

Alhomida, A. S. (2001). Evaluation of theophylline-stimulated changes in carnitine palmitoyltransferase activity in skeletal muscle and liver of rats. *Journal of Enzyme Inhibition*, *16*(2), 177–183. https://doi.org/10.1080/14756360109162367

Andrei, K. (2011). *Solubility and Physical Stability Improvement of Natural Xanthine*. *February*.

Apostol, I., Miller, K. J., Ratto, J., & Kelner, D. N. (2009). Comparison of different approaches
for evaluation of the detection and quantitation limits of a purity method: A case study using a capillary isoelectrofocusing method for a monoclonal antibody. *Analytical Biochemistry*, *385*(1), 101–106. https://doi.org/10.1016/j.ab.2008.09.053

Balakrishnan, P., Park, E. K., Song, C. K., Ko, H. J., Hahn, T. W., Song, K. W., & Cho, H. J. (2015). Carbopol-Incorporated thermoreversible gel for intranasal drug delivery. *Molecules*, *20*(3), 4124–4135. https://doi.org/10.3390/molecules20034124

Balato, N., Megna, M., Ayala, F., Balato, A., Napolitano, M., & Patruno, C. (2014). Effects of

climate changes on skin diseases. *Expert Review of Anti-Infective Therapy*, *12*(2), 171–181. https://doi.org/10.1586/14787210.2014.875855

Barnes, P. J. (2010). Theophylline. *Pharmaceuticals*, *3*(3), 725–747. https://doi.org/10.3390/ph3030725

Baroni, A., Buommino, E., De Gregorio, V., Ruocco, E., Ruocco, V., & Wolf, R. (2012). Structure and function of the epidermis related to barrier properties. *Clinics in Dermatology*, *30*(3), 257–262. https://doi.org/10.1016/j.clindermatol.2011.08.007

Bartlett, A., Krull, I., & Swartz, M. (2002). Validation of Bioanalytical. In *America* (Vol. 20, Issue 9).

Bartosova, L., & Bajgar, J. (2012). Transdermal Drug Delivery In Vitro Using Diffusion Cells.
Current Medicinal Chemistry, *19*(27), 4671–4677.
https://doi.org/10.2174/092986712803306358

Bäsler, K., Bergmann, S., Heisig, M., Naegel, A., Zorn-Kruppa, M., & Brandner, J. M. (2016).
The role of tight junctions in skin barrier function and dermal absorption. *Journal of Controlled Release*, *242*, 105–118. https://doi.org/10.1016/j.jconrel.2016.08.007

Bauer, J., Hoq, M. N., Mulcahy, J., Tofail, S. A. M., Gulshan, F., Silien, C., Podbielska, H., &
Akbar, M. M. (2020). Implementation of artificial intelligence and non-contact infrared thermography for prediction and personalized automatic identification of different stages of cellulite. *EPMA Journal*, *11*(1), 17–29. https://doi.org/10.1007/s13167-020-00199-x

Belouafa, S., Habti, F., Benhar, S., Belafkih, B., Tayane, S., Hamdouch, S., Bennamara, A., &
Abourriche, A. (2017). Statistical tools and approaches to validate analytical methods: Methodology and practical examples. *International Journal of Metrology and Quality Engineering*, *8*. https://doi.org/10.1051/ijmqe/2016030

Bernal, E. (2014). Limit of Detection and Limit of Quantification Determination in Gas Chromatography. *Advances in Gas Chromatography*. https://doi.org/10.5772/57341

Bird, D., & Ravindra, N. M. (2020). Transdermal drug delivery and patches—An overview. *Medical Devices & Sensors*, *3*(6), 1–15. https://doi.org/10.1002/mds3.10069

Blicharz, L., Rudnicka, L., & Samochocki, Z. (2019). Staphylococcus aureus: An underestimated factor in the pathogenesis of atopic dermatitis? *Postepy Dermatologii i Alergologii*, *36*(1), 11–17. https://doi.org/10.5114/ada.2019.82821

Boaventura, G., Krause, L., Queiroz, N., & Contreras, C. (2013). Cosmetics With Caffeine: Real Benefits Versus Marketing Claims. *Proceedings Of The 22nd Conference Of The International Federation Of Societies Of Cosmetic Chemists*, 533–536.

Borekova, M., Hojerova, J., Koprda, V., & Bauerova, K. (2008). Nourishing and health benefits of
coenzyme Q10. *Czech journal of food sciences*, *26*(4), 229.

Brodin, B., Steffansen, B., & Nielsen, C. U. (2002). Passive diffusion of drug substances: the concepts of flux and permeability. *Molecular Biopharmaceutics*, 18.

Campas-Baypoli, O. N., Sánchez-Machado, D. I., Bueno-Solano, C., Ramírez-Wong, B., & López-Cervantes, J. (2010). HPLC method validation for measurement of sulforaphane level in broccoli by-products. *Biomedical Chromatography*, *24*(4), 387–392. https://doi.org/10.1002/bmc.1303

Cao, Q. R., Ren, S., Park, M. J., Choi, Y. J., & Lee, B. J. (2007). Determination of highly soluble
L-carnitine in biological samples by reverse phase high performance liquid chromatography with fluorescent derivatization. *Archives of Pharmacal Research*, *30*(8), 1041–1046. https://doi.org/10.1007/BF02993974

Carrer, V., Alonso, C., Pont, M., Zanuy, M., Córdoba, M., Espinosa, S., Barba, C., Oliver, M. A.,
Martí, M., & Coderch, L. (2020a). Effect of propylene glycol on the skin penetration of drugs.
Archives of Dermatological Research, *312*(5), 337–352. https://doi.org/10.1007/s00403-019-02017-5

Carrer, V., Alonso, C., Pont, M., Zanuy, M., Córdoba, M., Espinosa, S., Barba, C., Oliver, M. A.,
Martí, M., & Coderch, L. (2020b). Effect of propylene glycol on the skin penetration of drugs.
Archives of Dermatological Research, *312*(5), 337–352. https://doi.org/10.1007/s00403-019-02017-5

Çelik, B., Sağıroğlu, A. A., & Özdemir, S. (2017). Design, optimization and characterization of
coenzyme Q10-and D-panthenyl triacetate-loaded liposomes. *International journal of nanomedicine*,
4869-4878.

Cheng, Y.-L., Lee, C.-Y., Huang, Y.-L., Buckner, C. A., Lafrenie, R. M., Dénommée, J. A., Caswell, J. M., Want, D. A., Gan, G. G., Leong, Y. C., Bee, P. C., Chin, E., Teh, A. K. H., Picco, S.,
Villegas, L., Tonelli, F., Merlo, M., Rigau, J., Diaz, D., … Mathijssen, R. H. J. (2016). We are
IntechOpen , the world ’ s leading publisher of Open Access books Built by scientists , for scientists TOP 1 %. *Intech*, *11*(tourism), 13. https://www.intechopen.com/books/advanced-biometric-technologies/liveness-detection-in-biometrics

Chin, E. L. H., da Silva, C., & Hegde, M. (2013). Assessment of clinical analytical sensitivity and specificity of next-generation sequencing for detection of simple and complex

mutations. *BMC Genetics*, *14*. https://doi.org/10.1186/1471-2156-14-6

Chowdhury, A. Z., Jahan, S. A., Islam, M. N., Moniruzzaman, M., Alam, M. K., Zaman, M. A., ... &
Gan, S. H. (2012). Occurrence of organophosphorus and carbamate pesticide residues in surface
water samples from the Rangpur district of Bangladesh. *Bulletin of environmental contamination and
toxicology*, *89*, 202-207.

Contin, M., Lucangioli, S., Martinefski, M., Flor, S., & Tripodi, V. (2011). Miniaturized HPLC
UV method for analysis of coenzyme Q10 in human plasma. *Journal of Liquid Chromatography and Related Technologies*, *34*(20), 2485–2494. https://doi.org/10.1080/10826076.2011.591028

Córdoba-Díaz, M., Nova, M., Elorza, B., Córdoba-Díaz, D., Chantres, J. R., & Córdoba-Borrego, M. (2000). Validation protocol of an automated in-line flow-through diffusion equipment for in vitro permeation studies. *Journal of Controlled Release*, *69*(3), 357–367. https://doi.org/10.1016/S0168-3659(00)00306-0

Crane, F. L. (2001). Biochemical functions of coenzyme Q10. *Journal of the American College of
Nutrition*, *20*(6), 591-598.

Czaplicki, S. (2013). Chromatography in Bioactivity Analysis of Compounds. *Column Chromatography*, *May*. https://doi.org/10.5772/55620

Davis, E. C., & Callender, V. D. (2010). Postinflammatory hyperpigmentation: A review of the
epidemiology, clinical features, and treatment options in skin of color. *Journal of Clinical and
Aesthetic Dermatology*, *3*(7).

De Wever, B., Kurdykowski, S., & Descargues, P. (2015). Human Skin Models for Research Applications in Pharmacology and Toxicology: Introducing NativeSkin ® , the “Missing Link”
Bridging Cell Culture and/or Reconstructed Skin Models and Human Clinical Testing . *Applied
In Vitro Toxicology*, *1*(1), 26–32. https://doi.org/10.1089/aivt.2014.0010

Dejaegher, B., & Heyden, Y. Vander. (2007). Ruggedness and robustness testing. *Journal of Chromatography A*, *1158*(1–2), 138–157. https://doi.org/10.1016/j.chroma.2007.02.086

Deplazes, E., Tafalla, B. D., Cranfield, C. G., & Garcia, A. (2020). Role of Ion-Phospholipid Interactions in Zwitterionic Phospholipid Bilayer Ion Permeation. *Journal of Physical Chemistry Letters*, *11*(15), 6353–6358. https://doi.org/10.1021/acs.jpclett.0c01479

Gad, S., Desoqi, M., El-Sawy, H., Khafagy, E., & Ghourab, M. (2021). Drug Delivery Systems for
Topical treatment of Inflammatory Skin Diseases. *Records of Pharmaceutical and Biomedical
Sciences*, *5*(Pharmacology-Pharmaceutics), 59-64.

Dewé, W., Marini, R. D., Chiap, P., Hubert, P., Crommen, J., & Boulanger, B. (2004). Development of response models for optimising HPLC methods. *Chemometrics and Intelligent Laboratory Systems*, *74*(2 SPEC.ISS.), 263–268. https://doi.org/10.1016/j.chemolab.2004.04.016

Dewi, S. R., Cahyono, A., P., A. R., & Mawardi, P. (2021). *The Comparison of the Effects of Caffeine Topical 0.25% and 0.5% as Anti-wrinkle Therapy*. *Rcd 2018*, 113–117. https://doi.org/10.5220/0008152001130117

Dien et al., 2013, & Pratik K. Mutha, Robert L. Sainburg, K. Y. H. (2008). 基因的改变NIH Public Access. *Bone*, *23*(1), 1–7. https://doi.org/10.1007/978-1-60327-325-1

Ditzinger, F., Price, D. J., Ilie, A. R., Köhl, N. J., Jankovic, S., Tsakiridou, G., Aleandri, S., Kalantzi, L., Holm, R., Nair, A., Saal, C., Griffin, B., & Kuentz, M. (2019). Lipophilicity and hydrophobicity considerations in bio-enabling oral formulations approaches – a PEARRL review. *Journal of Pharmacy and Pharmacology*, *71*(4), 464–482. https://doi.org/10.1111/jphp.12984

Djajadisastra, J., & Sutriyo, H. (2014). Percutane transport profile of caffeine and aminophyllin as anticellulite and the influences of other substances on in vitro penetration. *International Journal of Pharmacy and Pharmaceutical Sciences*, *6*(5), 532-38.

Dragicevic, N., & Maibach, H. I. (2017). Percutaneous penetration enhancers drug penetration into/through the skin: Methodology and general considerations. *Percutaneous Penetration Enhancers Drug Penetration Into/Through the Skin: Methodology and General Considerations*, *September*, 1–414. https://doi.org/10.1007/978-3-662-53270-6

Duracher, L., Blasco, L., Hubaud, J. C., Vian, L., & Marti-Mestres, G. (2009). The influence of
alcohol, propylene glycol and 1,2-pentanediol on the permeability of hydrophilic model drug through excised pig skin. *International Journal of Pharmaceutics*, *374*(1–2), 39–45. https://doi.org/10.1016/j.ijpharm.2009.02.021

Elias, P. M. (2012). Structure and function of the stratum corneum extracellular matrix. *Journal of Investigative Dermatology*, *132*(9), 2131–2133. https://doi.org/10.1038/jid.2012.246

Elmansi, H., Nasr, J. J., Rageh, A. H., El-Awady, M. I., Hassan, G. S., Abdel-Aziz, H. A., & Belal,
F. (2019). Assessment of lipophilicity of newly synthesized celecoxib analogues using reversed-phase HPLC. *BMC Chemistry*, *13*(1), 1–7. https://doi.org/10.1186/s13065-019-0607-6

Estévez, P. N., Tripodi, V., Buontempo, F., & Lucangioli, S. (2012). Coenzyme Q10 stability in
pediatric liquid oral dosage formulations. *Farmacia Hospitalaria*, *36*(6), 492–497. https://doi.org/10.7399/FH.2012.36.6.55

European Medicines Agency (EMA). (2017). Propylene glycol used as an excipient. *Committee for Human Medicinal Products (CHMP)*, *44*(October). www.ema.europa.eu/contact

Fleischer, D. M., Udkoff, J., Borok, J., Friedman, A., Nicol, N., Bienstock, J., Lio, P., Tollefson,
M., & Eichenfield, L. F. (2017). Atopic dermatitis: Skin care and topical therapies. *Seminars in
Cutaneous Medicine and Surgery*, *36*(3), 104–111. https://doi.org/10.12788/j.sder.2017.035

Fotaki, N. (2011). Flow-through cell apparatus (USP Apparatus 4): Operation and features. *Dissolution Technologies*, *18*(4), 46–49. https://doi.org/10.14227/DT180411P46

Fox, L. T., Gerber, M., Du Preez, J. L., Grobler, A., & Du Plessis, J. (2011). Topical and transdermal delivery of L-carnitine. *Skin Pharmacology and Physiology*, *24*(6), 330–336. https://doi.org/10.1159/000330385

Gad, S., Desoqi, M., El-Sawy, H., Khafagy, E., & Ghourab, M. (2021). Drug Delivery Systems
for Topical treatment of Inflammatory Skin Diseases. *Records of Pharmaceutical and Biomedical Sciences*, *5*(1), 59–64. https://doi.org/10.21608/rpbs.2021.62807.1094

Gao, Y., Ierapetritou, M. G., & Muzzio, F. J. (2013). Determination of the confidence interval
of the relative standard deviation using convolution. *Journal of Pharmaceutical Innovation*, *8*(2), 72–82. https://doi.org/10.1007/s12247-012-9144-8

Gautier, A., & Hinner, M. J. (2015). Site-Specific Protein Labeling: Methods and Protocols. *Site-Specific Protein Labeling: Methods and Protocols*, 1–267. https://doi.org/10.1007/978-1-4939-2272-7

Gelker, M., Müller-Goymann, C. C., & Viöl, W. (2018). Permeabilization of human stratum corneum
and full-thickness skin samples by a direct dielectric barrier discharge. *Clinical Plasma Medicine*, *9*,
34-40.

Gruber, J. V., Stojkoska, V., & Riemer, J. (2020). Retinol has a skin dehydrating effect that can be
improved by a mixture of water-soluble polysaccharides. *Cosmetics*, *7*(4), 80.

Guidelines for Percutaneous Absorption / Penetration. (1997). 39–54.

Gulaboski, R., Cordeiro, M. N. D. S., Milhazes, N., Garrido, J., Borges, F., Jorge, M., Pereira, C.

M., Bogeski, I., Morales, A. H., Naumoski, B., & Silva, A. F. (2007). Evaluation of the lipophilic
properties of opioids, amphetamine-like drugs, and metabolites through electrochemical studies at the interface between two immiscible solutions. *Analytical Biochemistry*, *361*(2), 236–243. https://doi.org/10.1016/j.ab.2006.11.006

Hamilton, D. F., Ghert, M., & Simpson, A. H. R. W. (2015). Interpreting regression models in
clinical outcome studies. *Bone and Joint Research*, *4*(9), 152–153. https://doi.org/10.1302/2046-3758.49.2000571

Hansen, S., Lehr, C. M., & Schaefer, U. F. (2013). Modeling the human skin barrier-Towards a
better understanding of dermal absorption. *Advanced Drug Delivery Reviews*, *65*(2), 149–151. https://doi.org/10.1016/j.addr.2012.12.002

Haq, A., & Michniak-Kohn, B. (2018). Effects of solvents and penetration enhancers on transdermal delivery of thymoquinone: Permeability and skin deposition study. *Drug Delivery*, *25*(1), 1943. https://doi.org/10.1080/10717544.2018.1523256

Haque, T., & Talukder, M. M. U. (2018). Chemical enhancer: A simplistic way to modulate barrier function of the stratum corneum. *Advanced Pharmaceutical Bulletin*, *8*(2), 169–179. https://doi.org/10.15171/apb.2018.021

HARRY, R. G. (1941). "Skin Penetration." *British Journal of Dermatology*, *53*(3), 65–82. https://doi.org/10.1111/j.1365-2133.1941.tb10505.x

Herndon, J. H., Jiang, L. I., Kononov, T., & Fox, T. (2016). An open label clinical trial to evaluate the efficacy and tolerance of a retinol and Vitamin C facial regimen in women with mild-to-moderate hyperpigmentation and photodamaged facial skin. *Journal of Drugs in Dermatology*, *15*(4), 476–482.

Herron, A. J. (2010). *Proceeding of the ACVP / ASVCP Concurrent Annual Meetings Pigs as Dermatologic Models of Human Skin Disease*.

Hogan, M. B., Peele, K., & Wilson, N. W. (2012). Skin Barrier Function and Its Importance at
the Start of the Atopic March. *Journal of Allergy*, *2012*(May), 1–7. https://doi.org/10.1155/2012/901940

Horwitz, W., & Albert, R. (2006). The Horwitz ratio (HorRat): a useful index of method performance
with respect to precision. *Journal of AOAC International*, *89*(4), 1095-1109.

Hussain, A., Khan, G. M., Jan, S. U., Shah, S. U., Shah, K., Akhlaq, M., Rahim, N., Nawaz, A., &
Wahab, A. (2012). Effect of olive oil on transdermal penetration of flurbiprofen from topical gel as enhancer. *Pakistan Journal of Pharmaceutical Sciences*, *25*(2), 365–369.

In, S., Yook, N., Kim, J. H., Shin, M., Tak, S., Jeon, J. H., Ahn, B., Park, S. G., Lee, C. K., & Kang,
N. G. (2019). Enhancement of exfoliating efficacy of L-carnitine with ion-pair method monitored by nuclear magnetic resonance spectroscopy. *Scientific Reports*, *9*(1), 1–9. https://doi.org/10.1038/s41598-019-49818-2

Institute of Medicine (US) Committee on Military Nutrition Research. (2001). *Caffeine for the Sustainment of Mental Task Performance: Formulations for Military Operations*. National Academies Press (US).

Ismail, R., Lee, H. Y., Mahyudin, N. A., & Abu Bakar, F. (2014). Linearity study on detection
and quantification limits for the determination of avermectins using linear regression. *Journal of Food and Drug Analysis*, *22*(4), 407–412. https://doi.org/10.1016/j.jfda.2014.01.026

Jain, S. K., Verma, A., Jain, A., & Hurkat, P. (2016). Transfollicular drug delivery: current perspectives. *Research and Reports in Transdermal Drug Delivery*, 1. https://doi.org/10.2147/rrtd.s75809

Jayanthi, M., Thirunavukkarasu, S. V., Nagarajan, V., Elangovan, S., & Raja, S. (2012). development and validation of RP-HPLC method for determination of glibenclamide in pharmaceutical dosage forms. *International Journal of ChemTech Research*, *4*(2), 593–601.

Jiang, W.-T., Tang, L.-X., Pan, J., Su, C.-J., Shen, Z., Hu, Z.-H., Zhan, Z.-B., & Shi, A.-M. (2022).
Development and validation of an UHPLC-Orbitrap-HRMS method for rapid determination of endogenous L-carnitine in patients on hemodialysis/peritoneal dialysis and its application to promote rational drug use. *Annals of Translational Medicine*, *10*(2), 103–103. https://doi.org/10.21037/atm-21-6784

Jung, Y. J., Yoon, J. H., Kang, N. G., Park, S. G., & Jeong, S. H. (2012). Diffusion properties of
different compounds across various synthetic membranes using Franz-type diffusion cells. *Journal of Pharmaceutical Investigation*, *42*(5), 271–277. https://doi.org/10.1007/s40005-012-0040-5

K. Bhal, S. (2007). Log P — Making Sense of the Value. *Advanced Chemistry Development*, 1–
4. www.acdlabs.com/logp

Kadam, A. S., Ratnaparkhi, M. P., & Chaudhary, S. P. (2014). Transdermal drug delivery: An overview.

Karau, M. G., Kihunyu, J. N., Kathenya, N. M., Wangai, L. N., Kariuki, D., & Kibet, R. H. (2010).
Determination of caffeine content in non-alcoholic beverages and energy drinks using HPLC-UV method. *African Journal of Drug and Alcohol Studies*, *9*(1), 15–21. https://doi.org/10.4314/ajdas.v9i1.61754

Kazakevich, Y., & Lobrutto, R. (2006). Stationary Phases. *HPLC for Pharmaceutical Scientists*,
75–138. https://doi.org/10.1002/9780470087954.ch3

Khan, A., Khan, M. I., Iqbal, Z., Shah, Y., Ahmad, L., & Watson, D. G. (2010). An optimized and
validated RP-HPLC/UV detection method for simultaneous determination of all-trans-Retinol (Vitamin A) and α-Tocopherol (Vitamin E) in human serum: Comparison of different particulate reversed-phase HPLC columns. *Journal of Chromatography B: Analytical Technologies in the Biomedical and Life Sciences*, *878*(25), 2339–2347. https://doi.org/10.1016/j.jchromb.2010.07.009

Khoshkam, R., & Afshar, M. (2014a). Validation of a Stability-Indicating RP-HPLC Method for
Determination of L -Carnitine in Tablets . *International Scholarly Research Notices*, *2014*, 1–7. https://doi.org/10.1155/2014/481059

Khoshkam, R., & Afshar, M. (2014b). Validation of a Stability-Indicating RP-HPLC Method for
Determination of <small class="sc">L</small>-Carnitine in Tablets. *International Scholarly Research Notices*, *2014*, 481059. https://doi.org/10.1155/2014/481059

Knott, A., Achterberg, V., Smuda, C., Mielke, H., Sperling, G., Dunckelmann, K., Vogelsang,
A., Krüger, A., Schwengler, H., Behtash, M., Kristof, S., Diekmann, H., Eisenberg, T., Berroth,
A., Hildebrand, J., Siegner, R., Winnefeld, M., Teuber, F., Fey, S., … Blatt, T. (2015). Topical
treatment with coenzyme Q10-containing formulas improves skin's Q10 level and provides antioxidative effects. *BioFactors*, *41*(6), 383–390. https://doi.org/10.1002/biof.1239

Kupiec, T. (2004). Quality-control analytical methods: high-performance liquid chromatography. *International Journal of Pharmaceutical Compounding*, *8*(3), 223–227. http://www.ncbi.nlm.nih.gov/pubmed/23924674

Krueger, J. G., & Bowcock, A. (2005). Psoriasis pathophysiology: current concepts of pathogenesis. *Annals of the rheumatic diseases*, *64*(suppl 2), ii30-ii36.

Krüger, A. (2010). Formulation, in vitro release and transdermal diffusion of selected retinoids (Doctoral dissertation, North-West University).

Lebonvallet, N., Jeanmaire, C., Danoux, L., Sibille, P., Pauly, G., & Misery, L. (2010). The evolution and use of skin explants: potential and limitations for dermatological research. *European journal of dermatology: EJD*, *20*(6), 671–684. https://doi.org/10.1684/ejd.2010.1054.

Leyden, J. J., Shergill, B., Micali, G., Downie, J., & Wallo, W. (2011). Natural options for the
management of hyperpigmentation. *Journal of the European Academy of Dermatology and*

Venereology, *25*(10), 1140–1145. https://doi.org/10.1111/j.1468-3083.2011.04130.x

Li, S., Jiang, M., Li, M., Hu, P., Xu, M., & Shu, C. (2022). Development and validation of a simple and sensitive HPLC method for the determination of related substances in regorafenib tablets. *Analytical Sciences*, *38*(3), 591–599. https://doi.org/10.1007/s44211-022-00068-9

Lin, T. K., Zhong, L., & Santiago, J. L. (2018). Anti-inflammatory and skin barrier repair effects
of topical application of some plant oils. *International Journal of Molecular Sciences*, *19*(1). https://doi.org/10.3390/ijms19010070

Longo, N., Frigeni, M., & Pasquali, M. (2016). Carnitine transport and fatty acid oxidation. *Biochimica et Biophysica Acta - Molecular Cell Research*, *1863*(10), 2422–2435. https://doi.org/10.1016/j.bbamcr.2016.01.023

López, L. C., Quinzii, C. M., Area, E., Naini, A., Rahman, S., Schuelke, M., Salviati, L., Dimauro,
S., & Hirano, M. (2010). Treatment of CoQ10 deficient fibroblasts with ubiquinone, CoQ analogs, and vitamin C: Time-and compound-dependent effects. *PLoS ONE*, *5*(7), 14–17. https://doi.org/10.1371/journal.pone.0011897

Ma, B., Wang, J., Sun, J., Li, M., Xu, H., Sun, G., & Sun, X. (2014). Permeability of rhynchophylline across human intestinal cell in vitro. *International Journal of Clinical and Experimental Pathology*, *7*(5), 1957–1966.

Manoharan, G. (2021). Quantitative Determination of L-Carnitine Tablet Formulation by A Validated Stability-Indicating Reversed-Phase HPLC Method. *South Asian Res J Pharm Sci*, *3*(3), 46–51. https://doi.org/10.36346/sarjps.2021.v03i03.003

Mansour, R. S. H., Hamdan, I. I., Salem, M. S. H., Khalil, E. A., & Sallam, A. A. (2021). HPLC
method development/validation and skin diffusion study of caffeine, methyl paraben and butyl paraben as skin-diffusing model drugs. *PLoS ONE*, *16*(3 March), 1–16. https://doi.org/10.1371/journal.pone.0247879

MASRIJAL, C. D. P., HARMITA, H., & ISKANDARSYAH, I. (2020). Improving Transdermal Drug
Delivery System for Medroxyprogesterone Acetate By Olive Oil and Dimethylsulfoxide (Dmso) As Penetration Enhancers: in Vitro Penetration Study. *International Journal of Pharmacy and Pharmaceutical Sciences*, *August*, 12–15. https://doi.org/10.22159/ijpps.2020v12i4.36762

Matsui, T., & Amagai, M. (2015). Dissecting the formation, structure and barrier function of the stratum corneum. *International Immunology*, *27*(6), 269–280. https://doi.org/10.1093/intimm/dxv013

Menon, G. K., Cleary, G. W., & Lane, M. E. (2012). The structure and function of the

Stratum corneum. *International journal of pharmaceutics*, *435*(1), 3-9.

Menditto, A., Patriarca, M., & Magnusson, B. (2007). Understanding the meaning of accuracy, trueness and precision. *Accreditation and Quality Assurance*, *12*(1), 45–47. https://doi.org/10.1007/s00769-006-0191-z

Mhatre V. Ho, Ji-Ann Lee, and K. C. M., & Dien et al., 2013. (2008). 基因的改变NIH Public
Access. *Bone*, *23*(1), 1–7. https://doi.org/10.1002/0471143030.cb1909s41.Three-Dimensional

Mitani, T., Takaya, T., Harada, N., Katayama, S., Yamaji, R., Nakamura, S., & Ashida, H. (2018). Theophylline suppresses interleukin-6 expression by inhibiting glucocorticoid receptor signaling in pre-adipocytes. *Archives of Biochemistry and Biophysics*, *646*(February), 98–106. https://doi.org/10.1016/j.abb.2018.04.001

Moghimipour, E., Tabassi, S. A. S., Kouchak, M., & Varghaei, H. (2012). Combination strategies for enhancing transdermal absorption of theophylline through shed snake skin. *Asian Journal of Pharmaceutical and Clinical Research*, *5*(SUPPL 2), 30–34.

Molteni, S., & Reali, E. (2012). Biomarkers in the pathogenesis, diagnosis, and treatment of psoriasis. *Psoriasis: Targets and Therapy*, 55-66.

Moraes, D. (2012). Letters The Coefficient of Determination : What. *Investigative Ophtalmology & Visual Science*, *53*(11), 6830–6832.

Mukherjee, S., Date, A., Patravale, V., Korting, H. C., Roeder, A., & Weindl, G. (2006). Retinoids in the treatment of skin aging: an overview of clinical efficacy and safety. *Clinical Interventions in Aging*, *1*(4), 327–348. https://doi.org/10.2147/ciia.2006.1.4.327

Musazzi, U. M., Casiraghi, A., Franzé, S., Cilurzo, F., & Minghetti, P. (2018). Data on the determination of human epidermis integrity in skin permeation experiments by electrical resistance. *Data in Brief*, *21*, 1258–1262. https://doi.org/10.1016/j.dib.2018.10.098

Mustapha, R., Lafforgue, C., Fenina, N., & Marty, J. (2011). Influence of drug concentration on the diffusion parameters of caffeine. *Indian Journal of Pharmacology*, *43*(2), 157–162. https://doi.org/10.4103/0253-7613.77351

National Center for Biotechnology Information. PubChem Compound Summary for CID 702, Ethanol. (https://pubchem.ncbi.nlm.nih.gov/compound/Ethanol; accessed on 21 March 2020).

National Center for Biotechnology Information. PubChem Compound Summary for CID 1030,
Propylene Glycol. https://pubchem.ncbi.nlm.nih.gov/compound/Propylene-Glycol. Accessed Feb. 27, 2024.

National Center for Biotechnology Information (2024). PubChem Compound Summary for CID 2153, Theophylline. Retrieved February 27, 2024

from https://pubchem.ncbi.nlm.nih.gov/compound/Theophylline.

National Center for Biotechnology Information (2024). PubChem Compound Summary for CID 445354, Retinol. Retrieved February 27, 2024 from https://pubchem.ncbi.nlm.nih.gov/compound/Retinol.

National Center for Biotechnology Information (2024). PubChem Compound Summary for CID 288, Carnitine. Retrieved February 27, 2024 from https://pubchem.ncbi.nlm.nih.gov/compound/Carnitine.

N'Da, D. D. (2014). Prodrug strategies for enhancing the percutaneous absorption of drugs. *Molecules*, *19*(12), 20780–20807. https://doi.org/10.3390/molecules191220780

Nakano, T., Yoshino, T., Fujimura, T., Arai, S., Mukuno, A., Sato, N., & Katsuoka, K. (2015).
Reduced expression of dermcidin, a peptide active against propionibacterium acnes, in sweat of patients with acne vulgaris. *Acta Dermato-Venereologica*, *95*(7), 783–786. https://doi.org/10.2340/00015555-2068

Neupane, R., Boddu, S. H. S., Renukuntla, J., Babu, R. J., & Tiwari, A. K. (2020). Alternatives
to biological skin in permeation studies: Current trends and possibilities. *Pharmaceutics*, *12*(2). https://doi.org/10.3390/pharmaceutics12020152

Ng, K. W. (2018). Penetration enhancement of topical formulations. *Pharmaceutics*, *10*(2), 10–12. https://doi.org/10.3390/pharmaceutics10020051

Ng, K. W., & Lau, W. M. (2015). Skin deep: The basics of human skin structure and drug penetration. *Percutaneous Penetration Enhancers Chemical Methods in Penetration Enhancement: Drug Manipulation Strategies and Vehicle Effects*, 3–11. https://doi.org/10.1007/978-3-662-45013-0_1

Nicolaidou, E., & Katsambas, A. D. (2014). Pigmentation disorders: Hyperpigmentation and hypopigmentation. *Clinics in Dermatology*, *32*(1), 66–72. https://doi.org/10.1016/j.clindermatol.2013.05.026
No, P. (2015). *LIST OF FIGURES Figure No. 3*(1), 3–7.

Nolan, K., & Marmur, E. (2012). Moisturizers: Reality and the skin benefits. *Dermatologic Therapy*, *25*(3), 229–233. https://doi.org/10.1111/j.1529-8019.2012.01504.x

Nutten, S. (2015). Atopic dermatitis: Global epidemiology and risk factors. *Annals of Nutrition and Metabolism*, *66*, 8–16. https://doi.org/10.1159/000370220

O'Byrne, S. M., & Blaner, W. S. (2013). Retinol and retinyl esters: biochemistry and physiology: thematic review series: fat-soluble vitamins: vitamin A. *Journal of lipid research*, *54*(7), 1731-1743.

Ojha, S., Gadwe, S., & Mulgund, S. (2013). *Newer stationary phases for reverse phase-liquid chromatographic analysis*. *1*(1), 98–109.

Oliphant, E. A., Purohit, T. J., Alsweiler, J. M., McKinlay, C. J. D., & Hanning, S. M. (2022).
Validation and application of a simple and rapid stability-indicating liquid chromatographic assay for the quantification of caffeine from human saliva. *Journal of Liquid Chromatography and Related Technologies*, *45*(1–4), 10–17. https://doi.org/10.1080/10826076.2022.2095402

Oliveira, L. D. M., Teixeira, F. M. E., & Sato, M. N. (2018). Impact of Retinoic Acid on Immune
Cells and Inflammatory Diseases. *Mediators of Inflammation*, *2018*. https://doi.org/10.1155/2018/3067126

Otberg, N., Patzelt, A., Rasulev, U., Hagemeister, T., Linscheid, M., Sinkgraven, R., Sterry, W.,
& Lademann, J. (2008). The role of hair follicles in the percutaneous absorption of caffeine. *British Journal of Clinical Pharmacology*, *65*(4), 488–492. https://doi.org/10.1111/j.1365-2125.2007.03065.x

Parsons, H. M., Ekman, D. R., Collette, T. W., & Viant, M. R. (2009). Spectral relative standard deviation: A practical benchmark in metabolomics. *Analyst*, *134*(3), 478–485. https://doi.org/10.1039/b808986h

Pathan, I. B., & Setty, C. M. (2009). Chemical penetration enhancers for transdermal drug delivery systems. *Tropical Journal of Pharmaceutical Research*, *8*(2), 173–179. https://doi.org/10.4314/tjpr.v8i2.44527

Patriche, E. L., Croitoru, O., Coman, G., Stefan, C. S., Tutunaru, D., & Cuciureanu, R. (2014).
Validation of HPLC method for the determination of retinol in different dietary supplements. *Romanian Biotechnological Letters*, *19*(6), 9875–9882.

Pena-rodríguez, E., Moreno, M. C., Blanco-fernandez, B., González, J., & Fernández-campos,
F. (2020). Epidermal delivery of retinyl palmitate loaded transfersomes: Penetration and biodistribution studies. *Pharmaceutics*, *12*(2). https://doi.org/10.3390/pharmaceutics12020112

Peirano, R. I., Hamann, T., Düsing, H. J., Akhiani, M., Koop, U., Schmidt-Rose, T., & Wenck, H.
(2012). Topically applied l-carnitine effectively reduces sebum secretion in human skin. *Journal of
Cosmetic Dermatology*, *11*(1), 30-36.

Performance, M. T., Committee, M. O., Isbn, N. B., Pdf, T., Press, N. A., Press, N. A., Academy, N., Academy, N., & Press, N. A. (2001). Caffeine for the Sustainment of Mental Task Performance. In *Caffeine for the Sustainment of Mental Task Performance*. https://doi.org/10.17226/10219

Permegear Cattalog, (2018).

Peters, F. T., Drummer, O. H., & Musshoff, F. (2007). Validation of new methods. *Forensic Science International*, *165*(2–3), 216–224. https://doi.org/10.1016/j.forsciint.2006.05.021

Phechkrajang, C. M. (2010). Chaotropic Effect in Reversed-phase HPLC : A Review. *Journal of*
Pharmaceutical Science, *37*(1–2), 1–7.

Piipponen, M., Li, D., & Landén, N. X. (2020). The immune functions of keratinocytes in skin
wound healing. *International Journal of Molecular Sciences*, *21*(22), 1–26.
https://doi.org/10.3390/ijms21228790

Pokhrel, P., Shrestha, S., Rijal, S. K., & Rai, K. P. (2016). A simple HPLC Method for the Determination of Caffeine Content in Tea and Coffee. *Journal of Food Science and Technology Nepal*, *9*(December), 74–78. https://doi.org/10.3126/jfstn.v9i0.16200

Pouliot, R., Angers, L., Dubois-Declercq, S., Masson, L.-C., Roy, B., Jean, J., & Morin, A. (2017). Effects of Freezing on Functionality and Physicochemical Properties of A 3D-Human Skin Model. *Journal of Dermatology & Cosmetology*, *1*(2), 24–31.
https://doi.org/10.15406/jdc.2017.01.00007

Prabakaran, R., Chenthilnathan, A., & Vikraman, S. (2014). Validation of simultaneous determination of vitamin a acetate and vitamin e acetate in multivitamin tablets by rp-hplc. *International Journal of Pharmaceutical Biological and Chemical Sciences*, *3*(2), 27–34.

Pranitha, K., Priya, J., & Ramathilagam, N. (2014). RP-HPLC Method Development and Validation for the Simultaneous Estimation of Metoprolol and Telmisartan in Tablet Dosage Form. *Ijpar*, *3*(1), 75–82.

Preparation of Calibration Curves, (2003)
Proksch, E., Fölster-Holst, R., & Jensen, J. M. (2006). Skin barrier function, epidermal proliferation and differentiation in eczema. *Journal of Dermatological Science*, *43*(3), 159–169. https://doi.org/10.1016/j.jdermsci.2006.06.003

Rachmin, I., Ostrowski, S. M., Weng, Q. Y., & Fisher, D. E. (2020). Topical treatment strategies to manipulate human skin pigmentation. *Advanced Drug Delivery Reviews*, *153*, 65–71. https://doi.org/10.1016/j.addr.2020.02.002

Rakuša, Ž. T., Kristl, A., & Roškar, R. (2021). Stability of reduced and oxidized coenzyme q10
in finished products. *Antioxidants*, *10*(3), 1–17. https://doi.org/10.3390/antiox10030360

Randall, M. J., Jüngel, A., Rimann, M., & Wuertz-Kozak, K. (2018). Advances in the biofabrication of 3D skin in vitro: Healthy and pathological models. *Frontiers in Bioengineering and Biotechnology*, *6*(OCT). https://doi.org/10.3389/fbioe.2018.00154

Rathore, A. S., Jat, R. C., Sharma, N., Tiwari, R., Ram, S., Of, C., & Email, C. A. (2013).

Available online at http // www.ijrdpl.com Review Article AN OVERVIEW : MATRIX TABLET
AS CONTROLLED DRUG DELIVERY SYSTEM. *2*(4), 482–492.

Ratner, B. (2009). The correlation coefficient: Its values range between 1/1, or do they. *Journal of Targeting, Measurement and Analysis for Marketing*, *17*(2), 139–142. https://doi.org/10.1057/jt.2009.5

Rawlings, A. V., & Harding, C. R. (2004). Moisturization and skin barrier function. *Dermatologic Therapy*, *17*(1), 43–48. https://doi.org/10.1111/j.1396-0296.2004.04s1005.x

Rendon, A., & Schäkel, K. (2019). Psoriasis pathogenesis and treatment. *International journal of molecular sciences*, *20*(6), 1475.

Roure, R., Oddos, T., Rossi, A., Vial, F., & Bertin, C. (2011). Evaluation of the efficacy of a topical cosmetic slimming product combining tetrahydroxypropyl ethylenediamine, caffeine, carnitine, forskolin and retinol, in vitro, ex vivo and in vivo studies. *International Journal of Cosmetic Science*, *33*(6), 519–526. https://doi.org/10.1111/j.1468-2494.2011.00665.x

Rodak, K., Kokot, I., & Kratz, E. M. (2021). Caffeine as a factor influencing the functioning of the human body—Friend or foe?. *Nutrients*, *13*(9), 3088.

Rudakov, F., Geiser, J. D., & Weber, P. M. (2018). Spatially resolved standoff trace chemical sensing using backwards transient absorption spectroscopy. *Optics Letters*, *43*(6), 1279-1282

Rüegg, R. A. B., & Dimenstein, R. (2020). Validation of an Analytical Method Based on High-Performance Liquid Chromatography for the Determination of Retinol in Chicken Liver. *OALib*, *07*(07), 1–12. https://doi.org/10.4236/oalib.1106181

Ruela, A. L. M., Perissinato, A. G., Lino, M. E. de S., Mudrik, P. S., & Pereira, G. R. (2016). Evaluation of skin absorption of drugs from topical and transdermal formulations. *Brazilian Journal of Pharmaceutical Sciences*, *52*(3), 527–544. https://doi.org/10.1590/s1984-82502016000300018

Sanabria de la Torre, R., Fernández González, A., Quiñones Vico, MI., Montero Vilchez, T., Arias Santiago, S. (2020). Bioengineered Skin Intended as In Vitro Model for Environmental Skin Impact Analysis. *Biomedicines*, *8*(11), 464.

Sarkar, M., Bag, P., Kumar, B., & Chawla, P. A. (2021). Development and Validation by Reverse Phase High Performance Liquid Chromatography Method for the Estimation of Piperine and Coenzyme Q10 in Bulk and Pharmaceutical Dosage Form. *Indian Journal of Pharmaceutical Sciences*, *83*(6), 1208–1214. https://doi.org/10.36468/pharmaceutical-sciences.875

Schafer, N., Balwierz, R., Biernat, P., Ochędzan-Siodłak, W., & Lipok, J. (2023). Natural Ingredients of Transdermal Drug Delivery Systems as Permeation Enhancers of Active Substances through the *Stratum Corneum*. *Molecular*

pharmaceutics, *20*(7), 3278–3297.
https://doi.org/10.1021/acs.molpharmaceut.3c00126

Schmook, F. P., Meingassner, J. G., & Billich, A. (2001). Comparison of human skin or epidermis models with human and animal skin in in-vitro percutaneous absorption. *International Journal of Pharmaceutics*, *215*(1–2), 51–56. https://doi.org/10.1016/S0378-5173(00)00665-7

seleem, mae moustafa, Abulfadl, Y., El Hoffy, N., & A. Ewida, H. (2022). Promising Role of
Caffeine in Collagen Resynthesis and UV Protection. *SSRN Electronic Journal*.
https://doi.org/10.2139/ssrn.4035592

Shabir, G. A. (1993). A Practical Approach to Validation of HPLC Methods Under Current Good. *Equipment and Instrumentation Qualification*, 29–37.

Sharma, S., Goyal, S., & Chauhan, K. (2018). A review on analytical method development and
validation. *International Journal of Applied Pharmaceutics*, *10*(6), 8–15.
https://doi.org/10.22159/ijap.2018v10i6.28279

Shuler, L., & Hickman, J. J. (2016). *systems* (Vol. 20, Issue 2).
https://doi.org/10.1177/2211068214561025.TEER

Shumin Yang and Yanqing Wu. (2013). We are IntechOpen , the first native scientific publisher of Open Access books TOP 1 % Nutritional Value of Soybean Meal. *Web of Science*,
29.

Söderquist, M. (2013). Eliminating Biological Change after Excision: Preserving Sample Quality—One
of the Goals of Heat-Stabilization Technology. *Genetic Engineering & Biotechnology News*, *33*(2), 16-
16.

Sorg, O., Antille, C., Kaya, G., & Saurat, J. H. (2006). Retinoids in cosmeceuticals. *Dermatologic Therapy*, *19*(5), 289–296. https://doi.org/10.1111/j.1529-8019.2006.00086.x

Srinivasan, B., Kolli, A. R., Esch, M. B., Abaci, H. E., Shuler, M. L., & Hickman, J. J. (2015). TEER measurement techniques for in vitro barrier model systems. *Journal of laboratory automation*, *20*(2),107-126.

Steinstraesser, L., Rittig, A., Gevers, K., Sorkin, M., Hirsch, T., Kesting, M., Sand, M., Al-Benna, S., Langer, S., Steinau, H.-U., & Jacobsen, F. (2009). A human full-skin culture system
for interventional studies. *Eplasty*, *9*, e5.
http://www.ncbi.nlm.nih.gov/pubmed/19198642%0Ahttp://www.pubmedcentral.nih.gov/articlerender.fcgi?artid=PMC2627306

Supe, S., & Takudage, P. (2021). Methods for evaluating penetration of drug into the skin: A

review. *Skin Research and Technology*, *27*(3), 299–308. https://doi.org/10.1111/srt.12968

Taleuzzaman, M. (2018). Limit of Blank (LOB), Limit of Detection (LOD), and Limit of Quantification (LOQ). *Organic & Medicinal Chem IJ*, *7*(5), 555722. https://doi.org/10.19080/OMCIJ.2018.07.555722

Tarafder, A., Vajda, P., & Guiochon, G. (2013). Accurate on-line mass flow measurements in supercritical fluid chromatography. *Journal of Chromatography A*, *1320*, 130-137.

Tessema, E. N., Bosse, K., Wohlrab, J., Mrestani, Y., & Neubert, R. H. H. (2021). Investigation
of ex vivo Skin Penetration of Coenzyme Q10 from Microemulsions and Hydrophilic Cream. *Skin Pharmacology and Physiology*, *33*(6), 293–299. https://doi.org/10.1159/000511443

Tokarska, K., Tokarski, S., Woźniacka, A., Sysa-Jędrzejowska, A., & Bogaczewicz, J. (2018).
Cellulite: A cosmetic or systemic issue? Contemporary views on the etiopathogenesis of cellulite. *Postepy Dermatologii i Alergologii*, *35*(5), 442–446. https://doi.org/10.5114/ada.2018.77235

United Nations Office on Drugs, Crime. Laboratory, & Scientific Section. (2009). Guidance for the Validation of Analytical Methodology and Calibration of Equipment Used for Testing of Illicit Drugs in Seized Materials and Biological Specimens: A Commitment to Quality and Continuous Improvement. United Nations Publications.

Van Zyl, J. M., Derendinger, B., Seifart, H. I., & Van der Bijl, P. (2008). Comparative diffusion
of drugs through bronchial tissue. *International Journal of Pharmaceutics*, *357*(1–2), 32–36. https://doi.org/10.1016/j.ijpharm.2008.01.028

Venkatesh, V., Elphine Prabahar, A., Venkata Suresh, P., Umamaheswari, C., & Rama Rao, N.
(2011). A new RP-HPLC method for simultaneous estimation of etophylline and theophylline in tablets. *Research Journal of Pharmacy and Technology*, *4*(1), 128–130.

Veryser, L., Boonen, J., Mehuys, E., Roche, N., Remon, J.-P., Peremans, K., Burvenich, C., &
De Spiegeleer, B. (2013). Transdermal Evaluation of Caffeine in Different Formulations and Excipients. *Journal of Caffeine Research*, *3*(1), 41–46. https://doi.org/10.1089/jcr.2013.0002

Wang, F. Y., Chen, Y., Huang, Y. Y., & Cheng, C. M. (2021). Transdermal drug delivery systems for fighting common viral infectious diseases. *Drug Delivery and Translational Research*, *11*(4), 1498–1508. https://doi.org/10.1007/s13346-021-01004-6

Wang, M., Wang, K., Liao, X., Hu, H., Chen, L., Meng, L., Gao, W., & Li, Q. (2021). Carnitine
Palmitoyltransferase System: A New Target for Anti-Inflammatory and Anticancer Therapy? *Frontiers in Pharmacology*, *12*(October), 1–16. https://doi.org/10.3389/fphar.2021.760581

Wang, W., Yang, J., Zhang, E., Lu, Y., & Cao, Z. (2017). L-Carnitine derived zwitterionic

betaine materials. *Journal of Materials Chemistry B*, *5*(44), 8676–8680. https://doi.org/10.1039/c7tb02431b

Willson, C. (2018). The clinical toxicology of caffeine: A review and case study. *Toxicology Reports*, *5*(April), 1140–1152. https://doi.org/10.1016/j.toxrep.2018.11.002

Woolery-Lloyd, H., & Kammer, J. N. (2011). Treatment of Hyperpigmentation. *Seminars in Cutaneous Medicine and Surgery*, *30*(3), 171–175. https://doi.org/10.1016/j.sder.2011.06.004

Yourick, J. J., Jung, C. T., & Bronaugh, R. L. (2008). In vitro and in vivo percutaneous absorption of retinol from cosmetic formulations: Significance of the skin reservoir and prediction of systemic absorption. *Toxicology and Applied Pharmacology*, *231*(1), 117–121. https://doi.org/10.1016/j.taap.2008.04.006

Yu, Y. Q., Yang, X., Wu, X. F., & Fan, Y. Bin. (2021). Enhancing Permeation of Drug Molecules
Across the Skin via Delivery in Nanocarriers: Novel Strategies for Effective Transdermal Applications. *Frontiers in Bioengineering and Biotechnology*, *9*(March), 1–17. https://doi.org/10.3389/fbioe.2021.646554

Zasada, M., & Budzisz, E. (2019). Retinoids: Active molecules influencing skin structure formation in cosmetic and dermatological treatments. *Postepy Dermatologii i Alergologii*, *36*(4), 392–397. https://doi.org/10.5114/ada.2019.87443

Zhou, L., Nyberg, K., & Rowat, A. C. (2015). Understanding diffusion theory and Fick's law through food and cooking. *Advances in Physiology Education*, *39*(1), 192–197. https://doi.org/10.1152/advan.00133.2014

7. Appendices

Document Viewer

Turnitin Originality Report

Processed on: 02-Mar-2023 9:51 PM SAST
ID: 2027268379
Word Count: 49973
Submitted: 1

Final Write up -1.docx By Jessica Elonga

Similarity Index	Similarity by Source	
14%	Internet Sources:	10%
	Publications:	9%
	Student Papers:	0%

mode:

<1% match (Internet from 05-Feb-2023)
https://www.researchgate.net/publication/327623073_The_Beneficial_Effect_of_Proanthocyanidins_and_Icariin_on_Biochemical_Markers_of_Bone_Turnover_in_Rats

<1% match (Internet from 12-Feb-2023)
https://www.researchgate.net/publication/235729112_Design_and_Evaluation_of_Microemulsion_Gel_System_of_Nadifloxacin

<1% match (Internet from 19-Feb-2023)
https://www.researchgate.net/publication/337653981_Fasten_simple_and_specific_stability_of_the_avant-garde_RP-HPLC_method_for_estimation_and_validation_of_nystatin_in_pharmaceutical_formulations_Production_and_Hosted_by

<1% match (Internet from 24-Feb-2023)
https://www.researchgate.net/publication/233519750_Intravaginal_Drug_Delivery_Systems_Design_Challenges_and_Solutions

<1% match (Internet from 27-Jan-2023)
https://www.researchgate.net/publication/264850947_Andean_indigenous_food_crops_nutritional_value_and_bioactive_compounds

<1% match (Internet from 14-Feb-2023)
https://www.researchgate.net/publication/309705639_A_Study_of_Method_Development_Validation_and_Forced_Degradation_for_Quantification_of_Buprenorphine_Hydrochl

<1% match (Internet from 05-Feb-2023)

UNIVERSITY OF THE WITWATERSRAND, JOHANNESBURG
7 York Road, Parktown, 2193 South Africa * Telephone (011)717-2363

28th January 2016

To: Whom it may concern,

Re: approval for the use of animal tissue samples collected from pigs euthanized for other purposes in *in vitro* diffusion studies

This letter is to confirm that Dr AD van Eyk does not require full animal ethics clearance to collect pig intestine and colon samples. The grant applicant, Dr Armorel van Eyk will be using skin samples from already euthanized animals, hence full animal ethics clearance is not required, as these animals have been euthanized for other purposes. The skin samples for *in vitro* diffusion studies will be collected with permission from the Central Animal Service Unit at the University of the Witwatersrand. A request for permission to the Animal ethics committee has been submitted.

The following student will be involved in these studies as of 2016: Jessica Elonga (student number 447226) for the degree Master of Science on Medicine (Pharmacology). The title of the project is: "*The in vitro diffusion characteristics across excised porcine skin of various compounds used topically in the treatment of adiposis edematosa"*.
These studies will be performed in the Division of Pharmacology, Department of Pharmacy and Pharmacology.

If you would like any further or more specific information in this regard, do not hesitate to contact me.
Yours sincerely,



Kennedy Erlwanger
(Chairman: Animal Ethics Screening Committee, University of the Witwatersrand)

Assoc Prof Kennedy H. Erlwanger
School of Physiology
Faculty of Health Sciences, University of the Witwatersrand
7 York Road, Parktown, 2193
SOUTH AFRICA

Private bag 3, Wits, 2050, South Africa.
Tel: +27 (0)11 717 2454
Fax: + 27 (0)11 643 2765
Email: Kennedy.Erlwanger@wits.ac.za